



UNIVERSITAT DE  
BARCELONA

# Characterization of striatal development in Huntington's Disease and its implication to the adult phenotype

Cristina Vila Torondel



Aquesta tesi doctoral està subjecta a la llicència **Reconeixement- NoComercial – SenseObraDerivada 4.0. Espanya de Creative Commons.**

Esta tesis doctoral está sujeta a la licencia **Reconocimiento - NoComercial – SinObraDerivada 4.0. España de Creative Commons.**

This doctoral thesis is licensed under the **Creative Commons Attribution-NonCommercial-NoDerivs 4.0. Spain License.**

# Characterization of striatal development in Huntington's Disease and its implication to the adult phenotype

**Doctoral degree  
by the University of Barcelona  
Doctoral Programme in Biomedicine**



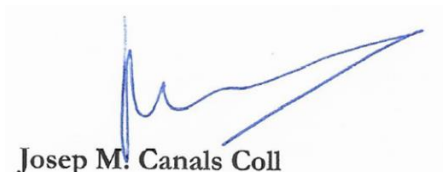
UNIVERSITAT DE  
BARCELONA

A handwritten signature in blue ink, appearing to be 'Cristina Vila Torondel', enclosed within a light blue rectangular border.

Dissertation submitted by:

**Cristina Vila Torondel**

This thesis has been supervised by Dr. Josep M. Canals Coll from the Laboratory of Stem Cells and Regenerative Medicine, Department of Biomedicine from the Faculty of Medicine and Health Science, University of Barcelona.

A handwritten signature in blue ink, appearing to be 'Josep M. Canals Coll', enclosed within a light blue rectangular border.

**Josep M. Canals Coll**



*«Siempre hice algo para lo que no estaba preparada. Creo que así es la manera de crecer»*

**Marissa Mayer**



*A los míos,*



# ACKNOWLEDGEMENTS

---





# ACKNOWLEDGEMENTS

Primer de tot, t'agrairé a tu, Pep. Gràcies per triar-me i apostar per mi. Fa gairebé 7 anys ens vam conèixer al curs d'estiu de la UB, junt amb el Jordi A., on veu despertar el meu interès i ganes de seguir-me formant en les cèl·lules mare i la medicina regenerativa. Recordo quan van sortir les llistes d'opcions per a fer el TFG, vaig veure el teu nom, i vaig tindre clar que allà era on volia començar la meua vida com a científica. El dia de l'entrevista vam parlar del desenvolupament, i recordo que vas veure claríssim el que necessitava. Vas dir-me: has de fer aquest projecte de desenvolupament en HD. Gràcies a això, ara soc una boja enamorada del desenvolupament embrionari. Com ja he dit, han passat casi 7 anys. Uns anys en els que he après tantíssimes coses, científiques i de la vida, uns anys que he gaudit de la ciència i del creixement personal. Som els dos molt torçuts, i algunes vegades em tingut diferències i ens hem enganxat en certes situacions jaja però haig de dir-te, i tots ho sabem, que si tornés a estar en el moment de triar TFG, tornaria a escollir-te. Gràcies per tot el coneixement i tota la part científica, però gràcies també per haver sapigut gestionar una persona tant difícil com jo i, sobretot, per tota la teva comprensió i recolzament a nivell personal que he rebut per part teva aquests anys. M'has vist créixer com a persona i com a investigadora i, per això, espero que sentis orgull amb aquesta Tesi. Gràcies Pep.

A mi familia. No fui una buena adolescente, y aunque llevo tiempo trabajando activamente en mejorar y pulir, todavía no soy (aunque poco me queda) la mujer en la que me quiero convertir. He sido un poco rebelde, complicada, desafiante, traviesa, cabezota, fiestera, y algunas cosas más. He tenido malos momentos, demasiados, algunos por mi culpa y otros por males ajenos a mí, pero, contra todo pronóstico, aquí estamos. Miro hacia atrás, a momentos cruciales de mi adolescencia, como el bachillerato y la selectividad, entrar en una carrera, y mi vida entonces era asquerosamente caótica i compleja. Miro a esa niña y la admiro por haber sabido seguir por el pequeño rayo luz que podía haber en esa turbia realidad. Pero esa niña tuvo el coraje, fuerza y tenacidad para hacerlo y, por eso, hoy quiero honrarla. Sigo sin saber cómo pudo hacerlo, pero sé seguro que debo daros las gracias a vosotros, no solo por apoyarme, sino por haberme criado dándome las armas necesarias para enfrentarme a situaciones pochas y superarlas, por enseñarme que es mi deber trabajar duro y no dejarlo nunca (aunque cueste), que es mi deber formarme y llegar a donde quiero llegar, aunque el mundo pese. Y ahora, esa pequeña niña (aparentemente) indefensa y completamente destruida, está a poco de convertirse en Doctora. Gracias y espero que eso os llene de orgullo, porque a mi si.

A Pepi. No solo tengo que agradecerte por formar parte, al igual que mis familia, en darme luz en esos momentos feos, sino también por todos los años que han venido después, hasta el día de hoy, por tu amor y apoyo incondicional, por ser mi compañero de vida con el que crecer (porque vaya dos éramos de niños, y menudos hombre y mujer en el que nos hemos convertido), por sufrir mis penas como si fueran tuyas, por disfrutar mis alegrías como si fueran tuyas y, por supuesto, por vivir los

nervios de esta Tesis como si fuera tuya jaja. Siempre te estaré agradecida por todo, y siempre intentaré ser el hogar al que puedas volver cuando sientas frío.

A Gertrudis. Aunque ya te incluya en el apartado de familia, tengo que hacer un párrafo dedicado en especial a ti. A las noches de chicas, a las tardes noches de panadería, pizzas y raviolis (buenísimos). Es mucho más fácil hacer una tesis cuando tienes momentos así en los que cargar pilas. Sé que a veces soy una hermana complicada, pero sabes que te amo y que siempre voy a intentar cuidarte más que a mí misma. Te quiero. Y aprovecho la sección para darte las gracias por el cuñado que me has dado. Ian, te quiero, y me encanta que volvamos a sentirnos adolescentes con nuestra vuelta al chumba chumba.

A les meves xuxitas. Ho sou tot. Hem crescut juntes, des de que ens cegàvem als panyals. A part de tot el recolzament, les risas, els bons moments, consells, festes i amor que tinc dia a dia amb vosaltres, gràcies per haver sapigut comprendre'm en els meus moments complicats, haver respectat les meves actuacions i, sobretot, haver decidit seguir al meu costat malgrat tot. Soc vostra per sempre, ja ho sabeu. Us estimo.

A mi Nurs. Eres luz en mi vida. Eres imprescindible. Ojalá así hasta hacernos viejecitas. Te quiero.

A Angelita i Aleix. Habéis sido (y sois) una parte muy importante de mi vida, pero, además, habéis compartido conmigo todo este proceso, desde cuando salí de la entrevista con Pep (Aleix, aún recuerdo que lo primero que hice al salir fue ir a la moto a sentarme y llamarte emocionada porque salí pensando que la entrevista había ido muy bien), hasta el día de hoy mientras escribo esto. Cojamos el camino que cojamos cada uno de nosotros, por mucho que se separen, siempre seréis parte de mi. Os quiero.

A mis cachorros, Max (sigo echándote de menos), Rona, Thai, Nala y Goku. No sabéis leer, pero os quiero pololitos míos. Una persona que no ha tenido bichis no conoce este amor. Habéis dado paz y amor a mis momentos difíciles. Me habéis acurrucado cuando estaba triste. Me habéis obligado a salir de mis bucles mentales en muchos momentos porque sois unos putos pesados, intensos, que reclamáis atención todo el puto rato (Nala, estás subiéndote encima de mí mientras escribo esto, y deseo matarte ahora mismo jaja). Aun así, antes me matan que dejar que os hagan daño. Os amo.

A todos mis amigos y amigas. He sido super afortunada y la vida me ha dado muchos y muy buenos, y como soy una empanada que, seguro que se deja de poner algún que otro nombre, no pondré ninguno. Gracias a todos vosotros por acompañarme en el camino y hacer de mi vida algo más divertido. Os pido perdón por el abandono que habéis recibido por mi parte durante estos últimos meses de doctorado. Se que me queréis igual y no me lo tenéis muy en cuenta. Os amo. Soy vuestra para siempre.

A les meves motomamis, el super team amb el que he tingut la sort de compartir aquests anys.

A ti Ana, una de las primeras que conocí al llegar al lab. Fuiste la primera en acogirme y enseñarme el mundo de los ratulinets. Más que eso, siempre te he visto como mi mami en el lab. También fuiste la primera a la que le conté mis cositas personales, por la confianza que me transmitías. Desprendes luz, una luz muy bonita. A ver si te lo crees de una vez. Gracias :)

A tu Georgina, amb la que m'identifico al 200% en tot. Som unes tarades, però entre bojes ens entenem. Fas que el camí que recorrem al lab sigui extremadament divertit. Les teves paellades, carndollades i demés ens donen la vida. Podem parlar seriosament sobre temes importants de la vida, però també podem morir de riure amb la tonteria mes tonta (perquè els nostres amics no poden estar a la platja de cap de les maneres, digali al Luigi). Tinc claríssim que ets una de les millor coses que m'emporto d'aquests 7 anys al lab. Gràcies!

A ti Cristi, la dupla perfecta que, junto con Georgina, formamos el trio fantástico. Te amo, te adoro, te miseo infinito en el lab. Mis intimidades se sienten solas desde que no estás aquí jaja. Gracias por las risas que me diste, gracias por dejarte llevar con mis locuras, gracias por enseñarme a Rosalía y gracias por existir en este mundo. Eres mágica, así que tengo claro que todo te irá bien en cualquier aspecto de la vida, hagas lo que hagas.

A tu Mireia, que també has estat al meu costat des del principi. Gràcies per aportar-me ordre, consells, recolzament i tot el que m'has aportat a mi i al lab. T'ho mereixes tot, perquè ets una lluitadora estupenda. Et desitjo el millor en la teva vida!

A mi Clelia, de ahora en adelante, married Clelia. Te amo, te amamos. Has dejado un vacío muy grande en el lab, pero me consuela saber que seguimos en contacto fuera. Gracias por estos años en el lab, gracias por abrirnos tus puertas de casa y dejarnos compartir tus momentos personales más maravillosos contigo. Cuenta conmigo para cualquier cosa científica que necesites, para cualquier cosa personal, para cuidar a baby Ander o para cuidar al posible (esper) futuro baby. Mi culo es tuyo.

A Francis. Francisquito de mi corazón. Creatio y Motomamis S.L. te necesitábamos en nuestras vidas. Gracias por todo lo bonito que nos has aportado estos años, y gracias por aguantar tanto tiempo rodeado de mujeres (locas) sin quejarte ni un solo segundo. Eres bueno, así que lucha siempre por lo que mereces, que no es poco. Nos vemos un día de estos.

A la Silvia, mi romántica Silvia. La teva presència en la nostra vida era inevitable. Ets maca, preciosa, divertida, sensata, serena i boja, i m'encanta. Com el teu cabell o la teva risa (molt forta i greu), que també m'encanten. No se, tot de tu m'encanta. Només espero que els nostres camins no se separin aquí, perquè em ficaria molt trista.

A la Cinta, o millor dit, Shinta. La meva amiga olímpica. Ets claríssimament fitxatge necessari pel lab. Eres lo que buscábamos. I no ho dic només per com treballes, que es obvi, sinó de cara a les motomamis. Gràcies per queixar-te amb mi de la shienschia, per riure i apreciar les tonteries com jo i,

per suposat, per portar un or al club. Tráeme una de oro, tráeme una de oro! No deixis de sortir amb les motomamis plis. Et desitjo tota la força i ànims per a acabar la teva tesi, tot i que coneixent-te, ho faràs genial. Pots demanar-me ajuda sempre que ho necessitis, estigui o no al lab. B MACSima.

A Inés, Inés, Inesita, Inés. Otro gran fichaje. No se si tendré espacio para escribir aquí todas nuestras tonterías absurdas, y eso me perturba, así que solo diré una cosa: dame una de laminar flow. Tengo demasiadas cosas bonitas que decir de ti, eres la mejor compañera que podría haber deseado. Solo espero que nuestros caminos sigan unidos durante mucho más tiempo. Ya pues, vamos hablando.

Al Marc. Aaaaai Markitus Markitus... piratiya. Gràcies per aguantar-me. Gràcies per ser el meu millor públic. Nada mas que añadir, señoría. Molta sort en la teva tesis, em tens aquí per tot el que necessitis!

Als nous fitxatges estupendos: Jordi A., Olga V. I alicé L.. A totes les persones que han estat al lab i que han fet aquest camí una mica menys dur. En especial a l'Anna V., l'Andrea C., l'Andrea H., el Philip, el David V., l'Andrés M., els Xavis, al Dani Q., a la Sandra, la Paola, el Dani T., i molts mes que m'estic deixant perquè soc una empanada.

A tot UPER CREATIO, tan blancs i nets, però tan bona gent tots.

A la histofamily. Tot i no formar part directa del histolab, sempre he sentit el vostre recolzament i calor. A moltes us he vist entrar, hem recorregut aquest dur camí del doctorar juntes i, ara, esteu convertint-vos en Doctors i Doctores preciosos. Y Maite, tu si que eres preciosa. Gràcies.

Gràcies en especial a l'Albert Giralt i al Dani de Toro. Sou un pou de sabiduria. Genis. Res mes a dir. Gràcies a la Silvia G., l'Ester P. i la Vero B. Simplement sou un referent per mi. Gràcies al Jordi Alberch qui, a part de descobrir en tu a un gran científic, també he descobert en tu una part humana molt maca, que es d'agrair. Espero que algun dia pugui quedar-me allò que tens a un tarro en l'armari del teu despatx.

A las millors secres, Núria, Carme i Mercè. I a les precioses joies de la Mercè.

A mis amichis de seguridad, que me hacen las pausas de café muy entretenidas.

Un especial agradecimiento al Dr. Francisco Londono y a la Dra. Anna Esteve por los análisis bioinformáticos.

Un últim agraïment, junt amb unes disculpes, a tota la gent important que m'estic oblidant. No m'ho tingueu en compte, ja sabeu com soc.

**Y mi último agradecimiento va para ti yayita mía. Muchas veces pienso que ojalá hubiera acabado esta Tesis un poco antes, para que vieras el fruto de todo lo que hemos estado hablando estos años, para que hubieras podido estar sentada entre el público mientras la defiendo. Pero igualmente sé que me estás viendo desde alguna parte, aun así, siento tu orgullo desde aquí, y eso me reconforta. Espero que tu más X haya estado a la altura de tus expectativas. Te echo infinitamente de menos. Te quiero.**

# SUMMARY

---



# SUMMARY

Huntington's disease (HD) is a devastating neurodegenerative disorder that manifests itself through motor, cognitive and behavioral symptoms. HD is a monogenic disease caused by CAG expansion in the huntingtin gene, which inversely correlates with the age of onset. Despite the ubiquitous expression of mutant huntingtin (mHtt), striatal-projection neurons, known as medium spiny neurons (MSN), are the most vulnerable cell type. Although the onset of the disease has been classically defined by the appearance of motor symptoms, which occur around the age of 40-50, recent studies have shown significant cognitive and mental dysfunction many years before motor onset. A key role of huntingtin in brain development has been described. For this reason and given that the mutation exists from the moment of conception, hypothesis about a possible developmental effect on HD started to emerge. Subtle effects during development can lead to deficiencies in the cellular homeostasis of evolving regional neuronal subpopulations, which in turn can result in adult-onset cell death by normally non-lethal environmental stressors. Neurodegenerative diseases can therefore represent an emerging class of developmental disorders characterized by little developmental abnormalities that cause no obvious deficits.

In this thesis we have studied and characterized these developmental alterations in a model of the disease, the zQ175 mouse. Our results show that mouse embryos that have inherited the mutation present a gene expression profile related to the pathophysiology described in adult patients with the disease, from early stages of development. In addition, we have detected that HD developmental alterations are specific to neuronal subpopulation. During the development of the mouse striatum, indirect pathway MSNs (iMSNs) are generated prematurely and excessively during the period of neurogenesis. However, these neurons exacerbately die during the natural period of programmed cell death, which occurs in postnatal stages. Thus, the striatal development of HD mice ends up with a striatum with a lower proportion iMSNs, generating an imbalance between their main neuronal populations. In addition, single-cell analysis allowed us to identify a specific neural progenitor cell (NPC) population differentially affected during HD development. The identification of subtle changes in specific populations of NPCs, and their subsequent follow-up to adults, may clarify neurodevelopmental's contribution to HD.

These results suggest that the subtle effects of the mutant huntingtin during development may cause significant alterations that spread to adults and contribute to the most common HD phenotypes.





# RESUM

La malaltia de Huntington (HD) és un trastorn neurodegeneratiu devastador, que es manifesta a través de símptomes motors, cognitius i conductuals. L'HD és una malaltia monogènica causada per una expansió de repetició CAG en el gen de la huntingtina, que es correlaciona inversament amb l'edat d'inici. Malgrat l'expressió ubíqua de la huntingtina mutada (mHtt), les neurones de projecció de l'estriat, conegudes com a neurones espinoses mitjanes (MSNs), són el tipus cel·lular més vulnerable. Tot i que l'aparició de la malaltia s'ha definit clàssicament per l'aparició dels símptomes motors, que es produeixen al voltant dels 40-50 anys, molts estudis recents han demostrat una disfunció cognitiva i psíquica important molts anys abans de l'aparició motora. S'ha descrit un rol clau de la huntingtina durant el desenvolupament del cervell. Per això, i atès que la mutació existeix des del moment de la concepció, recentment s'ha començat a hipotetitzar sobre una possible afectació del desenvolupament a l'HD. Efectes subtils durant el desenvolupament poden conduir a deficiències en l'homeòstasi cel·lular de les subpoblacions neuronals, que alhora poden produir la seva mort cel·lular en l'etapa adulta per estressors ambientals normalment no letals. Les malalties neurodegeneratives poden representar, per tant, una classe emergent de trastorns del desenvolupament caracteritzats per subtils anomalies desenvolupamentals que no causen dèficits evidents.

En aquesta tesi hem estudiat i caracteritzat aquestes alteracions en un model animal de la malaltia, el ratolí zQ175. Els nostres resultats mostren que els embrions de ratolí que han heretat la mutació, presenten un perfil d'expressió gènica relacionat amb la pato-fisiologia descrita en pacients adults amb la malaltia, ja des d'etapes primerenques del desenvolupament. A més, hem detectat que les alteracions del desenvolupament en HD són específiques de subpoblació neuronal. Durant el desenvolupament del nucli estriat del ratolí, les MSNs de la via indirecta (iMSNs) es generen prematurament i en excés durant el període de neurogènesi. No obstant això, aquestes neurones moren de forma exacerbada durant el període natural de mort cel·lular programada, que passa en etapes postnatales. Així doncs, el desenvolupament estriatal de ratolins HD acaba amb un estriat que presenta una menor proporció de neurones iMSNs, generant un desequilibri entre les seves principals poblacions neuronals. A més, l'anàlisi a nivell de cèl·lula única ens va permetre identificar una població específica de precursors neurals (NPCs) afectada diferencialment durant el desenvolupament d'HD. La identificació de canvis subtils en poblacions específiques de NPCs, i el posterior seguiment d'aquestes cap a l'adult, pot aclarir la contribució del neurodesenvolupament a l'HD.

Aquests resultats suggereixen que els efectes subtils de la huntingtina mutada durant el desenvolupament poden causar alteracions importants que es propaguen a l'adult i contribueixen als fenotips HD més comuns.



# INDEX

---



# INDEX

---

<b>ABBREVIATIONS</b> .....	1
<b>LIST OF FIGURES</b> .....	7
<b>LIST OF TABLES</b> .....	13
<b>INTRODUCTION</b> .....	17
1. <i>The Basal Ganglia and the Striatal Nuclei</i> .....	19
1.1. Basal Ganglia.....	19
1.2. The Striatal Nuclei .....	20
1.2.1. Striatal Neurons .....	20
1.2.2. Striatal cytoarchitecture: .....	21
1.2.3. Striatal Connections: .....	22
2. Brain Development.....	24
2.1. Embryogenesis .....	24
2.1.1. Fertilization and zygote formation.....	24
2.1.2. Blastocyst formation .....	25
2.1.3. Gastrulation.....	25
2.2. Nervous system development.....	26
2.2.1. Neurulation.....	26
2.2.2. Neural tube regionalization.....	27
3. The Striatal Development.....	28
3.1. Telencephalon regionalization .....	28
3.1.1. Subpallium .....	28
3.1.2. Pallial-Subpallial Boundary.....	29
3.1.3. Factors Involved in the dorso-ventral Telencephalic regionalization .....	30
3.2. Neural Progenitor Cells (NPCs) of the ventral Telencephalon.....	32
3.2.1. Neural Progenitor Cells Subtypes .....	32
3.3. Cell cycle vs Neurogenesis.....	34
3.4. Striatal Neurogenesis .....	36
3.4.1. Medium Spiny Neuron Neurogenesis .....	36
3.4.2. A novel source of Medium Spiny Neurons.....	38
3.4.3. Interneuron Neurogenesis .....	39
3.5. Striatal Migration and Reorganization .....	40
3.5.1. Striatal Radial Migration .....	40
3.5.2. Striatal Tangential Migration .....	41
3.5.3. Active Intermixing.....	42

3.6.	Striatal Connection's Formation.....	44
3.7.	Factors involved in the specification of striatal neuronal subtypes .....	45
3.7.1.	NPCs-related factors.....	45
3.7.2.	Direct pathway lineage-related factors .....	48
3.7.3.	Indirect pathway lineage-related factors .....	49
3.7.4.	Neuronal maturation-related factors .....	51
3.7.5.	Interneuron lineage-related factors:.....	52
4.	Developmental Alterations in Huntington's Disease.....	53
4.1.	Huntington's Disease and Huntingtin mutation.....	53
4.2.	HD Adult Pathophysiology.....	55
4.3.	Current Therapeutic Strategies.....	56
4.4.	Neurodevelopment in Huntington's Disease.....	57
4.4.1.	Huntingtin role during normal development.....	57
4.4.2.	Developmental alterations in HD models.....	57
4.4.3.	Developmental alterations in CAG expansion human carriers.....	58

<b>OBJECTIVES.....</b>	<b>59</b>
------------------------	-----------

<b>MATERIALS AND METHODS.....</b>	<b>63</b>
-----------------------------------	-----------

1	Animal Procedures.....	65
1.1.	General.....	65
1.2.	Huntington's Disease Mouse Model zQ175.....	65
1.3.	Reporter Mouse Lines Generation.....	66
2	Histological and Molecular Assays .....	67
2.1	Embryonic sample obtention for histological analysis.....	67
2.2	Adult sample obtention for histological analysis .....	67
2.3	Cryosectioning.....	67
2.4	Immunohistochemistry (IHC) .....	68
2.5	EdU analysis.....	69
2.4.1.	S-phase labelling.....	69
2.4.2.	Birthdating.....	69
2.4.3.	Neurogenesis .....	69
2.4.4.	EdU Detection.....	70
5.1.	Fluorescence <i>in situ</i> hybridization (FISH) .....	71
5.1.2.	Probe design.....	71
5.1.3.	FISH .....	71
5.2.1.	Sample Obtention.....	72

5.2.2. RNA extraction.....	72
5.2.3. cDNA synthesis.....	72
5.2.4. Q-PCR.....	72
2.6 Image adquisition.....	72
2.7 Measurement of volumes and in vivo cell counts.....	73
3 Bulk RNA-sequencing.....	74
3.1 Sample obtention for bulk RNA-seq analysis .....	74
3.1.1. Sampling and rapid freezing of tissue with 2-methyl-butane (isopentane) .....	74
3.1.2. Sterilizing Membrane Slides .....	74
3.1.3. Sectioning.....	74
3.1.4. Hematoxylin and eosin staining .....	75
3.1.5. Laser Micro-Dissection (MDL) .....	76
3.1.6. RNA Isolation.....	77
3.2 Bulk RNAseq Downstream Analysis.....	77
4 Single Cell RNA-sequencing.....	78
4.1 Introduction .....	78
4.2 Sample obtention for single cell RNA-seq analysis .....	78
4.2.1. Embryo obtention ans manteinance .....	78
4.2.2. Striatal dissection .....	79
4.2.3. Cell disgregation and quantification .....	80
4.2.4. Sample delivery and sequantiation .....	80
4.3 Bioinformatic Analyses of scRNA-seq data .....	80
<b>RESULTS.....</b>	<b>81</b>
<b>1 CHAPTER I: finding HD developmental alterations</b>	
<i>Transcriptomic analysis of HD striatal developmental abnormalities .....</i>	<i>83</i>
1.1. Differential expression analysis of wt and Q175 regions .....	83
1.2. Protein-coding DEGs .....	86
1.3. TEC genes .....	92
1.4. Non-coding DEGs .....	93
1.4.1. Long non-coding RNAs (lncRNAs).....	95
1.5. Differential expression analysis of wt and Q175 maturation patterns .....	96
1.5.1. Wt and HD striatal neurons are generated following distinct maturation patterns.....	96
1.5.2. Striatal lineage-specific transcriptional alterations.....	98
<b>2 CHAPTER II: defining HD developmental alterations</b>	
<i>Histological characterization of HD striatal developmental abnormalities.....</i>	<i>99</i>
2.1. NPCs cell cycle status is affected during Q175 development.....	99



2.2.	Q175 early NPCs undergo to a precocious cell cycle exit, compromising the NPCs pool maintenance .....	101
2.3.	Specific iMSNs are prematurely generated during HD development causing an early striatal subpopulation imbalance .....	103
2.4.	Interneuronal striatal lineage also undergo developmental abnormalities in HD embryos .....	107
3	<b>CHAPTER III: finding iMSNs alterations' origin</b>	
	<i>Characterization of developmental lineage-specific alterations in HD.....</i>	<i>108</i>
3.1.	Computational integration of different scRNA-seq datasets .....	108
3.1.1.	Annotation and identification of cluster identities.....	109
3.2.	Finding specific HD affected clusters.....	111
3.3.	HELT-expressing subpopulation .....	112
3.4.	HELT-expressing subpopulation is affected in zQ175 embryos .....	112
	<b>DISCUSSION.....</b>	<b>115</b>
1	<i>HD-related hallmarks are present in zQ175 embryos from early development.....</i>	<i>117</i>
1.1.	Transcriptional dysregulation .....	117
1.1.1.	TEC genes .....	117
1.1.2.	Long non-coding RNAs.....	118
1.2.	Endocytosis and Vesicle Transport Impairment .....	120
1.3.	Mitochondrial dysfunction, metabolism and cellular stress .....	121
1.4.	Neuronal Synaptic functionality and calcium homeostasis .....	122
2	<i>Specific NPCs and Neuronal subpopulations are imbalanced along development in HD.....</i>	<i>123</i>
2.2.	HD embryos display aberrant proliferative, neurogenic and maturation programs during HD striatal development .....	124
2.3.	Direct and indirect pathway imbalance starts from early development in HD .....	126
2.3.1.	Precocious and enhanced neurogenesis of iMSNs.....	127
2.3.2.	Specific iMSNs cell death during postnatal development.....	127
2.3.3.	HD striatum ends up with an imbalance in dMSNs/iMSNs populations .....	128
2.4.	Striatal Interneuron developmental alterations .....	129
2.5.	Targeting HELT-expressing subpopulation as a candidate for HD.....	130
3	<b>INTEGRATIVE DISCUSSION .....</b>	<b>133</b>
	<b>CONCLUSIONS.....</b>	<b>135</b>
	<b>BIBLIOGRAPHY.....</b>	<b>139</b>

# ABBREVIATIONS

---



# *Abbreviations*

<b>EdU</b>	5-ethynyl-2'-deoxyuridine
<b>AchE</b>	Acetylcholinesterase
<b>A2A/Adora2A</b>	Adenosine A2A receptor
<b>AD</b>	Alzheimer's Disease
<b>ALS</b>	Amyotrophic Lateral Sclerosis
<b>AP</b>	Antero-Posterior
<b>asRNA</b>	Antisense RNA
<b>aIP</b>	Apical IPs Intermediate Progenitor
<b>ADHD</b>	Attention deficit and hyperactivity disorder
<b>BG</b>	Basal Ganglia
<b>bIP</b>	Basal IPs Intermediate Progenitor
<b>BP</b>	Basal Progenitor
<b>bRB</b>	Basal Radial Glia
<b>bHLH</b>	Basic helix-loop-helix
<b>BMP</b>	Bone Morphogenic Protein
<b>BSA</b>	Bovine Serum Albumin
<b>CB</b>	Calbindin
<b>CR</b>	Calretinin
<b>CGE</b>	Caudal Garglionic Eminence
<b>CNS</b>	Central Nervous System
<b>ChAT</b>	Choline acetyltransferase
<b>Casp3</b>	Cleaved Caspase 3
<b>DIV</b>	Day in vitro
<b>DEGs</b>	Differentially expressed genes
<b>dMSN</b>	Direct pathway Medium Spiny Neuron
<b>D1/DRD1</b>	Dopamine D1 receptor
<b>D2/DRD2</b>	Dopamine D2 receptor
<b>dMGE</b>	Dorsal Medial Garglionic Eminence
<b>DBHS</b>	Drosophila Behavior Human Splicing
<b>DYN</b>	Dynorphin
<b>EGR-1</b>	Early Growth Response 1
<b>E</b>	Embryonic day
<b>ER</b>	Endoplasmic reticulum
<b>Enk</b>	Enkephalin
<b>Eph</b>	Ephrin Receptor
<b>EGF</b>	epidermal growth factor
<b>EST</b>	Expressed sequence tag
<b>FDR</b>	False Discovery Rate
<b>FGF</b>	Fibroblast growth factor
<b>FISH</b>	Fluorescence in situ hybridization
<b>G1</b>	Gap1
<b>G2</b>	Gap2

<b>GEM</b>	Gel bead in emulsion
<b>GE</b>	Gene expanded
<b>GNE</b>	Gene non-expanded
<b>GO</b>	Gene Ontology
<b>GW</b>	Gestational week
<b>GP</b>	Globus Pallidus
<b>Gpe</b>	Globus Pallidus external segment
<b>Gpi</b>	Globus Pallidus internal segment
<b>GAD-2</b>	Glutamic acid decarboxylase
<b>Gro</b>	Groucho
<b>HBSS</b>	Hanks' Balanced Salt solution
<b>hESC</b>	Human Embryonic Stem Cell
<b>Htt</b>	Huntingtin
<b>iPSC</b>	Induced Pluripotent Stem Cell
<b>iMSN</b>	Indirect pathway Medium Spiny Neuron
<b>ICM</b>	Inner Cell Mass
<b>INM</b>	Interkinetic nuclear migration
<b>IP</b>	Intermediate Progenitor
<b>IN</b>	Interneuron
<b>KO</b>	Knock-out
<b>LMD</b>	Laser mycodissection
<b>LGE</b>	Lateral Garglionic Eminence
<b>Lhx2</b>	LIM Homeobox 2
<b>lncRNA</b>	Long non-coding RNAs
<b>MPO</b>	Mammalian Phenotype Ontology
<b>MZ</b>	Mantle zone
<b>MGE</b>	Medial Garglionic Eminence
<b>MSN</b>	Medium Spiny Neuron
<b>met-ENK</b>	met-enkephalin
<b>MB</b>	Midbrain
<b>M</b>	Mitosis
<b>mHtt</b>	Mutant Huntingtin
<b>NPC</b>	Neural Progenitor Cell
<b>NE</b>	Neuroepithelial
<b>Ngn-1</b>	Neurogenin-1
<b>Ngn-2</b>	Neurogenin-2
<b>NPY</b>	Neuropeptide Y-positive
<b>Nr4a1</b>	Nuclear Receptor Subfamily 4 Group A Member 1
<b>ORF</b>	Open reading frame
<b>OP</b>	Other Progenitor
<b>oRG</b>	Outer Radial Glia
<b>PSPB</b>	Pallial-subpallial boundary
<b>PFA</b>	Paraformaldehyde
<b>PD</b>	Parkinson's Disease
<b>PV</b>	Parvalbumin
<b>PH3</b>	Phosphohistone 3

<b>P</b>	Postnatal day
<b>POA</b>	Preoptic area
<b>qPCR</b>	Quantitative-polymerase chain reaction
<b>RG</b>	Radial glia
<b>ROS</b>	Reactive oxygen spieces
<b>RA</b>	Retinois Acid
<b>RRA</b>	Retrorubral area
<b>rRNA</b>	Ribosomic RNA
<b>RIN</b>	RNA integrity number
<b>SNP</b>	Short Neural Precursor
<b>SEGs</b>	Single exon genes
<b>snRNA</b>	Small nuclear RNA
<b>snoRNA</b>	Small nucleolar RNA
<b>Sst</b>	Somatostatin
<b>Shh</b>	Sonic Hedgehog
<b>STR</b>	Striatum
<b>SAP</b>	Subapical Progenitor
<b>SP</b>	Substance P
<b>SN</b>	Substantia Nigra
<b>SNc</b>	Substantia Nigra pars compacta
<b>SNr</b>	Substantia Nigra pars reticulata
<b>STN</b>	Subthalamic Nucleus
<b>SVZ</b>	Subventricular zone
<b>SC</b>	Superior colliculus
<b>S</b>	Syntesis
<b>ncRNA</b>	The non-coding RNAs
<b>TALE</b>	Three amino acid loop extension
<b>TEC</b>	To be Experimentally Confirmed
<b>TH</b>	Tyrosine hydroxylase
<b>UMI</b>	Unique molecular identifier
<b>VIP</b>	Vasoactive intestinal peptide
<b>vMGE</b>	Ventral Medial Gaglionic Eminence
<b>vPall</b>	Ventral Pallium
<b>VTa</b>	Ventral Tegmental area
<b>VZ</b>	Ventricular zone
<b>WGE</b>	Whole Gaglionic Eminence
<b>wt</b>	wild-type
<b>ZF</b>	zinc finger motif
<b>GABA</b>	$\gamma$ -aminobutyric acid
<b><math>\mu</math>OR</b>	$\mu$ -opioid receptor



# LIST OF FIGURES

---





# *List of Figures*

<b>Figure 1.</b> Basal ganglia structure (A) and function (B).	19
<b>Figure 2.</b> Morphology of the different interneuron subtypes.	20
<b>Figure 3.</b> Striosome and matrix compartmentalization.	21
<b>Figure 4.</b> Schematic representation of cortical and striatal circuits involved in HD.	22
<b>Figure 5.</b> Emrbyogenic process showing the different cell stage from the fertilization to the blastocyst.	24
<b>Figure 6.</b> Gastrulation process showing the three germ layers arised from the blastocyst.	25
<b>Figure 7.</b> Neurulation and neural tube formation.	26
<b>Figure 8.</b> Neural tube regionalization.	27
<b>Figure 9.</b> Striatal developmental milestone.	28
<b>Figure 10.</b> Representation of coronal hemisections of the mouse telencephalon during embryonic development.	29
<b>Figure 11.</b> Regionalization of the Telencephalon.	29
<b>Figure 12.</b> Picture showing the different NPCs described in the striatal GZ.	32
<b>Figure 13.</b> (A) Cell cycle phases and checkpoints. (B) Summary of different signals that regulate transition from NPCs into neuronal differentiation.	34
<b>Figure 14.</b> Summary of the different linages and their generation along the striatal development.	37
<b>Figure 15.</b> Emx1-lineage cells contribute to multiple neural subtypes in the basal forebrain.	38
<b>Figure 16.</b> Summary of the different interneuron subtypes generated by the three main interneuronal sources: MGE, CGE and POA.	39
<b>Figure 17.</b> Schematic representations depicting cell migration for striatal development.	40
<b>Figure 18.</b> Schematic drawings of transversal hemisections through the developing telencephalon summarizing the chemorepellent and chemoattractive cues that drive interneuron migration to the cortex (A) or the striatum (B).	42
<b>Figure 19.</b> Establishment and maturation of the developing striatum.	44
<b>Figure 20.</b> The main transcription factor network regulating the fate determination of striatal MSNs.	47
<b>Figure 21.</b> Prevalence of HD worldwilde.	53
<b>Figure 22.</b> Schematic representation of the genetic basis of HD.	53
<b>Figure 23.</b> (A) Post-mortem image of a healthy and Huntington's disease brain. (B) Schematic representation of the direct and indirect inhibitory pathways underlying choreic and dyskinesic HD symptoms.	54
<b>Figure 24.</b> Scheme sumarizing the main HD pathophysiological hallmarks.	55
<b>Figure 25.</b> Summary of the ongoing clinical trials for HD.	56
<b>Figure 26.</b> Abnormal brain development in HD mutation carriers.	58

<b>Figure 27.</b> Q140 mouse model genetics. ....	65
<b>Figure 28.</b> Schematic representation of the mouse crossmates performed to obtain the reporter mice. .....	66
<b>Figure 29.</b> Schematic representation of S-Phase labelling experiments. ....	69
<b>Figure 30.</b> Schematic representation of birthdating analysis. ....	69
<b>Figure 31.</b> Schematic representation of the neurogenesis experiments. ....	69
<b>Figure 32.</b> Illustration of the EdU Click-it kit reaction. ....	70
<b>Figure 33.</b> Click iT® reaction cocktails. T' .....	70
<b>Figure 34.</b> Schematic of the RNAscope assay procedure. I .....	71
<b>Figure 35.</b> Slides: Glass, PEN-membrane (25mm x 76mm). ....	74
<b>Figure 36.</b> Hematoxylin-eosin staining protocol. ....	75
<b>Figure 37.</b> Image showing the Leica Laser Micro-dissection system. ....	76
<b>Figure 38.</b> Laser Micro-capture technique. ....	76
<b>Figure 39.</b> Image of the RNeasy Micro Kit (74004 Qiagen). ....	77
<b>Figure 40.</b> Chromium System is 10x GemCode™ Technology. ....	78
<b>Figure 41.</b> A) Schematic representation and images of the dissection LGEs at E14.5 .....	79
<b>Figure 42.</b> Schematic representatation of the methodology followed by the bulk RNA-seq analysis. .....	83
<b>Figure 43.</b> Principal Component Analysis (PCA) of the region comparison between genotypes. ....	84
<b>Figure 44.</b> Heatmap (A) and DEGs biotypes (B) of the MZ differential analysis. ....	85
<b>Figure 45.</b> Diagram of the mHtt-cell protein interactions described. ....	87
<b>Figure 46.</b> Enrichment analysis showing the distribution of the HD up-regulated DEG's related functions. ....	89
<b>Figure 47.</b> Enrichment analysis showing the distribution of the HD down-regulated DEG's related functions. ....	90
<b>Figure 48.</b> Pie-charts showing the blast2go (A) and the GO enrichment (B) analysis of the DE TECs. .....	92
<b>Figure 49.</b> Differentiation program in wt vs HD mice. ....	96
<b>Figure 50.</b> Lineage-specific alterations within the HD MZ. ....	98
<b>Figure 51.</b> Cell cycle progression is altered during striatal development in HD. ....	100
<b>Figure 52.</b> HD embryos undergo a premature cell cycle exit in the early developmental stages, followed by a reduction of the cell birth at later stages. ....	101
<b>Figure 53.</b> NPCs pool is compromised during HD development. ....	102
<b>Figure 54.</b> Lineage-specific iMSNs neurogenesis is increased at both neurogenic waves during HD striatal development. ....	103
<b>Figure 55.</b> iMSN population is increased at E18.5 HD striatum. ....	104
<b>Figure 56.</b> iMSN population is reduced in the P21 HD striatum. ....	105

<b>Figure 57.</b> Specific iMSNs population cell death occurs during the normal post-natal cell death period in HD mice. ....	106
<b>Figure 58.</b> Interneuron neurogenesis is increased at E14.5 HD striatal development. ....	107
<b>Figure 59.</b> Single cell dataset computational integration. ....	108
<b>Figure 60.</b> UMAPs showing the distribution of putative glutamatergic and GABAergic markers. ....	109
<b>Figure 61.</b> UMAPs showing the distribution of putative striatal NPC's markers.....	109
<b>Figure 62.</b> UMAPs showing the distribution of putative striatal dMSNs/iMSNs/IN's markers..	110
<b>Figure 63.</b> Distribution of wt and HD cells among the different clusters.....	111
<b>Figure 64.</b> Identity of the cells from the clusters of interest.....	112
<b>Figure 65.</b> Fluorescent <i>In Situ</i> Hybridization (FISH) of HELT.....	113
<b>Figure 66.</b> Relative expression of HELT RNA in wt/ctr and HD samples. ....	113
<b>Figure 67.</b> Scheme summarizing the main HD pathophysiological hallmarks.....	117
<b>Figure 68.</b> Contribution of coding vs noncoding RNAs in the human genome.....	118
<b>Figure 69.</b> Generation of speckles (A) and paraspeckles (B) from lncRNA molecules. ....	119
<b>Figure 70.</b> Graphical summary of the endocytic and vesicle transport alterations found in the HD embryos by bulk RNA-seq. ....	120
<b>Figure 71.</b> Diagram of the mHtt-cell protein interactions described.....	121
<b>Figure 72.</b> Graphical summary of the calcium-related DEGs dysregulated in HD embryos.....	122
<b>Figure 73.</b> Summary of the main regionalization-related genes affected in HD embryos.....	123
<b>Figure 74.</b> Hypothesis for the NPCs alterations observed in HD embryos.....	126
<b>Figure 75.</b> Types of NSC divisions in the ventricular zone are determined by spindle orientation and the inheritance of cell fate determinants.....	125
<b>Figure 76.</b> Huntington's disease (HD) transiently alters cortical circuitfunction by decreasing synaptic activity, increasing excitability, and reducing the complexity of dendritic arborization. ....	127
<b>Figure 77.</b> Temporal biases in interneuron origin. ....	129
<b>Figure 78.</b> HELT/Mgn KO mice. ....	130
<b>Figure 79.</b> Diagram illustrating the genetic network controlling the generation of midbrain-derived GABAergic neurons.....	131
<b>Figure 80.</b> HELT mRNA expression along brain development. ....	132
<b>Figure 81.</b> Schematic summary of the iMSN lineage developmental abnormalities. ....	134



# LIST OF TABLES

---



## *List of Tables*

<b>Table 1.</b> Sumarry of the Antibodies used during this tesis. ....	68
<b>Table 2.</b> List of the most significant terms obtained from the KEGG pathway and the Mammalian Phenotype Ontology analysis of the protein-coding DEGs (including up- and down-regulated DEGs). ....	86
<b>Table 3.</b> Gene Ontology (GO) Enrichment of the DEGs ontained. ....	88
<b>Table 4.</b> Gene Ontology (GO) Enrichment of the up-regulated DEGs in the MZ of HD embryos. ....	91
<b>Table 5.</b> Gene Ontology (GO) Enrichment of the down-regulated DEGs in the MZ of HD embryos. ....	91
<b>Table 6.</b> List of the non-coding DEGs down-regulated in HD MZ. ....	93
<b>Table 7.</b> List of the up-regulated non-coding DEGs in the HD MZ. ....	94
<b>Table 8.</b> List of long non-coding RNAs up-regulated in HD embryos. ....	95
<b>Table 9.</b> KEGG Pathway Analysis of the up- and down-regulated. ....	97





# INTRODUCTION

---



# Introduction

## 1. The Basal Ganglia and the Striatal Nuclei

### 1.1. Basal Ganglia

The basal ganglia (BG) consist of a group of interconnected subcortical nuclei that play an important role in motor, cognitive and limbic functions<sup>1</sup>. Anatomically, the basal ganglia is formed by:

- The **striatum** (STR), originated from the telencephalon, which includes the caudate and putamen in human and primates.
- The **substantia nigra** (SN), originated from the mesencephalon. The substantia nigra is divided into two major subnuclei; the substantia nigra **pars compacta** (SNc) consisting of dopaminergic neurons, whereas the substantia nigra **pars reticulata** (SNr) is made up of GABAergic projection neurons.
- The **globus pallidus**, which consists of two parts, the **internal** and **external** segments of the globus pallidus, commonly referred to as GPi and GPe, respectively.
- The **subthalamic nucleus** (STN), a small almond-shaped nucleus located laterally just below the thalamus at the junction between the diencephalon and midbrain.

Together, these nuclei form multiple loops linking the BG to the cortex, thalamus and brainstem (Figure 1). Although BG function has been classically related to the motor function regulation, the role of the BG has expanded from being principally motor-based<sup>2,3</sup> to the cognitive and emotional domains. They have been involved in reinforcement learning<sup>4,5</sup>, goal-directed behaviours<sup>6</sup>, response selection under competition<sup>7,8</sup>, decision making and in working memory<sup>9,10</sup>.

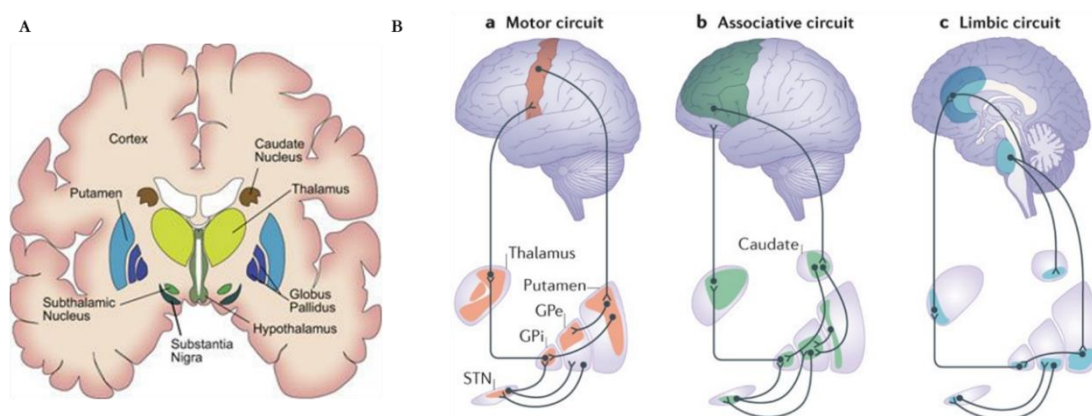


**Figure 1. Basal ganglia structure (A) and function (B).** The basal ganglia not only are connected to motor cortical areas (motor cortex, supplementary motor cortex, premotor cortex, cingulate motor area and frontal eye fields), as classically defined, but also have connections with a wide range of non-motor areas of the cortex<sup>11,12</sup>. Therefore, they influence motor (a), cognitive (or associative; b) and emotional (c) processing. *Image modified from Jahanshahi, et al. (2015).*

## 1.2. The Striatal Nuclei

The striatum is one of the most prominent subcortical regions in the brain of mammals, taking up an approximate volume of 10 cm<sup>3</sup> in the human brain<sup>13</sup>. It is a heterogeneous structure that receives afferents from several cortical and subcortical structures and projects to various basal ganglia nuclei.

### 1.2.1. Striatal Neurons:

#### 1.2.1.1. Striatal Medium Spiny Neurons

Aproximately 90-95% of striatal neurons are spiny projection neurons, also known as medium spiny neurons (MSNs). They have a medium sized soma (10-15 µm of diameter) and they are plenty of dendritic spines. They show a long axon to establish connections out of the striatal nuclei, and use the inhibitory neurotransmitter  $\gamma$ -aminobutyric acid (GABA). MSNs are segregated into two diferent subpopulations based on their projection targets and of the main receptors and neuropeptides they express<sup>14</sup>:

- **Striatonigral MSNs** or direct pathway MSNs (dMSNs), expressing high levels of the Dopamine receptor D1 (**DRD1**) and muscarinic M4 receptors, as well as dynorphin (DYN) and substance P (**SP**).
- **Striatopallidal MSNs** or indirect pathway MSNs (iMSNs), expressing high levels of the Dopamine receptor D2 (**DRD2**) and the adenosine A2A receptor (**A2A**), as well as their immunoreactivity for enkephalin (**Enk**).

#### 1.2.1.2. Interneurons

The remaining 5-10% of neurons in the striatum are non-projecting interneurons (INs), which can be divided into two main types: **medium-sized GABAergic** cells and **large cholinergic** (ChAT) cells<sup>15</sup> (Figure 2). Medium-sized GABAergic interneurons can be further classified into three subtypes based on the presence of certain chemicals<sup>16</sup>:

- Parvalbumin-positive (PV)
- Somatostatin-positive (Sst), neuropeptide Y-positive (NPY) and nitric oxide synthase-positive.
- Calretinin (CR)-positive.

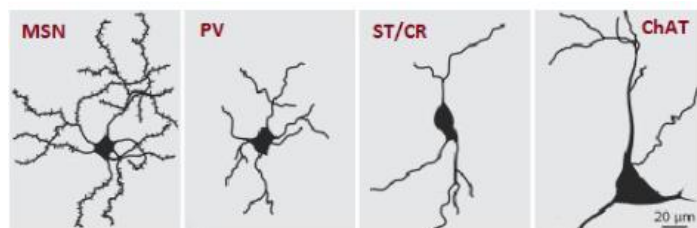


**Figure 2. Morphology of the different interneuron subtypes.**  
*Image modified from Kreitzer (2009).*

An additional population of tyrosine hydroxylase (TH) expressing interneurons has been found in the striatum of several species, including primates, rat, mouse and human<sup>17</sup>. These neurons are up-regulated after denervation of dopaminergic input from the midbrain<sup>18</sup> and their morphology, electrophysiological properties and distribution have been characterized<sup>19</sup>.

### 1.2.2. Striatal cytoarchitecture:

The striatum is a seemingly uniform region of the brain when examined using cytoarchitectural techniques, but when some specific markers are used, two distinct subdivisions can be found: **striosomes** (or patches) and **matrix** compartments. These compartments were first identified in the 1970s using the enzyme acetylcholinesterase (AChE) and further studies have revealed unique immunohistochemical and neuronal connection patterns of each compartment (Figure 3-A).

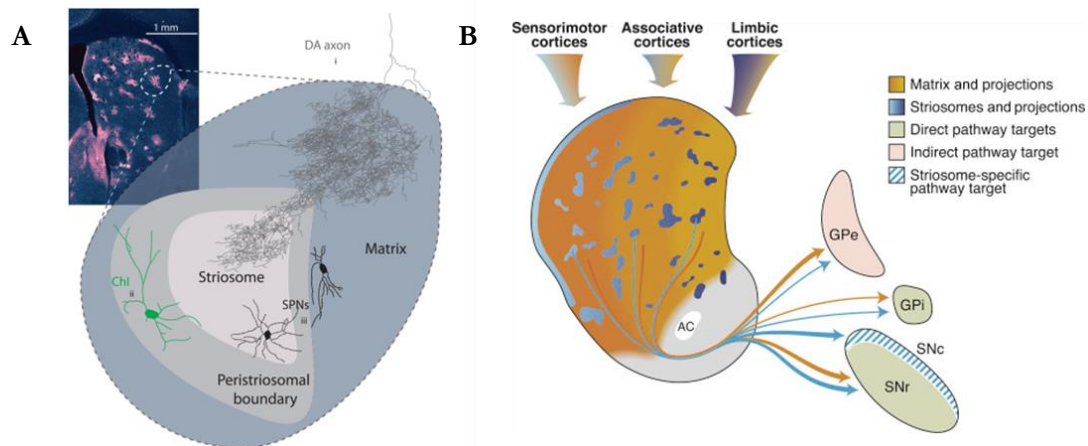


**Figure 3. Striosome and matrix compartmentalization.** (A) Scheme showing the different cell types inhabiting the different striatal departments. (B) Diagram showing the different inputs and outputs regarding this striatal striosome/matrix cytoarchitecture. *Image modified from Crittenden, J. R. (2016) and Graybiel, A. M. (2011).*

#### Striosomes

- Striosomes occupy only the 10–15% striatal volume.
- Histochemically defined by a high expression level of  $\mu$ -opioid receptor ( $\mu$ OR), substance P (SP), DRD1, met-enkephalin (met-ENK), CR, Nuclear Receptor Subfamily 4 Group A Member 1 (Nr4a1), pro-dynorphin, glutamic acid decarboxylase (GAD-2), and Early Growth Response 1 (EGR-1).
- Functionally, striosomal MSNs preferentially project to the SNc (direct pathway).

#### Matrix

- Histochemically defined by a high expression level of calbindin (CB), Sst, ENK, DRD2, and cholinergic markers including AChE and ChAT.
- Functionally, matrix MSNs preferentially project to the GPe, GPi (indirect).

#### Peristriosomal boundary

- Occupied by ChAT, Sst<sup>+</sup> and CR<sup>+</sup> INs<sup>20</sup>.

## Matrisomes

- Constitute clusters of corticostriatal afferent terminals and output cells of the matrix, grouped according to their targets<sup>21–23</sup>.
- Histochemically defined by a high expression level of the Ephrin receptor (Eph) A7<sup>24,25</sup>.
- Show a less organized mosaic pattern that partially overlaps with  $\mu$ OR-expressing areas<sup>24</sup>.

There have been reported upward of 60 genes differentially expressed in the striosomes and matrix, indicating that both compartments show different gene expression profiles<sup>26</sup>. This striosome/matrix organization is particularly important during development, and the use of axonal tracers allowed the understanding of how this compartmentalization segregates MSNs on the basis of their afferent and efferent projections<sup>27</sup> (Figure 3-B). Moreover, striosomes and matrix compartments have been differently involved in pathological processes including Parkinson's Disease (PD), HD, attention deficit and hyperactivity disorder (ADHD), and others<sup>26,28</sup>.

### 1.2.3. Striatal Connections:

The striatum acts as a central computational station, by integrating relevant inputs from throughout the central nervous system (CNS) and selecting the appropriate response to a set of environmental cues.

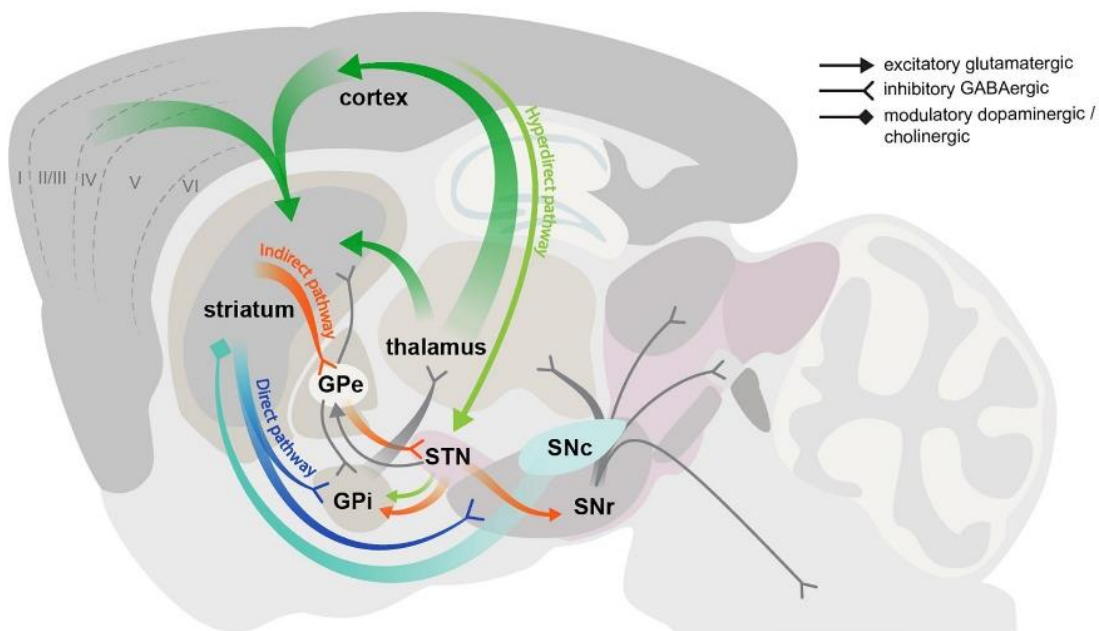


**Figure 4. Schematic representation of cortical and striatal circuits involved in HD.** GPe, external segment of the globus pallidus; GPi, internal segment of the globus pallidus; SNc, substantia nigra pars compacta; SNr, substantia nigra pars reticulata; STN, subthalamic nucleus. *Image adapted from Blumenstock and Dudanova (2020).*

#### 1.2.3.1. *Striatal Afferences:*

The striatum receives input from various regions of the brain, including the neocortex, limbic regions, and the thalamus. Different regions of the **cortex** project to different extents to the striosomes and matrix compartments. For example, limbic and frontal cortical regions such as the orbitofrontal, anterior cingulate, and insular cortices tend to connect with the striosomes, while somatosensory, motor, and association cortices mainly connect with the matrix<sup>29</sup>. The **thalamus** also plays a significant role in connecting to the striatum, with different nuclei connecting to different compartments. Additionally, the striatum receives dopaminergic inputs from the ventral tegmental area (VTA), the **SNc** and the retrorubral area (RRA), which also differentially project to the matrix and striosomes<sup>30</sup>: dopaminergic cells of the VTA and RRA were found to project only to the matrix, as well as dopaminergic projections from the dorsal SNc; whereas ventral SNc neurons and dopaminergic neurons located in the SNr project into the striosomes<sup>27</sup> (Figure 4).

#### 1.2.3.2. *Striatal Efferences:*

Once the striatum processes the input information, it sends its response through two different pathways within the BG (Figure 4), both GABAergic and therefore, inhibitory:

- The direct pathway (or striatonigral pathway) project directly to the iGP or to the SNr, which directly arrive to the thalamus<sup>31</sup>.
- The indirect pathway (or striatopallidal pathway) project to the eGP. These axons that arrive to the eGP are sent to inhibit glutamatergic neurons of the STN, which simultaneously project to the iGP and the SNr<sup>31</sup>.

Finally, the integrated information is sent to the thalamus which returns this information to the cortex, through the thalamus, closing the circuit known as cortico-striato-thalamo-cortical<sup>1,11,27,32</sup>. Activity of the direct pathway will disinhibit the thalamus, thus, increasing activity in the cortex and promoting movement. Activity of the indirect pathway will inhibit the thalamus, thus, decreasing activity in the cortex, leading to the inhibition of movement. The balance between both direct and indirect signals is essential for the correct function of the basal ganglia.



## 2. Brain Development

Multicellular organisms are formed by a relatively slow process of progressive changes that is called **development**. The study of animal development has traditionally been called **embryology**, referring to the process that occurs between fertilization and the birth of the developing organism. But development does not end at birth even in adulthood. Most organisms never stop developing. Every day we replace about a gram of skin cells, and inside our bone marrow there is the development of millions of new red blood cells every minute of our lives. Thus, the discipline of developmental biology encompasses not only embryonic studies but also other developmental processes that take place in adult organisms. Thus, developmental biology creates a framework where molecular biology, physiology, cell biology, anatomy, cancer research, immunology and even evolutionary processes and ecology studies are integrated. Likewise, the study of development has become an essential pillar for the understanding of other areas of biology.

Here, we will discuss how the brain, specifically the striatal nuclei, is formed. We will start from the very beginning, with a slight introduction of the embryogenic process, followed by a more detailed explanation of the striatal developmental process.

### 2.1. Embryogenesis

#### 2.1.1. Fertilization and zygote formation:

Fertilization refers to the fusion of male and female gametes, leaving half of the genetic material of the cells of an organism (46 chromosomes) due to the chromosomal reduction they have suffered with meiosis. The result of this fusion is the restoration of the genetic endowment of the human being, a new cell provided with a nucleus and 46 chromosomes, 23 of maternal origin and 23 of paternal origin, called **zygote**<sup>33</sup>. The first mitotic division of the zygote results in an embryo of 2 cells, which will divide into 4 symmetrical cells. The zygote increases in size, multiplies its cells, and undergoes strong cellular changes. During the initial stages of development, the zygote can acquire other names depending on its appearance such as morula (due to its blackberry shape) and blastula<sup>33</sup>.

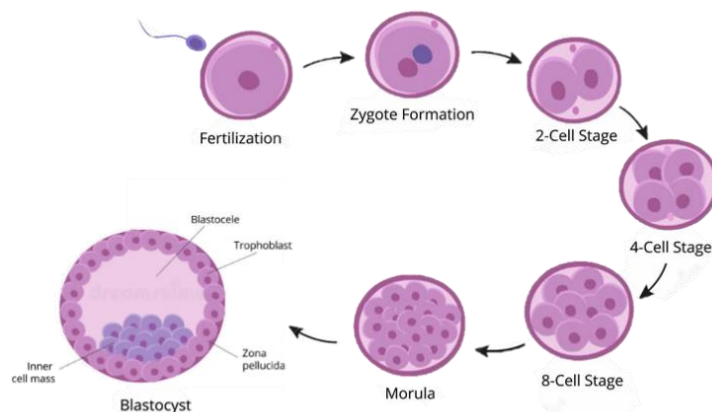


Figure 5. Emrbyogenic process showing the different cell stage from the fertilization to the blastocyst. Image obtained from the webside Freepik.

### 2.1.2. Blastocyst formation:

Cells in the blastula undergo rapid cell divisions to form the **blastocyst**. When the embryo becomes a blastocyst, it acquires a certain shape and cell differentiation begins<sup>34</sup>. There are two types of cells in the blastocyst:

- **Trophoblast** or trophoctoderm: its cells are responsible for forming the placenta.
- **Inner cell mass (ICM)**: its cells give rise to the foetus and all parts of the future baby's body.

The internal cavity of the blastocyst is called the blastocoele and is filled with fluid. The blastocyst emerges from the membrane that protects it (zona pellucida) and begins to adhere to the endometrium<sup>33,34</sup>.

### 2.1.3. Gastrulation:

Gastrulation is the process in which the inner cell mass of the blastocyst is converted into the trilaminar embryonic disc, which is comprised of the three germ layers<sup>35</sup>: ectoderm, mesoderm and endoderm (Figure 6). The gastrulation process starts with the formation of a transient structure, known as primitive streak, along the midline of the epiblast. Its formation marks the major body axes of the embryo<sup>35</sup>. Once the primitive streak is formed, major movements of cells from the external surface to the interior of the embryo will create the three-layered body plan and set the stage for development of the first organs<sup>36,37</sup>. The resulting embryo is known as a gastrula.

- The **ectoderm**, that gives rise to epidermis, the nervous system, and to the neural crest in vertebrates.
- The **mesoderm**, that gives rise to many cell types such as muscle, bone and connective tissue.
- The **endoderm**, that gives rise to epithelium of the digestive system and respiratory system, and organs associated with the digestive system, such as the liver and pancreas.

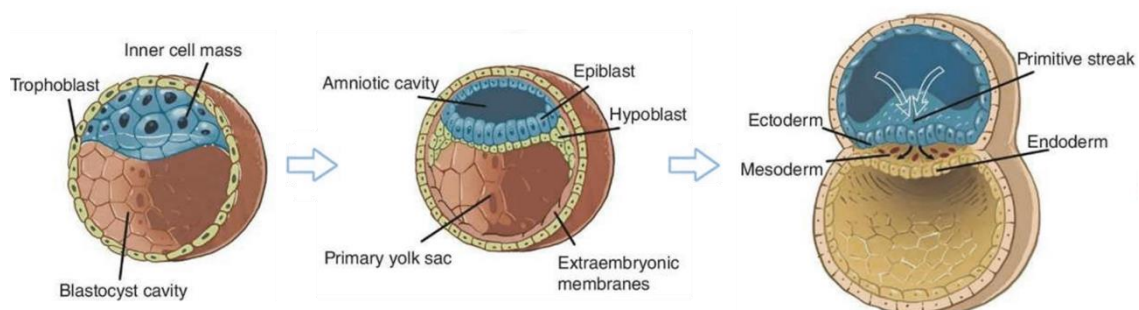


**Figure 6. Gastrulation process showing the three germ layers arising from the blastocyst.** *Image edited from the website Pocket Dentistry.*

## 2.2. Nervous system development

A fundamental feature of the nervous system development is the precise temporal sequence of cell type generation. The first neural cells, **neuroepithelial** (NE) cells, arise from the pluripotent stem cells of the early blastocyst that differentiate from the ectoderm towards the neuroectoderm through a process named **neural induction**.

### 2.2.1. Neurulation:

Neurulation marks the beginning of the formation of the central nervous system. The first event of neurulation is the formation of a thickened area of cells, called the **neural plate**. This ectoderm thickening is induced by a flexible rod-shaped body known as the **notochord**<sup>38</sup>. The growth of the neural plate begins from the cranial (head of the embryo) to the caudal (tail of the embryo) (Figure 7). These regions determine the future brain position at the cranial and the spinal cord towards the caudal<sup>39</sup>.

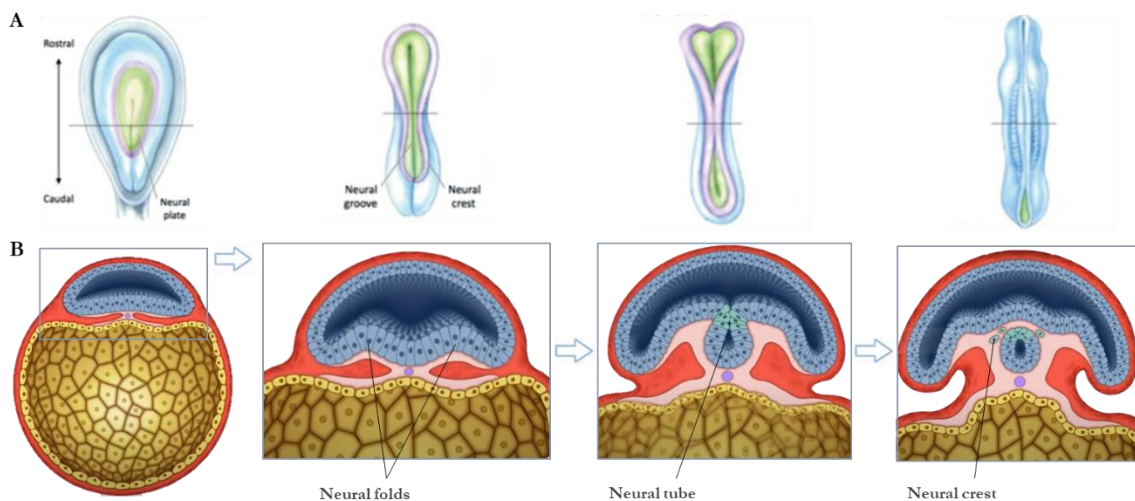


**Figure 7. Neurulation and neural tube formation.** Diagram showing a dorsal (A) and a coronal (B) view of the neural tube formation and closure. *Image edited from the website Quizlet.*

The lateral edges of the neural plate become elevated and move together to form the neural folds. Then, the neural folds fuse together, and the neural plate transforms to the **neural tube**. During the closure of the neural tube, cells from the crest of the neural fold detach, forming a new cell population called the **neural crest**. Once the neural tube is completely fused, the process of neurulation is complete. The anterior end of the neural tube will develop into the brain, the posterior portion will become the spinal cord, and the neural crest will give rise to peripheral structures.

### 2.2.2. Neural tube regionalization

The initial step in the neural tube regionalization process involves the establishment of an anterior-posterior (AP) axis and the division of brain vesicles. AP neural patterning occurs shortly after the beginning of neural development, where neural cells with similar growth and specialization potential are prompted to express specific homeodomain transcription factors along the AP axis<sup>40</sup>. As a result, the main section of the neural tube in vertebrates forms the spinal cord, while the more forward region is split into three primary vesicles during the initial vesicle stage: the forebrain (prosencephalon), midbrain (mesencephalon), and hindbrain (rhombencephalon)<sup>40</sup>.

In the subsequent vesicle stage, the forebrain undergoes further division into two areas: the front part called the anterior **telencephalon** and the back part called the posterior diencephalon. The midbrain is positioned behind the diencephalon, and the hindbrain gives rise to the metencephalon and myelencephalon (Figure 8). These five vesicles, along with the spinal cord, together constitute the six regions of the fully developed CNS.

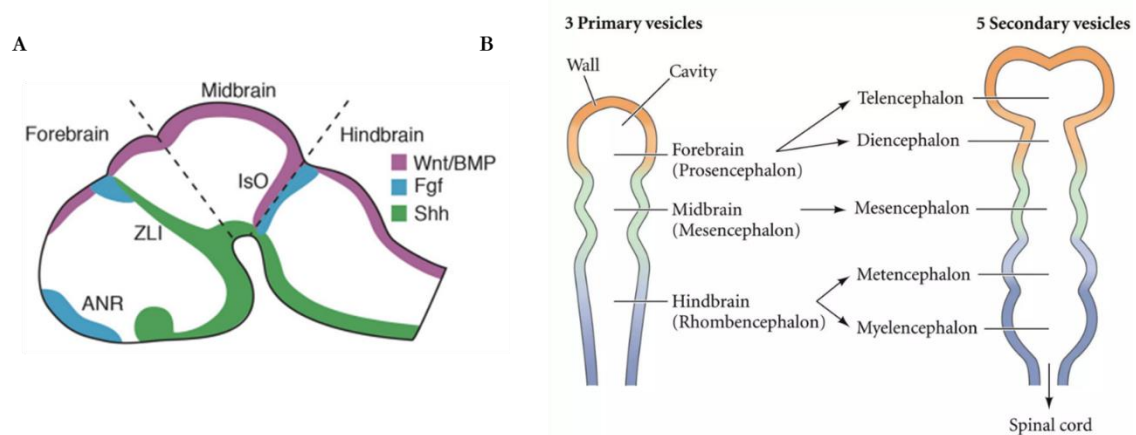


**Figure 8. Neural tube regionalization.** (A) Diagram showing the principal regions of morphogen expression. Rostral expression of Fgf defines the anterior neural ridge (ANR). The zona limitans intrathalamica (ZLI) is defined by a narrow band of Shh expression, with Fgf and BMP/Wnt coexpression dorsally at the border between the presumptive telencephalon and diencephalon. Caudally, the isthmus organizer (IsO) marks the boundary between the midbrain and hindbrain territories (B) Diagram showing the 3 primary and its 5 secondary vesicles generated during the neural tube regionalization. *Image edited from Suárez et al. 2014 and from the book Developmental Biology (6th edition, S. Gilbert).*

Signals triggered by Sonic Hedgehog (**Shh**) are critical for development of the ventral portion of the spinal cord, brain stem, diencephalon and portions of the ventral telencephalon. Just below the neural tube there is the notochord, however, it ends at the telencephalic-diencephalic boundary. Signals mediated by Bone Morphogenic Proteins (**BMPs**) and **Wnts** are critical for development of the dorsal portions of the neural tube<sup>41</sup>, including the dorsal telencephalon, cerebellum, and dorsal spinal cord, and for specification of the neural crest.

### 3. The Striatal Development

The striatal development starts with the induction and regionalization of the Telencephalon, when the striatal primordia is induced, around the embryonic day (E) 10.5 in mice (Figure 9).

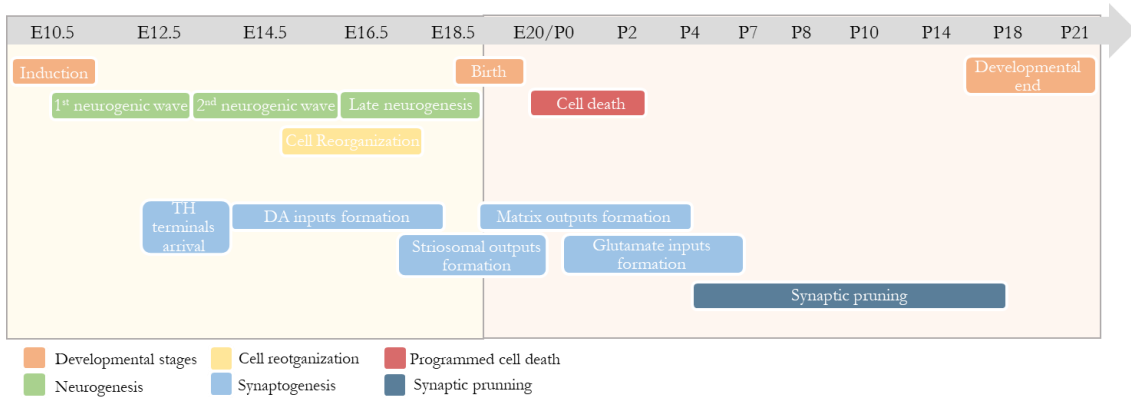


**Figure 9. Striatal developmental milestone.** Summary of the major developmental events occurring in the LGE development from its induction (~E10.5) to the developmental end (P21).

#### 3.1. Telencephalon regionalization

A combination of morphogenic and proliferative movements between E9 and E11 in mice, establishes further discrete proliferative regions within the telencephalon, which is the most rostral part of the neural tube, dividing it into: the dorsal telencephalon (**pallium**) which gives rise to the neocortex and its glutamatergic neurons, and the ventral telencephalon (**subpallium**) which forms the striatum and is the origin of cells that populate the olfactory bulb, globus pallidus and some cells that also populate the cortex.

##### 3.1.1. Subpallium:

The ventral telencephalon is further divided into three prominent bulges, collectively referred to as the whole ganglionic eminence (WGE). These eminences are formed due to the rapid migration of postmitotic neurons in the ventral telencephalon and give rise to the different parts of the striatum<sup>42,43</sup> (Figure 10):

- Lateral Ganglionic Eminence (**LGE**), which gives rise to the striatal **MSNs** and olfactory bulb IN.
- Medial Ganglionic Eminence (**MGE**), which produces neurons in the globus pallidus and basal forebrain, as well as cholinergic and GABAergic **INs** in the striatum, cortex, and hippocampus.
- Caudal Ganglionic Eminence (**CGE**), which generates a variety of projection neurons and INs found in different regions such as the cerebral cortex's layer V, hippocampus, and amygdala, most of which are GABAergic and CR positive INs<sup>42,43</sup>.



Within the surrounding neural epithelium of the developing telencephalon, there are two proliferative zones, the ventricular zone (VZ) and the subventricular zone (SVZ) from which both projection neurons and GABAergic INs are born before migrating to the regions they populate in the adult brain.

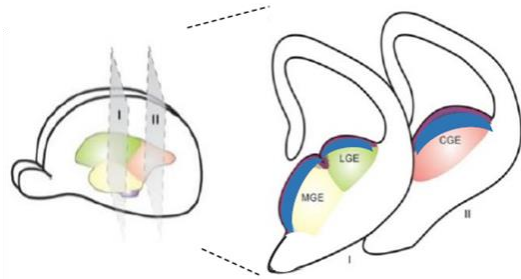


**Figure 10. Representation of coronal hemisections of the mouse telencephalon during embryonic development.** The different progenitor's domains of the subpallium formed by the LGE and MGE in the most rostral section and CGE in the most caudal section. This representation also shows the ventricular zone (VZ) in maroon and subventricular (SVZ) in blue of the eminences. *Image modified from Sultan et al. (2013).*

### 3.1.2. Pallial-Subpallial Boundary:

In the embryonic telencephalon, the pallial-subpallial boundary (PSPB) separates the ventral Pax6<sup>+</sup> pallium from the dorsal Gsh2<sup>+</sup> subpallium<sup>44</sup> (Figure 11). Because of that, PSPB is a region comprised of a complex intermix of molecularly distinct progenitor pools and shows combinatorial codes of regionally expressed TFs with intrinsic potential to generate very distinct neuronal cell types<sup>45</sup>. In line, PSPB is inhabited by NPCs from both the ventral-most aspect of the pallium (vPall) and from the dLGE. NPCs in the PSPB transiently express that defines this region as a molecularly distinct from the rest of the telencephalon, including: Er81, Tgfr $\alpha$ , Sfrp2, Dbx1, SP8 and mTsh1<sup>45</sup>. All of these factors are regulated by the major regulators of the dorso-ventral patterning, Pax6 and Gsh2<sup>45,46</sup>.

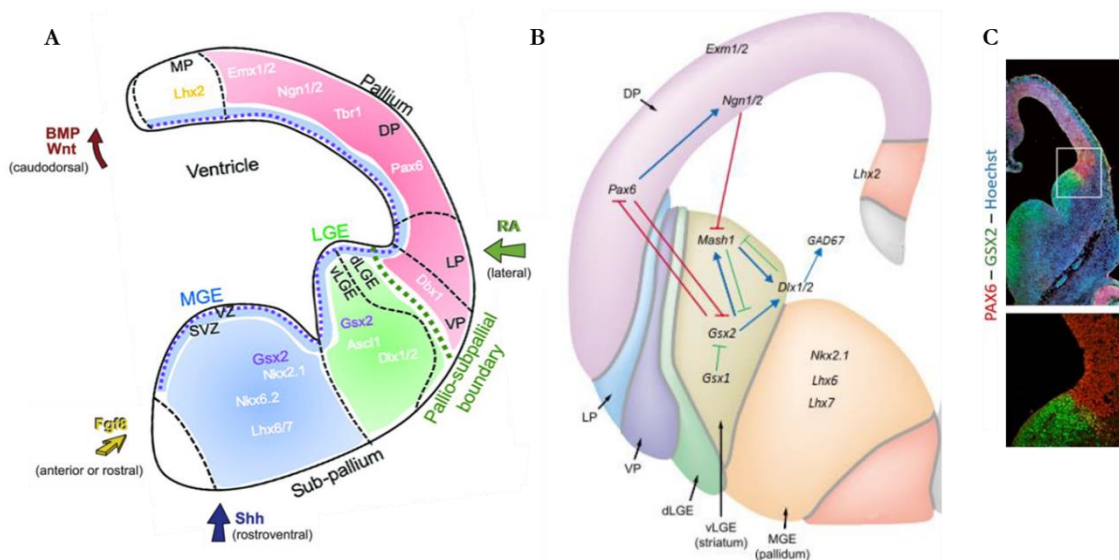


**Figure 11. Regionalization of the Telencephalon.** **A)** Schematic representation of a coronal section in the E12.5 mouse brain showing the distinct territories within the telencephalon. Dorsally there is the pallium, divided in medial pallium (MP), dorsal pallium (DP), lateral pallium (LP) and ventral pallium (VP). In the subpallium can be identified the eminences: dorsal LGE (dLGE), ventral LGE (vLGE) and MGE. **B)** Schematic representation of a mouse coronal section at E12.5 showing signalling pathways (BMPs, RA, Shh and Fgf8) and TFs controlling telencephalon regionalization. **C)** Coronal section through E12.5 brain processed by IF for Pax6 and Gsh2. Bottom, high-magnification views of the PSB. *Image edited from Schuurmans and Guillemot (2002) and Modo, M. (2019).*

### 3.1.3. Factors Involved in the dorso-ventral Telencephalic regionalization

The regionalization of the telencephalon is accompanied by the expression of transcription factors that interact with each other while maintaining these regional identities and defining different populations of progenitors<sup>47</sup>.

#### Factors involved in the dorsal determination:

Signaling of BMPs and Wnts is not only involved in early stages of development during neural tube formation but also in dorsal determination of the telencephalon. Thus, different members of the family of BMPs (BMP-2,4,5,6,7) and Wnts (Wnt-2b, 3a, 5a,7b,8b) are expressed in the dorsomedial line of cortical primordium<sup>48,49</sup> (Figure 11).

**BMPs** are secreted by the dorsal non-neural ectoderm and their inhibition is required to induce dorsalization of the telencephalon. This can be explained because BMPs are responsible for maintaining Gli expression. This idea is reinforced by the fact that in the ventral neural tube synthesizes inhibitors of BMPs such as Noggin, Chordin and Follistatin. Additionally, if the part that emits BMPs is removed, the cortical size is reduced as well as the expression of LIM Homeobox 2 (Lhx2), one of the most dorsal cortical markers<sup>50</sup>.

**Wnts** function as caudalizing agents in the initial antero-posterior orientation of the neural tube, however, later Wnts are crucial for the generation of the dorsal telencephalon<sup>51</sup>. Specific concentrations of Wnts are needed to induce regionalization and expression of Pax6, a dorsal telencephalic marker<sup>52</sup>. Wnt signaling is active in the pallium at E11.5 and E16.5 but not in the subpallium<sup>53</sup>. And, in the absence of signaling of the canonical Wnt pathway signalling, there is ectopic expression of ventral markers such as Gsh2, Dlx2, and Ascl1 in the dorsal telencephalon, along with the repression of dorsal markers such as Emx1, 2, and 3<sup>53</sup>.

Different concentrations of morphogenetic molecules cause cells to express specific transcription factors. It is a complex process that requires very fine regulation<sup>52,54–59</sup>. These transcription factors contribute to the maintenance of regional determination of the cells, since they can inhibit the expression of genes corresponding to other regions. Thus, pro-neural genes such as Neurogenin-1 (**Ngn-1**) and Neurogenin-2 (**Ngn-2**) have been described as promoting dorsalization of the telencephalon by repression of Mash-1, a ventral proneural gene<sup>60,61</sup>, or Pax6 which does so by repressing the expression of another ventral transcription factor, the Gsh2<sup>62,63</sup> (Figure 11). Other factors such as Emx-1, Emx-2 and Gli-3 are key regulators of dorsal determination during telencephalic development<sup>64–66</sup>, as well as Tlx, Lhx2, Foxg1 and COUP-TF1 (also known as Nr2f1) as shown by studies conducted with mutant mice that have null alleles of these genes<sup>50,61,67–70</sup>.

### Factors involved in ventral telencephalic determination:

Ventral regionalization can be explained by some basic molecular mechanisms. First, the specification of ventral progenitor domains in the CNS requires Shh signaling as well as inhibition of signaling by BMPs<sup>71–73</sup>. Secondly, Retinoic Acid (**RA**) is a key signal in the specification of intermediate progenitor domains. And finally, Fibroblast growth factor (**FGF**) signaling is also crucial, especially in the specification of the most ventral progenitor domains<sup>74</sup>.

In the forebrain, the influence of **Shh** signaling depends on its concentration, but also on the stage of the cell. It has been described that Shh signaling can induce the expression of ventral genes such as Nkx2.1. Shh and Nkx2.1 are expressed in MGE, but not in the LGE<sup>75,76</sup>. However, there are evidences that Shh is involved in the induction of LGE<sup>77</sup>. Thus, experiments have determined that during a narrow time window (E10.5-E11.5) in the development of the rat, the Shh protein can induce the expression of LGE-related genes such as *Dlx*, *GAD-67*, *Islet-1/2* or *Ikaros*. Therefore, the progressive development of ventral telencephalic structures is Shh-responsive dependent. Thus, it has been suggested that in early development, Shh signaling results in induction of MGE, while later Shh signaling induces LGE<sup>77</sup>.

**RA** also plays an important role in neuronal specification and regionalization of forebrain development<sup>41,56,78–81</sup>. At early stages of telencephalic development, inhibition of RA results in general disturbance of forebrain growth and development<sup>80</sup>. Interestingly, RA is also involved in the specification and differentiation of the intermediate region of LGE in the telencephalon<sup>56</sup>.

Finally, another signaling pathway that seems to be involved in the determination of ventral telencephalic structures is **FGF**. Mutant embryos that do not express FGF-8 show a reduction in the expression of the ventral marker Nkx2.1 as well as alterations in the midline of the ventral telencephalon<sup>82,83</sup>. One of the targets of FGF signaling is the transcription brain factor 1 (BF-1)<sup>84</sup>. This transcription factor is involved in regional specification as well as regulation of cell proliferation<sup>85–87</sup>.



### 3.2. Neural Progenitor Cells (NPCs) of the ventral Telencephalon

The ventral telencephalon is composed of several types of progenitor cells that are responsible for generating new neurons<sup>88–90</sup>. These progenitor cells can be divided into different subtypes based on their location, morphology and molecular characteristics. Lineage tracing studies have shown that Radial Glial (RGs) cells in the ventral telencephalon give rise to a variety of progenitor cells, including SNPs, SAPs, BPs and postmitotic neurons (Figure 12). Additionally, the expression of different transcription factors such as ETV1/Er81, Pax6, Gsh2, Ascl1, Dlx1/2 and Notch signaling, have been shown to regulate the fate of these progenitor cells and control the ordered production of different neuronal populations in the ventral telencephalon<sup>71–73,91</sup>.

#### 3.2.1. Neural Progenitor Cells Subtypes

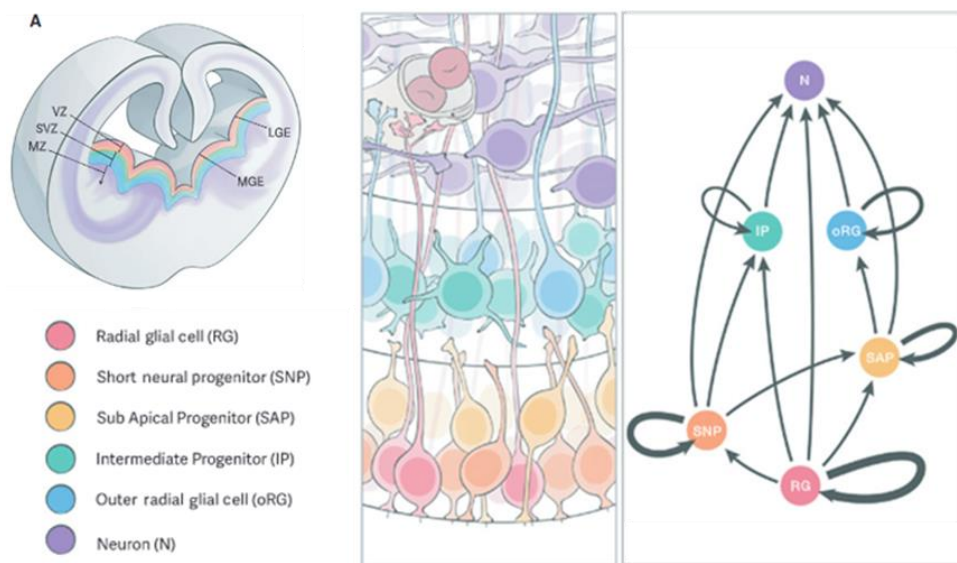


**Figure 12. Picture showing the different NPCs described in the striatal GZ.**

*Image edited from Turrero García, M., and Harvell, C. C. (2017).*

#### Radial Glia cells

The first NPCs found in the ventral telencephalon are the RGs, which come from the initial subpallial population of NE cells that appear at E10.5 in mice<sup>92</sup>.

- They divide themselves at the ventricular wall. RGs perform an evolutionary conserved movement known as interkinetic nuclear migration (INM): they undergo into the S-phase of the cell cycle at the basal part of the VZ and then mitosis occurs at the ventricular surface, moving between these two locations throughout G1 and G2 phases<sup>93,94</sup>.
- These RGs have a bipolar morphology and exhibit a basal process that anchors them to the ventricular surface and an apical process that extends towards the pial surface<sup>93,94</sup>.
- RGs from the ventral telencephalon share the main biological characteristics and expression marker patterns with those RGs from other developing regions of the CNS<sup>93,94</sup>.

- RGs play a critical role in the generation of neurons and glia, and they also serve as a scaffold for the migration of newborn neurons<sup>95–98</sup>.
- The RG's daughter progenitor cells consist of additional RGs plus a diverse population of other progenitors, such as further progenitors that inhabit both VZ and SVZ, and young neurons that migrate to the MZ<sup>93,94</sup>.

#### Short Neural Precursors (SNPs)

Another progenitor cell subtype found in the ventral telencephalon is the SNP. These cells have a rounded morphology and tend to lack processes during division<sup>93</sup>. They are typically found in the VZ and are thought to be involved in the generation of **intermediate progenitor cells** (IPs)<sup>94,99</sup>.

#### Intermediate Progenitors (IPs)

Ventral IPs generally undergo a single round of division, giving rise to two cells with neuronal morphology, suggesting that they could be the last step within the progenitor's lineage<sup>100</sup>. Some IPs self-renewal events has been also reported. IPs can be divided into **apical IPs** (aIPs), located near the ventricle, and **basal IPs** (bIPs), wich undergo several rounds of transit-amplifying divisions before they reach the terminal neurogenic division<sup>94,101,102</sup>.

#### Subapical Progenitors (SAPs)

Additionally, the ventral telencephalon also contains **other progenitor** (OPs) cells that divide at subapical positions away from the ventricular surface, these have been named SAPs<sup>94</sup>. They are found in the ventricular zone and are thought to be involved in the generation of IPs.

#### Basal Progenitors (BPs)

The SVZ of the ventral telencephalon contains progenitor types that lack a process during division and resemble BPs, as well as progenitors that retain one or more processes and resemble RGCs.

#### Outer Radial Glia (oRG)

The latter progenitors divide in the basal aspects of the ventral telencephalon and are called oRG or **basal RGs** (bRGs)<sup>94,103</sup>. They have self-renewal capacity and they usually come from the asimetric division of the bipolar SAPs<sup>94,103</sup>.

### 3.3. Cell cycle vs Neurogenesis

The decision between division and differentiation has a significant impact on the number and characteristics of the produced offspring cells, ultimately shaping the overall structure and function of the central nervous system. Consequently, the process of cell division needs to be tightly regulated.

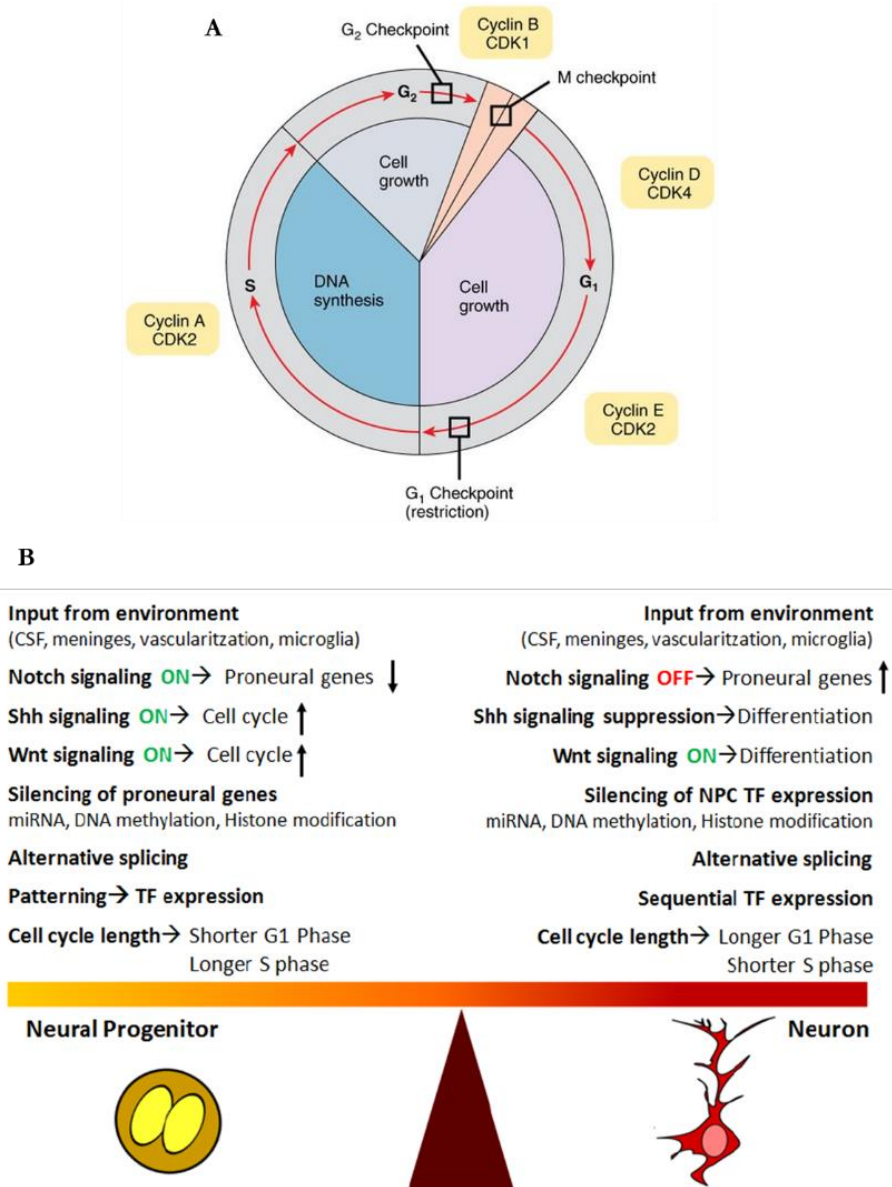


Figure 13. (A) Cell cycle phases and checkpoints. (B) Summary of different signals that regulate transition from NPCs into neuronal differentiation. Image edited from OpenStax: CNX and Paridaen and Huttner (2014).

The cell cycle consists of four consecutive phases: G<sub>1</sub> (Gap1), S (Synthesis), and G<sub>2</sub> (Gap2), collectively known as interphase, and M phase (Mitosis) (Figure 13).

- During G<sub>1</sub>, the cell increases in size and synthesizes mRNA and proteins in preparation for subsequent division steps. This phase is also when the cell is responsive to external signals that influence the decision to either exit the cell cycle and enter the dormant G<sub>0</sub> phase or proceed past the restriction point and commit to further cell divisions.

- In the S phase, the cell replicates its nuclear DNA.
- The G2 phase follows DNA replication and occurs before mitosis. During this phase, the cell generates the components necessary for the formation of the spindle.
- Finally, in the M phase, nuclear division and cytokinesis (division of the membrane and cytoplasm) occur, resulting in the formation of two independent cells.

The cell cycle process incorporates several checkpoints to regulate and ensure the successful completion of crucial events<sup>104</sup>. Each phase of the cycle involves specific processes that must be completed before advancing to the next phase.

- The G1 checkpoint, located at the end of the G1 phase, just before entering the S phase, is the initial checkpoint. It plays a critical role in determining whether the cell should divide, delay division, or enter the dormant G0 phase instead of continuing the cycle. Neurons, which are fully differentiated cells that no longer divide, enter the G0 phase. The G1 checkpoint evaluates the availability of all necessary conditions, such as nutrients and enzymes, required for DNA synthesis.
- The G2 checkpoint ensures the successful completion of DNA replication during the S phase and confirms the cell's readiness for mitosis.
- During mitosis, the metaphase checkpoint (M checkpoint) serves as a crucial checkpoint, ensuring proper alignment and pairing of all chromosomes on the spindle, thereby indicating the cell's readiness to undergo division<sup>104</sup>.

The duration of the G1 and S phases represents a crucial mechanism for regulating the balance between cell division and differentiation. When differentiation is induced, the G1 phase is doubled in length. This extension of the G1 phase leads to an increase in neurogenic divisions and premature differentiation. Conversely, a shortening of the G1 phase promotes proliferative divisions and the expansion of precursor cells<sup>105</sup>. The length of the S phase reflects the requirement for precise DNA replication and repair during NPC expansion versus differentiation. Expanding NPCs have a S phase that is more than 3 times longer than those NPCs that have already committed to differentiation. This suggests that unrestricted NPCs have a greater need for accurate DNA replication and repair, as any errors would be inherited by a larger number of progeny compared to restricted NPCs<sup>106</sup>.

### 3.4. Striatal Neurogenesis

Neurogenesis is defined as the process of generating new neurons from stem and committed NPCs. It involves a series of steps including cell division, the production of migratory precursors, differentiation, and integration into neural networks<sup>107</sup>. In addition to giving rise to all the neurons of the CNS, these progenitor cells also produce the two types of macroglial cells: astrocytes and oligodendrocytes<sup>108,109</sup>.

During the initial stages of neurogenesis in the ganglionic eminences, most cell divisions occur on the surface of the VZ. As development progresses, some cells begin dividing at deeper locations, marking the emergence of the SVZ (around E11 in the mouse MGE and E12 in the LGE)<sup>110</sup>, which expands in size and number of dividing cells until it eventually becomes the primary site of progenitor proliferation around the middle stages of neurogenesis (E13-E14)<sup>94,110,111</sup>. This expansion of the SVZ is linked with an increase in the diversity of NPCs present in the ganglionic eminences, which may contribute to the production of different types of neurons.

#### 3.4.1. Medium Spiny Neuron Neurogenesis:

NPCs inhabiting the LGE are the main source of the different neurons of the MSNs lineage, following a time-dependent neurogenic program that expands from E11.5 to E18.5 (Figure 14).

##### 1<sup>st</sup> neurogenic wave:

Neurogenic onset in the early LGE (around E10) is marked by the expression of Tis21 (Btg2) in RGs, which self-renew themselves over multiple rounds of division to generate several types of IPs and SNPs. In the early phase of this lineage, RGs may generate neurons directly or throughout aIPs with a dynamic Ascl1 expression pattern. Early RGs sequentially give rise to both apical and basal IPs and generate both striosomal and matrix MSNs. Early aIPs, which show high expression levels of Ascl1, are committed to produce striosomal MSNs with likely no more than one single round of amplification. Thus, neurons generated during the first neurogenic wave will give rise preferentially to **striosomal dMSNs**. These neurons will constitute the 10-15% of the neurons of the adult striatum<sup>112</sup>.

##### 2<sup>nd</sup> neurogenic wave:

During an abrupt transition that occurs around E13.5, RGs shift to generate bIPs, which are fate-restricted to generate matrix MSNs. Then, around E14.5 to E17.5 phase, Ascl1<sup>+</sup> bIPs first give rise to further matrix MSNs and then switch to glial cells production. By contrast, Dlx1<sup>+</sup> bIPs remain dividing and generating matrix MSNs throughout the later phase of LGE neurogenesis. At the final stage, around E18.5, Dlx1<sup>+</sup> bIPs are finally restricted to generate peri-striosomal MSNs. A similar ratio of direct/indirect MSNs are generated from both aIPs and bIPs-mediated neurogenesis, with a bias towards iMSNs at the end of bIPs neurogenesis. Thus, neurons generated during the second

neurogenic wave will give rise preferentially to **matrix iMSNs**. These neurons comprise the 80-85% of the adult MSNs<sup>112</sup>.

#### Late neurogenesis:

In the last phase of embryonic development, during the terminal rounds of neurogenesis at E18.5, remaining *Dlx1*<sup>+</sup> bIPs give rise to the peri-striosomal MSNs<sup>113</sup>. This MSNs will project to both pallidal segments and the SNr, as the typical pattern of a matrix MSN<sup>20,114</sup>. Additionally, neurogenic divisions occurring during this last embryonic period, switch to the gliogenic lineage, giving rise to astrocytes and oligodendrocytes<sup>93,115,116</sup>.

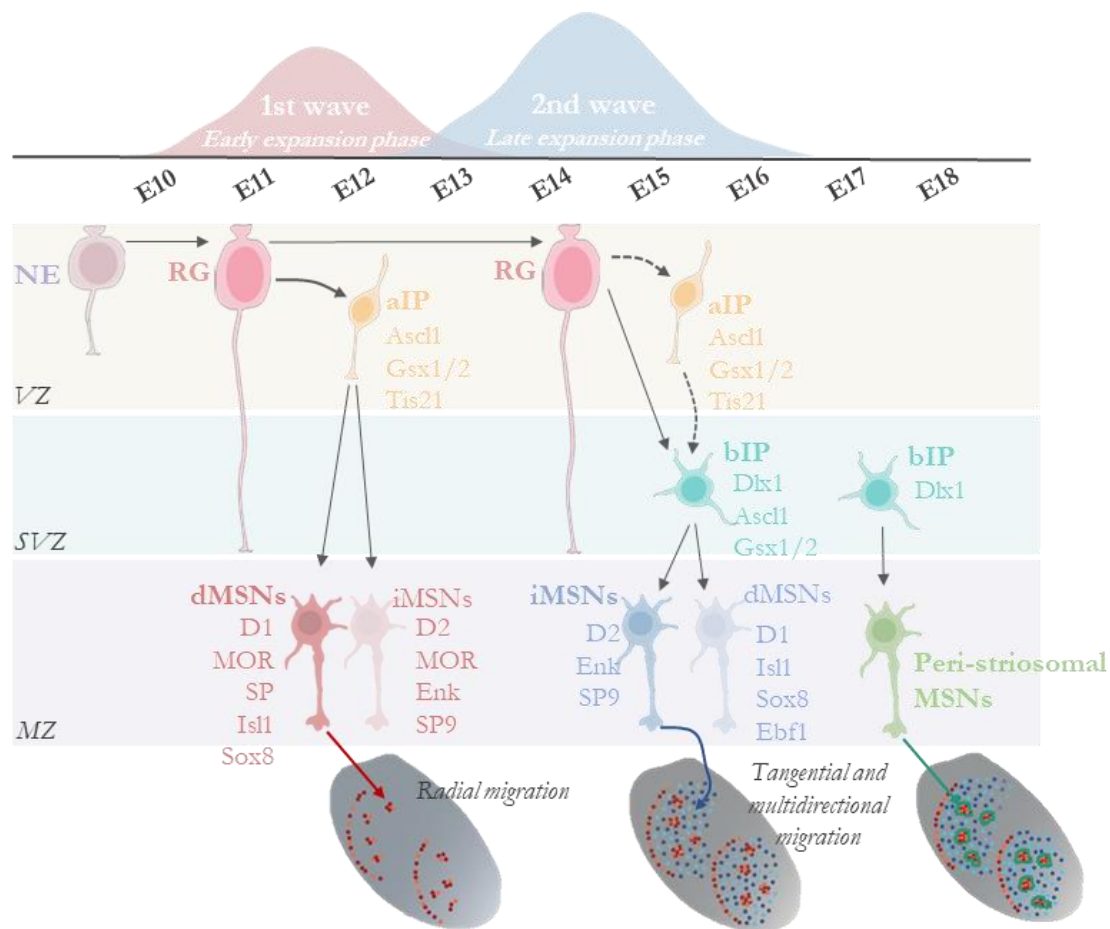


**Figure 14. Summary of the different lineages and their generation along the striatal development.** The molecular identity of the different neuronal progenitors is indicated by the expression of transcription factors (*Gsx1/2*; *Tis21*; *Ascl1*; *Dlx1*), whereas the molecular identity of mature striosomal and matrix MSNs appears in red and blue, respectively. E: embryonic day n; MZ: mantle zone; SVZ: subventricular zone; VZ: ventricular zone. Image edited from Lebonc M. *et al.* (2020) and Kelly S. *et al.* (2018).



### 3.4.2. A novel source of Medium Spiny Neurons:

Although striatal MSN's origin has been classically defined as arising from LGE progenitors, a novel origin has been recently described. A distinct group of cells, derived from the Emx1 lineage, has been defined as a new source of two distinct neuronal populations in the mature basal forebrain: inhibitory MSNs in the striatum and distinct subclasses of excitatory neurons in the amygdala.

Emx1-lineage MSNs display several specific characteristics that distinguish them from the classic non-Emx1-lineage MSNs<sup>117,118</sup>. Striatal Emx1-lineage MSNs, although they are located along the dorso-ventral and rostro-caudal axes, they are disproportionately localized in the dorsal portion of the striatum. Moreover, these MSNs are also preferentially located into the striatal patches<sup>117</sup>.

Little is known about Emx1-lineage progenitors and progeny, but it has been shown that both timing and genetic heterogeneity may play a role in determining cell fate decisions and their differentiation into striatal or amygdalar neurons (Figure 15):

- Emx1 cells from the amygdalar lineage express Pax6, and they are generated between E9.5 and E11.5<sup>119</sup>.
- Emx1 cells from striatal lineage express Gsh2 and Dlx2<sup>118</sup>, and they are generated between E11.5 and E15.4.

These newly born neurons migrate from the pallium ventrally into the striatum. The differential fates of ventrally migrating Emx1-derived cells whose ultimate destination is striatum or amygdala, may also be influenced by external cues located at the PSPB. This area expresses different molecules which are locally secreted, such as Sfrp2, Tgfa and Fgf7<sup>117,120</sup>.

Striatal Cell Subtypes				Amygdala Cell Subtypes	
Neurons	Astrocytes	Oligodendrocytes	NG2 cells	Tbr1+ neurons	Glia
44 %	9%	25%	22%	100%	0%
Neuronal Subtypes				Neuronal Subtypes	
DARPP-32+ MSNs		Calretinin+ Interneurons		Lateral Nucleus	Basolateral Nucleus
95%		<1%		Pyramidal-like excitatory neurons	Burst-firing excitatory neurons
MSN Subtypes				100%	100%
Patch neurons	Matrix neurons	D1-like Nigral MSNs	D2-like Pallidal MSNs		
91%	9%	25%	75%		

**Figure 15. Emx1-lineage cells contribute to multiple neural subtypes in the basal forebrain.** *Image edited from Cacas, L. A., et al. (2009).*

### 3.4.3. Interneuron Neurogenesis:

Interneurons are born in different subpallial domains, from where they migrate out to eventually invade their final destination. Although the MGE is the main source of telencephalic interneurons, CGE and the preoptic area (POA) are also involved in IN neurogenesis<sup>121</sup> (Figure 16).

- Striatal IN represents the 5-10% of the striatal neurons and come from the MGE.
- Cortical IN represents the 20-30% of the cortical neurons and come from the MGE (60%) and from the CGE and POA (40%).

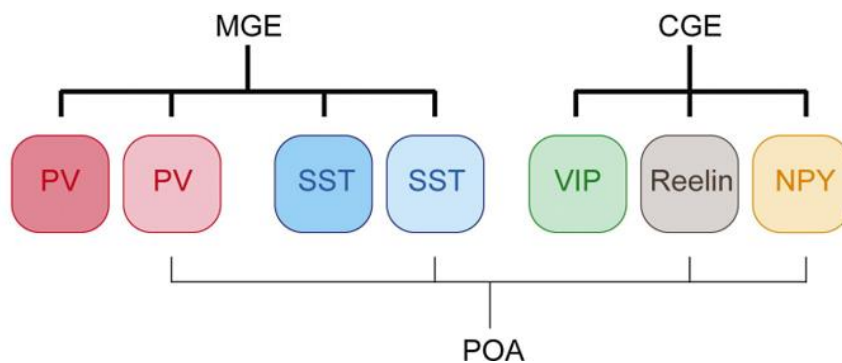


**Figure 16. Summary of the different interneuron subtypes generated by the three main interneuronal sources: MGE, CGE and POA.** Image edited from Bartolini, G., Ciceri, G., and Marín, O. (2013).

Around E9, Shh signalling induces the expression of the transcription factors Nkx2.1 and its downstream effector Lhx6 in the NPCs inhabiting the MGE<sup>122</sup>. Both specifically define the MGE neuroepithelium. In a cascade of events, Lhx6 and its downstream effectors Sox6 and Satb1 mark the cellular identity acquisition and positioning. Different concentrations of Shh in the MGE distinguishes two different territories:

- Dorsal MGE (**dMGE**), a region with high shh levels, which is enriched in Nkx6.2 and Gli1-expressing cells. NPCs coming from dMGE will generate preferentially **Sst**<sup>+</sup> IN, which co-express **CR**, **NPY** and **NOS**.
- Ventral MGE (**vMGE**), a region with lower shh levels, which is enriched in Dlx5/6 and Lhx6-expressing cells. NPCs from the vMGE will give rise mainly to **PV**<sup>+</sup> IN.

These IN are born between E12.5 and E16.5, with a peak at E14.5.

The other major source of IN is the CGE. INs derived from this region virtually express the serotonin receptor 5HT3aR. These IN can be further divided into those that co-express Vasoactive intestinal peptide (VIP) and CR, and those VIP<sup>-</sup> but Reelin<sup>+</sup> IN. CGE-derived IN are late-born cells with a peak of generation around E16.5.

Once the different INs are born, they migrate tangentially to their final location. Interactions between different environmental cues and cell surface receptors mark a key role during this process of migration (see section 3.4.2).



### 3.5. Striatal Migration and Reorganization

Cell migration plays an essential role in the formation of tissues during development. Thus, neuronal migration is one of the critical processes during the early stages of histogenesis of the striatum. Two major forms of neuronal migration during striatum formation have been described (Figure 17): **radial migration** and **tangential migration**, which supply MSNs and interneurons to the striatum, respectively<sup>123</sup>.

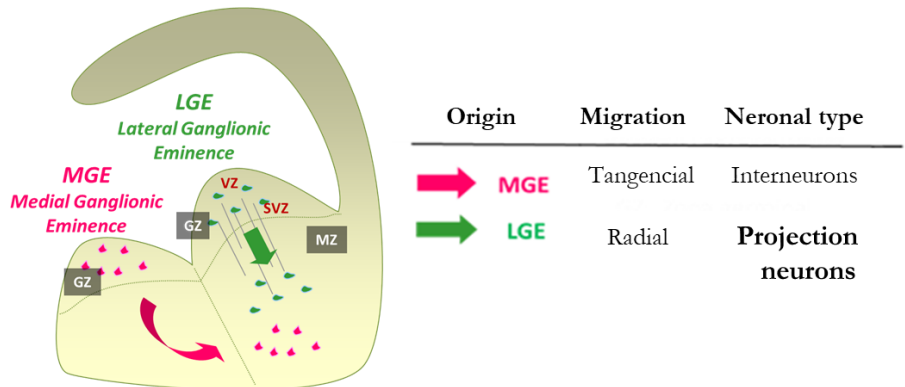


**Figure 17. Schematic representations depicting cell migration for striatal development.** St, striatal nuclei; Ctx, cortex. *Modified from Dra. Martín-Ibañez R.*

#### 3.5.1. Striatal Radial Migration

MSNs begin their migratory path from the VZ-SVZ of the LGE. When a progenitor receives the appropriate signals to differentiate into striatal projection neuron, it begins its migratory path towards the MZ where it will finish its differentiation and mature. This process is relatively short and RGs cells are necessary to carry out this migration during their differentiation process. The first evidence that progenitors reached the postmitotic region using the fibers of the RG is described by Ramón y Cajal, using Golgi marking in sections of the cerebral cortex<sup>124</sup>. Later, Rakic and collaborators describe through different techniques that young post-mitotic neurons find their way to their final destination, through the intricacies of cellular bundles, following the long fibers of the RG during the development of the cerebral cortex and cerebellar<sup>125,126</sup>. In these brain structures, RG cells are formed from the neural tube during early VZ development. Each RG cell has its soma in the VZ and elaborates a process that expands through the neural tube wall until it reaches the pial surface, where it is anchored to the basement membrane<sup>127–129</sup>. Once neuronal production ceases, RG retracts its anchors from the ventricular and pial surface and differentiates into astrocytes, or neurons<sup>130–134</sup>. This type of migration is particularly prominent during the formation of laminar structures such as the neocortex<sup>125,126</sup> and the hippocampus<sup>27,135</sup>.

In the striatum it has been described that the fibers of the RG originate in the VZ of the LGE and project to the striatum with an orientation perpendicular to that of the ventricular surface, suggesting that they are the ones that mark the route of the migration of the striatal precursors<sup>90,136,137</sup>. Since

LGE neural precursors are the primary source of striatal MSNs<sup>138,139</sup>, one can establish that MSNs generated in the GZ of the LGE migrate to the MZ through radial migration processes.

The radial migration process at the level of the striatum nucleus is controlled by several mechanisms, one of them is the expression of certain transcription factors. Among them, Dlx family of transcription factors has been described: Dlx-1 and Dlx-2. These factors are expressed following a temporally restricted pattern in VZ-SVZ of the LGE and MGE and are necessary for the MSNs of the striatum matrix to migrate radially to their final positions. Studies of loss of function of these genes result in an abnormal accumulation of neuronal precursors in the SVZ that produce severe structural alterations in the striatum<sup>139</sup>.

Another mechanism of regulation of radial migration is carried out by guide molecules found in the area and that are essential for the establishment of the stereotyped organization of the nervous system<sup>140,141</sup>. Hamasaki et al. demonstrated that netrin-1 is a guide molecule that is expressed in the VZ of the LGE during telencephalon development and that it regulates the radial migration of striatal MSNs of the matrix<sup>142</sup>.

### 3.5.2. Striatal Tangential Migration

Tangential migration occurs in multiple regions of the central nervous system and contributes to tangential dispersal of clonally related cells. Tangential migration comprises different types of cell movements that diverge mainly in the type of substrate used by migrating cells. In certain cases, neurons that migrate tangentially follow growing axons to reach their final destination. While in other cases, neurons do not follow specific cellular substrates but disperse individually. Regardless of the type of migration, cells that move tangentially do not seem to respect regional boundaries and migrate through the different subdivisions of the telencephalon and even traverse long axonal pathways<sup>143–146</sup>.

Tangential migration of neuronal precursors is indispensable for telencephalon formation during development<sup>62</sup>. MGE has been identified as the largest source of cells that migrate tangentially by distributing themselves through different structures of the telencephalon such as the cerebral cortex, hippocampus, GP and striatum<sup>128,147–149</sup>.

Striatal interneurons form local neural circuits in both compartments of the striatum and although they represent less than 10% of striatal neurons exert an important influence on the function of the striatum nucleus<sup>27,150</sup>. Several studies establish that during the embryonic stage these interneurons migrate tangentially from their place of birth to their final destination<sup>123</sup>. Marin et al. described that a subpopulation of precursors expressing the homeodomain protein Nkx2.1 migrate tangentially from MGE to the developing striatum where cells subsequently differentiate into ChAT<sup>+</sup>, CR<sup>+</sup>, or PV<sup>+</sup> interneurons<sup>151</sup>. Uterine transplants of MGE cells show that these cells populate the striatum by tangential migration<sup>152</sup>. Thus, evidence derived from these and other studies suggests that striatal interneurons derive mainly from MGE via tangential migration.

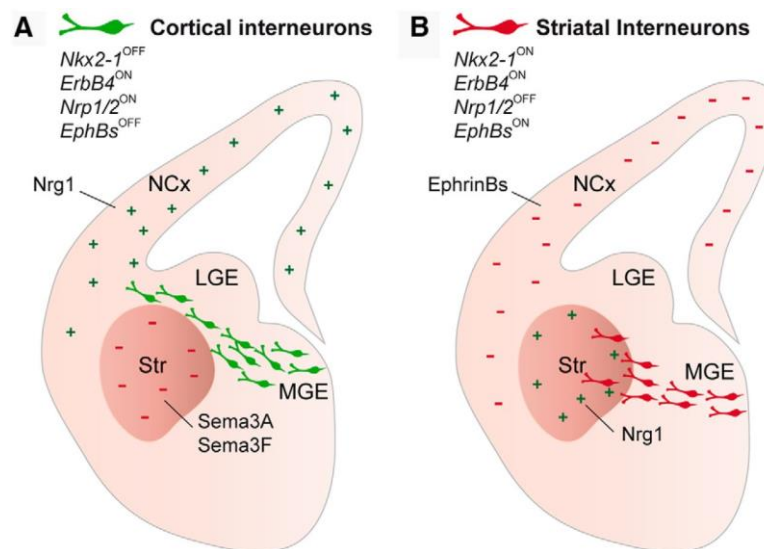


Figure 18. Schematic drawings of transversal hemisections through the developing telencephalon summarizing the chemorepellent and chemoattractive cues that drive interneuron migration to the cortex (A) or the striatum (B). NCx, neocortex; Str, striatum. Image edited from Villar-Cerviño, et al. (2015).

The capacity for tangential migration is controlled by several transcription factors essential for cell dispersal, such as Mash1 and Lhx6<sup>148,153–155</sup>. However, there are extrinsic signals that play a really important role in controlling cell migration, the most important are chemoattractant factors, such as Cxcr4 or GDNF<sup>156,157</sup>, and chemorepellents, such as Slit or Semaphorins 3A/3F<sup>151,158</sup>. For example, semaphorins 3A and 3F act as repulsive keys that inhibit the entry of migrating cells from MGE to the striatum and, therefore, these cells are redirected towards the cortex<sup>128</sup> (Figure 18).

### 3.5.3. Active Intermixing

In mouse, the striosomal and matrix neurons initially remain intermix and spread uniformly around the striatal primordium. Striosomes, which are firstly generated during the first neurogenic wave, develop concomitantly with the arrival of dopaminergic afferents from the SN, which reach the striatum at E14 and cluster at the patches by E19<sup>159</sup>. Then, after E16-E19, striosomal neurons start to form cellular aggregates positive for SP<sup>27</sup> and DARPP-32<sup>160</sup> whereas matrix neurons surround the striosomes constituting a mosaic pattern<sup>161</sup>. Thus, striosome neurons can display homophilic adhesive properties, providing a first hint about potential mechanisms controlling striatal compartmentalization<sup>161,162</sup>. Then, late born neurons will migrate and occupy ventrolateral spaces causing the passive movement of the striosomal neurons that were there towards dorsomedial locations<sup>163</sup>. In this migration process, matrix neurons intermingle with striosome neurons<sup>161</sup> and once striosomal neurons aggregate, neurons from the second wave of neurogenesis surround them so that shortly after birth the matrix and striosome neurons are fully segregated<sup>164</sup>. Finally, by postnatal day (P) 2 a complete segregation has formed<sup>161</sup>.

Hence, mouse studies indicate that the formation of striatal compartments obey extrinsic factors such as incoming cortical or nigral axons<sup>72,165</sup> and intrinsic factors (including generation timing and contact-dependent cell sorting by expression of different cell adhesion molecules). Although the exact factors controlling the formation of both striatal compartments are not well known, several studies evidenced some intrinsic factors that might be involved in specific processes of the striatal compartmentalization. Among them, transcription factors such as *Dlx-1/2* and *Ebf-1* are involved in the generation and migration of striatal matrix neurons<sup>139</sup>, as well as *Ebf-1*<sup>139,166,167</sup>. Moreover, there are some proteins controlling striosomes-matrix compartmentalization. For example, *Cadherin 8*, a cell adhesion molecule predominantly expressed in the striatal matrix and suggested to be involved in the formation of the striatal compartmentalized structures during brain development<sup>168</sup>. Ephrins and their receptors have also been described as guidance cues that control matrix/striosome compartmentalization<sup>25,165</sup>. It was described that Ephs were highly enriched in the matrix compartment and that selective interaction between Ephrin ligands and Ephs could regulate compartmental organization of the striatum<sup>25</sup>. Then, it was demonstrated that EphA4 and its ephrin ligand displayed specific temporal patterns of expression and function that played a significant role in the spatial segregation of matrix and striosome neurons<sup>165</sup>. Thus, suggesting that the family of Ephs/Ephrins is involved in the formation of the mosaic pattern of the striatum, supporting a model whereby the temporal control of membrane-bound cues is tightly linked to the spatial organization of this structure<sup>165</sup>.

### 3.6. Striatal Connection's Formation

The development of the striatum does not end at the embryonic level, but the formation of connections, the establishment of circuits and the maturation of pathways does not occur until the early stages of postnatal age. The striatonigral route is the earliest to form. Dopaminergic terminals from the SN reach the striatum around E14.5 in mice<sup>159</sup> (Figure 19). Although dopaminergic terminals from NS reach the striatum during embryonic development, the main innervation occurs during the first postnatal week<sup>169</sup>. Then, during the first postnatal week, matrix iMSNs establish connections with their targets, the SNr and the GPe. During this time, glutamatergic inputs coming from the cortex and thalamus begin to take shape. Between P2 and P7, the physiological cell death period occurs, when approximately 30% of the striatal neurons undergo cell death<sup>164</sup>. It has been shown that MSNs which have already sent projections to the substantia nigra (SN) or the globus pallidus externa (GPe) by P2 tend to preferably survive the natural death period<sup>164</sup>.

Between the first to the fourth postnatal week, the microcircuit maturation continues, and the pathway is not considered fully formed until the end of the first postnatal month<sup>170</sup>.

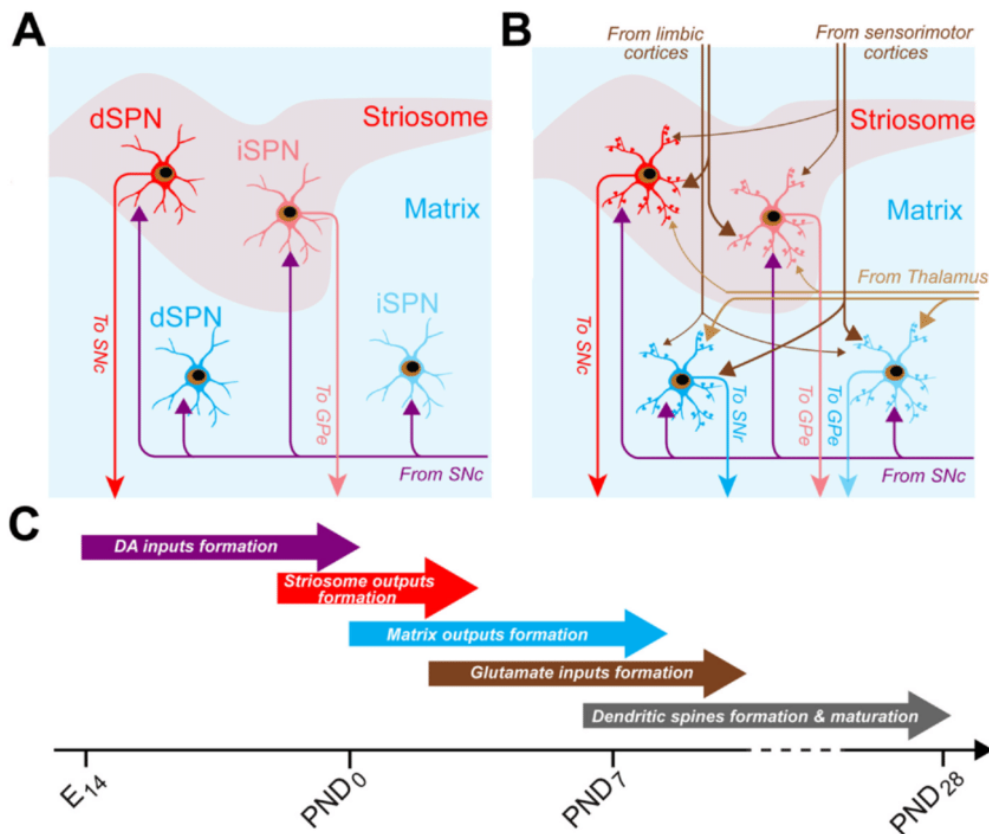


**Figure 19. Establishment and maturation of the developing striatum. (A-B)** Schematic summary showing the sequential maturation of the striatum. **(C)** Timeline showing the different key steps involved in the maturation of the developing striatum. E: embryonic day; GPe: external globus pallidus; P: postnatal day; SNc: substantia nigra pars compacta; SNr: substantia nigra pars reticulata. *Image edited from Lebouc, M., et al. (2020).*

### 3.7. Factors involved in the specification of striatal neuronal subtypes

The development of the striatum is a complex process that is regulated by several genetic and environmental factors. The expression of different transcription factors defines different parent populations and contributes to the specification of different striatal neuronal subtypes. These factors can influence the development of the striatum at various stages, including cell proliferation, migration, and differentiation.

#### 3.7.1. NPCs-related factors:

##### **Retinoic Acid**

RA is involved in the determination of striatal neurons<sup>171</sup>. Several studies show that the signaling machinery of RA as synthesis and degradation enzymes are enriched in the LGE<sup>172–174</sup>. Likewise, RA levels in the LGE are higher than in other regions of the developing telencephalon<sup>81,171</sup>. In addition, RA is also involved in the regulation of gene expression of factors involved in the development of the striatum such as *Meis2*<sup>175</sup> or *Nolz-1*<sup>176,177</sup>.

##### **GSX1/2**

*Gsx2*, also known as *Gsh2*, is the first gene to be detected in the developing forebrain between E9 and E10 expressing itself in dLGE, vLGE and MGE. *Gsh2*-deficient mice have ectopic expression of dorsal genes (*Pax6* and *Ngn2*) in LGE and have a loss of expression of *Ascl1* and *Dlx2* genes in this same region<sup>71,178</sup>. Thus, *Gsh2* plays an essential role in the development of the striatum while maintaining the molecular identity of early precursors. In the *Gsh2* knock-out (KO), the LGE size at E12 is reduced<sup>179</sup> and, consequently, at E18.5 the striatum shows a reduction in the total number of striatal MSNs, with a reduction in the *DARPP-32*<sup>+</sup> and *Foxp1*<sup>+</sup> MSNs<sup>71,178</sup>. However, it seems that the absence of *Gsh2* alters the striosomes and matrix differently. By labelling striosomes with  $\mu$ -OR receptor, they showed a reduced size in the E18.5 striatum of *Gsh2* deficient mice. These results support the idea that *Gsh2* is necessary for the first wave of neurogenesis that includes VZ progenitors (early progenitors), which are associated with the generation of striosome neurons. In fact, the apparent correct generation of matrix neurons could be explained by the expression of *Gsx1* that could compensate for the loss of *Gsh2* in later stages<sup>180</sup>, since the double mutant mouse for *Gsx1* and *Gsh2* presents serious problems in both compartments<sup>180,181</sup>. *Gsx1*, or *Gsh1*, is a gene closely related to *Gsh2*, mainly expressed in MGE and vLGE from E12.5 while *Gsh2* is expressed in dLGE progenitors and relatively low in vLGE and MGE<sup>180–183</sup>. Pei et al. have shown that *Gsx1* works similarly to *Gsh2* by differentially regulating the maturation of LGE progenitors<sup>184</sup>. Specifically, *Gsh2* keeps LGE progenitors in an undifferentiated state and promotes VZ progenitor self-renewal, while an increase in *Gsx1* levels in *Mash1*-expressing cells leads to *Gsh2* repression and transition from VZ to SVZ, promoting progenitor maturation and acquisition of neuronal phenotypes. These new results indicate that the two *Gsx* genes are closely related and control in a balanced way the proliferation and differentiation of neuronal progenitors in LGE<sup>184</sup>.

### **Mash1**

Mash1 or, also known as Ascl1, is a transcription factor of the type bHLH (basic helix-loop-helix) that has a main role in the correct development of the ventral telencephalon depending on its expression of Gsh2<sup>60,71,178,185</sup>. Mash1 is expressed in the proliferative region (both VZ and SVZ) of the LGE and MGE of the telencephalon<sup>186</sup>. There are many studies showing evidence that suggests that Mash1 could be above Dlx2 in the neurogenic cascade of transcription factors<sup>60,61,144,186</sup>. This hypothesis is reinforced by different studies: the first, Mash1 and Dlx1/2 show patterns where their expression overlaps in the VZ and SVZ of the ventral telencephalon<sup>186</sup>. Second, Horton et al. have shown that Mash1-deficient mice have a small number of cells expressing Dlx genes in the SVZ from nodal eminence to E12.5<sup>187</sup>. Third, ectopic expression of Mash1 leads to an increase in Dlx1/2 levels in neocortical neurons<sup>61</sup>. Finally, chromatin immunoprecipitation analysis for the Mash1 protein indicates that it can bind, in vitro and in vivo, to enhancer I12b, which is located in the intergenic region of Dlx1/2 and that, at least in part, is responsible for the expression of Dlx genes in GABAergic projection neurons and interneurons that are in differentiation<sup>188</sup>. In addition, Mash1 has been shown to be sufficient to induce ectopic expression of ventral markers in dorsal telencephalon neurons via Dlx1/2<sup>60,61</sup>.

Mash1 is necessary for the specification of neural precursors and control their production times<sup>60</sup>. For example, in the Mash1 KO mouse, most LGE progenitors showed early expression of SVZ markers in VZ cells. However, these precursors were still able to differentiate into striatal neurons. Thus, expression of Dlx1/2 and GAD67 (GABAergic neuron's marker) was detected in the ventral telencephalon<sup>60</sup>. When analyzing the expression of other striatal markers in the striatum of this mouse at E18.5, the expression of TH did not change and that the expression of D2 and ENK was simply slightly reduced, indicating that these striatal neurons can be generated despite the absence of Mash1. Thus, it seems that the function of Mash1 in the progenitors of the LGE seems to be redundant, and a population of neuronal genes still undefined must exist being able to perform the same functions. However, in the ventral telencephalon, interneurons are also generated that can migrate from the dLGE to reach the olfactory bulb or from the MGE to reach the cortex. In the Mash1-deficient mouse, a reduction in the number of GABAergic interneurons in both the olfactory bulb and cortex is observed, suggesting that Mash1 is required for the generation and/or migration of olfactory or cortical GABAergic interneurons<sup>60</sup>. In fact, these mice present a reduction of neuronal precursors in SVZ and MGE accompanied by a reduction in size<sup>60</sup>.

The expression of Gsh2 in the mouse deficient for Mash1 does not change to E12.5, but at E18.5 there is an increase in cells expressing Gsh2, this suggests that Mash1 also plays a role in repressing the expression of Gsh2 late in development<sup>189</sup>.

Mash1 regulates many genes with diverse molecular functions, this suggests a direct control of both genes that have a role in early and more advanced stages of neurogenesis. In addition, Mash1 also plays an important role in coordinating the neurogenesis program through the successive phases of proliferation, cell cycle exit and differentiation<sup>91</sup>.



## **Dlx**

The Dlx gene family is also involved in the generation of striatal neurons, specifically in projection neurons. This family is composed of six members, of which Dlx1 and Dlx2 are expressed in the VZ and SVZ of the two nodal eminences<sup>190</sup>, while Dlx5 and Dlx6 are expressed in the SVZ and MZ of the two eminences. This family of genes is involved in the generation of late neurons of the striatum<sup>139</sup> since mice deficient in Dlx1/2 show a disruption of the SVZ accompanied by the alteration in the differentiation of the neurons that will form the striatal matrix, but in no case affects the generation of early neurons. In addition, these Dlx1/2-deficient mice lose expression of Dlx5 and Dlx6, indicating that the expression of Dlx1 and Dlx2 precedes that of Dlx5 and Dlx6<sup>190</sup>. Moreover, in the double KO for Dlx1/2 there is a decrease in the expression of the mature MSN marker, Ctip2<sup>183</sup>.

## **Meis2**

Meis genes (Meis 1-3) belong to the TALE (three amino acid loop extension) superclass of homeobox genes<sup>191</sup>. They form heteromeric complexes with other transcriptional regulators, including the related PBC family, members of the Hox clusters or bHLH protein<sup>192,193</sup>. In the developing mouse brain, the Meis2 gene is expressed in the telencephalon, diencephalon, cerebellum, pons and medulla<sup>81,178</sup> as well as in the striatum of the adult mouse brain<sup>81</sup>. Meis2 displays region-specific patterns of expression from E10.5 until birth, defining distinct subterritories in the developing telencephalon and being highly expressed in intermediate progenitors of the telencephalon<sup>178</sup>. Meis family members have been shown to function as regulators of cell proliferation and differentiation in many tissues during animal development<sup>194,195</sup>. Interestingly, it was shown that RA signalling is sufficient to induce the expression of Meis2, promoting an intermediate character in telencephalic cells<sup>56</sup>. In the Meis2 conditional KO (Dlx5/6-CIE; Meis2<sup>F/F</sup>) mouse, LGE precursor cells failed to fully differentiate into MSNs, leading to an expansion of the SVZ. As a result, the majority of MSNs were not generated<sup>196</sup>. Recent experiments revealed that Six3 and Zfp503 are crucial direct downstream targets of Meis2 in controlling the specification of the D1 and D2 MSNs<sup>196</sup> (Figure 20).

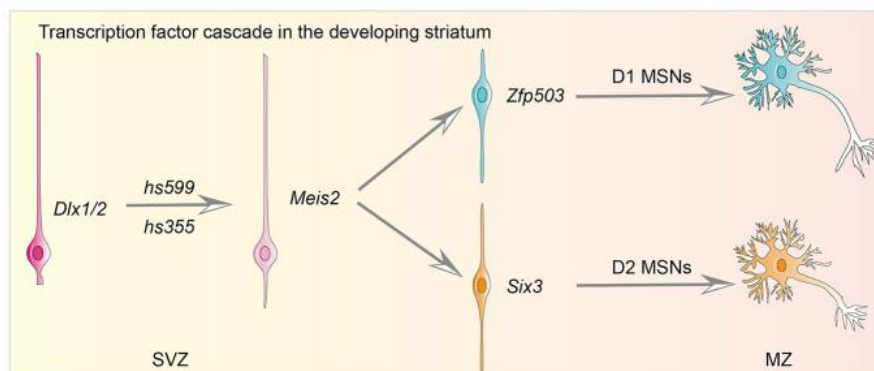


**Figure 20. The main transcription factor network regulating the fate determination of striatal MSNs.** First, Dlx1/2 promote the expression of Meis2 by enhancers such as hs599 and hs355. Then, Meis2 promotes Zfp503 or Six3 expression to further determine precursor cell fate (D1 or D2 MSNs). Cx, cortex; LV, lateral ventricle; MSN, medium-sized spiny neurons; MZ, mantle zone; Str, striatum; SVZ, subventricular zone; VZ, ventricular zone. *Image edited from Su, Z., et al. (2022).*



### 3.7.2. Direct pathway lineage-related factors:

#### **Zfp503**

Zfp503, or also known as Nolz1, is a member of the Noc/Nlz-Elbow (eIB)-Tlp (NET) family of transcription factors that are involved in regionalization and differentiation during the development of many species studied<sup>197–199</sup>. This transcription factor is strongly expressed in vLGE without being expressed in MGE or dLGE<sup>176</sup> suggesting a specific striatal function. Nolz1 begins to be expressed at E11.5 but its expression is strongly reduced in postnatal stages although low levels of expression are maintained in adults<sup>176,177</sup>. Interestingly, this family of transcription factors cannot interact directly with DNA, indicating that they need to establish a physical interaction with other transcription factors. In *Drosophila*, the eIB analogue has been shown to interact with Groucho (Gro) proteins, forming large protein complexes that act as transcriptional co-representatives<sup>200</sup>.

In previous publications of our group, the role of Nolz1 during the development of LGE was analyzed<sup>177</sup>. Nolz1 showed a high expression in proliferating NPCs of the LGE SVZ<sup>177</sup>. Low levels of Nolz1 were detected in the MZ and in the adult striatum. In concordance, the overexpression of Nolz1 promotes cell cycle exit and negatively regulates the proliferation in telencephalic organotypic cultures<sup>177</sup>. In addition, in LGE-derived primary cultures, the Nolz1 over-expression promotes the acquisition of neuronal phenotypes, showing an increase in the number of  $\beta$ -III-tubulin<sup>+</sup> and Map2<sup>+</sup> neurons. Interestingly, it was also found that Gsh2 is necessary for the expression of Nolz1 since its expression is lost in the Gsx1 KO mice<sup>201</sup>. Moreover, it has been recently found that interactions between Nolz-1 and Dlx1/2 genes are critical for the developmental processes by which the striatum is divided into dorsal and ventral districts<sup>201</sup>.

#### **Ebf-1**

Ebf-1 codes for a transcription factor containing a DNA-binding domain with an atypical ZF and a non-basic HLH dimerization domain<sup>202</sup>. The Ebf family of transcription factors includes Ebf-1, 2, 3, and O/E-4 in mammals<sup>202–205</sup>. Ebf-1 is expressed in the striatum during embryonic development<sup>205</sup>. Striatal alterations have been reported in the Ebf1 KO mice, related to the neuronal differentiation, in the transition between SVZ and MZ, leading to an atrophy of the perinatal striatum<sup>166</sup>. However, these defects are not a consequence of an altered cell migration from proliferative areas (SVZ and VZ) to MZ since the patterns of BrdU-labeled cells in Ebf1-deficient mice are not altered. More recent publications describe the involvement of Ebf1 in the development of striatonigral neurons<sup>206,207</sup>. Lobo et al. developed a protocol to separately study the striatopallidal and striatonigral populations by using transgenic animals expressing either EGFP protein under the control of Chrm4, M4-EGFP (specific to striatonigral neurons) or, D2, D2-EGFP (specific to striatopallidal neurons). It was then identified that Ebf1 is highly enriched in the striatonigral population<sup>207</sup>. In addition, in the Ebf-1 KO mice, there was also found a strong reduction in terminal contacts towards SN. In contrast, striatopallidal MSNs and their projections are relatively intact in the mouse Ebf1<sup>-/-</sup> <sup>207</sup>. Thus,

all these results point to the importance of factor Ebf1 in the development and correct formation of connections of striatonigral MSNs.

### **Zfp521**

The transcription factor Zfp521 is a nuclear transcription factor of 1311 amino acids with 30 ZFs distributed along its sequence forming clusters of 5-7 ZFs<sup>208</sup>. The human analogue EHZF/ZNF521 shares 95% identity with the murine protein sequence Zfp521/Evi3<sup>209</sup>.

ZNF521 was first identified in humans in early CD34+ hematopoietic progenitors<sup>210</sup>. However, it is expressed in different tissues in humans such as the brain, muscle, heart, kidneys, spleen, lymph node, placenta, thymus and fetal liver. In the striatum, the expression of Zfp521 is enriched in postnatal and adult striatonigral neurons since Lobo and company identified elevated levels of mRNA of this transcription factor in this population<sup>206</sup>. The same study showed that Ebf1 expression was also enriched in this same striatonigral population. These data suggest that both transcription factors could play an essential role for striatonigral MSNs. In addition, Lobo and co also described a reduction in mRNA levels of Zfp521 in the Ebf-1 KO mice, suggesting that the expression of Ebf-1 could act above Zfp521 in the cascade of transcription factors involved in striatal development<sup>206</sup>.

### **Isl1**

The LIM homeodomain TF Islet1 (Isl1) is mostly expressed in the SVZ and MZ of the vLGE during embryogenesis. It colocalizes with *Dlx* genes and its coexpression marks a specific population of progenitors that give rise to MSNs. However, Isl1 protein is also expressed by a progenitor population of the MGE that develops into cholinergic interneurons<sup>73,211</sup>. In Isl1 conditional mutants (Isl1<sup>-/-</sup>), DARPP-32 staining revealed a 43% reduction in striatal size, and alterations in both the patch and matrix compartments. Indeed, a specific reduction in the DARPP-32 innervations along the striatonigral tract was detected, whereas striatopallidal innervations were unchanged; suggesting a specific affectation of the direct pathway MSNs<sup>212</sup>. On the other hand, loss of Isl1 results in a nearly complete loss of striatal cholinergic interneurons<sup>212,213</sup>. Interestingly, the expression of *Gsh2*, *Mash1*, and *Dlx* in E14.5 Isl1 KO mice was not altered, suggesting they are upstream of Isl1 expression<sup>181,212</sup>. However, Isl1 expression was maintained, although at lower levels, in the LGE of triple *Dlx1/2*<sup>-/-</sup> and *Mash1*<sup>-/-</sup> mutant mice, demonstrating its role in LGE specification is independent of *Dlx* and *Mash1*<sup>214</sup>. Ebf1 expression, which is required for the correct differentiation of striatonigral neurons and the striatal matrix compartment<sup>206,215,216</sup>, was also apparently similar between the Isl1<sup>-/-</sup> mice and the controls.

### 3.7.3. Indirect pathway lineage-related factors:

#### **Ikaros**

Ikaros is the founding member of a small family of DNA-binding proteins that form zinc finger motifs (ZFs), which also includes *Helios*, *Aiolos*, *Eos*, and *Pegasus*<sup>217</sup>. Ikaros was first identified in

the hematopoietic system, but later it was also seen that it had a role in the development of ENK<sup>+</sup> neurons of the striatum nucleus, specifically playing an active role in their neurogenesis<sup>218,219</sup>.

Ikaros is specifically expressed in the LGE<sup>77</sup>, being restricted its expression to the MZ between E14.5 and P3, with a peak of expression approximately to E18.5, and disappearing its expression to P15<sup>219</sup>. Ikaros is below *Dlx* in the cascade of transcription factors that controls striatal development, as Ikaros expression is strongly reduced in the double *Dlx1/2* KO mouse at E15.5 and E18.5<sup>214,219</sup>. However, in the *Ebf-1* KO mice Ikaros expression remain unchanged to E18.5. These results suggest that both Ikaros and *Ebf1* are involved in the development of striatal MSNs but acting on distinct neuronal populations.

In humans, IKAROS1 (analogous to murine Ikaros), is also expressed during human striatal development in a subpopulation of neurons belonging to the caudate and putamen nuclei<sup>220</sup>.

### **Helios**

Another member of the Ikaros family of transcription factors is Helios (*Ikzf2*; *He*). Our group has described its expression in LGE from E14.5 having a peak expression at E18.5 and disappearing during postnatal development at P15<sup>221</sup>. During embryonic development, Helios is expressed by two distinct cell populations: a small population in the SVZ that colocalizes with nestin positive NPCs, and a larger population in the MZ that colocalizes with Map2 (marker of differentiated neurons)<sup>221</sup>. In fact, Helios has been described as a marker of matrix neurons since Helios does not colocalize with NeuN or DARPP-32 (striosomal markers in late embryonic stages and early postnatal stages) at P3<sup>221</sup>. In addition, Helios expression in different KO mice has been studied for different LGE-related transcription factors. Helios expression disappears in the *Dlx1/2* and the *Gsh2* KO mice, however, its expression is maintained in *Mash1* mutants suggesting that it is involved in a MSNs lineage independent of *Mash1*<sup>221</sup>. In fact, Helios expression levels do not change in the *Ebf-1* nor in the Ikaros KO mice. In addition, the relationship between Helios and Ikaros was studied by immunohistochemistry and the lack of colocalization between these two transcription factors points to a parallel expression in two different populations of neuronal precursors<sup>221</sup>.

### **SP8/SP9/ Six3**

The *Sp9* gene, which contains a zinc finger TF, is active in both dMSNs and iMSNs' progenitors in the SVZ. However, only the postmitotic iMSNs continue expressing it. Studies have shown that *Sp9* is necessary for the production, differentiation, and survival of iMSNs, as its absence causes 95% of them to be lost<sup>222</sup>. Additionally, *Sp9* promotes the expression of specific genes (*Drd2*, *Adora2a*, *P2ry1*, *Gpr6*, and *Grik3*) that are iMSNs markers<sup>222</sup>. *Sp8*, a paralog of *Sp9*, is primarily expressed in the dorsal LGE of the SVZ. The ventral LGE generates MSNs, and *Sp9* is broadly expressed in these regions, while *Sp8* is weakly expressed there<sup>223,224</sup>. However, the function and targets of *Sp8* in the vLGE remain unknown. A recent study, which used conditional SP8/SP9 deletion, demonstrates that mice lacking these transcription factor lose nearly all iMSNs due to reduced neurogenesis in the

LGE. However, dMSNs are mostly unaffected by the deletion. SP8 and SP9 work together to activate the transcription factor Six3, which is expressed in a specific area of the LGE subventricular zone<sup>225</sup>. When Six3 is conditionally deleted, the formation of most iMSNs is prevented, resembling the phenotype of Sp8/9 mutants (Figure 20). Moreover, they found that SP9 directly binds to the promoter and a possible enhancer of Six3<sup>225</sup>.

#### 3.7.4. Neuronal maturation-related factors:

##### ***Ctip2***

Ctip2 or Bcl11b is a transcription factor expressed in the cortex and striatum from early embryonic stages to adulthood<sup>226,227</sup>. Interestingly, in the striatum it is only expressed in MSNs, specifically marking this neuronal population from early embryonic stages onwards<sup>228</sup>. In addition, it is also used as a marker of the V layer of the cortex<sup>226</sup>.

In Ctip2 KO mice, MSNs birth and migration to the striatal primordia is not affected, since the expression of immature MSN markers such as Meis2 and Nolz1 remains unchanged<sup>228</sup>. However, the differentiation of these neurons is affected, with a marked decrease in the expression of Foxp1 to E15.5. These data indicate that in the absence of Ctip2, MSNs can be specified from their parents and migrate to MZ, but they are not able to differentiate<sup>228</sup>. On the other hand, the INs are not altered in the Ctip2 KO. In fact, in the absence of Ctip2, labeling for Reelin,  $\mu$ -OR, and GluR1 (striosomal markers) reveals an alteration of the striosomes that can be observed compared with the striatum of control mice. In conclusion, these results indicate that Ctip2 is necessary for the development and maturation of MSNs and for the correct compartmentalization of MSNs in striosomes and matrix.

##### ***Foxp1***

Foxp1 belongs to a subfamily of genes called winged-helix/forkhead whose expression is detected from E12.5 in the developing telencephalon and continues into adulthood<sup>229</sup>. Foxp1 is expressed in both the striatum and cortex, in the CA1 region of hippocampal neurons, as well as in other regions of the central nervous system<sup>229,230</sup>.

In the mouse, Foxp1 is expressed in the SVZ at E12 and in the SVZ and MZ at E14 in the striatum<sup>230</sup>. As increased expression of Foxp1 is observed in MZ, it has been associated with neurons that have already completed their migration and already differentiated rather than in neural precursors that are proliferating in VZ or SVZ<sup>229,230</sup>. Specifically, Foxp1 is thought to be associated with matrix MSNs, since the projection neurons of the striosomes are specified prior to E12.5<sup>230</sup>. In fact, it has been suggested that Foxp1 is below the transcription factors Dlx 5/6 since both genes have overlapping expression profiles<sup>230</sup>, hypothesizing on a cascade of transcription factors for the development and formation of matrix neurons, such as Dlx1/2-Dlx5/6-Foxp1. In addition, it has been observed that Foxp1 colocalizes with Ctip2<sup>228</sup> and that it seems that it depends on it, since the expression of Foxp1 is decreased in the Ctip KO mice to E15.5<sup>228</sup>.

### 3.7.5. Interneuron lineage-related factors:

#### **Nkx2.1**

The Nkx2.1 homeodomain protein in the mouse begins to be expressed in the most ventral region of the pallium approximately at E9<sup>5,231</sup>. Later in embryonic development, almost all proliferating cells found in MGE and cells in the most ventral part of the preoptic region express Nkx2.1. In the Nkx2.1 KO mice, the MGE region expresses LGE-specific markers<sup>231</sup>. In the MZ of these mice the striatum expands at the expense of the ventral pallium<sup>231</sup>. MGE and POA give rise to cortical and striatal INs<sup>232,233</sup> as well as cholinergic projection neurons<sup>231,234,235</sup>. In the MGE-derived cortical INs, Nkx2.1 expression is repressed while migrating outside the MGE. On the other hand, most of the MGE-derived striatal INs maintain its Nkx2.1 expression<sup>151,236,237</sup>. In fact, when forcing Nkx2.1 expression in cortical interneurons, they change their migration and they finally locate within the striatum<sup>237</sup>. In addition, oligodendrocytes, including a transient population of the cerebral cortex, are also generated from progenitors expressing Nkx2.1<sup>237</sup>. Nkx2.1 continues to be expressed postnatally in several neuronal subtypes in subcortical regions<sup>151</sup>.

## 4. Developmental Alterations in Huntington's Disease

### 4.1. Huntington's Disease and Huntingtin mutation

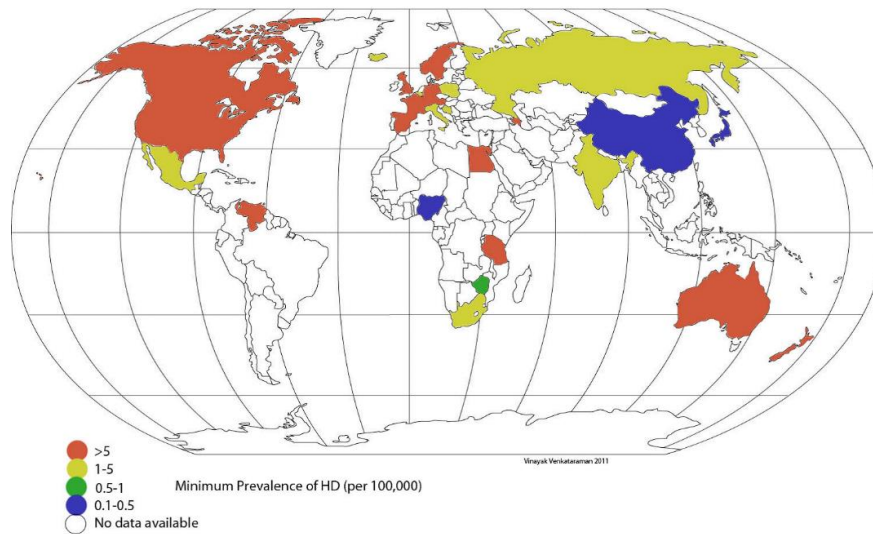


Figure 21. Prevalence of HD worldwilde. Image edited from Warby et al. (2009).

HD is an inherited neurodegenerative disorder characterized by motor, psychiatric and cognitive dysfunction<sup>238,239,240</sup>. It has a prevalence between 1-10 affected individuals per 100,000 people regarding ethnicity and geographical location<sup>241,242</sup> (Figure 21). HD is inherited in an **autosomal dominant** manner, caused by a mutation in the IT15 gene, located on the short arm of chromosome 4. This gene encodes for a 350 kDa protein called **huntingtin (Htt)**, which has a **polyglutamine repeat** in exon 1.

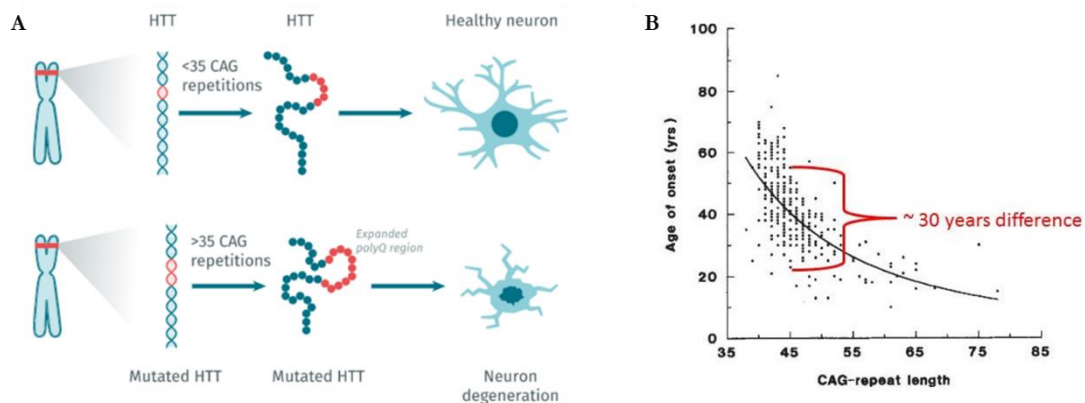
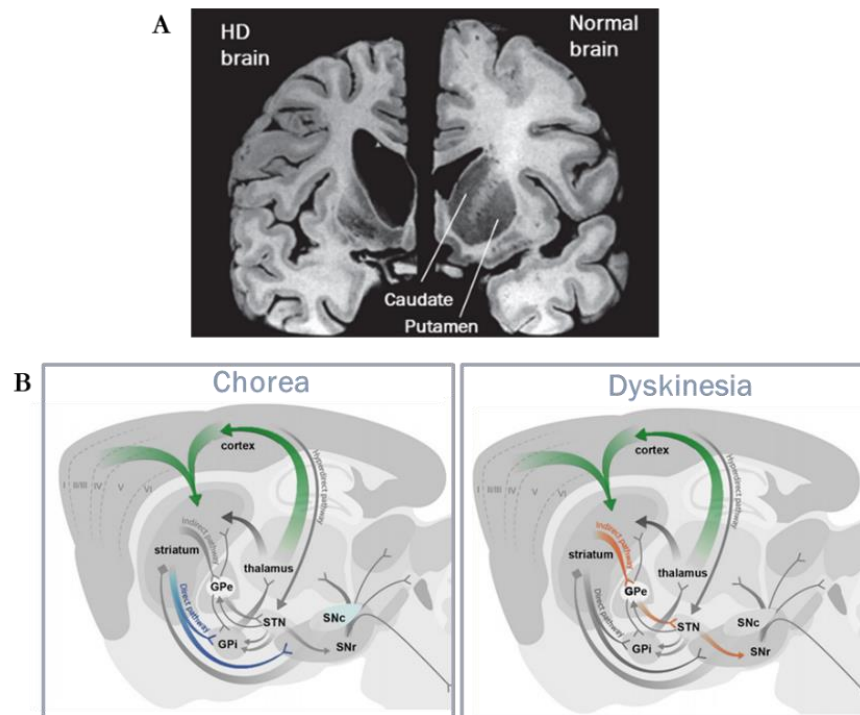


Figure 22. Schematic representation of the genetic basis of HD. Image edited from Bates, G. P., et al. (2015) and Andrew, S. E., et al. (1993).

When this repeat exceeds 35 times, the protein acquires toxic properties and the symptoms of the disease inevitably appear (Figure 22). Individuals with a CAG repeat number between 36 and 39, which is known as the reduced-penetrance repeat length range, may develop HD but very late in life. When the number of CAG repeats is higher than 39, a person will develop HD within a normal lifespan, appearing between the ages of 35 and 50 and worsens progressively until death of the patient, usually 15-20 years later. Patients with more than 80 CAG repeats will develop the disease before the

age of 10, what is known as Juvenile onset's HD. In fact, there is an inverse correlation between the number of CAG repeats and the age of onset of the disease: the more repeats, the earlier the onset and the more severe the symptoms.

Histopathologically, it is known that the **caudate and putamen** nuclei, which are part of the basal ganglia, are the most affected brain regions<sup>243,244</sup>. Additionally, there is significant cortical neurodegeneration with associated neuronal death<sup>243,245</sup>. However, this cortical neurodegeneration is more secondary and occurs in later stages of the disease<sup>246</sup>.



**Figure 23. (A)** Post-mortem image of a healthy and Huntington's disease brain. **(B)** Schematic representation of the direct and indirect inhibitory pathways underlying choreic and dyskinesic HD symptoms. Image edited from Bates, G. P., et al. (2015) and Blumenstock and Dudanova (2020).

These **symptoms** primarily affect motor function, with progressive loss of control of both voluntary and involuntary movements, including uncontrollable, rapid, chorea-like movements of the trunk and limbs. Emotional dysfunction, personality changes, and progressive intellectual decline are also common. It is known that lesions in the basal ganglia can produce hyperkinetic symptoms (exaggerated involuntary movements) or hypokinetic symptoms (loss of motor ability)<sup>247</sup>. This led to the proposal and identification of two distinct main pathways in the BG; the direct (excitatory) pathway and the indirect (inhibitory) pathway<sup>14,27,248</sup>. In fact, the motor symptoms in HD initially have a hyperkinetic course with chorea, exaggerated and uncontrolled non-stereotyped movements<sup>249</sup>. Later, the symptoms progress to a hypokinetic phase with loss of ability to generate movement, rigidity, and dystonia<sup>250</sup>. This suggests that the primarily affected pathway would be the indirect (loss of movement inhibition) to which later the degeneration of the direct pathway (loss of excitation or movement production) would be added.



## 4.2. HD Adult Pathophysiology

While the genetic cause of HD is well understood, the number and variety of molecular changes associated with the disease are not fully understood. It is known that toxicity in HD is caused by a gain of function of the mutant huntingtin protein, but it is possible that a loss of function of the normal huntingtin protein also contributes to the disease. Researchers have identified several potential mechanisms of pathogenesis in HD and are currently focusing on identifying potential therapeutic targets that could help to ameliorate the symptoms of this debilitating disorder.

The mutation in the huntingtin gene is the starting point for a series of events that lead to the degeneration and death of these neural populations. However, the molecular mechanisms that result in the selective death of striatal neurons are still unknown. Huntingtin is present in all brain neurons and in other non-neuronal tissues, and its expression does not particularly correlate with the pattern of neuronal degeneration.

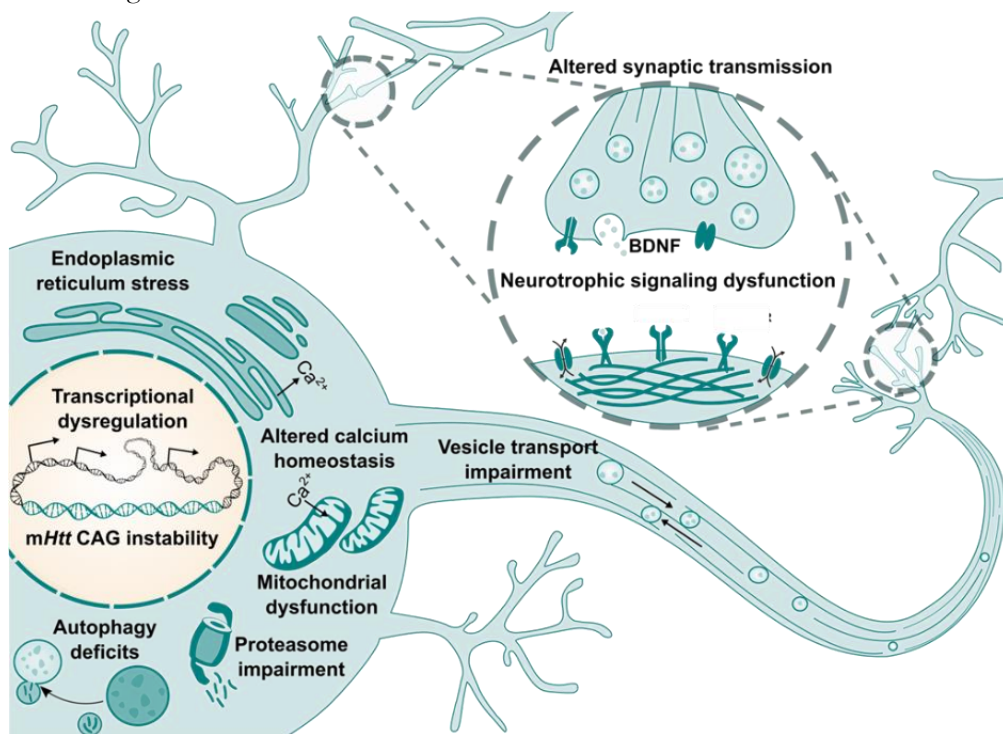


Figure 24. Scheme summarizing the main HD pathophysiological hallmarks.

*Edited from Dra. Nuria Suelves.*



### 4.3. Current Therapeutic Strategies

There is currently no disease-modifying or curative treatment for HD. The treatments that are available target specific symptoms and include movement-suppressing drugs, antidepressants, and physical therapy<sup>251</sup>:

Chorea medication	Antipsychotic medication	Antidepressants (SSRIs)	Mood stabilizers
<ul style="list-style-type: none"> <li>• Tetrabenazine</li> <li>• Deutetrabenazine</li> </ul>	<ul style="list-style-type: none"> <li>• Olanzapine</li> <li>• Risperidone</li> </ul>	<ul style="list-style-type: none"> <li>• Citalopram</li> <li>• Fluoxetine</li> <li>• Sertraline</li> </ul>	<ul style="list-style-type: none"> <li>• Lamotrigine</li> <li>• Carbamazepine</li> </ul>

There are currently several ongoing clinical trials trying to target different aspects of the disease (Figure 25). Regarding the whole spectrum of therapeutic strategies, the huntingtin lowering trials are the most significant ones. Their rationale is to diminish the levels of the expression of the mutated protein that causes the disease. Nevertheless, there is still not cure for Huntington's Disease.

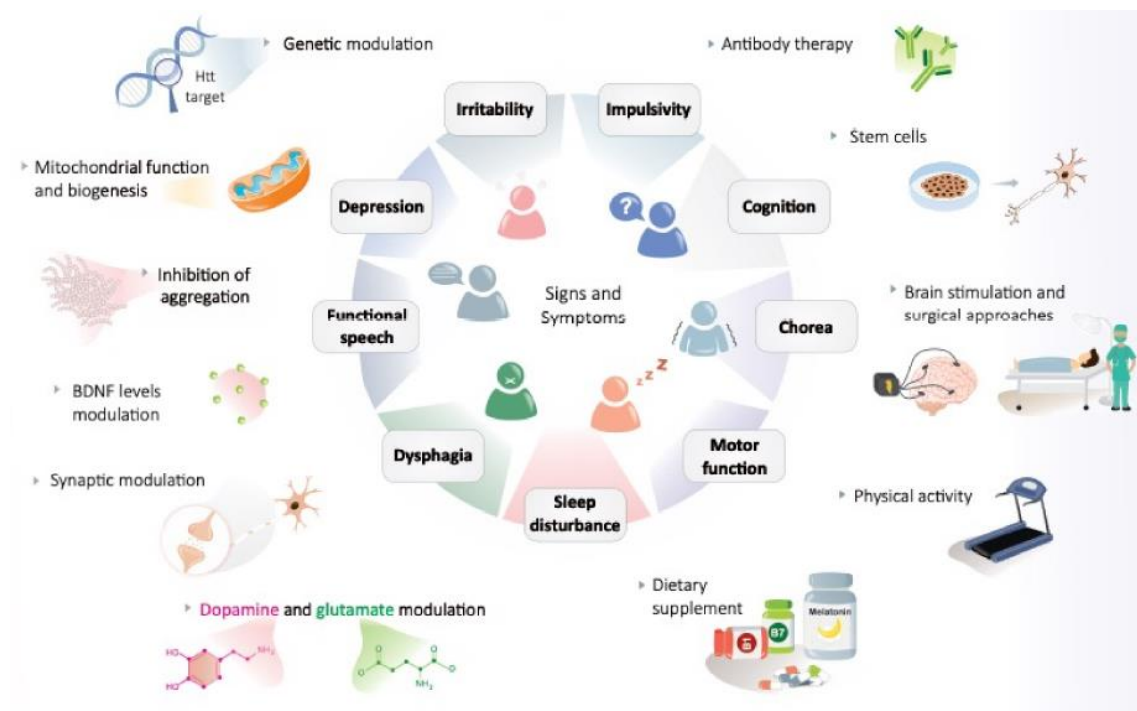


Figure 25. Summary of the ongoing clinical trials for HD. Edited from Kim et al. (2021).

## 4.4. Neurodevelopment in Huntington's Disease

### 4.4.1. Huntingtin role during normal development

Htt is crucial for the organism development, and the absence of Htt is lethal in mice around developmental day E7.5–8.5<sup>252,253</sup>. In this line, the decreased level of wild-type Htt (10–15% of normal levels) in mouse embryos, followed by reconstitution of Htt expression to normal level on postnatal day 21, resulted in progressive striatal and cortical neuronal degeneration and motor incoordination later in life<sup>254</sup>. Moreover, mice with a deletion of Htt in Gsh2 lineages exhibit striatal neurodegeneration and motor deficits, similar to those observed in HD<sup>255</sup>. A recent study also confirmed these findings by performing a cell-type specific deletion of Htt in MSNs using transgenic mice<sup>256</sup>. The loss of Htt in iMSNs led to a reduction of GABAergic synapses in the GPe and behavioral hyperactivity, while the loss of Htt in dMSNs led to increased inhibition of the SNr and hypoactivity in mice. These specific deletions of Htt induced HD-like alterations in adulthood, including MSN loss, motor alterations, and reactive gliosis observed in 10-month-old mice. These results suggest that Htt is necessary for maintaining basal ganglia circuit integrity and that the loss of function of the protein during the earlier developmental period may contribute to the adult alterations observed in HD. Htt is also essential for the mitotic spindle formation and orientation. Htt depletion during embryonic cortical neurogenesis leads to an incorrect spindle orientation, resulting in a decreased number of proliferating progenitors and an increase in differentiation due to an imbalance in symmetric vs. asymmetric divisions<sup>257–259</sup>.

### 4.4.2. Developmental alterations in HD models

HD-related developmental alterations have been recently described in a large variety of *in vitro* HD models, while less is known in the *in vivo* HD models. HD-associated defects are found in human embryonic stem cells (hESCs) as early as the neurulation stage, showing morphogenic alterations in the neural tube due to a loss of function of the huntingtin protein<sup>16</sup>. In keeping with this view, the HD-iPSC consortium has demonstrated that HD-derived induced pluripotent stem cells (iPSCs) show differentially expressed genes versus control cells during *in vitro* differentiation, with one third of these genes having functions in pathways regulating neuronal development and maturation<sup>260</sup>. Furthermore, knock-in mouse models of HD exhibit impairments in striatal striosome and matrix functional compartmentalization and aberration in the maintenance and maturation of MSN neural stem cell precursors<sup>17</sup>. During the postnatal phase, there were modifications in the striatal cytoarchitecture, characterized by a decrease in the expression of the striosomal marker,  $\mu$ OR, at P2, while the matrix marker, calbindin, exhibited a modified mosaic pattern at P7. These anomalies were solely observed in the striatum, which suggests that there is a particular variation in the maturation of striatal neurons and an increased susceptibility to damage<sup>261</sup>. Additionally, it has been observed in zQ175 mice, that the growth of dendritic spines in the striatum appears to be accelerated at P21, but without any notable alteration in the number of cortical or thalamic striatal synapses<sup>262</sup>. On the other

hand, in Q140 mice the quantity of VGLUT2-positive axodendritic thalamic terminals in the striatum is reduced by 40% at 1 month in comparison to wt mice<sup>263</sup>. Moreover, during the first postnatal week, HD mice have less corticallayer 2/3 excitatory synaptic activity than wild-type mice, express fewer glutamatergic receptors, and show sensorimotor deficits<sup>264</sup>. Intriguingly, recent research has demonstrated that expressing mHtt selectively during development, starting from the embryonic phase to P21, is enough to create an HD-like phenotype in later adult stages, which specifically involves striatal neurodegeneration, motor coordination impairments, modified corticostriatal connectivity, and altered striatal electrophysiological activity<sup>254</sup>.

#### 4.4.3. Developmental alterations in CAG expansion human carriers

By histologically analyze cortical tissue from gestational week (GW) 13 fetuses carrying the CAG expansion, it was shown that mHTT is not correctly located at junctional complexes and disrupts the polarity of human and mouse neuroepithelium. This interferes with the cell cycle of apical progenitors, resulting in fewer proliferating cells and more neural progenitors entering lineage specification prematurely. Large-scale studies in humans (PREDICT-HD and TRACK-HD) showed reduced striatal size in premanifest individuals<sup>18–20</sup>. A recent study in children and adolescents (age 6–18) with a parent or grandparent diagnosed with HD underwent MRI. Seventy-five individuals were HTT gene-expanded (GE) and 97 individuals were gene-nonexpanded (GNE). Age-related striatal volume changes differed significantly between the GE and GNE groups, with initial hypertrophy and more rapid volume decline in GE (Figure 26). A similar age-dependent group difference was observed for the globus pallidus, but not in other major regions. This diminished striatal volume could be seen up to 15 years before the appearance of the first symptoms<sup>19–21</sup>, suggesting that pathogenesis of HD begins with abnormal brain development.

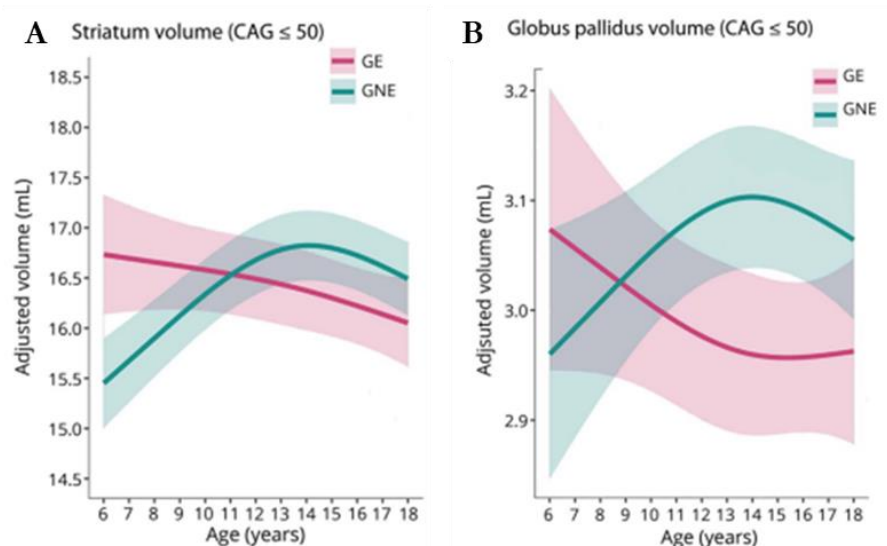


**Figure 26. Abnormal brain development in HD mutation carriers. A)** Mean estimated age-dependent change of striatal volume in the GE (red) and GNE (green) groups. **B)** Mean estimated age-dependent change of the globus pallidus. Image edited from Van Der Plas, E., et al. (2019).

# OBJECTIVES

---



# *OBJECTIVES*

## **Objectives**

In this thesis we aimed to characterize the specific developmental alterations that occur during the striatal development in HD.

1. To characterize the developmental gene expression profile in HD mouse model.
2. To study neurogenesis during HD development.
3. To identify specific NPCs subpopulations altered during HD development.



# MATERIALS AND METHODS

---





# Materials and Methods

## 1 Animal Procedures

### 1.1. General

Animals were housed with access to food and water *ad libitum* in a colony room kept at 19-22 °C and 40-60% humidity, under a 12:12 h light/dark cycle. Experimental procedures involving the use of animals were performed according to the European (2010/63/EU) Guide for the Care and Use of Experimental Animals and the ARRIVE guidelines. They were approved by the Animal Experimentation Ethics Committee of the University of Barcelona (14/19 P9).

### 1.2. Huntington's Disease Mouse Model zQ175

As a HD model we used the zQ175 mouse model (B6J.129S1-Httm1Mfc/190ChdJ) which was obtained from CHDI (CHDI-81003003).

Since the identification of the mutation HTT in 1993, many mouse models of HD have been created to explore the disease. Among these models, full-length Htt knock-in (KI) models most accurately imitate the human disease genetically because the expression of the mutant Htt is in the correct genetic and protein context. Nonetheless, most KI mouse models in which the expanded CAG repeat is inserted into the mouse Htt typically show more subtle behavioral, histopathological, and molecular phenotypes compared to the transgenic models that overexpress mutant Htt<sup>265</sup>.

The zQ175 knock-in model of HD, was generated by replacing the mouse full-length mouse Htt locus with the mutant human HTT exon 1. The zQ175 mouse model, was originated from a spontaneous germline expansion in the CAG copy number in the CAG 140 knock-in colony (Figure 27), exhibiting clear behavioral impairments in both heterozygous and homozygous mice<sup>266,267</sup>. The zQ175 model displayed decreased body weight, motor deficits, brain atrophy, altered brain metabolites, and a reduction in striatal gene markers<sup>267</sup>.

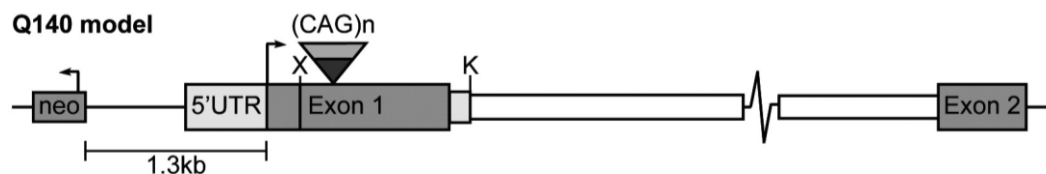


**Figure 27. Q140 mouse model genetics.** A spontaneous expansion of the CAG copy number within the exon 1 gave rise to the zQ175 HD mouse model.

### 1.3. Reporter Mouse Lines Generation

With the objective of selectively label and analyse the three different striatal neuron subpopulations (dMSNs, iMSNs and Interneurons), we used these four different reporter mice:

- DRD1-CRE line was generated by the laboratory of Dr. Ming Xu (B6;129-Tg(Drd1-cre)120Mxu/Mmjax)<sup>268</sup>, which was available in our lab.
- A2A-CRE line was generated by the laboratory of Dr. Alban de Kerchove<sup>269</sup>, which is available in our lab.
- Nkx2.1-CRE line was kindly provided by Dr. Egea J., which was available in our lab.
- tdTomato reporter mice was used to recombine with DR1, A2A or Nkx2.1-mediated CRE expression, (B6.Cg-Gt(ROSA)26Sortm14(CAG-tdTomato)Hze/J), which was available in our lab.

C57BL/6J (WT) and zQ175 (HD mouse model) were used and cross mated with reporter mice Drd1-CRE-Tomato (for tracking dMSNs cells), A2A-CRE-Tomato (for tracking iMSNs cells) and Nkx2.1-CRE-Tomato (for tracking interneurons) to obtain: wt/Q175;Drd1-CRE;tdTomato, wt/Q175;A2A-CRE;tdTomato and wt/Q175;Nkx2.1-CRE;tdTomato.

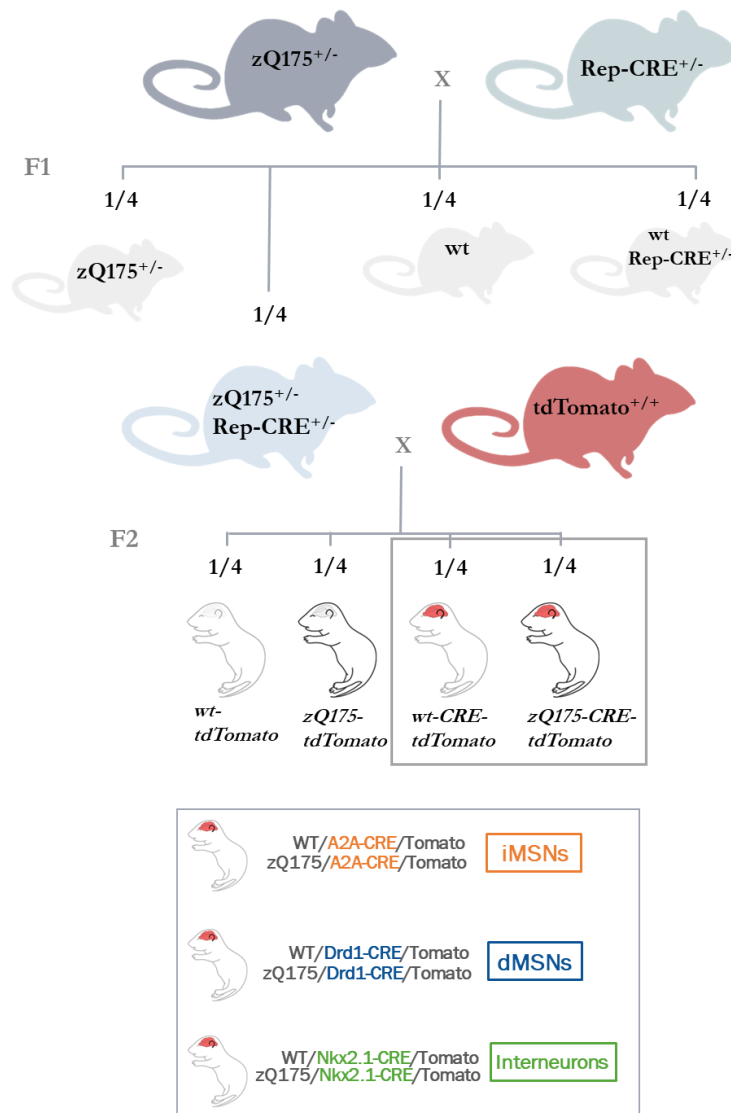


**Figure 28.** Schematic representation of the mouse crossmates performed to obtain the reporter mice.

## 2 *Histological and Molecular Assays*

---

### 2.1 Embryonic sample obtention for histological analysis

Wt females and zQ175 males were cross mated to obtain wt and HD littermates. The day of pregnancy, determined by the first detection of a vaginal sperm plug in daily inspection, was considered E0.5. Females were sacrificed by cervical dislocation at different developmental stages (E12.5, E14.5, E16.5 and E18.5) and embryos were taken by a caesarean section.

#### For embryonic fixed tissue:

Embryo heads were collected and fixed in 4% paraformaldehyde (PFA, Merk Millipore) overnight, cryoprotected following a 15%-30% sucrose/PBS gradient, and finally precooled in 2-methyl-butane for two minutes and then stored at -80°C.

#### For embryonic fresh/frozen tissue:

Some samples were directly precooled in 2-methyl-butane for two minutes and then stored at -80°C for specific antibody's requirement.

### 2.2 Adult sample obtention for histological analysis

For postnatal analysis, mice were deeply anesthetized with pentobarbital and intracardially perfused with PBS and a 4% PFA solution in 0.1 M phosphate buffer. Brains were removed and post-fixed overnight in the same solution, washed three times with PBS, cryoprotected with 15%-30% sucrose gradient in PBS and frozen in dryice cooled methylbutane (Sigma).

### 2.3 Cryosectioning

Serial coronal sections (16 µm) of the brain are obtained using a cryostat (Termo Fisher). Samples were embeded in Tissue-Tek® O.C.T.™ (Sakura, 4583) and allowed to freeze. Brain slices were collected into EpreDia™ SuperFrost Plus™ Adhesion slides (Termo Fisher, 12312148).

#### For embryonic tissue:

- Criostat object temperature: -16°C
- Criostat chamber temperature: -19°C
- Number of series: 6 (stages until E14.5) and 8 (stages from E16.5).

#### For postnatal tissue:

- Criostat object temperature: -21°C
- Criostat chamber temperature: -24°C
- Number of series: 10

## 2.4 Immunohistochemistry (IHC)

Fluorescent immunolabeling was performed for the following analysis:

- Phosphohistone 3 (PH3) labelling for the cell cycle phase analysis at E12.5, E14.5 and E16.5.
- Cleaved Caspase 3 (Casp3) labelling for the cell death analysis at E12.5, E14.5, E16.5, E18.5 and P5.

Fluorescent immunolabeling was performed according to the following protocol:

Tissue fresh-frozen samples were treated with fresh PFA 4% for 10 minutes (this step was avoided when working with fixed-frozen samples). Then, 3 washes with PBS were performed and tissue sections were blocked for 1 h in PBS containing 0.3% Triton X-100 and 1% bovine serum albumin (BSA) to avoid non-specific binding. Following the blocking step, samples were incubated overnight at 4°C in PBS containing 0.3% Triton X-100 and 1% BSA with the corresponding primary antibodies. Next day, tissue sections were washed three times with PBS and were incubated for 2 hours at RT with the secondary antibody in PBS + 0.3% Triton X-100 and 1% BSA. Finally, tissue sections were mounted in DAPI Fluoromount-G (SouthernBiotech, 0100-20) (60 µl/slide). No signal was detected in control preparations from which the primary antibody was omitted.

Antigen	Origin	Reference	Dilution	Company
Cleaved Caspase 3 (C-Casp 3)	Rabbit	9661S	1:200	Cell Signaling Technology
Phosphohistone 3 (PH3)	Mouse	9706S	1:500	Cell Signaling Technology
Alexa-488 anti mouse	Donkey	715-545-150	1:500	Jackson Immuno Research
Alexa-488 anti rabbit	Donkey	711-545-152	1:500	Jackson Immuno Research

Table 1. Summary of the Antibodies used during this thesis.

## 2.5 EdU analysis

The 5-ethynyl-2'-deoxyuridine (EdU, C10337 Invitrogen) is a nucleotide analogous to thymidine that is incorporated into DNA during its synthesis. EdU is used to assay DNA synthesis in cell culture and detect cells in embryonic, neonatal and adult animals which have undergone DNA synthesis.

EdU solution was freshly prepared in PBS and intraperitoneally injected in pregnant mice (50mg/Kg) at the specific time points of interest.

### 2.4.1. S-phase labelling

To label S-Phase cells, wt pregnant females (crossmated with zQ175 males) were injected intraperitoneally with EdU. EdU is administered at E12.5, E14.5, and E16.5. After 30 minutes, embryos were taken by caesarean section and processed as described in section 2.1.

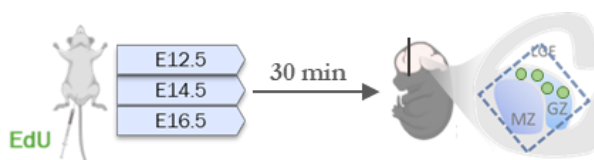


Figure 29. Schematic representation of S-Phase labelling experiments.

### 2.4.2. Birthdating

To study birthdating, wt pregnant females (crossmated with zQ175 males) were injected intraperitoneally with EdU. EdU is administered at E12.5, E14.5, and E16.5, and the embryos were subsequently allowed to develop until E18.5, when embryos were taken by caesarean section and processed as described in section 2.1.

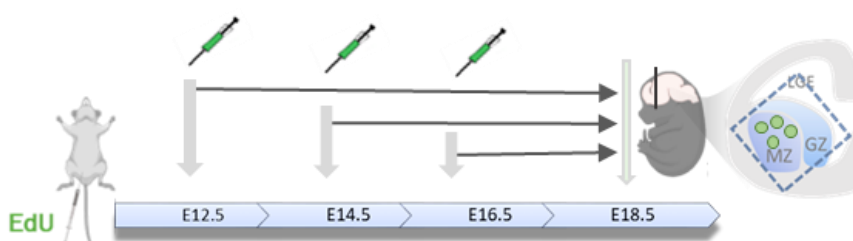


Figure 30. Schematic representation of birthdating analysis.

### 2.4.3. Neurogenesis

To study neurogenesis, tdTomato pregnant females (crossmated with Q175;Drd1-CRE, Q175;A2A-CRE or Q175;Nkx2.1-CRE males) were injected intraperitoneally with EdU. EdU is administered at E12.5, E14.5, and E16.5, and the embryos were subsequently allowed to develop until E18.5, at which point embryos were taken by caesarean section and processed as described in section 2.1.

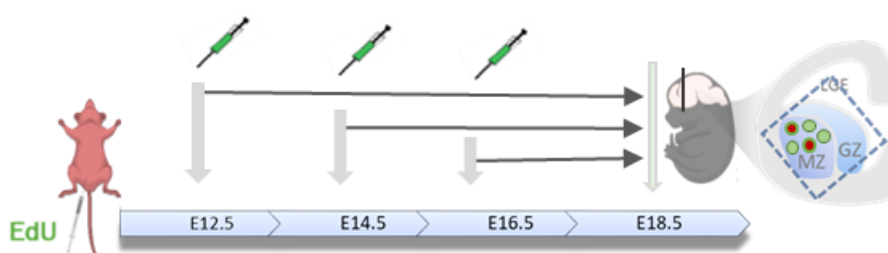
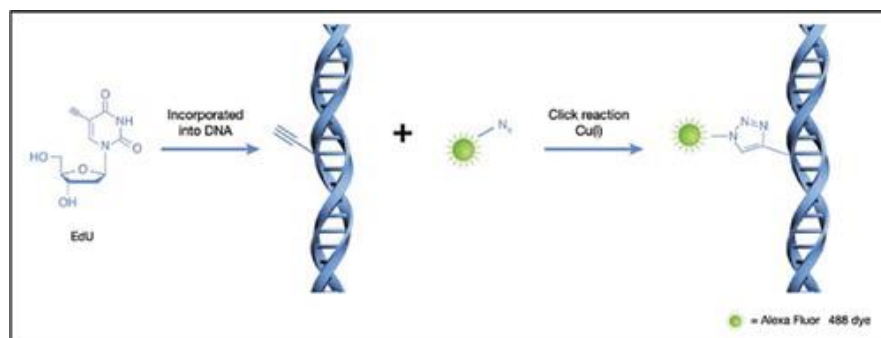


Figure 31. Schematic representation of the neurogenesis experiments.

## 2.4.4. EdU Detection

The detection of EdU is based on a copper-catalyzed covalent reaction between an acid and a base. In this reaction the EdU acts as a base and the fluorescent marker Alexa Fluor acts as an acid. Thanks to the small size of this Alexa Fluor acid, using an aldehyde-based fixation and a permeabilization with detergent is sufficient for the fluorescent marker to reach the built-in EdU (Figure 32).



**Figure 32. Illustration of the EdU Click-it kit reaction.** The click reaction between the ethynyl group of the incorporated EdU in the doublestranded DNA and the Alexa Fluor 488 azide. The illustration represents the formation of the triazole bond between the alkyne and the azide.

The slides with the tissue were washed 3 times with PBS and the commercial Click *iT* Edu Alexa Fluor 488 Imaging Kit (C10337, Invitrogen) was used for the detection of EdU. The slides were incubated with the EdU Click *iT* reaction following the manufacturer's instructions.

Click *iT*® Edu reaction: 1 reaction was used for 2 slides (250 µl/slide) (Figure 33). Depending on the number of slides of each analysis, different total reaction volumes were prepared. All the reactives are provided by the kit and the mix must be prepared just before using (after 30 minutes the reaction is lost). The slides were incubated for 30 minutes with the Click *iT*® Edu reaction at RT, then slides were washed twice with PBS and mounted with DAPI-Fluoromount G (SouthernBiotech, 0100-20) (60 µl/slide).

Reaction components	Number of reactions							
	1	2	5	10	15	30	50	100
PBS, D-PBS, or TBS	438 µL	875 µL	2.19 mL	4.38 mL	6.57 mL	13.2 mL	21.9 mL	43.8 mL
CuSO <sub>4</sub> (Component F)	10 µL	20 µL	50 µL	100 µL	150 µL	300 µL	500 µL	1 mL
Fluorescent dye azide (prepared in step 1.3)	2.5 µL	5 µL	12.5 µL	25 µL	37.5 µL	75 µL	125 µL	250 µL
Reaction Buffer Additive (prepared in step 5.1)	50 µL	100 µL	250 µL	500 µL	750 µL	1.5 mL	2.5 mL	5 mL
Total reaction volume	500 µL	1 mL	2.5 mL	5 mL	7.5 mL	15 mL	25 mL	50 mL

**Figure 33. Click *iT*® reaction cocktails.** Table from the Manual of Click-*iT*® EdU Flow Cytometry Assay Kits of Life Technologies.

## 5.1. Fluorescence *in situ* hybridization (FISH)

Fluorescent *in situ* hybridization is a very useful method to observe and quantify specific RNA species *in situ*, as it can detect target RNA within intact cells. FISH was performed for the HELT labelling in cryosections of E14.5 and E16.5 wt and Q175 embryos.

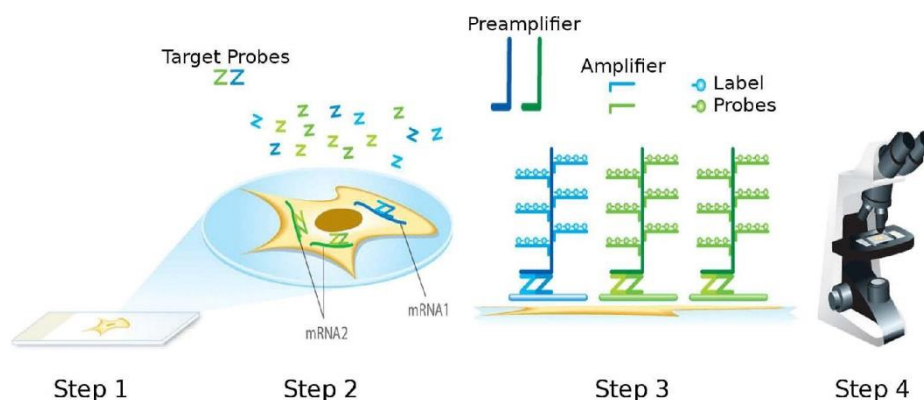


**Figure 34. Schematic of the RNAscope assay procedure.** In step 1, cells or tissues are fixed and permeabilized to allow for target probe access. In step 2, target RNA-specific oligonucleotide probes (Z) are hybridized in pairs (ZZ) to multiple RNA targets. In step 3, multiple signal amplification molecules are hybridized, each recognizing a specific target probe, and each unique label probe is conjugated to a different fluorophore or enzyme. In step 4, signals are detected using a fluorescent microscope. Wang et al. (2012) J. Molec. Diag. 14:22.

### 5.1.2. Probe design:

We first customized a new probe for HELT RNA. To do so, we performed a multiple sequence alignment of the different splice variants of the RNA, by using the CLUSTAL 2.1 software.

- Helt bHLH transcription factor (Helt)  
NCBI Reference Sequence: NM\_173789.4
- Mus musculus helt bHLH transcription factor (Helt), transcript variant X1  
NCBI Reference Sequence: XM\_006509389.3
- Mus musculus helt bHLH transcription factor (Helt), transcript variant X2  
NCBI Reference Sequence: XM\_011242213.2
- Mus musculus helt bHLH transcription factor (Helt), transcript variant X3  
NCBI Reference Sequence: XM\_030243446.1

From that analysis, we selected the nucleotide region that was conserved among the different variants:

```

1  agcttttagc agaatttgcc aactacttcc actacgggta ccacgagtgc atgaagaacc tggcgacta cctcaccacc gttgagcggg
91  tggagaccaa agacaccaag tatgcgcgca tctcgcctt cttgcaatcc aaggcccgcc tggcgccgga gccacacatt
171 cgcgcgtct cgttccgga gccagatttc tctatcagc tgcattgagc aagccagag ttccggggcc acagccagg
251 tgaagccaca atgtcccgcc agggggctac ccagggtca ttccatggc ctctggagc tgccgcagc ccagcactgc cttactgtc
341 cagcgcgacg gtacctctcc ccagccggc acagcagcac agcccttct tggctccgat gcagggcctg gaccggcatt
421 atctcaatct gatcgccat ggccaccca acggcctcaa cctgcacag cccagcacc ctccgtgct ctga

```

### 5.1.3. FISH:

FISH was performed using the RNAscope Multiplex Fluorescent Detection Kit (PN 320851), with the HyBEZ™ II Hybridization System for Manual Assays, following the manufacturer's instructions.



## 5.2. Quantitative Polymerase Chain Reaction

Quantitative PCR was performed to quantify the relative RNA expression of HELT in:

- LGEs from E12.5 and E14.5 wt and Q175 embryos.
- MGEs from E12.5 and E14.5 wt and Q175 embryos.
- Striatum from E16.5 wt and Q175 embryos.

### 5.2.1. Sample Obtention

The striatal tissues of interest (LGEs, MGEs and striatum as a whole) were microdissected and rapidly flash-frozen in precooled in 2-methyl-butane, separately.

### 5.2.2. RNA extraction

Total RNA was extracted using the RNeasy Micro Kit (74004 Qiagen), following the manufacturer's instructions.

### 5.2.3. cDNA synthesis

Total RNA (500 ng) was used to synthesize cDNA using random primers with the High-Capacity cDNA Reverse Transcription Kit (Applied Biosystems, CA4368813) according to the manufacturer's instructions.

### 5.2.4. Q-PCR

The cDNA was then analyzed by quantitative-polymerase chain reaction (qPCR) as previously described (Martín-Ibáñez et al. 2007) using the TaqMan gene expression assays (Applied Biosystems, 4304437). To specifically recognize mHELT, we used the TaqMan probe Mm00723333\_g1 (FAM-MGB). We used 18S (HS99999901\_s1, Taqman) gene expression as an internal loading control. QPCR was carried out in reaction buffer containing 12.5 µl Brilliant qPCR Master Mix (Stratagene), 1.25 µl TaqMan gene expression assays, and 20–30 ng of cDNA. To provide negative controls and exclude contamination by genomic DNA, the reverse transcriptase was omitted in the cDNA synthesis step, and samples were subjected to the PCR reaction in the same way for each TaqMan gene expression assay.

The qPCR data was analyzed using the 7500 System SDS Software. Cts were extracted and quantified using the formula:

$$\Delta Ct = Ct (HELT) - Ct (18S)$$

$$\Delta\Delta C = \Delta Ct - (\text{media of HELT LGE E14.5 WT Cts})$$

All qPCR assays were performed with at least 3 samples for each condition of study and with at least two technical replicates. Analysis and graphs were performed using GraphPad, and the results were expressed as LogFoldChange ( $2^{-\Delta\Delta Ct}$ ).

## 2.6 Image acquisition

Images were taken using a Confocal LSM880 Zeiss Microscope from the Unitat de Microscòpia Òptica Avançada (CCiTUB) service of the University of Barcelona (UB).

## 2.7 Measurement of volumes and in vivo cell counts

### Cell number quantification:

Unbiased stereological counts were performed using the Visiopharm's newCAST™ (VIS) software. The number of positive cells in the striatum, GZ or MZ, was estimated using the optical dissector method. The chosen grid size was 5-8 % of total counted area. The unbiased counting frame was positioned randomly, thereby creating a systematic random sample of the area. Sections were viewed under a 40x objective. Gundersen coefficients of error were all less than 0.10.

### Volume quantification:

The volumes of certain brain regions such as striatal GZ or MZ in embryos, or postnatal brains were measured using the VIS software software attached to an Olympus microscope (Olympus Danmark A/S, Ballerup, Denmark). Consecutive 16 µm-thick sections (10 sections/animal) for adult mice or 16 µm-thick sections (6 sections/animal) for embryos/postnatal mice were viewed, and the borders of the anatomical landmarks were outlined. The volumes were calculated by multiplying the sum of all section areas (µm<sup>2</sup>) by the distance between successive sections (16 µm) as described in (Canals et al. 2004).

### Statistical analysis:

All results are expressed as the mean of independent experiments  $\pm$ s.e.m. and results were analysed using Student's t-test. We considered statistical significance  $p < 0.05$  (\*) and  $p < 0.01$  (\*\*).

### 3 Bulk RNA-sequencing

---

#### 3.1 Sample obtention for bulk RNA-seq analysis

Laser microdissection (MDL) was performed at the development stage E16.5 in order to isolate and obtain the GZ and MZ regions of LGE, for subsequent RNA analysis. A minimum of 4 biological replicates per genotype were used.

##### 3.1.1. Sampling and rapid freezing of tissue with 2-methyl-butane (isopentane)

We first pre-freezed 2-methyl-butane (Sigma Chemical Co.) in dry ice, controlling its temperature with a thermometer to ensure a good freezing. A good rapid freezing process will minimize the appearance of cracks.

The pregnant female is sacrificed by cervical dislocation at gestational stage E16.5 (considering the vaginal plug E0.5) and the embryos were taken by caesarean section. The heads were obtained by beheading and submerged in the 2-methyl-butane immediately for 2 minutes. After this time, heads were deposited in an Eppendorf (1.5 ml) in dry ice to maintain the temperature. A section of the embryo (tail or leg) was also taken for genotyping (PCR). This procedure was performed embryo by embryo, not simultaneously to avoid confusion between any frozen and body and thus obtain a correct genotyping of each sample. The queues were stored at -20°C if DNA is not extracted instantly. Frozen heads are stored at -80°C until the day of their sectioning.

##### 3.1.2. Sterilizing Membrane Slides

Special Glass, PEN-membrane (25 mm x 76mm) slides were used.

Slides were covered cover with RNasa ZAP for 5 minutes.

Subsequently, they were washed with H<sub>2</sub>O DEPC and allowed to dry.

Finally, they were irradiated with UV light for 30 minutes.

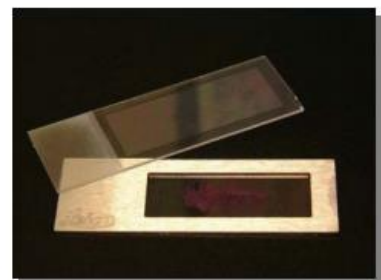


Figure 35. Slides: Glass, PEN-membrane (25mm x 76mm).

##### 3.1.3. Sectioning

The striatal primordium was sectioned at 16µm starting from the more rostral to the more caudal striatum. The cryostat was previously cleaned with ethanol and RNasa ZAP to avoid contamination. The 16 µm sample sections were immediately placed on the slides for laser microdissection (MembraneSlides).

- Object temperature: -16 °C
- Knife temperature: -19 °C

### 3.1.4. Hematoxylin and eosin staining

Once all the striatal tissue was cryosectioned and placed on the slides, we immediately proceed to the hematoxylin and eosin protocol to stain cells and be able to recognize both GZ and MZ in the microdissection step.



**Figure 36. Hematoxylin-eosin staining protocol.** Hydration of the samples, staining with hematoxylin, washing with PBS-DEPC, staining with eosin and final dehydration of the samples.

1. 100% Ethanol (1')
2. 95% Ethanol (30'')
3. 70% Ethanol (30'')
4. 50% Ethanol (30'')
5. Hematoxylin (Sigma Aldrich) 1 minute
6. PBS DEPC (10'')
7. PBS DEPC (20'')
8. Eosin solution (Sigma Aldrich) 10 seconds
9. 70% ethanol (30'')
10. 95% ethanol (30'')
11. 100% ethanol (1') or air-dry at room temperature

Once dry, the slides were stored in sterile falcons (50 ml) at -80°C until microdissection.

Important:

All the material was treated with RNase ZAP (clamps, doors, surfaces, etc.) H<sub>2</sub>O-DEPC and PBS-DEPC (both at 0.1%) were used. They were prepared by adding 1 ml of DEPC in 1 liter of MQ/PBS water, and leaving it in bell o/n. The next day, the DEPC was inactivated by autoclaving 15 minutes the solutions to break the DEPC into carbon dioxide and ethanol. The glass material was previously baked at 180°C for at least 8 hours. The whole procedure was done as quickly and coldly as possible, and the staining was done immediately after sectioning, without exceeding 30 minutes.

### 3.1.5. Laser Micro-Dissection (MDL)



Figure 37. Image showing the Leica Laser Micro-dissection system.

Slides with fixed and tinted cuts were left to defrost and can now be used for MDL. The microdissection was performed using the Leica Laser Microdissection Microscope D7000 (Figure 37) (following manufacturer's instructions). The slides were loaded onto the sample holder (slider) and loaded from 1 to 3 Eppendorf (RNase-free) 0.5 ml collection holder. Then, the position of the sample holder was selected (there are three possible if 3 doors are placed at once) and the section of the desired tissue for dissection was labelled with the MDL software, using the desired increases (Figure 38). The laser started and it was verified that the micro-dissected sections had been collected in the collection tube.

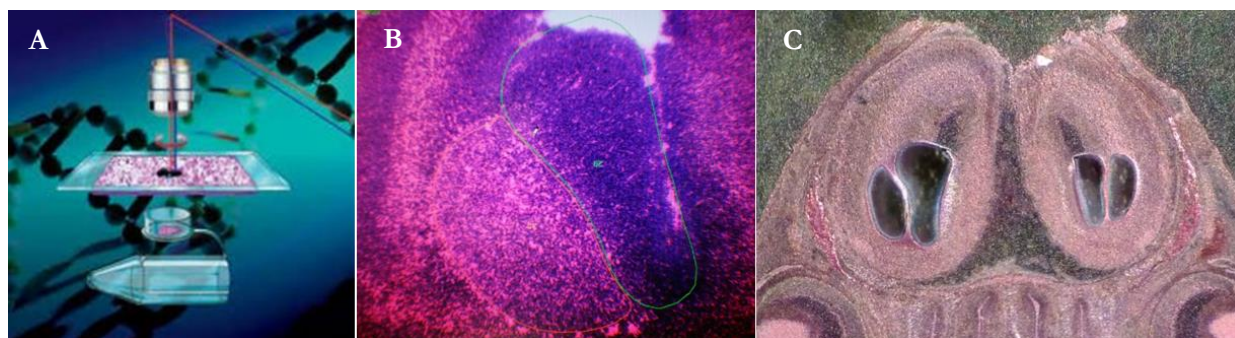


**Figure 38. Laser Micro-capture technique.** **A)** Schematic illustration of the laser capture technique: laser goes through the tissue, cuts it and the small piece falls to the tube tip. **B)** Example image of a E16.5 sample with the GZ and MZ region selection drawn, before laser activation. **C)** Example of an E16.5 tissue section after the laser region isolation.

The tubes were discharged very carefully (taking care that the sample does not jump), the lid was carefully closed and a small stirring was made to make the samples stay at the bottom of the tube. The lid was opened again and 75  $\mu$ l of Buffer RLT and 5  $\mu$ l of RNA-carrier were added. The samples were kept in carbonic snow until they reach the laboratory, where they were stored at  $-80^{\circ}\text{C}$  until the day of RNA extraction.

The laser microdissector is a service of IDIBAPS, whose MDLs are carried out in the Department of Functional Genomics of the Esther Koplowitz Center (CEK).

### 3.1.6. RNA Isolation

Samples of laser-dissected micro-dissected tissue present a particular challenge for molecular analysis, since nucleic acids must be purified from a very small amount of initial material. In addition, fixing and staining steps can compromise the integrity of RNA. RNeasy Kits allow efficient purification of total RNA from small to large amounts of starting material, including samples such as microdissected tissues and from small numbers of cells down to single cells.



Figure 39. Image of the RNeasy Micro Kit (74004 Qiagen).

RNA extraction of the collected samples (32 samples) was carried out with the RNeasy Micro Kit (74004 Qiagen), following the manufacturer's instructions. RNA was quantified using Nanodrop 1000 (Thermo Fisher Scientific Inc). The RNA obtained was sent to the National Center for Genomic Analysis (CNAG/CRG) for sequencing. RNA concentration, RNA purity and RNA integrity number (RIN) was quantified and showed optimal conditions.

## 3.2 Bulk RNAseq Downstream Analysis

Paired-end sequencing of total RNA was performed, with a read length of 75 base pairs with an Illumina HiSeq 2000 apparatus. Alignment/mapping was done with STAR/2.5.3a, and RSEM/1.3.0 software was used to quantify the abundance of RNA-seq transcripts. The *Mus musculus* reference genome GRCm38 was used and gencode vM21 was used for annotations.



## 4 Single Cell RNA-sequencing

### 4.1 Introduction:

The complex and intricate workings of biological systems arise from the collaborative actions of individual cells, each fulfilling its own unique role in the larger ensemble. However, due to this complexity, traditional bulk RNA-seq methods often fall short in gene expression research of organisms, tissues, or cell populations. The Single Cell Gene Expression solutions allows you to perform molecular and cellular characterization of cells. The 10X Genomics Chromium system (figure 40) uses a speedy technique that involves encapsulating individual cells in droplets through a process called gel bead in emulsion (GEM). This process involves labeling each gel bead with oligonucleotides that include a distinct barcode, a 10 bp unique molecular identifier (UMI), sequencing adapters/primers, and a 30 bp oligo-dT that is anchored.

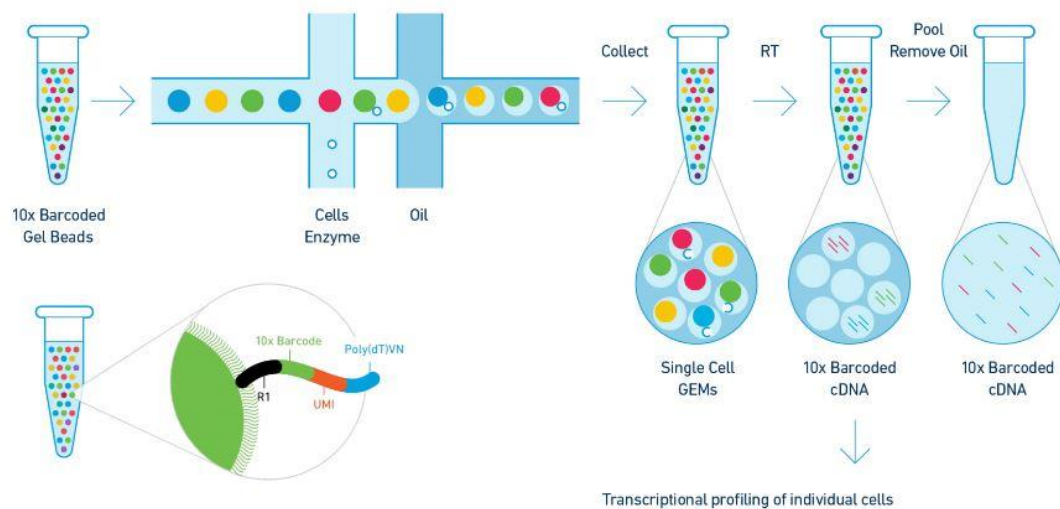


Figure 40. Chromium System is 10x GemCode™ Technology.

### 4.2 Sample obtention for single cell RNA-seq analysis

#### 4.2.1. Embryo obtention and maintenance

Wt females and zQ175 males were cross mated to obtain wt and HD littermates. Females were sacrificed by cervical dislocation at E14.5 and embryos were taken by a cesarean section and placed in 1xPBS on ice to clean the excess blood. Embryos were then placed in a new Petri dish with 1xPBS on ice. There, with the help of scissors and tweezers, the uterus was removed, and embryos were carefully separated between them, very careful not to break the umbilical cord. Then, an embryo was placed in a third Petri dish with 1xPBS under the magnifying glass. With the help of two tweezers, a small hole in the placenta was done, near the tail region, to take a little piece of the tail for genotyping.

This process was repeated with all embryos. Each embryo was placed in its corresponding well of the 12-wells plate, previously prepared with supplemented Hanks' Balanced Salt solution (HBSS) on ice. Finally, the 12 wells plate with the embryos was placed in a box with ice, inside the cold room. Meanwhile, DNA from the tail samples is extracted and samples are genotyped.

#### 4.2.2. Striatal dissection

Once known the genotype of each embryo, one of the embryos of interest was taken from the 12-wells plate and placed in a Petri dish with 1xPBS under the magnifying glass. The head was fixed by the eye using tweezers, the skin and the skull layers were removed, and the brain was isolated. Then, two scalpels were taken: one to hold the brain by the trunk and the other to open the right hemisphere until striatum was accessible. Then, the LGE (or striatum as a whole in E16.5) is removed by placing one scalpel on one side of the region and making "spoon" towards the other scalpel until it is removed. This process is repeated to isolate the LGE of the other hemisphere. Finally, both LGEs were placed in a 10ml tube prepared with 1 ml of HBSS, this will represent an n. We repeated this process with the second embryo of interest. Just 2 embryos (1 wt and 1 zQ175) from a littermate were processed each day.

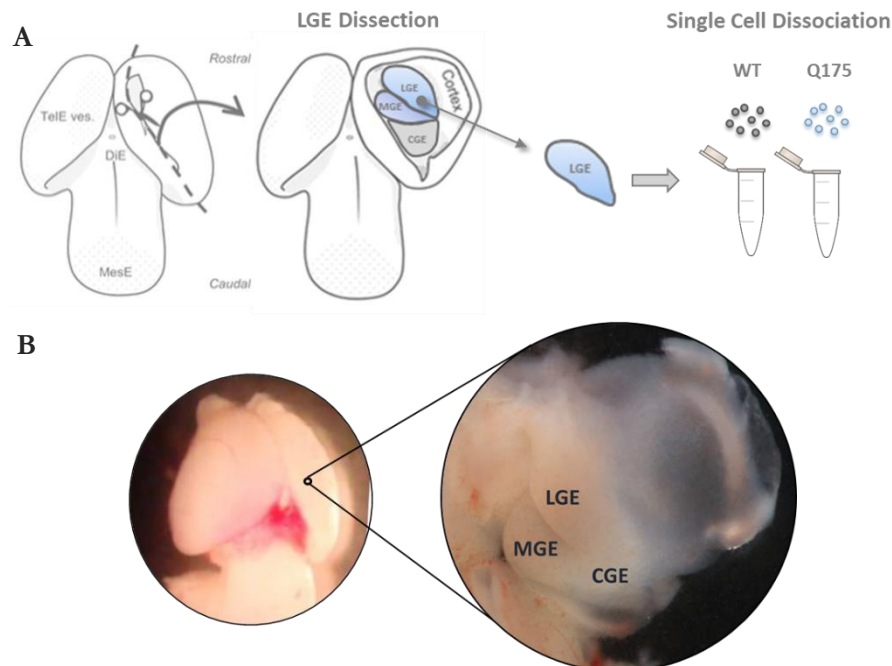


**Figure 41.** **A)** Schematic representation and images of the dissection of LGEs at E14.5: hemispheres were opened and LGE was isolated to dissociate cells into single-cell suspension for scRNA-seq. **B)** Images of the dissection process: opened right hemisphere showing the two ganglionic eminences, LGE and MGE.



#### 4.2.3. Cell disaggregation and quantification

Once we have the LGEs from the two embryos, we dissociate the tissue mechanically, using a previously flaming Pasteur pipette (up to 0.2-0.5 mm), by piping up and down the suspension 10 times. Then, Trypan Blue (T8154, Sigma) staining was used to quantify the total number of alive/death cells obtained.

#### 4.2.4. Sample delivery and sequantiation

Single cell suspensions are delivered in ice to the National Center for Genomic Analysis (CNAG/CRG). Illumina Sequencing Analysis Viewer, Illumina run specifications, FastQC, and Quality control alignment INS-017.

### 4.3 Bioinformatic Analyses of scRNA-seq data

To investigate human striatal development in both control and HD models, six human stem cells lines (three control-HD pairs: 1 hESC line and iPSC lines) were in vitro differentiated in the lab towards a striatal MSNs fate<sup>270</sup>. Three control and three HD PSC lines are differentiated towards MSNs using our in vitro differentiation protocol and analysed at the gene expression and functional level at various time points.

Single cell analysis was performed using the Smart-Seq2 protocol. Reads were aligned with STAR and gene expression was estimated with RSEM (GRCh38/GENCODE v32). Sample analysis was performed with Seurat. A graph-based clustering approach was employed for clustering the cells followed by UMAP dimensionality reduction. Finally, marker genes for each cluster were determined.

# RESULTS

---



# RESULTS

## 1 CHAPTER I: finding HD developmental alterations

### *Transcriptomic analysis of HD striatal developmental abnormalities*

Striatal primordia is formed by two important and very distinct regions, the proliferative zone or GZ and the post-mitotic zone or MZ. To study possible alterations during striatal development in HD, we isolated both GZ and MZ of E16.5 HD and wt mouse embryos using the laser capture microdissection (Leica LSM6) and then analyzed their transcriptomes by bulk RNA-seq. Two different analyses were performed from the obtained transcriptomic datasets (Figure 42).

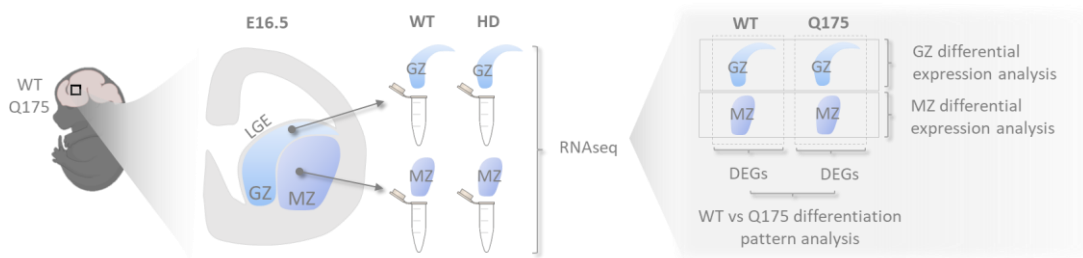


**Figure 42. Schematic representation of the methodology followed by the bulk RNA-seq analysis.** Wt and Q175 embryos were taken and GZ and MZ were isolated by laser micro-capture to specifically isolate the RNAs from both regions separately. After sequencing, two different analyses were performed: we first compared the gene expression pattern of both regions between genotypes, and then we extracted the differentiation expression pattern among each genotype and finally compare these patterns between genotypes.

#### 1.1. Differential expression analysis of wt and Q175 regions

We first compared the transcriptomic profiles from each region between genotypes. Applying Hierarchical Clustering of the GZ biological replicates did not cluster together and showed high variability (Figure 43 A-B). Only three genes presented significant False Discovery Rate ( $FDR < 0.05$ ) differences between genotypes, corresponding to one snRNA and two processed pseudogenes (IDs: Gm24924, Gm9030 and Gm13502, respectively). These genes presented very high  $\log_2$ FoldChange values: -20.996, 6.594 and 3.233, respectively. Applying Hierarchical Clustering of the MZ samples, all biological replicates clustered together showing robust results in the MZ (Figure 43 C, Figure 44 A). Highly significant ( $FDR < 0.05$ ) differences were observed between both genotypes. 1094 genes were differentially expressed genes (DEGs) in the MZ of HD embryos at E16.5, most of them (887 genes) being up-regulated (Figure 44 B). Different biotypes were dysregulated in HD samples, including “*To be Experimentally Confirmed*” (TECs) genes (50%), protein-coding genes (37%) and non-coding RNA (ncRNA) molecules (13%) (Figure 44 B). Down-regulated genes correspond mostly to protein-coding genes while up-regulated genes correspond to TECs, protein-coding genes and ncRNA (Figure 44 B). Within the protein-coding genes, approximately half of them were up-regulated and half down-regulated.

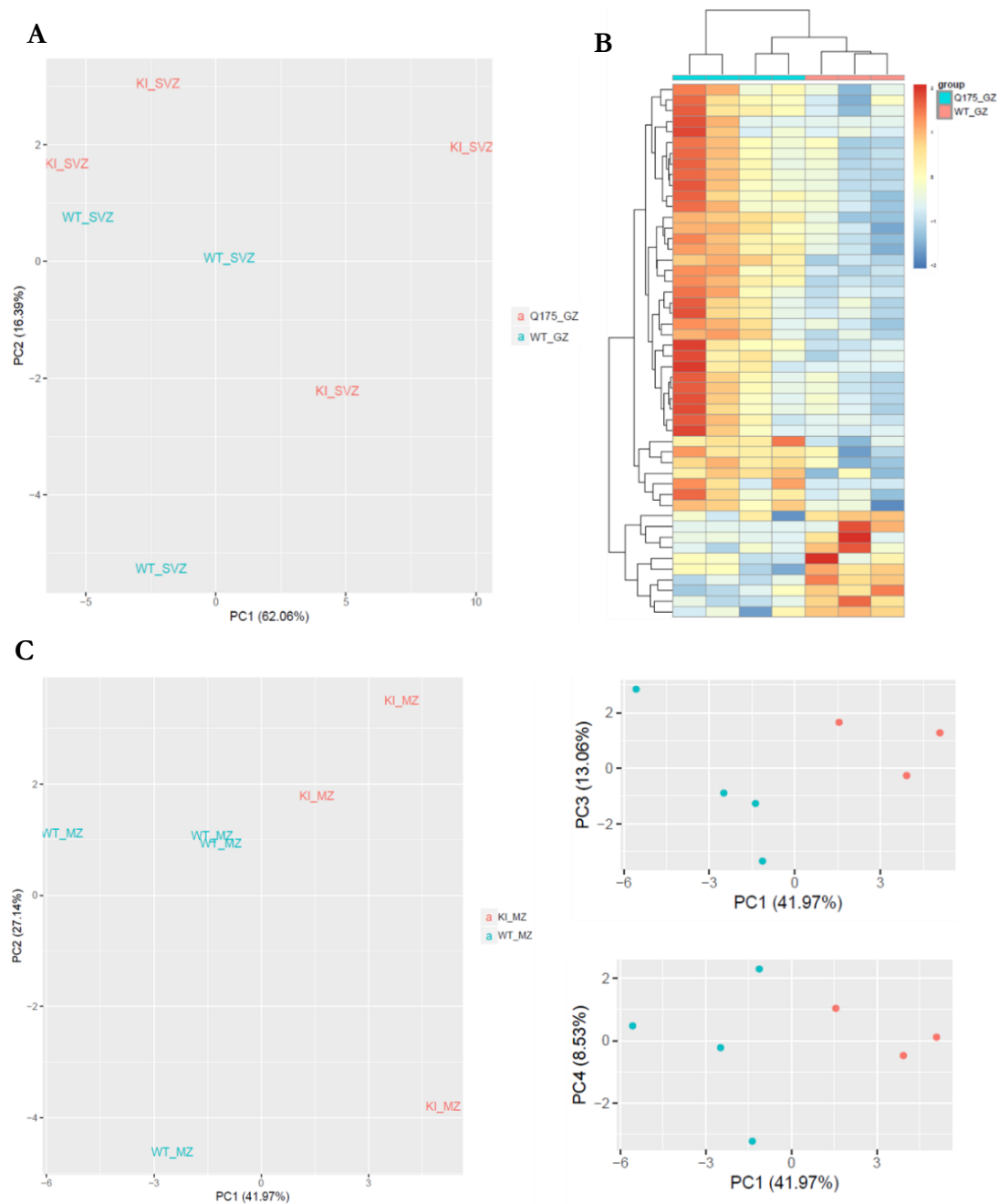


**Figure 43. Principal Component Analysis (PCA) of the region comparison between genotypes.** PCA **(A)** and Heatmap **(B)** obtained in the GZ comparison show a bad segregation of the samples. **(C)** Three different PCAs of the MZ comparison showing that HD and wt samples cluster together regarding genotype.

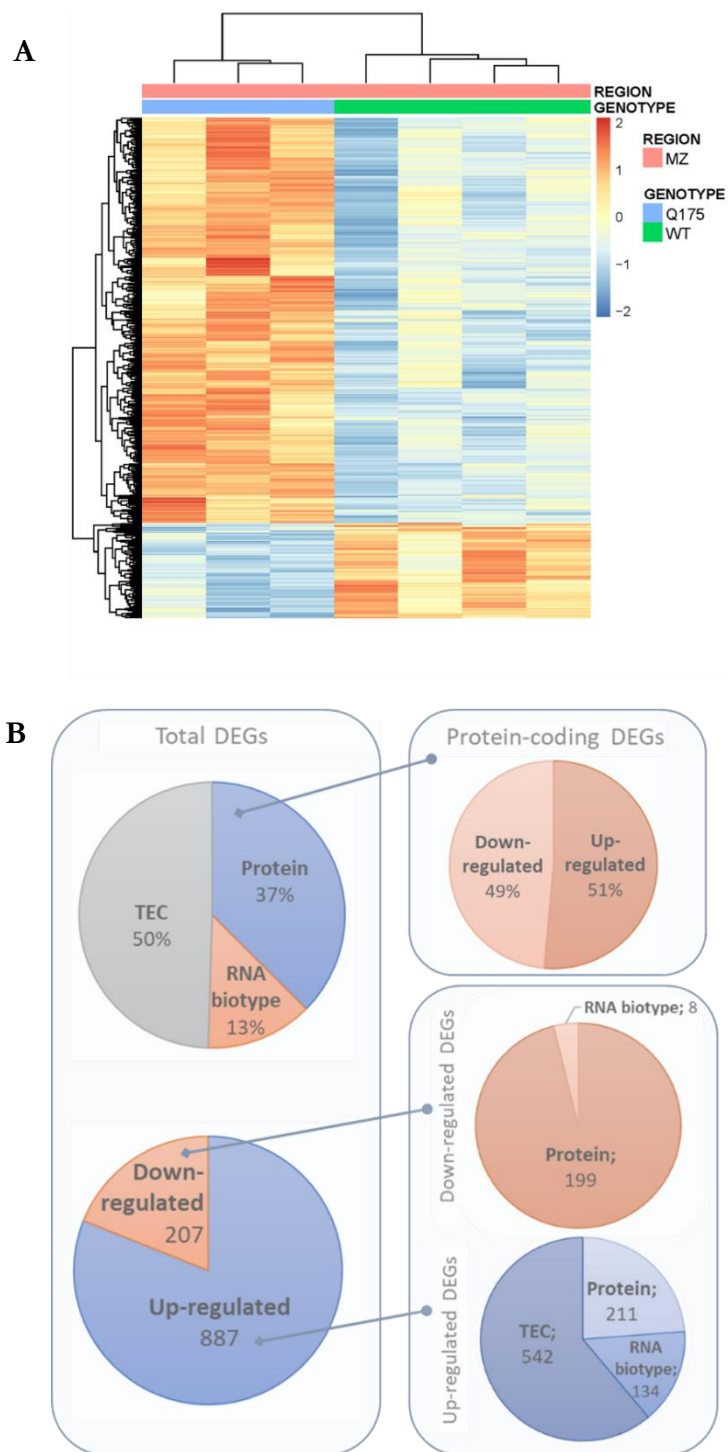


Figure 44. Heatmap (A) and DEGs biotypes (B) of the MZ differential analysis.

## 1.2. Protein-coding DEGs

The comparison of the gene expression between wt and Q175 mice pointed out different expression profiles between genotypes regarding the protein-coding genes, so we performed gene enrichment and Kegg Pathway analysis to understand the biological implication of the altered genes.

Interestingly, the Kegg Pathway analysis showed that the most enriched family of genes were related to neurodegenerative diseases: HD, PD, Alzheimer's Disease (AD), Amyotrophic Lateral Sclerosis (ALS) and other neurological diseases such as spinocerebellar ataxia (Table 2). Moreover, the Mammalian Phenotype Ontology (MPO) (Monarch, an integrative data and analytic platform connecting phenotypes to genotypes across species) related the HD altered gene expression with developmental abnormalities and movement conditions. This analysis also pointed out other important cellular events such as metabolism, proteolysis and cellular signaling.

<b>All protein-coding DEGs</b>			
<b>Category</b>	<b>term description</b>	<b>gene count</b>	<b>FDR</b>
KEGG_PATHWAY	Huntington disease	33	2.93E-13
KEGG_PATHWAY	Prion disease	31	3.09E-13
KEGG_PATHWAY	Parkinson disease	28	5.21E-12
KEGG_PATHWAY	Alzheimer disease	32	5.83E-11
KEGG_PATHWAY	Amyotrophic lateral sclerosis	30	1.53E-09
KEGG_PATHWAY	Oxidative phosphorylation	16	4.03E-07
KEGG_PATHWAY	Spinocerebellar ataxia	15	5.43E-06
KEGG_PATHWAY	Proteasome	8	0.00019
KEGG_PATHWAY	Thermogenesis	15	0.00098
KEGG_PATHWAY	Glycolysis / Gluconeogenesis	7	0.0094
KEGG_PATHWAY	Carbon metabolism	9	0.0166
KEGG_PATHWAY	cGMP-PKG signaling pathway	10	0.0348
MPO	Prewaning lethality	134	5.23E-05
MPO	Abnormal survival	142	0.0001
MPO	Behavior/neurological phenotype	126	0.0004
MPO	Abnormal behavior	121	0.00042
MPO	Mortality/aging	146	0.00046
MPO	Growth/size/body region phenotype	125	0.002
MPO	Abnormal motor capabilities/coordination/movement	88	0.0036
MPO	Abnormal voluntary movement	56	0.0036
MPO	Abnormal nervous system physiology	62	0.0079
MPO	Abnormal locomotor behavior	52	0.0097
MPO	Abnormal synaptic transmission	39	0.0097
MPO	Nervous system phenotype	99	0.0152
MPO	Prenatal lethality	72	0.0251
MPO	Abnormal neuron morphology	50	0.0251
MPO	Embryonic lethality prior to organogenesis	35	0.0399
MPO	Embryonic lethality prior to tooth bud stage	38	0.0399

**Table 2.** List of the most significant terms obtained from the KEGG pathway and the Mammalian Phenotype Ontology analysis of the protein-coding DEGs (including up- and down-regulated DEGs).

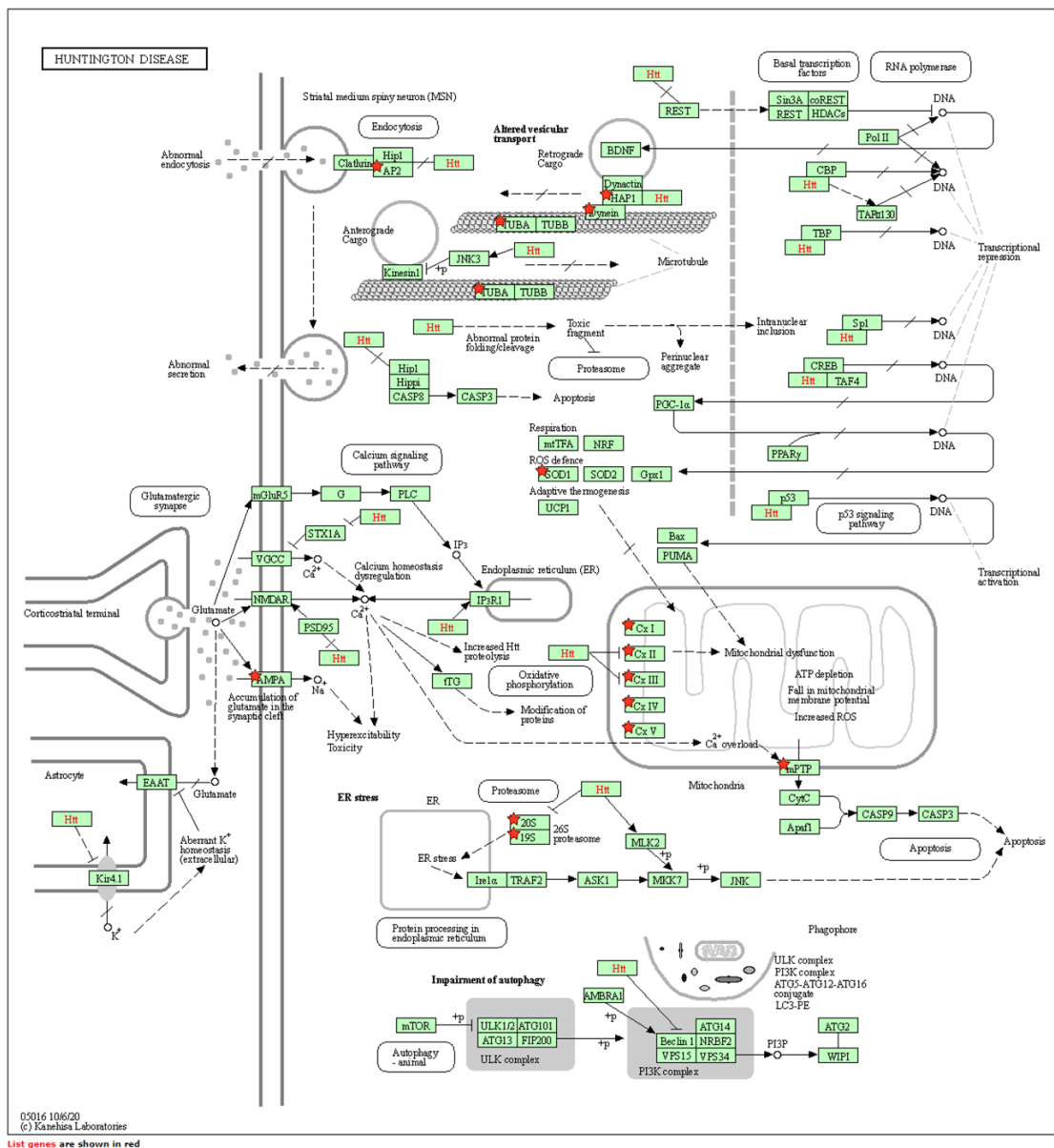


**Figure 45. Diagram of the mHtt-cell protein interactions described.** Image taken from KeggPathways' analysis. The stars mark the distribution of the DEGs obtained.

Regarding the HD pathways, the KEGG pathway's obtained diagram (Figure 45) showed that altered DEGs were distributed among important HD pathophysiological alterations such as an abnormal endocytosis, altered vesicular transport, reactive oxygen species (ROS) defense, mitochondrial dysfunction, glutamatergic synapse and proteasome and endoplasmic reticulum (ER) stress.



The Gene Ontology (GO) enrichment analysis pointed out that genes disrregulated in the HD emrbyos were also related with cell cycle, splicing events, and the proteolytic pathway.

Annotation Cluster 1		Enrichment Score: 13.48		
	Term	Count	P_Value	Benjamini
UP_KEYWORDS	Cell cycle	83	8.0E-17	4.2E-15
UP_KEYWORDS	Cell division	58	7.3E-15	1.9E-13
UP_KEYWORDS	Mitosis	41	6.2E-11	1.3E-9
Annotation Cluster 2		Enrichment Score: 7.98		
	Term	Count	P_Value	Benjamini
UP_KEYWORDS	Spliceosome	24	7.0E-9	1.1E-7
UP_KEYWORDS	mRNA processing	41	1.0E-8	1.6E-7
UP_KEYWORDS	mRNA splicing	35	1.6E-8	2.2E-7
Annotation Cluster 3		Enrichment Score: 7.61		
	Term	Count	P_Value	Benjamini
UP_KEYWORDS	Proteasome	23	3.5E-15	1.0E-13
UP_KEYWORDS	Threonine protease	11	2.4E-8	3.2E-7
UP_KEYWORDS	Protease	32	1.8E-1	5.0E-1
Annotation Cluster 4		Enrichment Score: 6.44		
	Term	Count	P_Value	Benjamini
UP_KEYWORDS	Chromosome	46	2.1E-7	2.6E-6
UP_KEYWORDS	Centromere	23	4.2E-7	5.0E-6
UP_KEYWORDS	Kinetochore	19	5.3E-7	6.0E-6

**Table 3. Gene Ontology (GO) Enrichment of the DEGs ontained.**

We then performed GO enrichment analysis of the up- and down-regulated protein-coding genes, separately, to understand the biological implication of the altered genes. The functions of the HD up-regulated DEGs were mainly related with neuronal function (Figure 46). Up-regulated DEGs were significantly enriched in cell differentiation processes, including cell adhesion and axon/dentrite formation, synapse formation and channel activity (Table 4).

Conversely, the functions of the down-regulated DEGs were largely spread along different biological processes, being the cell cycle one of the most enriched ones (Figure 47). The functions of the HD down-regulated DEGs were significantly enriched in important biological processes, including metabolism and ATP production, mitochondrial function, proteasomal function, exosomes, protein transport and REDOX processes (Table 5).



Figure 46. Enrichment analysis showing the distribution of the HD up-regulated DEG's related functions.



Figure 47. Enrichment analysis showing the distribution of the HD down-regulated DEGs' related functions.

<i>Category</i>	<i>Term</i>	<i>Count</i>	<i>P-Value</i>	<i>Benjamini</i>
GOTERM_BP_DIRECT	homophilic cell adhesion via plasma membrane adhesion molecules	13	5.90E-08	4.50E-05
GOTERM_MF_DIRECT	ion channel activity	12	1.50E-06	4.30E-04
GOTERM_MF_DIRECT	calcium ion binding	23	3.30E-06	4.50E-04
GOTERM_CC_DIRECT	nucleoplasm	38	3.20E-05	7.70E-03
GOTERM_CC_DIRECT	centriole	8	9.60E-05	1.20E-02
GOTERM_BP_DIRECT	membrane depolarization during action potential	5	1.40E-04	5.40E-02
GOTERM_CC_DIRECT	Z disc	8	1.90E-04	1.40E-02
GOTERM_CC_DIRECT	axon initial segment	4	2.30E-04	1.40E-02
GOTERM_CC_DIRECT	postsynaptic membrane	10	2.90E-04	1.40E-02
GOTERM_BP_DIRECT	regulation of ion transmembrane transport	8	3.30E-04	8.50E-02
GOTERM_MF_DIRECT	nucleic acid binding	27	4.10E-04	3.40E-02
GOTERM_MF_DIRECT	voltage-gated ion channel activity	8	4.80E-04	3.40E-02
GOTERM_CC_DIRECT	postsynaptic density	10	5.00E-04	2.00E-02
GOTERM_BP_DIRECT	photoreceptor cell maintenance	5	5.80E-04	1.10E-01
GOTERM_MF_DIRECT	poly(A) RNA binding	24	1.10E-03	6.30E-02
GOTERM_BP_DIRECT	synaptic transmission, glutamatergic	4	2.70E-03	3.60E-01
GOTERM_CC_DIRECT	dendrite	13	2.70E-03	9.50E-02

**Table 4. Gene Ontology (GO) Enrichment of the up-regulated DEGs in the MZ of HD embryos.**

<i>Category</i>	<i>Term</i>	<i>Count</i>	<i>P-Value</i>	<i>Benjamini</i>
GOTERM_CC_DIRECT	mitochondrion	57	3.00E-17	8.70E-15
GOTERM_CC_DIRECT	extracellular exosome	70	4.40E-16	6.40E-14
GOTERM_CC_DIRECT	myelin sheath	18	3.60E-12	3.40E-10
GOTERM_CC_DIRECT	mitochondrial inner membrane	23	1.60E-11	1.10E-09
GOTERM_CC_DIRECT	cytosol	42	5.80E-08	3.40E-06
GOTERM_CC_DIRECT	proteasome complex	9	1.90E-07	9.10E-06
GOTERM_BP_DIRECT	transport	42	5.20E-07	4.40E-04
GOTERM_CC_DIRECT	nucleus	89	9.00E-07	3.50E-05
GOTERM_CC_DIRECT	proteasome core complex	6	9.70E-07	3.50E-05
GOTERM_BP_DIRECT	proton transport	8	1.80E-06	7.40E-04
GOTERM_CC_DIRECT	cytoplasm	94	2.30E-06	7.40E-05
GOTERM_MF_DIRECT	threonine-type endopeptidase activity	6	2.60E-06	7.70E-04
GOTERM_BP_DIRECT	antigen processing and presentation of exogenous peptide antigen via MHC class I	6	1.10E-05	3.10E-03
GOTERM_CC_DIRECT	respiratory chain	7	1.70E-05	5.00E-04
GOTERM_CC_DIRECT	mitochondrial proton-transporting ATP synthase complex	5	2.10E-05	5.50E-04
GOTERM_BP_DIRECT	proteolysis involved in cellular protein catabolic process	7	2.20E-05	4.60E-03
GOTERM_MF_DIRECT	protein complex binding	14	5.70E-05	8.60E-03
GOTERM_BP_DIRECT	ATP synthesis coupled proton transport	5	7.40E-05	1.20E-02
GOTERM_MF_DIRECT	endopeptidase activity	8	1.20E-04	1.20E-02
GOTERM_CC_DIRECT	mitochondrial proton-transporting ATP synthase complex, coupling factor F(o)	4	1.70E-04	3.70E-03
GOTERM_MF_DIRECT	hydrogen ion transmembrane transporter activity	5	2.60E-04	1.90E-02
GOTERM_BP_DIRECT	protein transport	17	3.10E-04	4.30E-02
GOTERM_MF_DIRECT	proton-transporting ATP synthase activity, rotational mechanism	4	3.20E-04	1.90E-02
GOTERM_BP_DIRECT	oxidation-reduction process	18	4.60E-04	5.50E-02
GOTERM_BP_DIRECT	substantia nigra development	5	5.50E-04	5.80E-02
GOTERM_MF_DIRECT	poly(A) RNA binding	24	6.00E-04	3.00E-02

**Table 5. Gene Ontology (GO) Enrichment of the down-regulated DEGs in the MZ of HD embryos.**

### 1.3. TEC genes:

Among the 1094 DEGs in the MZ, half of them encode for unknown genes that correspond to TEC genes (Figure 44 B). This TEC category is used for non-spliced expressed sequence tag (EST) clusters that have polyA features. This gene category was created for the ENCODE project to highlight regions that could indicate the presence of protein-coding genes that require experimental validation. Interestingly, all TECs obtained in this analysis were up-regulated in the MZ of HD samples and, moreover, all of them were monoexonic. After performing a blast2go, some of the TECs presented matches and a predicted GO associated (Figure 48 A). We performed a GO enrichment analysis to deeper analyze their possible biological implication. Half of the TECs presented associated predictions, with an enrichment in gene families related with important pathways, including nervous system development and social and locomotory behavior, among many others (Figure 48 B).

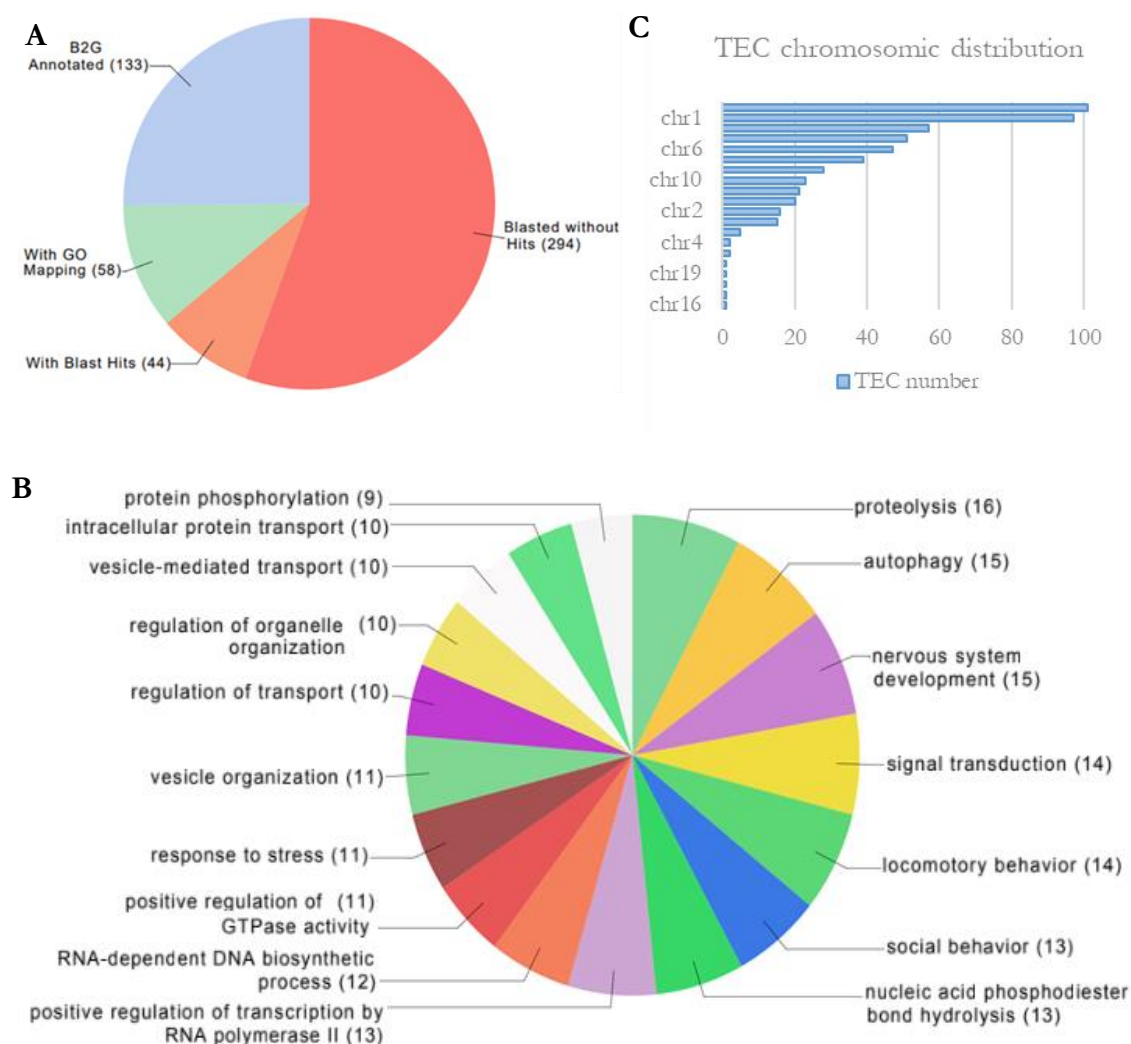


Figure 48. Pie-charts showing the blast2go (A) and the GO enrichment (B) analysis of the DE TECs. C) Distribution of the TECs along the different chromosomes. The majority of the TECs are concentrated in 4 chromosomes: 1, 6, 10 and 2.

## 1.4. Non-coding DEGs

Due to its relevance in the regulation of development, we also focused our attention on the non-coding RNAs (ncRNAs). Among the 1094 DEGs in the MZ, a 13% were ncRNAs. Most of them were up-regulated in HD embryos (Figure 44 B), and only 7 non-coding DEGs were found (Table 6).

Among the down-regulated genes, 3 different types of molecules were detected:

- Ribosomal RNA (**rRNA**).
- Small nuclear RNA (**snRNA**) molecules, which are involved in the processing of pre messenger RNAs.
- Small nucleolar RNA (**snoRNA**) molecules which are involved in the post-transcriptional modification of other RNAs.

Among the up-regulated genes, 2 different types of molecules were detected:

- **Antisense RNAs (asRNA)**, which overlap the genomic span of a protein-coding locus on the opposite strand.
- Different **Pseudogenes**, which are molecules that have homology to known protein-coding genes but contain a frameshift and/or stop codon(s) which disrupts the open reading frame (ORF).

In the up- and down-regulated genes, the non-coding DEGs were predicted ncRNA without annotations (*see “Gm-number” in the name*) (Tables 6 and 7). Only few ncRNAs of the up-regulated genes present associated annotations, such as the asRNAs Kcnq1ot1, Nespas and Zfhx2os, and the pseudogenes Pcdhgb8, Mageb16-ps2, Zcchc9-ps, Wdr46-ps and Mir99ahg.

<i>Down-regulated non-coding DEGs</i>			
Name	Biotype	log2FC	padj
n-R5-8s1	rRNA	-0.49	4.25E-02
Gm22486	snoRNA	-0.79	3.59E-02
Gm22422	snoRNA	-0.95	4.31E-02
Gm23472	snRNA	-1.22	2.39E-02
Gm23444	snRNA	-1.22	2.39E-02
Gm22973	snRNA	-1.37	2.97E-03

Table 6. List of the non-coding DEGs down-regulated in HD MZ.



<i>Up-regulated non-coding DEGs</i>			
Name	Biotype	log2FC	padj
Gm16070	antisense_RNA	0.80	4.81E-02
Kcnq1ot1	antisense_RNA	0.79	6.57E-03
Nespas	antisense_RNA	0.61	2.72E-03
Gm38336	antisense_RNA	0.55	4.31E-02
Zfx2os	antisense_RNA	0.50	2.42E-02
D030055H07Rik	antisense_RNA	0.41	2.13E-02
4732440D04Rik	antisense_RNA	0.38	1.54E-02
B230334C09Rik	antisense_RNA	0.37	8.94E-04
Gm9856	antisense_RNA	0.32	4.77E-02
Pcdhgb8	polymorphic_pseudogene	0.55	3.69E-03
Mageb16-ps2	processed_pseudogene	1.34	4.92E-02
Gm15739	processed_pseudogene	1.29	1.11E-03
AC161250.2	processed_pseudogene	1.29	1.43E-02
Gm18212	processed_pseudogene	1.17	6.64E-04
Gm8261	processed_pseudogene	1.13	2.92E-02
Gm15828	processed_pseudogene	1.13	3.67E-06
Gm14776	processed_pseudogene	1.09	1.36E-02
CT025642.2	processed_pseudogene	1.05	7.04E-03
Gm8855	processed_pseudogene	1.03	2.85E-02
Gm12369	processed_pseudogene	1.00	3.23E-04
Zcchc9-ps	processed_pseudogene	1.00	1.49E-03
Gm13689	processed_pseudogene	0.97	4.54E-03
AC154729.1	processed_pseudogene	0.96	4.57E-03
AC147240.1	processed_pseudogene	0.92	1.06E-03
Gm19046	processed_pseudogene	0.91	3.56E-02
Gm6611	processed_pseudogene	0.90	1.99E-03
Gm16228	processed_pseudogene	0.79	4.76E-02
Gm11652	processed_pseudogene	0.77	2.21E-02
Gm14021	processed_pseudogene	0.77	3.62E-03
Gm15681	processed_pseudogene	0.76	1.71E-08
Wdr46-ps	processed_pseudogene	0.76	0.002414
Gm20491	processed_pseudogene	0.69	0.013659
Gm11839	processed_pseudogene	0.59	0.020394
1700030C10Rik	processed_transcript	1.01	0.034941
B230216N24Rik	processed_transcript	0.70	2.84E-05
Gm28373	processed_transcript	0.69	0.049273
Gm43813	processed_transcript	0.67	0.017719
Gm26871	processed_transcript	0.62	3.18E-05
A330076H08Rik	processed_transcript	0.57	0.001877
6430590A07Rik	processed_transcript	0.56	2.55E-05
BC039771	processed_transcript	0.55	0.018322
A330023F24Rik	processed_transcript	0.54	0.01894
Gm12940	processed_transcript	0.50	0.029612
C230004F18Rik	processed_transcript	0.48	0.041077
Mir99ahg	processed_transcript	0.37	0.042457
Gm17229	transcribed_processed_pseudogene	1.08	2.77E-05
AC155270.1	transcribed_processed_pseudogene	1.01	0.017385
Gm19035	transcribed_processed_pseudogene	0.90	3.20E-07
Gm15666	transcribed_processed_pseudogene	0.79	3.36E-05
Gm16523	transcribed_processed_pseudogene	0.74	0.00018
Gm10033	transcribed_unprocessed_pseudogene	0.35	0.018568
Gm36858	unprocessed_pseudogene	0.78	3.38E-07
Gm18150	unprocessed_pseudogene	0.75	0.013517

Table 7. List of the up-regulated non-coding DEGs in the HD MZ.

#### 1.4.1. Long non-coding RNAs (lncRNAs):

The up-regulated non-coding genes in the HD samples were also enriched in lncRNAs, generally defined as transcripts with more than 200 nucleotides that are not translated into protein. As in the other ncRNAs, most of the HD up-regulated lncRNAs are predicted genes (Table 8). However, some important lncRNAs with associated annotations came up in HD mouse samples: nuclear paraspeckle assembly transcript 1 (Neat1), ganglioside-induced differentiation-associated-protein 10 (Gdap10), metastasis associated lung adenocarcinoma transcript 1 (Malat1), myocardial infarction associated transcript (Miat) and five prime to xist (Ftx).

<i>Up-regulated non-coding DEGs</i>							
Name	Biotype	log2FC	padj	Name	Biotype	log2FC	padj
Gm29113	lincRNA	1.32	5.25E-03	Gm3294	lincRNA	0.52	2.72E-03
Gm29325	lincRNA	1.26	9.63E-04	C78859	lincRNA	0.51	1.04E-04
Gm10287	lincRNA	1.23	5.25E-09	Malat1	lincRNA	0.49	8.05E-05
Gm30382	lincRNA	0.92	9.12E-06	Gm9916	lincRNA	0.48	2.50E-03
Gm26601	lincRNA	0.86	4.09E-08	Miat	lincRNA	0.47	1.88E-03
Gm4425	lincRNA	0.74	3.34E-02	C130073E24Rik	lincRNA	0.46	2.85E-02
Gm45159	lincRNA	0.71	1.99E-11	Gm9801	lincRNA	0.46	4.83E-03
CT010478.1	lincRNA	0.69	4.88E-02	A230057D06Rik	lincRNA	0.43	3.48E-02
Gm26945	lincRNA	0.69	6.74E-05	Ftx	lincRNA	0.41	2.99E-03
B830012L14Rik	lincRNA	0.67	4.14E-03	A330008L17Rik	lincRNA	0.40	1.47E-03
2610037D02Rik	lincRNA	0.66	7.32E-05	2900076A07Rik	lincRNA	0.39	1.24E-02
9530059O14Rik	lincRNA	0.65	1.02E-05	Gm45250	lincRNA	0.39	3.78E-02
Neat1	lincRNA	0.63	1.44E-03	Gm21781	lincRNA	0.38	7.21E-05
5330434G04Rik	lincRNA	0.59	1.46E-05	Gm20342	lincRNA	0.36	4.93E-02
Gm26853	lincRNA	0.55	7.16E-08	AI480526	lincRNA	0.36	2.41E-03
Gdap10	lincRNA	0.54	3.26E-04	6720427I07Rik	lincRNA	0.35	4.95E-02
Gm15328	lincRNA	0.54	7.83E-04	Gm3764	lincRNA	0.33	4.34E-02
AC163040.1	lincRNA	0.53	1.35E-02	Mir124a-1hg	lincRNA	0.23	2.94E-02
A430106G13Rik	lincRNA	0.53	1.95E-04	Mir124-2hg	lincRNA	0.21	3.23E-02

Table 8. List of long non-coding RNAs up-regulated in HD embryos.



## 1.5. Differential expression analysis of wt and Q175 maturation patterns

### 1.5.1. Wt and HD striatal neurons are generated following distinct maturation patterns:

Striatal GZ contains striatal NPCs that will exit the cell cycle at different developmental stages and will migrate to the striatal MZ while differentiating and maturing into functional MSNs. We wanted to know if genetic regulation program from the proliferative state to the mature state was altered in HD development respect to controls. To do so, we compared the gene expression patterns from the GZ and the MZ within the same genotype and, once we know which genes were regulated during this transition in each genotype, we extract the DEGs between the wt and HD to find differences (Figure 49 A).

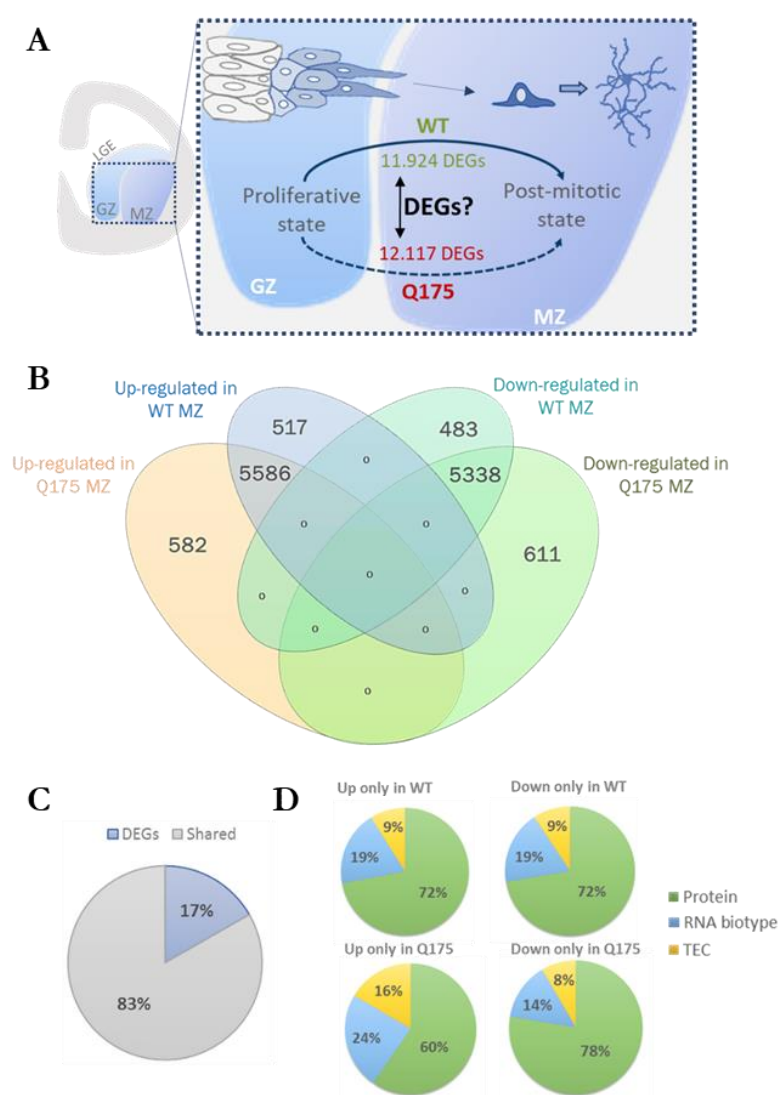


**Figure 49. Differentiation program in wt vs HD mice.** **A)** Graphical summary of the comparisons. **B)** Venn Diagram showing the total number of DEGs specific for each contidion. **C)** Pie chart showing the shared/non-shared DEGs between wt and HD differenciacion pattern. **D)** Pie charts shpwing the DEGs biotypes for each condition.

Results show that HD neuronal differentiation and maturation is governed by distinct regulation patterns respect to controls, thus indicating that striatal neurons are generated throughout different developmental pathways than wt striatal neurons. Around 12.000 genes are up- or down-regulated in the GZ to MZ transition, from the proliferative to the post-mitotic state. 83% of these changes in gene expression are shared between genotypes, but a 17% of these genes are differentially regulated in Q175 embryos with respect to wt (Figure 49 C).

A Venn Diagram was performed to see how these DEGs were specifically distributed: up-regulated in Q175 but not in wt, down-regulated in Q175 but not in wt, up-regulated in wt but not in Q175 and down-regulated in wt but not in Q175 (Figure 49 B). We finally performed enrichment analyses of these 17% of genes to know which pathways this DEGs are involved in. Genes that are erroneously up-regulated during HD differentiation program were enriched in cellular processes related with signalling pathways and formation of cholinergic and serotonergic synapses (Table 9). On the counterpart, the enrichment analysis from the down-regulated genes in HD differentiation program revealed important cellular pathways including gene expression regulation by splicing, autophagy and protein degradation and immune response (Table 9).

<i>Category</i>	<i>Term</i>	<i>Count</i>	<i>P-Value</i>	<i>Benjamini</i>
<b>Up only in Q175</b>				
KEGG_PATHWAY	Cholinergic synapse	8	6.40E-04	1.20E-01
KEGG_PATHWAY	ABC transporters	5	2.90E-03	2.60E-01
KEGG_PATHWAY	Estrogen signaling pathway	6	8.80E-03	5.40E-01
KEGG_PATHWAY	Morphine addiction	5	3.30E-02	1.00E+00
KEGG_PATHWAY	Circadian entrainment	5	3.80E-02	1.00E+00
KEGG_PATHWAY	Retrograde endocannabinoid signaling	5	4.50E-02	1.00E+00
KEGG_PATHWAY	Rap1 signaling pathway	7	6.00E-02	1.00E+00
KEGG_PATHWAY	Gastric acid secretion	4	6.70E-02	1.00E+00
KEGG_PATHWAY	Lysosome	5	7.40E-02	1.00E+00
KEGG_PATHWAY	PI3K-Akt signaling pathway	9	8.60E-02	1.00E+00
KEGG_PATHWAY	Serotonergic synapse	5	9.30E-02	1.00E+00
<b>Down only in Q175</b>				
KEGG_PATHWAY	Proteasome	8	4.50E-05	8.60E-03
KEGG_PATHWAY	Spliceosome	9	8.20E-03	6.10E-01
KEGG_PATHWAY	Fc gamma R-mediated phagocytosis	7	9.60E-03	6.10E-01
KEGG_PATHWAY	Leukocyte transendothelial migration	8	1.40E-02	6.70E-01
KEGG_PATHWAY	Protein processing in endoplasmic reticulum	8	7.30E-02	1.00E+00
KEGG_PATHWAY	Epstein-Barr virus infection	7	7.50E-02	1.00E+00
KEGG_PATHWAY	Natural killer cell mediated cytotoxicity	6	7.80E-02	1.00E+00

Table 9. KEGG Pathway Analysis of the up- and down-regulated.

### 1.5.2. Striatal lineage-specific transcriptional alterations:

Alterations in NPCs behavior can compromise cell fate decisions and neuronal generation, differentially affecting the two main striatal neurons, dMSNs and iMSNs. We therefore performed z-score analysis comparing our RNAseq dataset with the D1- and D2-specific markers previously described<sup>271</sup> to find specific transcriptional alterations in these two populations. HD embryo up-regulated gen's list was enriched in D2-MSN specific markers while HD embryo down-regulated gen's list was enriched in D1-MSN specific markers, suggesting striatal lineage-specific transcriptional alterations in Q175 embryos (Figure 50 A).

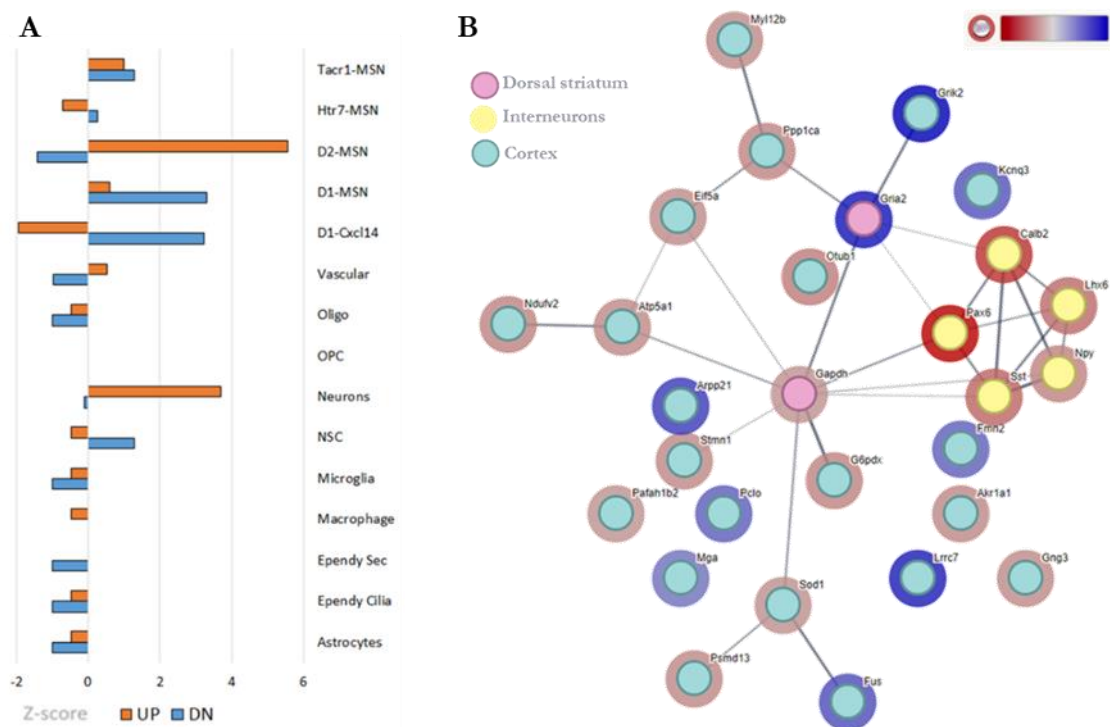


**Figure 50. Lineage-specific alterations within the HD MZ. A)** Z-score analysis showing the enrichment of iMSNs-lineage specific markers within the up-regulated DEGs, but an enrichment of dMSNs-lineage specific markers within the down-regulated DEGs **B)** StrinDB diagram showing some striatal (pink)/interneuronal (yellow)/cortical (cyan) related DEGs and their interactions. Blue and red circles correspond to HD up- and down-regulation, respectively.

Moreover, tissue enrichment analysis pointed out HD affected genes related with other lineages such as cortical and interneuronal. HD embryos have a reduction in the expression of genes that encode for the main neuropeptides expressed by the different interneurons: Sst, NPY and CR (Figure 50 B). Regarding cortical markers, HD embryos have some up- and some down-genes. Remarkably, this analysis also pointed out two affected genes related with the dorsal part of the striatum, where the PSPB is formed. In this line, an important PSPB gene, Pax6, is down-regulated in the HD embryos.

## 2 *CHAPTER II: defining HD developmental alterations*

### *Histological characterization of HD striatal developmental abnormalities*

---

The transcriptomic analysis suggests that developmental alterations in Q175 embryos are related to cell cycle progression of the striatal NPCs and to the maturation and differentiation pattern. The study also showed that some HD-related developmental abnormalities are d/iMSNs-lineage specific. We aimed to deeply analyse and characterize and define the specific striatal developmental alterations occurring in the Q175 mouse model. To do so, we performed different histological analysis, including cell cycle phase labelling, birthdating analyses and finally lineage-specific neurogenesis analysis by using Cre-reporter mice.

#### 2.1. NPCs cell cycle status is affected during Q175 development

As RNA-seq data suggested alterations in the proliferative rates and cell cycle progression, we performed proliferation studies in wt and HD mouse embryos at different embryonic stages (E12.4, E14.5, E16.5). Both S- and M-phases were analyzed by EdU and PH3 labelling, respectively.

Significant differences were found in both S and M-phases between genotypes (Figure 51) along the different stages. At E12.5, zQ175 embryos display an increase in the number and proportion of S-phase cells in the germinal region, while a reduction in the number and proportion of M-phase cells in that region. No differences were found in the number and proportion neither in the S-phase cells nor in the M-phase cells in striatal GZ at E14.5. Conversely, an increase in the number of M-phase cells in the zQ175 embryos at E16.5 was detected, but a significant decrease in the number of S-phase cells in this region.

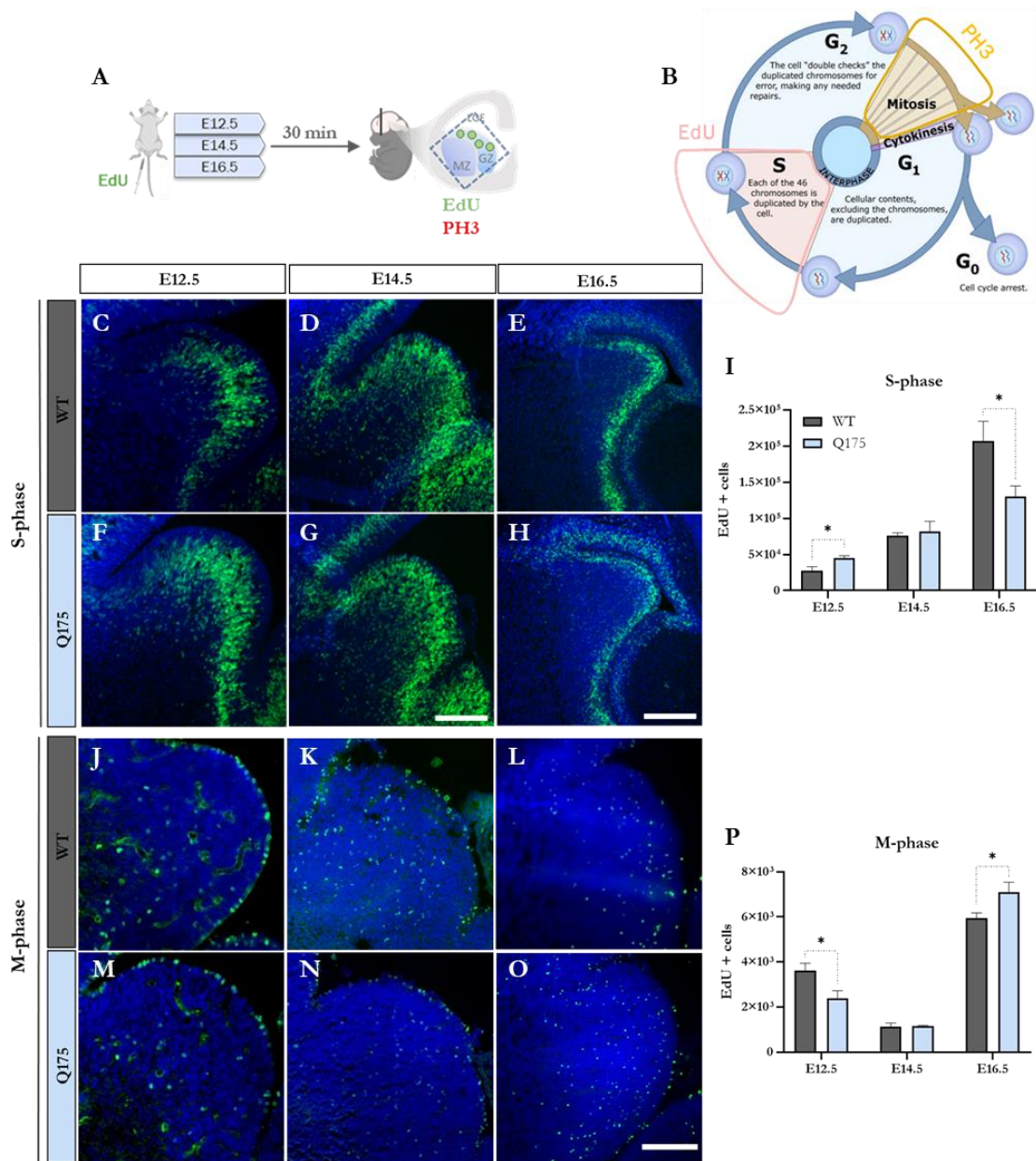


**Figure 51. Cell cycle progression is altered during striatal development in HD.** **A)** Schematic summary of the cell cycle phase labelling. **B)** Image showing the cell cycle phases that were labelled in this experiment. Representative pictures of the S-phase cells in both wt (**C-E**) and Q175 (**F-H**) embryos at different stages (E12.5-E16.5). Scale bar C/D/F/G: 150  $\mu$ m. Scale bar E/H: 400  $\mu$ m. Representative pictures of the M-phase cells in both wt (**J-L**) and Q175 (**M-O**) embryos at different stages (E12.5-E16.5). Scale bar: 150  $\mu$ m Stereological quantification of the total number of S-phase (EdU positive) (**I**) and M-phase (PH3 positive) (**P**) cells within the striatal GZ of wt and HD embryos. All results are expressed as the mean of independent experiments  $\pm$ s.e.m. and results were analysed using Student's t-test. We considered statistical significance  $p < 0.05$  (\*) and  $p < 0.01$  (\*\*).



## 2.2. Q175 early NPCs undergo to a precocious cell cycle exit, compromising the NPCs pool maintenance

As proliferation was affected during HD striatal development, we analyzed if these alterations were affecting the striatal neurogenic events. To do that, we performed birth-dating assays with EdU incorporation paradigms. We injected different pregnant mice at different developmental stages (E12.5, E14.5 and E16.5) and then allowed embryos to develop until E18.5, when brains were harvested. HD embryos displayed aberrant birth-dating rates at all stages. We found an increase in the generation of cells at E12.5, but a decrease at E16.5 and a tendency at E14.5 (Figure 52).

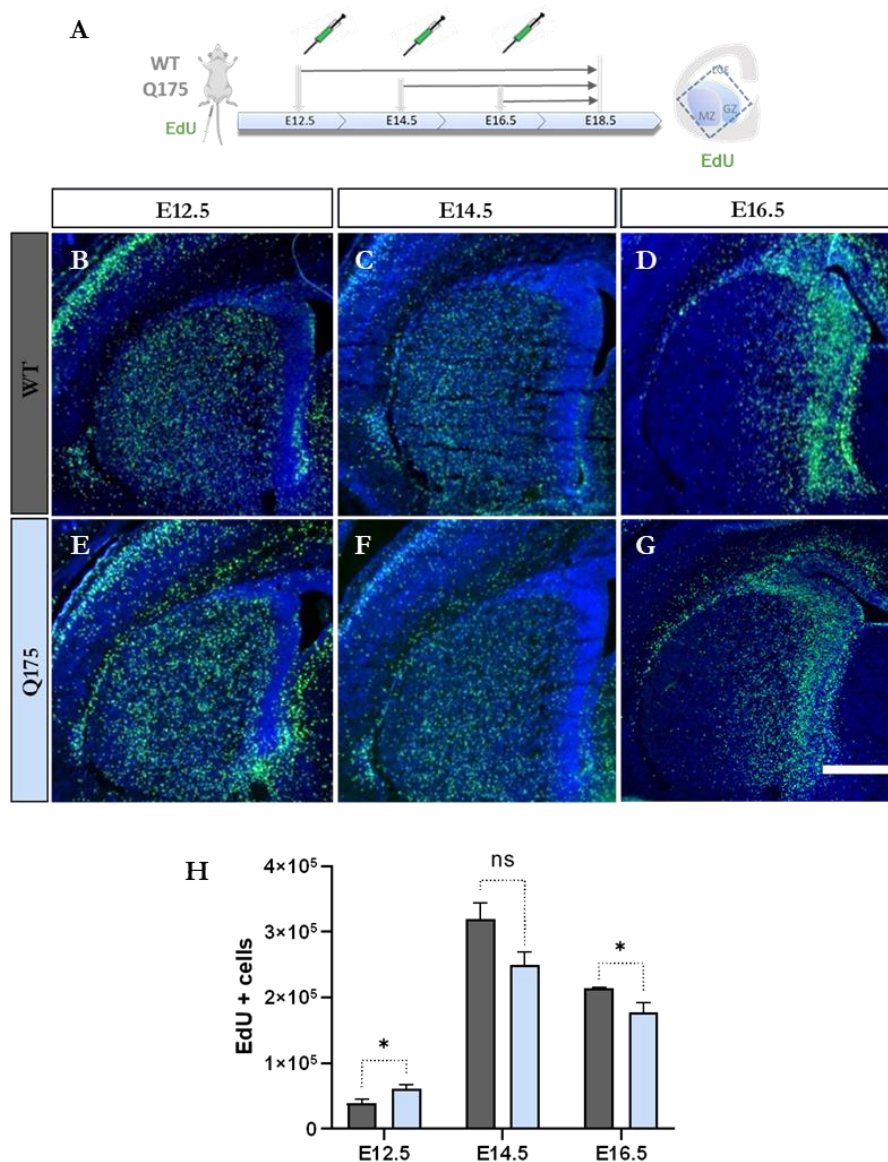


**Figure 52. HD embryos undergo a premature cell cycle exit in the early developmental stages, followed by a reduction of the cell birth at later stages.** **A)** Schematic summary of the birthdating analyses. Representative pictures embryonic E18.5 striatum showing in green the cells that were born at the different stages in both wt (**B-D**) and Q175 (**E-G**). **H)** Stereological quantification showing the cell cycle exit rates at E12.5, E14.5 and E16.5 of wt and HD mice. All results are expressed as the mean of independent experiments  $\pm$  s.e.m. and results were analysed using Student's t-test. We considered statistical significance  $p < 0.05$  (\*) and  $p < 0.01$  (\*\*). Scale bar: 400  $\mu$ m.

Alterations in the cell cycle status of NPCs and that its precocious cell cycle exit could be exhausting the striatal NPCs pool (Figure 53 A). We quantified the total number of cells inhabiting the GZ, by counting the total number of DAPI cells, and the total volume of this region embryonically (E12.5-E16.5) and postnatally (P5). Interestingly, HD samples did not display significant differences neither in the total number of cells in the GZ nor in the volume of that region at three E12.5, E14.5 and E16.5 stages respect to controls (Figure 53 B-C). NPCs pool consumption consequences are detectable at P5, when the GZ population is importantly decreased (Figure 53 B).

We secondly studied if the NPC's found alterations were causing or were caused by cell death events. We quantified the number of Casp3 positive cells in the GZ (E12.5-P5) and found a huge increase in NPCs cell death from E18.5 to postnatal period (Figure 53 C).

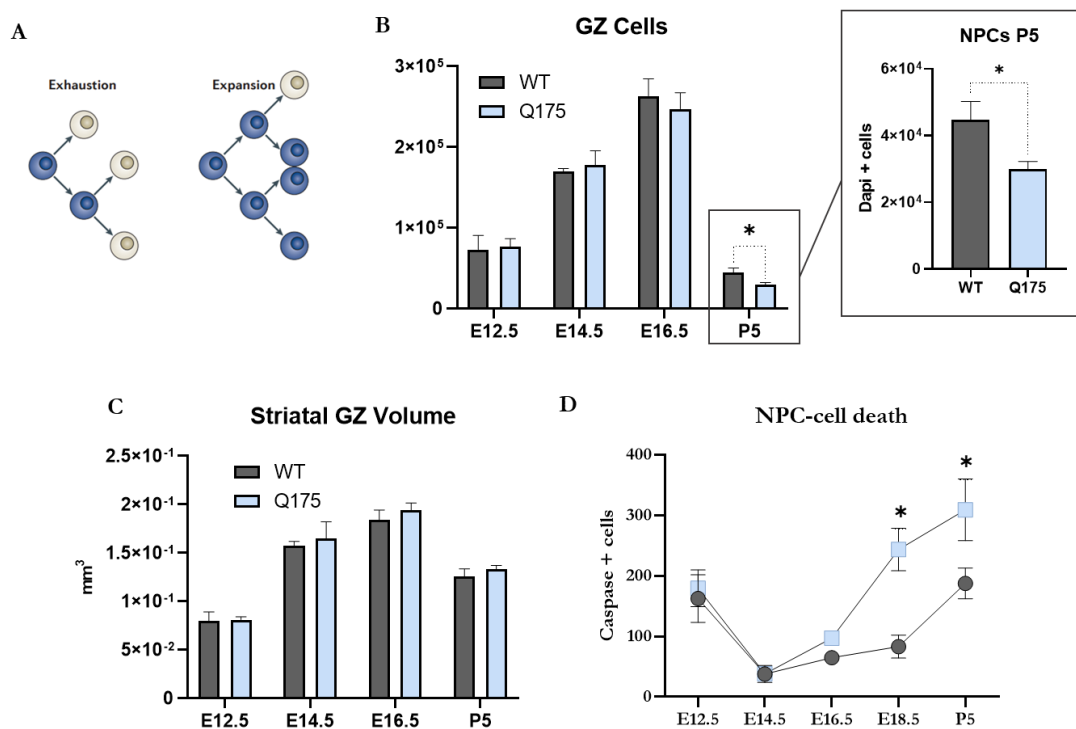


**Figure 53. NPCs pool is compromised during HD development. A)** Schematic representation of the NPC pool expansion vs exhaustion events. **B)** Stereological quantification of the total number of cells (DAPI) in the GZ at E12.5, E14.5, E16.5 and P5 of wt and HD mice. **C)** Stereological quantification of the total GZ volume (mm<sup>3</sup>) of wt and HD embryos at different developmental stages. **D)** Stereological quantification of the NPC's cell death (Casp<sup>+</sup> cells) at different developmental stages of wt and HD mice. All results are expressed as the mean of independent experiments  $\pm$  s.e.m. and results were analysed using Student's t-test. We considered statistical significance  $p < 0.05$  (\*) and  $p < 0.01$  (\*\*).

### 2.3. Specific iMSNs are prematurely generated during HD development causing and early striatal subpopulation imbalance

Briefly, dMSNs are mostly generated throughout the first neurogenic wave, while iMSNs are more prompt to be generated along later neurogenic waves. To deeper analyze if birth-dating alterations were affecting specific striatal subpopulation neurogenesis, and as RNAseq analysis suggested lineage-specific alterations, we injected EdU to wt/Q175;Drd1-CRE;tdTomato and wt/Q175;A2A-CRE;tdTomato pregnant dams at both E12.5 and E14.5 stages and allow embryos to develop until E18.5, when samples are obtained and analysed (Figure 54 A).

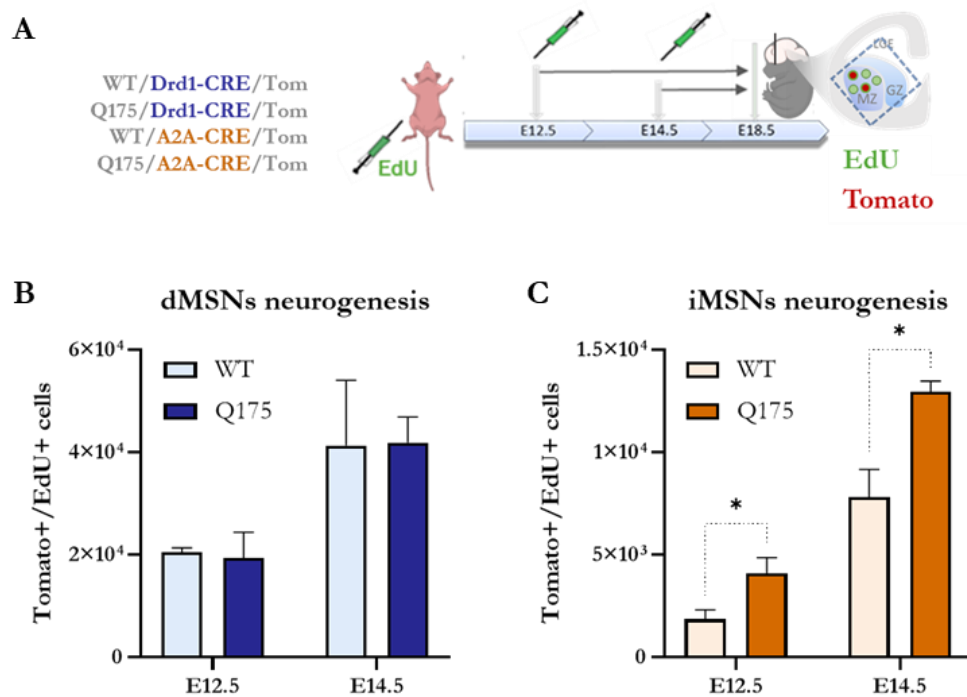


**Figure 54. Lineage-specific iMSNs neurogenesis is increased at both neurogenic waves during HD striatal development.** **A)** Schematic summary of the dMSNs/iMSNs neurogenesis analyses. Stereological quantification showing no differences in the iMSNs neurogenesis (**B**) and an increased iMSNs generation (**C**) in the HD embryos respect to the controls. All results are expressed as the mean of independent experiments  $\pm$ s.e.m. and results were analysed using Student's t-test. We considered statistical significance  $p < 0.05$  (\*) and  $p < 0.01$  (\*\*).

We quantified the number of EdU/tdTomato double positive cells, and we found that specific iMSNs neurogenesis was defectively increased in both neurogenic waves. Conversely, we did not observe dMSNs-specific neurogenic differences at these stages (Figure 54). As the transcriptomic analysis suggested an imbalance among these striatal subpopulations, and we found an increase in the iMSNs generation, we wanted to confirm histologically if dMSNs and iMSNs populations were imbalanced in HD development. To do so, we quantified the total tdTomato positive cells at E18.5 using both wt/Q175;Drd1-CRE;tdTomato and wt/Q175;A2A-CRE;tdTomato mouse lines (Figure 55 A). At this stage, we found no significant reduction of dMSNs total cells and, conversely, an important increase of iMSNs total cells in striatal MZ of Q175 embryos (Figure 55 B-C).



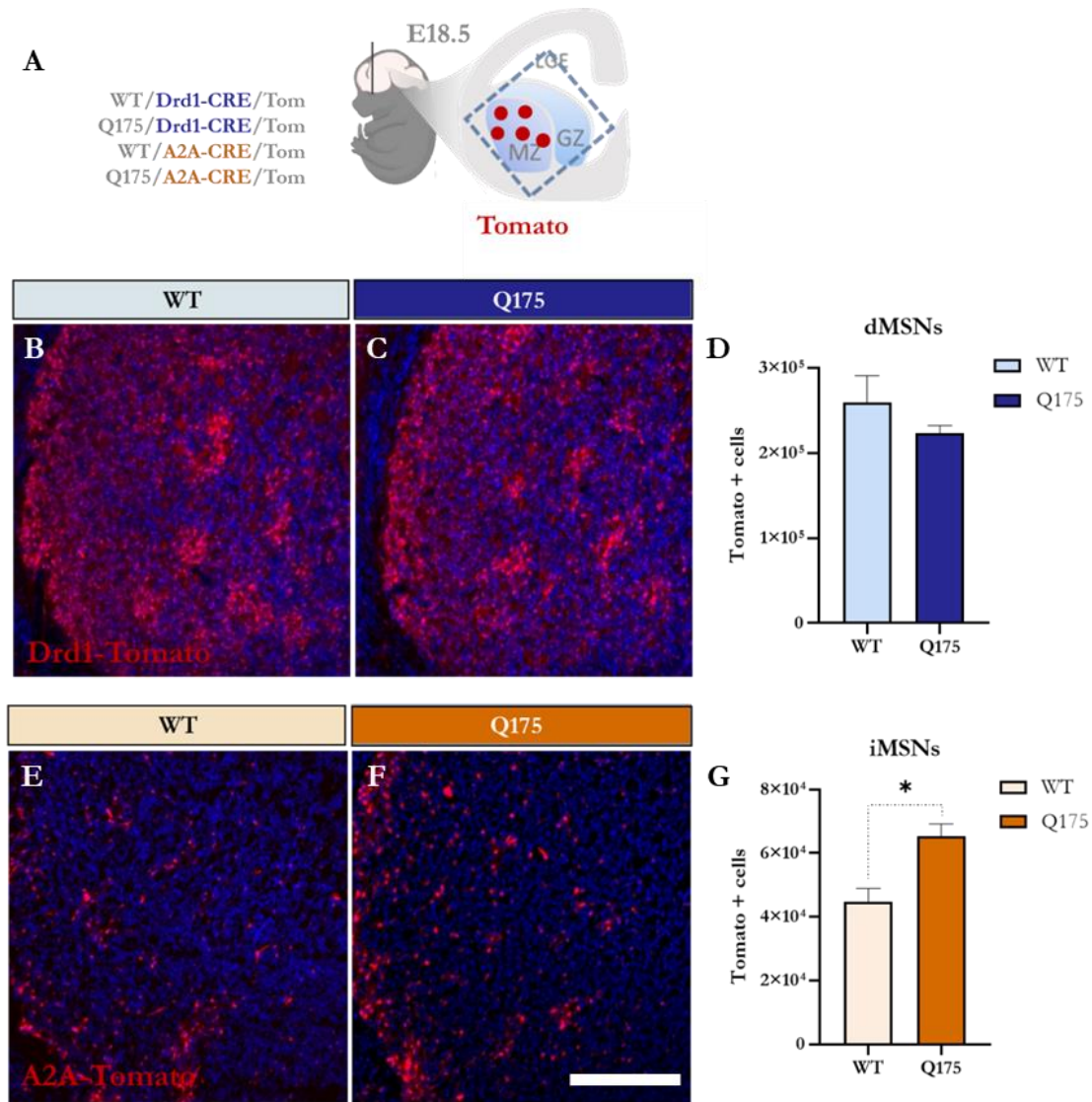


**Figure 55. iMSN population is increased at E18.5 HD striatum.** **A)** Schematic summary of the population analyses. Representative pictures of the dMSN population (red cells) inhabiting the embryonic E18.5 striatum of both wt (**B**) and Q175 (**C**) embryos. Representative pictures of the iMSN population (red cells) inhabiting the embryonic E18.5 striatum of both wt (**E**) and Q175 (**F**) embryos. Stereological quantification showing the total number of dMSNs (**D**) and iMSNs (**G**) populations in the E18.5 striatum. All results are expressed as the mean of independent experiments  $\pm$  s.e.m. and results were analysed using Student's t-test. We considered statistical significance  $p < 0.05$  (\*) and  $p < 0.01$  (\*\*). Scale bar: 200  $\mu$ m.

We then analyzed how this population imbalance was affected at the end of development, whether if it was maintained or somehow compensated during postnatal development. We therefore quantified the total tdTomato positive cells at P21, when development ends, using both wt/Q175;Drd1-CRE;tdTomato and wt/Q175;A2A-CRE;tdTomato mouse lines (Figure 56 A). Unexpectedly, Q175 mice displayed a decrease in the total number of iMSN population but not in the dMSN population in the mature P21 striatum (Figure 56 B-G).

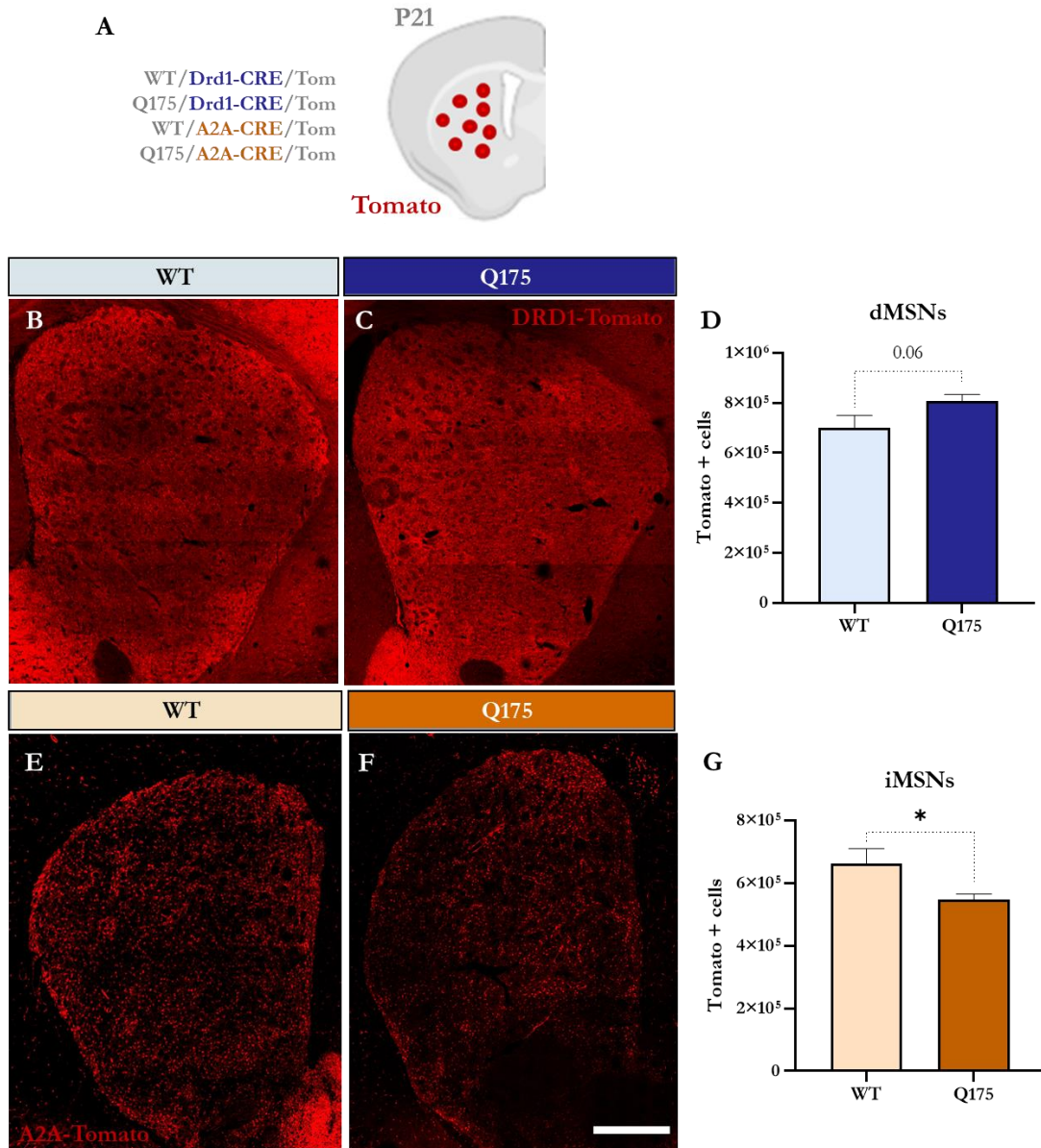


**Figure 56. iMSN population is reduced in the P21 HD striatum. A)** Schematic summary of the population analyses. Representative pictures of the dMSN population (red cells) inhabiting the P21 striatum of both wt (**B**) and Q175 (**C**) mice. Representative pictures of the iMSN population (red cells) inhabiting the P21 striatum of both wt (**E**) and Q175 (**F**) mice. Stereological quantification showing the total number of dMSNs (**D**) and iMSNs (**G**) populations in the P21 striatum. All results are expressed as the mean of independent experiments  $\pm$ s.e.m. and results were analysed using Student's t-test. We considered statistical significance  $p < 0.05$  (\*) and  $p < 0.01$  (\*\*). Scale bar: 500  $\mu$ m.

We then wanted to elucidate why iMSNs population was diminished postnatally, while there was an increased iMSN generation embryonically. As a natural period of cellular programmed cell death is occurring during P3-P7, we quantified the iMSNs population at P5 by using the A2A reporter mice (Figure 57 A). Q175 mice have a decreased iMSNs population as early as P5 (Figure 57 B-D). We then analyse the natural programmed cell death occurring in P5 by quantifying the number of c-Casp 3 positive cells in the P5 striatal MZ, and we found no differences in the total number of death cells (Figure 57 E). To study if the decrease in the iMSNs population was due to an increased specific cell death, we quantified the number of Casp3/tomato double positive within the MZ and we found a specific iMSN cellular death at P5 in Q175 puppies (Figure 57 F).

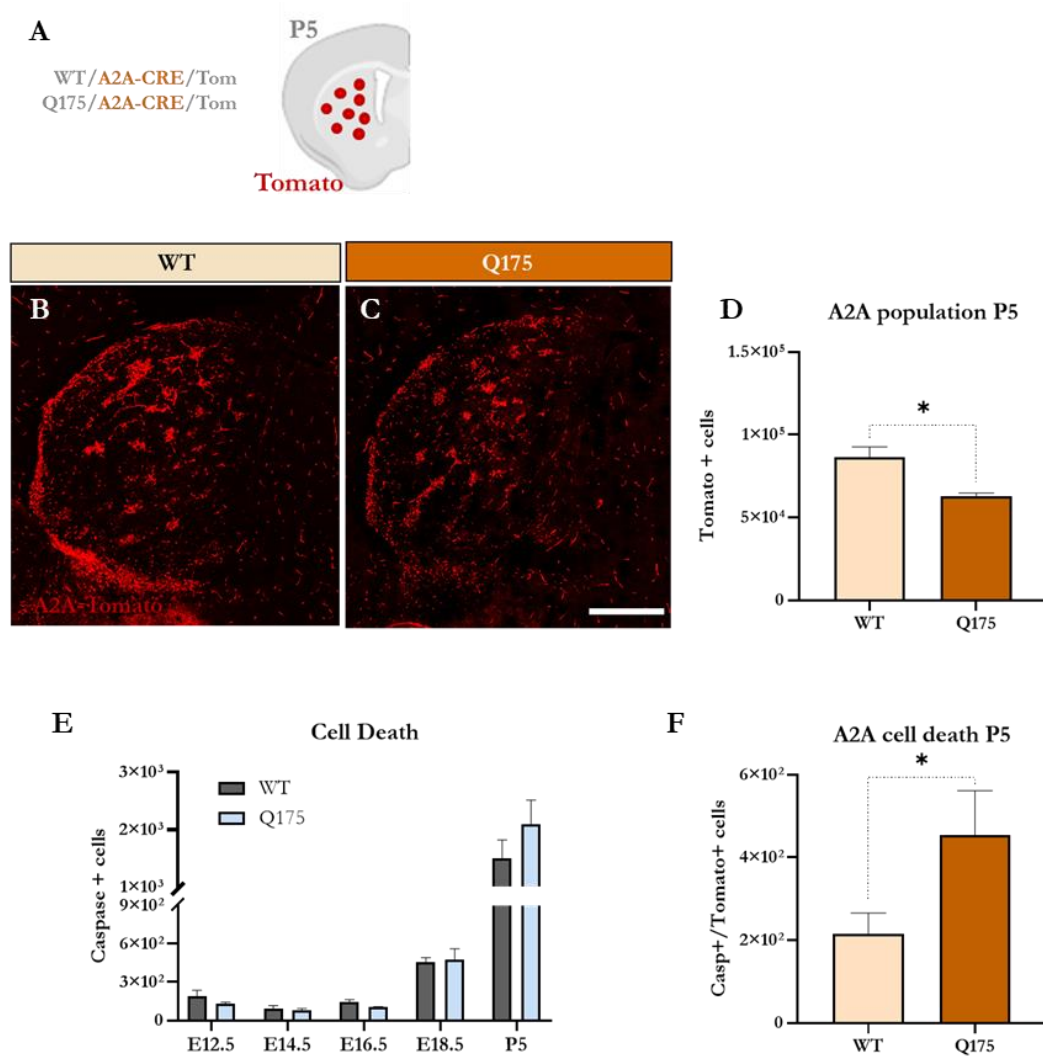


**Figure 57. Specific iMSNs population cell death occurs during the normal post-natal cell death period in HD mice.** **A)** Schematic summary of the A2A P5 population studies. **B-C)** Representative images of the A2A population in the wt (B) and HD (C) P5 striatum. **D)** Stereological quantification of the total number of iMSNs cells inhabiting the P5 striatum of both wt and HD mice. **E)** Stereological quantifications of the cell death occurring from E12.5 until P5, in both wt and HD mice. **F)** Stereological quantification of the specific iMSNs cell death (double Casp3<sup>+</sup>/Tom<sup>+</sup> cells) occurring at P5. All results are expressed as the mean of independent experiments  $\pm$ s.e.m. and results were analysed using Student's t-test. We considered statistical significance  $p < 0.05$  (\*) and  $p < 0.01$  (\*\*). Scale bar: 500  $\mu$ m.

## 2.4. Interneuronal striatal lineage also undergo developmental abnormalities in HD embryos:

The bulk RNA-seq analysis suggested that HD embryos had a specific reduction in the interneuron population at E16.5. To deeper study specific IN HD alterations, we injected EdU to wt/Q175;Nkx2.1-CRE;tdTomato pregnant dams at both E12.5 and E14.5 stages and allow embryos to develop until E18.5, when samples are obtained and analysed. We also quantified the total number of IN population at E18.5.

We found an increase in the IN production at E14.5 in HD embryos. Conversely, no stadistically significant differences were found in the final IN population at E18.5, but a tendency to a diminished IN population.

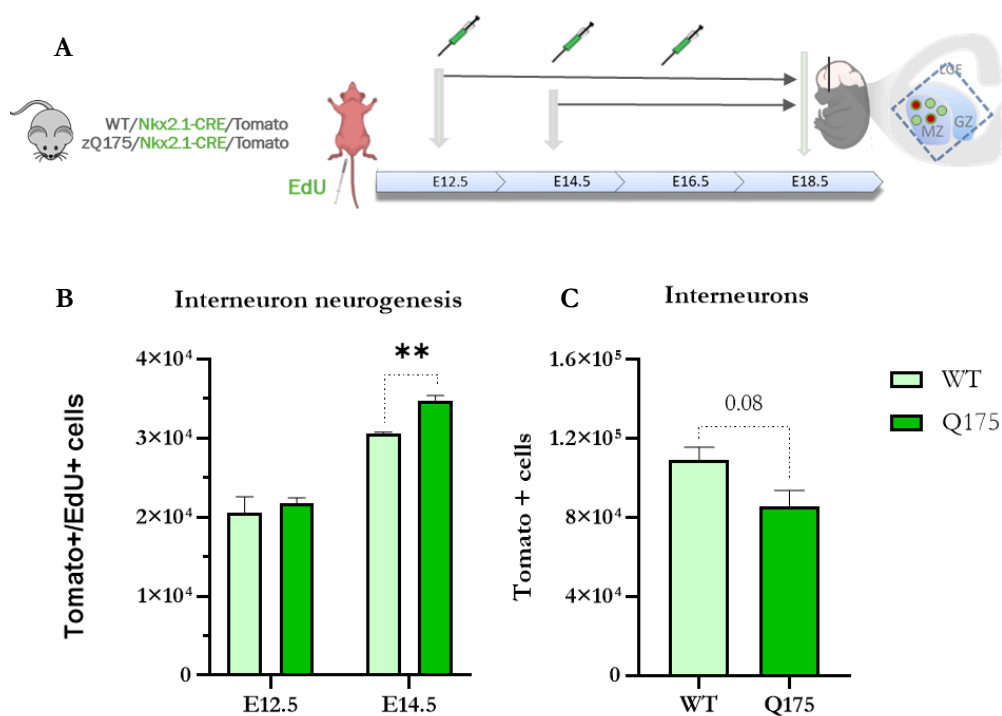


**Figure 58. Interneuron neurogenesis is increased at E14.5 HD striatal development.** **A)** Schematic summary of the IN neurogenesis analyses. Stereological quantification showing no differences in the iMSNs neurogenesis **(B)** Stereological quantification of the IN neurogenesis at both E12.5 and E14.5 in wt and HD embryos. **(C)** Stereological quantification of the IN total number of cells at the E18.5 striatum. All results are expressed as the mean of independent experiments  $\pm$ s.e.m. and results were analysed using Student's t-test. We considered statistical significance  $p < 0.05$  (\*) and  $p < 0.01$  (\*\*).



### 3 CHAPTER III: finding iMSNs alterations' origin

#### Characterization of developmental lineage-specific alterations in HD

After defining the lineage specific alterations occurring along the striatal development in HD, we wanted to elucidate the origin of all of them at the NPCs level. Conversely to other brain regions, normal striatal development is not widely understood. Some insights have been shown regarding the striatal NPCs heterogeneity and their progenies, but we are still not able to clearly define the different striatal neuronal precursor different populations and their lineages.

#### 3.1. Computational integration of different scRNA-seq datasets

What causes these NPCs alterations, and whether if they are affecting all striatal NPCs or specific subpopulations remain still unknown. To comprehensively resolve this issue, we used scRNA-seq (10X Genomics) to profile distinct NPCs subpopulations of early wt and Q175 LGEs. To comprehensively resolve the LGE NPCs heterogeneity during normal striatal development, and then detect disturbances during striatal HD development, we used scRNA-seq (10X Genomics) to profile distinct NPCs subpopulations from E14.5 Q175 LGEs. We also used an available dataset previously generated in the lab (Phil Sanders, unpublished data), which consists in scRNA-seq data from different days in vitro (DIVs) of our *in vitro* differentiation protocol from human pluripotent stem cells to striatal neurons<sup>270</sup>. To increase the robustness of the study, we computationally integrated the mouse E14.5 scRNA-seq data and the human *in vitro* data and with the public human fetal scRNA-seq dataset<sup>272</sup> (accession number: E-MTAB-8894) to finally enrich our study (Figure 59 A).

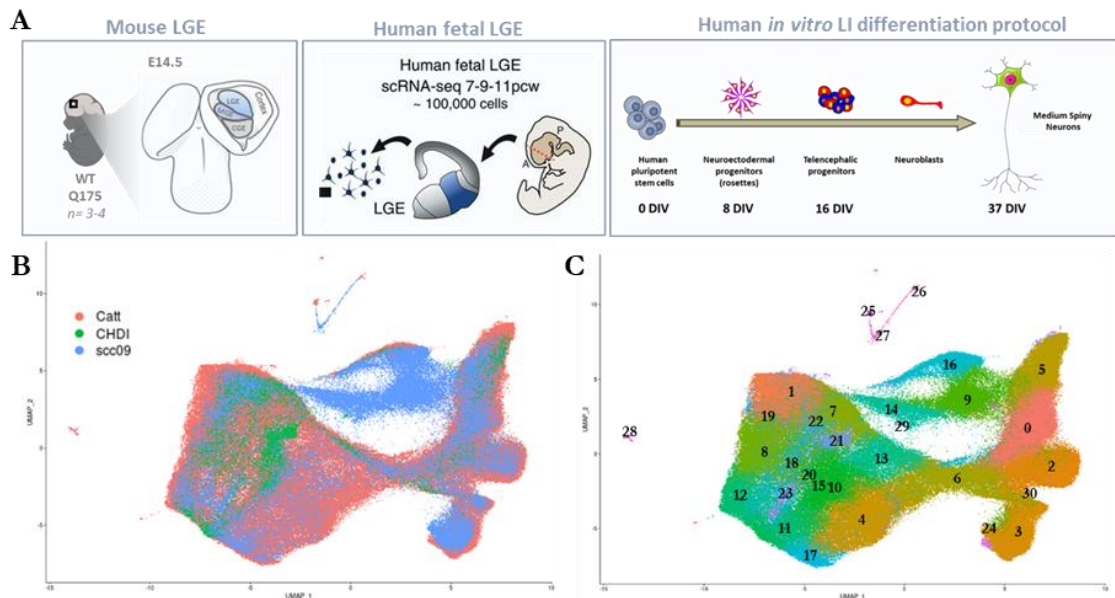


**Figure 59. Single cell dataset computational integration.** A) Summary of the used datasets to perform the integration: wt and HD samples from E14.5 mouse LGEs, human fetal samples of control 7-11 wpc LGEs and control and HD cells differentiated *in vitro* throughout the striatal lineages. B) UMAP showing the integration of cells coming from the different datasets. C) UMAP showing the different clusters that were generated from the integration (30 in total).

By computationally integrating these 3 different human and mouse developmental scRNA-seq datasets, we obtained a robust developmental landscape that pointed out different subpopulations and lineages (Figure 59 B). We were able to discriminate 30 clusters and their transcriptional signatures (Figure 59 C) which were then classified according to canonical markers (Figures 60-62). The clustering analysis pointed out the three main striatal lineages: dMSNs, iMSNs and interneurons.

### 3.1.1. Annotation and identification of cluster identities:

By selecting putative known markers and plotting them in the obtained UMAP, we could clearly identify the identity of the main clusters.

Firstly, we identified GABAergic clusters, by the expression of GAD2, and specifically GABAergic MSNs, marked by the expression of FOXP1 and FOXP2. We were also able to detect some clusters enriched in cortical markers, such as TBR1, EMX2 and the glutamateric marker SLC17A6. Then, we identified the cells enriched in striatal NPC's and Neuroblast (NB) markers, such as Gsh2/Gsx2, Ascl1/Mash1 and the Dlx family.

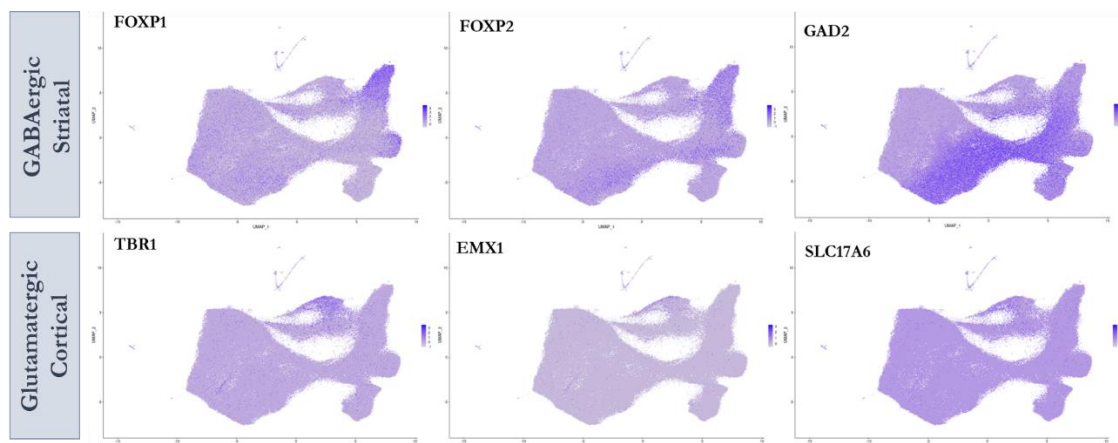


Figure 60. UMAPs showing the distribution of putative glutamatergic and GABAergic markers.

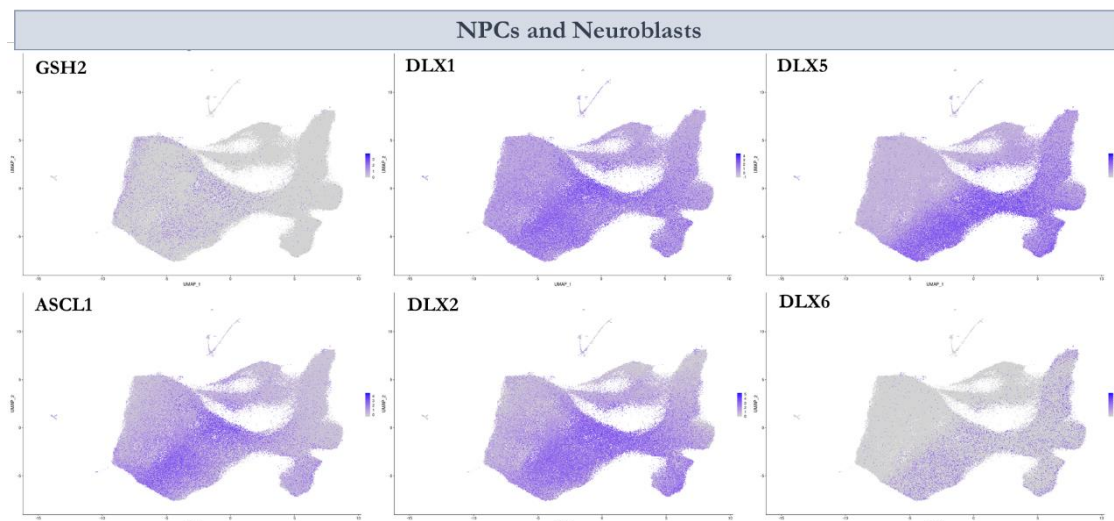


Figure 61. UMAPs showing the distribution of putative striatal NPC's markers.

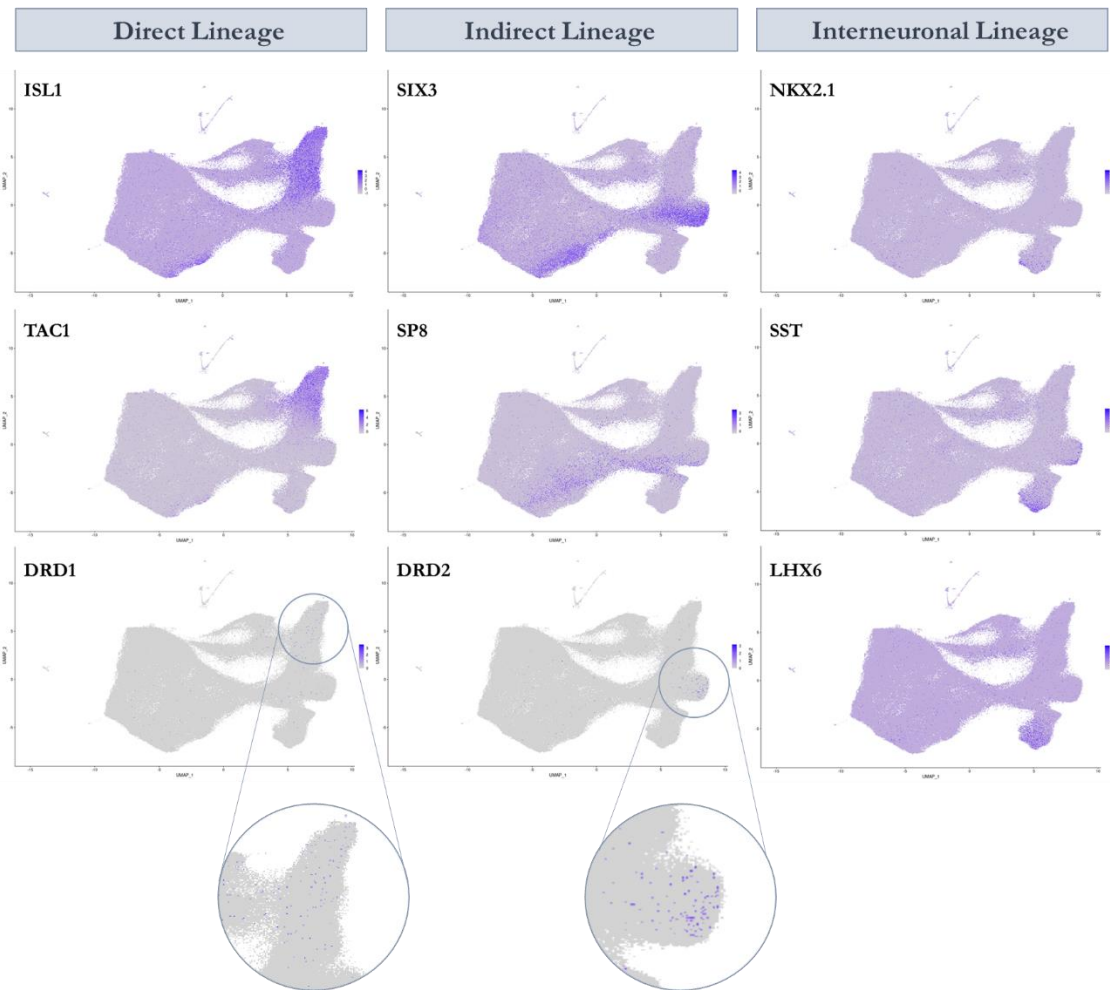


Figure 62. UMAPs showing the distribution of putative striatal dMSNs/iMSNs/IN's markers.

Moreover, we were also capable of identify the 3 different striatal lineages:

- Direct pathway lineage, marked by a high expression of ISL1, TAC1 and DRD1.
- Indirect pathway, marked by a high expression of SIX3, SP8 and DRD2.
- Interneuronal lineage, marked by a high expression of NKX2.1, SST and LHX6.

### 3.2. Finding specific HD affected clusters:

We then looked for cluster-specific HD alterations, detectable in our developmental model. As two of the three datasets used for this clustering were combining wt and HD cells, we were able to quantify the different contribution of the wt and HD cells to each cluster. The analysis pointed out two specific clusters, clusters 10 and 13, which showed a significant decreased contribution of HD cells. These two clusters were formed by cells enriched in striatal NPC's markers such as *Ascl1* and the *Dlx* family (Figure 63).

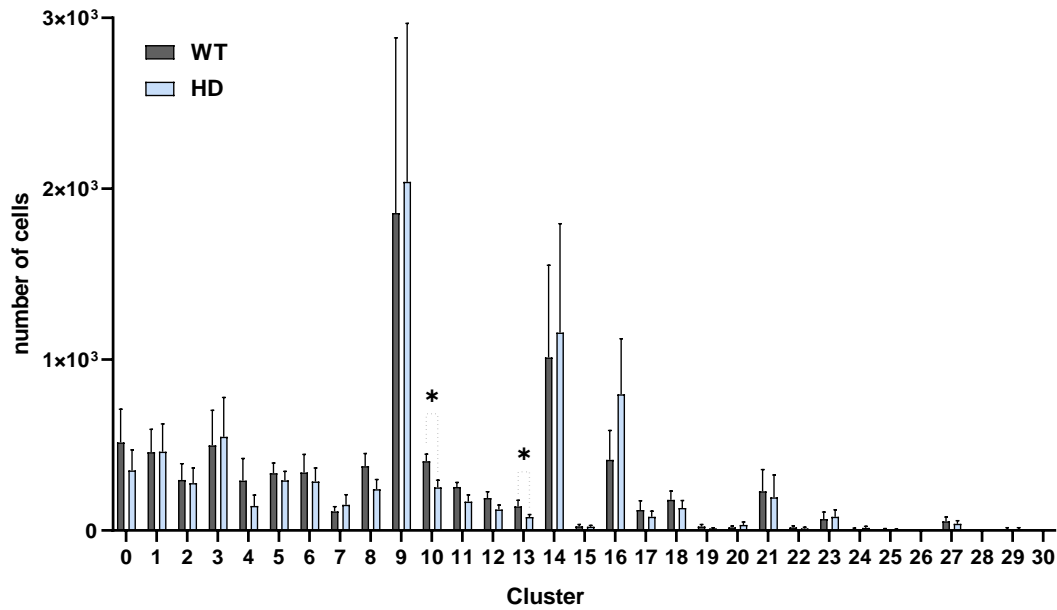


**Figure 63. Distribution of wt and HD cells among the different clusters.** The graph shows the mean of wt/ctr human/mouse number of cells and the mean of Q175/HD human/mouse number of cells within the 30 clusters. All results are expressed as the mean of independent experiments  $\pm$ s.e.m. and results were analysed using Student's t-test. We considered statistical significance  $p < 0.05$  (\*) and  $p < 0.01$  (\*\*).

We then wanted to find specific markers that identify these clusters specifically, genes that were expressed in those clusters but not in the others. To do so, we looked for specific markers by comparing the list of genes expressed by cells in the clusters 10 and 13 and the gene list of genes expressed by cells of the remaining clusters. We obtained a Venn Diagram showing that only 3 genes were non-overlapping between the 10-13 cluster gene's list and the rest of cluster's gene list (Figure 64 A).



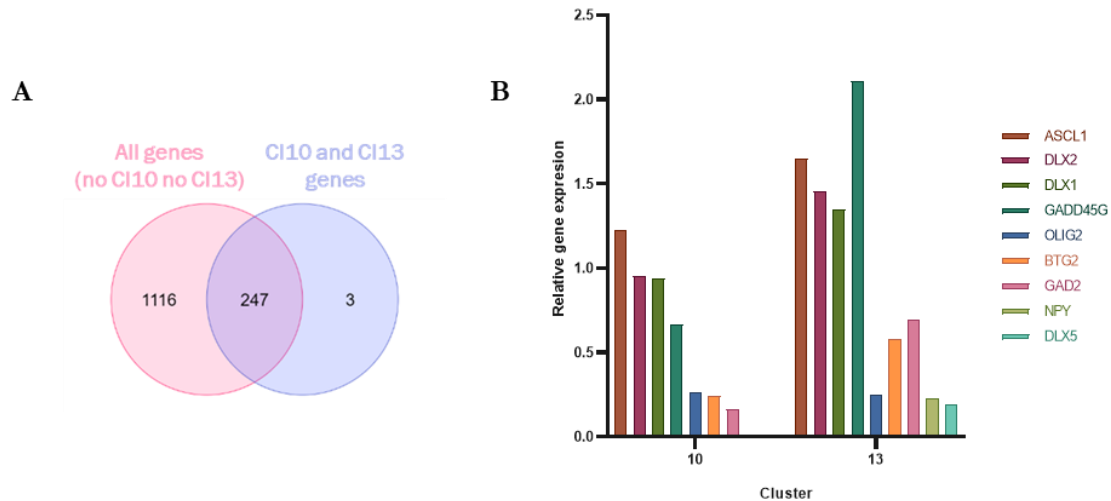


**Figure 64. Identity of the cells from the clusters of interest.** **A)** Relative gene expression of the main putative markers expressed within clusters 10 and 13. **B)** Venn Diagram showing the overlapping and non-overlapping number of genes between the clusters 10 and 13 respect the rest of the clusters.

### 3.3. HELT-expressing subpopulation:

We focused on one of the 3 genes that was selectively enriched in the affected clusters: HELT, also known as Megane (Mgn) or Heslike. We then check for the expression of putative striatal markers along both clusters 10 and 13, those which were specifically affected in HD cells and that specifically expressed HELT, and we discovered that this cluster of cells expressed NPCs specific genes, such as Tis21 (Btg2), Mash1 (Ascl1), Dlx1/2, among others, suggesting that these cells conform a population of progenitors residing de SVZ (Figure 64 B).

### 3.4. HELT-expressing subpopulation is affected in zQ175 embryos:

To further corroborate and analyze these results, we first validated HELT expression in E14.5 and E16.5 brain slices of wt embryos with the FISH technique, by designing a specific probe to detect the mouse HELT RNA. HELT was specifically expressed in the striatal GZ, mainly in the SVZ, at both E14.5 and E16.5 (Figure 65 A-E).

We then check HELT RNA expression in a *bulk* RNA-seq dataset available in our lab (Phil Sanders, unpublished data), which comes from the expression analysis of different DIVs from our *in vitro* cell differentiation protocol, which differentiated control and HD human iPSCs and ESCs towards the striatal MSNs lineage<sup>270</sup>. We found a reduction in HELT expression in all HD cell lines respect to controls (Figure 66 A).

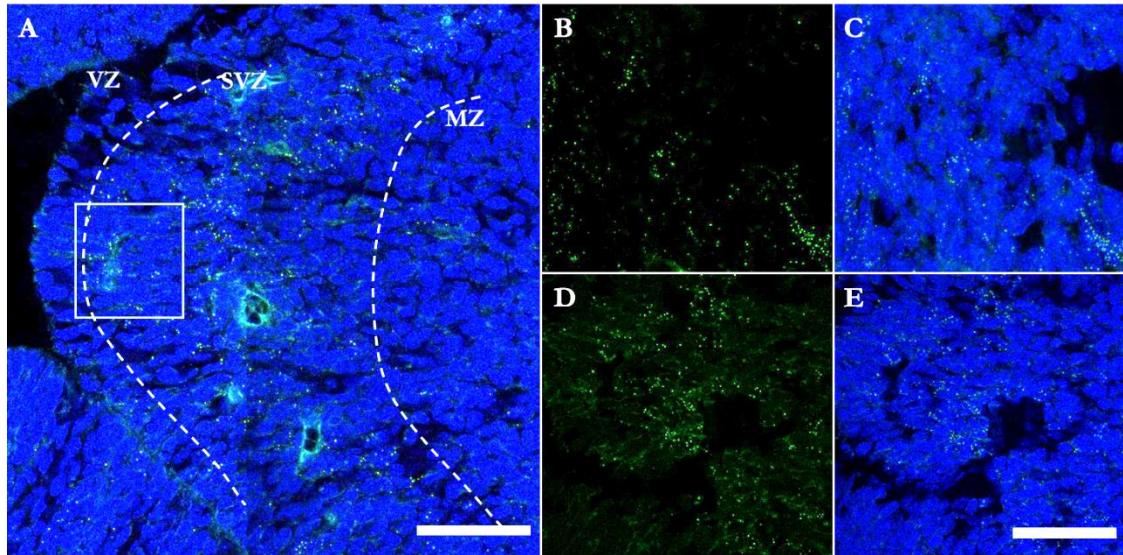


**Figure 65. Fluorescent *In Situ* Hybridization (FISH) of HELT.** A) Mosaic (taken at 40X) of the striatal GZ at E16.5 showing HELT RNA expression in cells preferentially located within the SVZ. Representative images (taken at 63X) of the HELT RNA expression in the SVZ of E14.5 (B-C) and E16.5 (D-E) embryos. Each green dot represents a single HELT-RNA molecule. VZ: ventricular zone; SVZ: sub-ventricular zone; MZ: mantle zone.

To validate HELT differential expression between wt and HD embryos, we quantified the the relative levels of HELT RNA expression by qPCR. To do so, we isolate the LGEs and the MGEs of E12.5 and E14.5 wt and HD embryos and the striatum of E16.5 wt and HD embryos. We found an increase in the RNA expression of HELT in HD NPCs at E12.5 and E14.5, but a later decrease at E16.5 (Figure 66 B). No differences in the RNA levels were found neither in the MGE at E12.5 nor at E14.5 (Figure 66 C).

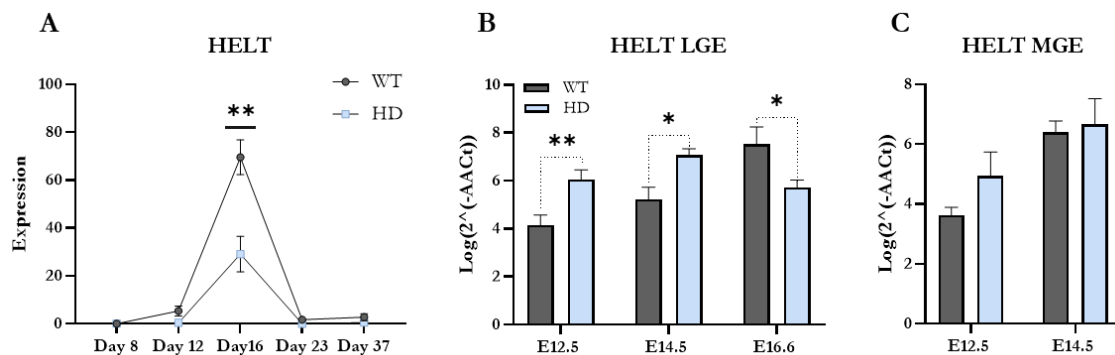


**Figure 66. Relative expression of HELT RNA in wt/ctr and HD samples.** A) Quantification of HELT expression in ctr and HD human cells from bulk RNA-seq datasets from our lab. Quantification of HELT RNA by qPCR of LGE (B) and MGE (C) tissues at different developmental stages. All results are expressed as the mean of independent experiments  $\pm$  s.e.m. and results were analysed using Student's t-test. We considered statistical significance  $p < 0.05$  (\*) and  $p < 0.01$  (\*\*).



# DISCUSSION

---



# DISCUSSION

## 1 HD-related hallmarks are present in zQ175 embryos from early development:

Gene expression analysis carried out by bulk RNAseq pointed out an altered expression pattern in HD embryos. HD altered genes were related with many important adult HD-related hallmarks (Figure 67).

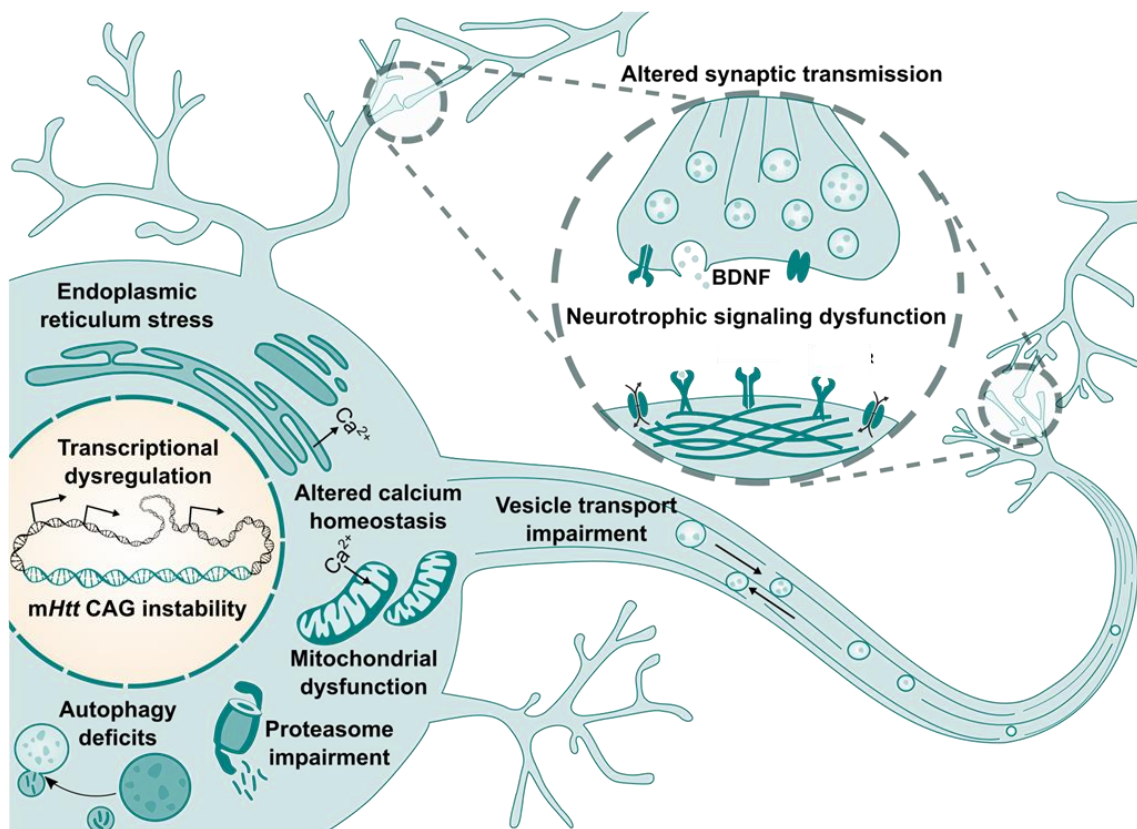


Figure 67. Scheme summarizing the main HD pathophysiological hallmarks. *Edited from Dra. Nuria Suelves.*

### 1.1. *Transcriptional dysregulation*

Many of the genes that were deregulated in HD samples encode for DNA binding proteins and proteins involved in the processing and metabolism of RNAs, as well as alterations in genes encode for proteins related to chromatin remodeling processes, suggesting that both alterations in gene transcription and epigenetic alterations may be occurring in HD development.

#### 1.1.1. TEC genes:

Of the total DEGs present in HD embryos, 50% correspond to TECs, predictions, genes whose products still must be experimentally characterized. Of the other 50% of DEGs, a large part

corresponds to genes that are predicted, without functional annotations or without bibliography in this regard. Interestingly, all the TECs overexpressed in the HD embryos are monoexonic. It has been proposed that the expression of a large proportion of human single exon genes (SEGs) in testis and neuro-specific are associated with several types of cancer, neurological and developmental disorders<sup>273</sup>.

The *Mus musculus* genome has currently around 3000 TEC genes and we found around 500 up-regulated. It's possible that some regions of the body, such as brain, express more TECs than the rest of the tissues as the brain is more complex and many genes have been recently discovered or predicted. This fact shows that there is still a great lack of knowledge about the striatal development and the molecules that regulate it. In addition, the TEC's enrichment analysis predictions were related to HD pathological events, suggesting that within this list of "unknown" genes, there might be key molecules that bring us closer to finding a cure or treatment or, at least, that allow us to better understand the disease.

#### 1.1.2. Long non-coding RNAs:

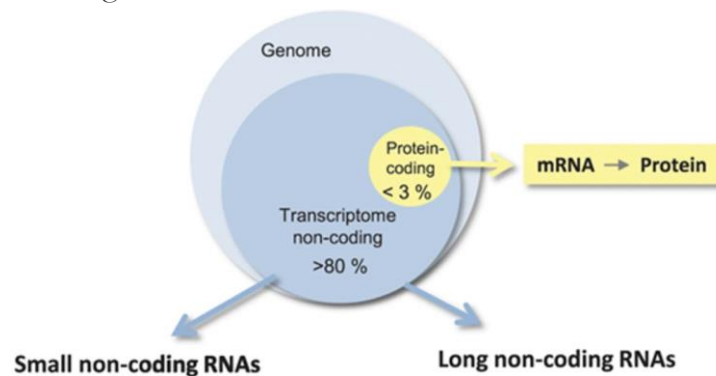


**Figure 68. Contribution of coding vs noncoding RNAs in the human genome.** Edited from: Uchida, S., & Dimmeler, S. (2015).

Advances in genomic analysis have revealed that genes that encode for proteins only account for less than 3% of the total transcribed genome. Conversely, more than the 80% of the transcribed genome correspond to RNAs without coding capacity (Figure 68), including lncRNAs. LncRNAs are RNAs of more than 200 bases in length, with low or no potential to encode for protein<sup>274</sup>. These RNAs often act as epigenetic regulators through chromatin remodeling<sup>275</sup>, as well as splicing regulators, transcription factor regulators, and mRNA stability regulators<sup>276</sup>. LncRNAs are involved in many biological processes such as cell proliferation and survival<sup>277</sup>. In addition, lncRNAs are pretty stable, they are expressed in a tissue-dependent manner, and they are deregulated in human diseases, including cancer and neurological diseases. Of the total of the 38 differentially expressed lncRNAs found in the bulk RNA-seq analysis, we focused on two of them, Malat1 and Neat1, which are highly conserved within the mammalian lineage suggesting a significant function of them<sup>278</sup>. Moreover, both are altered in neuro-degenerative diseases such as HD, PD and AD<sup>279–282</sup>.



Malat1, also known as Neat2, is an lncRNA that has been related to the modulation of genes associated with the development of dendrites and synapses, as well as with cell proliferation<sup>281,283</sup>. The other lncRNA, Neat1, has been closely related to cell survival and defense<sup>284</sup>. It has been described that the up-regulation of Neat1 promotes the cell survival when the cell is under chronic stress situations, such as prolonged proteasome inhibition, hypoxia or oxidative stress<sup>285</sup>. On the other hand, the down-regulation of Neat1 leads to a significant increase in cell death<sup>286</sup>.

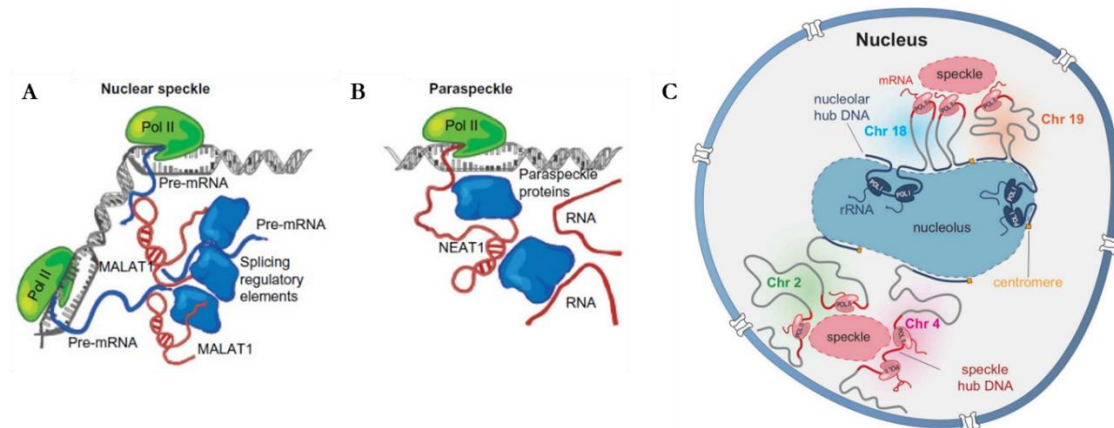


**Figure 69. Generation of speckles (A) and paraspeckles (B) from lncRNA molecules.** Arrangement of these structures in the cell nucleus, specifically in the interchromatinic space. **C)** Model for how higher-order inter-chromosomal hubs shape 3-dimensional. (A, B) (C). Edited from: Quinodoz, S. A. (2018) and Huarte, M., & Marín-Béjar, O. (2015).

Malat1 and Neat1 have been described as essential pieces for the integrity of the architecture of nuclear bodies. Within mammalian cells' nucleus, there are various granular structures such as speckles, paraspeckles, nucleoli, cajal bodies and polycomb bodies. These bodies play roles in several biological processes, such as gene transcription, RNA processing, ribosome formation, chromatin alteration, and protein breakdown<sup>287,288</sup>. Specifically, nuclear speckles, which are part of the spliceosome, contribute to pre-mRNA splicing and the generation of mature mRNA molecules. Neat1 and Malat1 are located exclusively in nuclear paraspeckles and speckles, respectively. Paraspeckles are a relatively new class of sub-nuclear bodies found in the inter-chromatinic space of mammalian cells<sup>283,289,290</sup> (Figure 69). These are structures formed by the interaction between lncRNA molecules and members of the *Drosophila* Behavior Human Splicing (DBHS) family of proteins. These structures retain certain RNAs, playing a role in controlling gene expression during various cellular processes, including differentiation, viral infection and stress response<sup>291</sup>. These studies support that the up-regulation of these two lncRNAs occurs in the presence of cell stress, suggesting this over-expression as a neuro-protective mechanism against neuronal damage<sup>286</sup>.

HD samples show an over-expression of these two lncRNAs, suggesting that during development in HD cells may already be suffering from a certain degree of stress such as oxidative stress. We suggest that this may be existing since alterations in mitochondrial function and in oxidative stress response proteins are affected in HD embryos, as we will discuss below.



## 1.2. *Endocytosis and Vesicle Transport Impairment*

HD DEGs were also related to important intracellular pathways: endocytosis and intracellular transport (Figure 45).

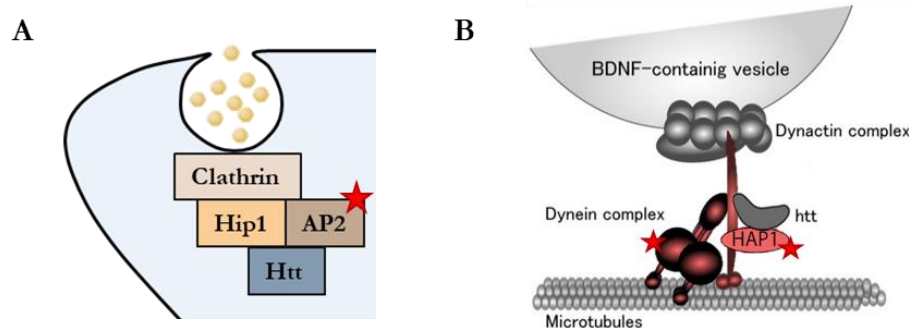


**Figure 70. Graphical summary of the endocytic and vesicle transport alterations found in the HD embryos by bulk RNA-seq. (A)** Down-regulation of genes encoding for proteins of the AP2 clathrine-dependent endocytosis, such as Ap2s1. **(B)** Down-regulation of genes encoding for proteins of the dynein complex, such as Dnah7 and Hap1.

One of the genes that was down-regulated in the HD samples is the Ap2s1. The coding protein is a main component of the AP-2 adaptor protein complex, which participates in multiple vesicular transport pathways as well as in the selection of the load and formation of vesicles (Figure 70 A). AP-2 is also involved in clathrine-mediated endocytosis, joining directly to the clathrine and to different membrane components.

Another downregulated gene is the Huntingtin-associated protein 1 (Hap1). The coding protein is specifically associated with Htt (Figure 70 B), and both are involved in anterograde vesicular traffic functions, with Hap1 allowing the binding between Htt and transporter proteins and load. Hap1 has been related with neurite growth, axonal transport and secretion of BDNF, transport of autophagosomes, transport of GABA receptors to synapses and their recycling, ciliogenesis and with the regulation of transcription through interaction with transcription factors<sup>292–294</sup>. Recently, it has been described that polymorphisms in the protein Hap1 modify the age of onset of disease<sup>295</sup> suggesting an important role of this protein in the pathogenesis of HD. It has been shown that both proteins (AP-2 and Hap1) interact directly with each other, being key pieces for defects in vesicular transport and BDNF described in HD<sup>296,297</sup>

Finally, we also found alterations in the gene that codes for the protein Dynein Axonemal Heavy Chain 7 (Dnah7), which is one of the Top10 DEGs with the highest exchange value (data not shown). This dynein interacts directly with the protein Hap1 (Figure 70 B). Both Ap2 and Hap1 are down-regulated, while Dnah7b is up-regulated in HD samples. Many other coding genes for proteins related to intracellular traffic are altered in HD samples, supporting the hypothesis that there are transport defects during HD development.

### 1.3. Mitochondrial dysfunction, metabolism and cellular stress

Many of the altered genes in HD samples correspond to metabolism-related genes, which concentrate on the biosynthesis and metabolism of glycans and lipids as well as carbon metabolism, including glycolysis/gluconeogenesis (Table 2). Several studies have shown alterations in HD metabolism, both lipid and carbon<sup>298–300</sup>. However, nothing has been described about glycan metabolism in HD.

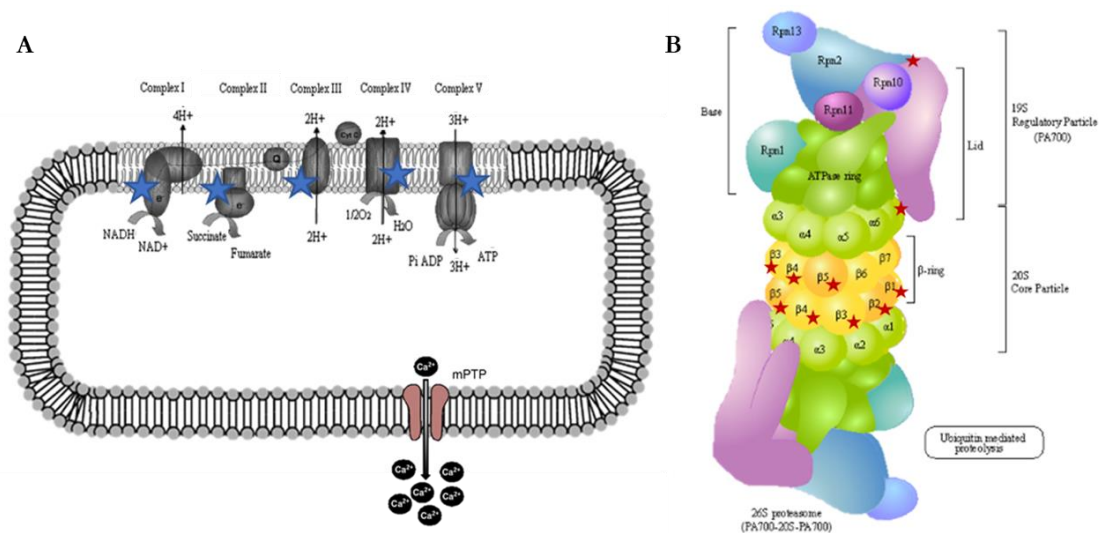


**Figure 71. Diagram of the mHtt-cell protein interactions described.** Image taken from KeggPathways' analysis. The stars mark the distribution of the DEGs obtained.

The three most enriched terms in the pathway analysis of the HD DEGs were neuro-degenerative diseases: HD, PD and AZ (Table 2). The alterations are mainly focused on mitochondria. Patients with HD have metabolic abnormalities as well as energy dysfunction<sup>301</sup>. The main contributing factor to this is the effect of the mHtt in mitochondria: increases mitochondrial fragmentation, alterations in biogenesis and mitochondrial transport, as well as reduced expression of the enzymes responsible for ATP production via oxidative phosphorylation<sup>301</sup>. The results show a decrease in several genes encoding for proteins involved in the respiration chain (Figure 71 A), suggesting alterations in mitochondria and energy production during development in HD mouse embryos.

The enrichment analysis also pointed out downregulation of proteasome-related genes (Figure 71 B). Mutant protein accumulation is a common feature of neurodegenerative diseases. Many evidences implicate the ubiquitin-proteasome pathway in the failure of cells to degrade mutant huntingtin in HD<sup>302–304</sup>. Ineffective elimination of misfolded and oxidate proteins by the proteasome, autophagy pathways and exocytosis lead to accumulation of toxic protein oligomers and aggregates into neurons<sup>305</sup>. Additionally, oxidative stress has a direct impact on the proteasome itself<sup>305</sup>. HD embryos also have alterations in genes encoding for oxidative stress response. Down-regulation of the gene that codes for the superoxide protein dismutase [Cu-Zn] (Sod1), responsible for eliminating radicals

and ROS, is found in HD embryos. Other genes encoding for oxidative stress response proteins are altered in HD embryos (Il18bp, Apex2, Fndc1, Krit1, Cygb, among others).

These results support the hypothesis that small situations cellular stress and energy availability deficits are already generated during HD development.

#### 1.4. *Neuronal Synaptic functionality and calcium homeostasis:*

In the DEGs enrichment analysis (Tables 4 and 5) terms such as ion transport, membrane depolarization and signaling pathways, among others, appear. The MSNs receive mainly cortical glutamatergic inputs. Glutamate activates receptors, including NMDAs, which cause a massive increase in the concentration of intracellular calcium in the neuron. An excess of stimulation by this glutamate leads to induced neuronal death, which is known as in excito-toxicity by glutamate and is believed to be one of the main contributors to HD degeneration.

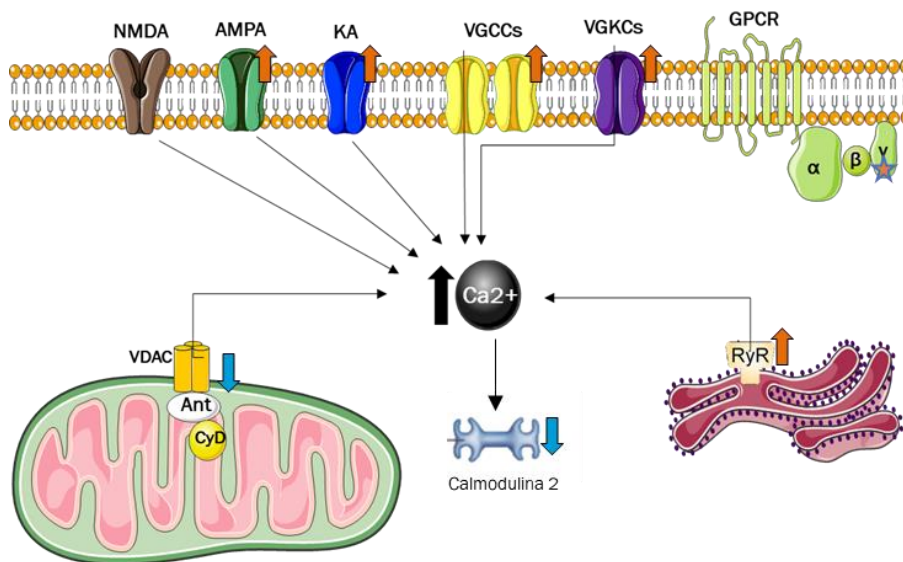


**Figure 72. Graphical summary of the calcium-related DEGs dysregulated in HD embryos.** Orange arrows show down-regulated DEGs and blue arrows show up-regulated DEGs. Blue/orange star shows up and down-regulates DEGs within the same protein subunits.

The results (Figure 72) show an increase in genes encoding for glutamate receptors, as well as an increase in genes encoding for plasma membrane calcium channels and endoplasmic reticulum, suggesting greater glutamatergic stimulation and a greater increase in intracellular calcium in neurons in HD samples. This subtle loss of homeostasis during development can increase throughout adult life and end up generating large situations of excito-toxicity by glutamate that led to neuronal degeneration in the striatum.

## 2 Specific NPCs and Neuronal subpopulations are imbalanced along development in HD

### 2.1. Telencephalic patterning-related alterations:

The regionalization of the telencephalon represents a critical step in brain development, being essential to determine the subsequent cell specification. Pax6, in the telencephalon, is an essential factor for dorso-ventral specification in the PSPB, and it is required for pallial cell identity specification. This barrier is located in the most dorsal part of the LGE, and is marked by the antagonistic action of different transcription factors<sup>306,307</sup> (Figure 73). In the mutant Pax6<sup>-/-</sup> this PSPB is lost<sup>70,308</sup>, cortical and striatal cells have defects in segregation<sup>306</sup>, as well as defects in tangential migration and an increase in the number of GABAergic INs from MGE/LGE in the cortex<sup>309,310</sup>. Pax6 also regulates neurogenesis and regulates the normal progression of the cell cycle in neural progenitors. In addition, Pax6 is an important neuro-genetic determinant of radial glia<sup>311</sup>, and controls neuronal migration by the regulation of adhesion molecules.

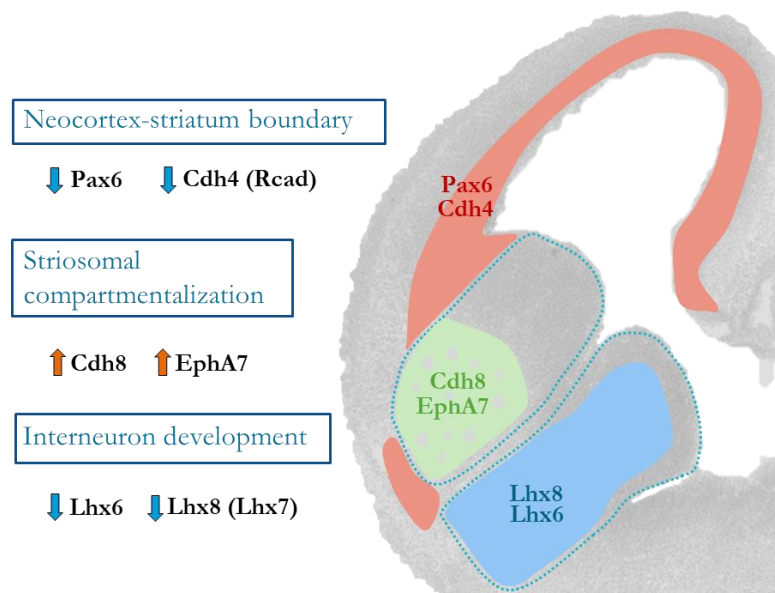


Figure 73. Summary of the main regionalization-related genes affected in HD embryos.

The bulk RNAseq analysis showed that HD embryos have a decreased expression of the gene encoding for **Pax6**. Moreover, they also have an altered expression of genes encoding for two cadherines, **Cdh8** and **Cdh4** which are up and downregulated in HD embryos, respectively. Cdh4 is positively regulated by Pax6 and is involved in the maintenance of the PSPB as well as in the axonal growth<sup>312</sup>. Cdh8 is predominantly expressed in the striatal matrix and engages with cell aggregation and cell classification during development<sup>168,313</sup>. In addition, HD embryos also have a reduced expression of genes encoding for the proteins **Lhx6** and **Lhx8**, two highly conserved transcription factors that take important roles in the patterning and cell fate determination during development<sup>314</sup>, as well as in the migration of GABAergic interneurons from the MGE to the cortex. Moreover, HD

embryos have an increase in the expression of the gene encoding for the ephrine receptor A7 (**EphA7**). EphA7 expression identifies a novel “matrisome” striatal compartment. Neurons conforming this compartment, reside within the striatal matrix but send their axons to the globus pallidus and SNr. It has been shown that EphA7 and ephrin-A5 may participate in the formation of this matrisome subcompartment and its projections<sup>24</sup>. Moreover, alteration in other migration-related molecules, such as protocadherines, have been detected in HD samples at E16.5. Alteration in such important regulators may give rise, on the one hand, to failures in cell fate acquisition and migration to their target areas and, on the other hand, to defects in the striatal cytoarchitecture formation.

## 2.2. HD embryos display aberrant proliferative, neurogenic and maturation programs during HD striatal development

Many of the cellular events described above can influence and define the cell cycle progression<sup>315,316</sup>. On the one hand, cellular proliferation is an energy-consuming activity that is controlled by checkpoints of the cell cycle<sup>317,318</sup>. Cells that make the decision to divide should be metabolically prepared to support the energetic demand imposed by proliferation. On the other hand, different cellular stressor sources can also affect the cell cycle checkpoints and alter the cell cycle progression and decisions. In this line, the GO analysis of the bulk RNA-seq showed that dysregulated genes in HD embryos are related to cell cycle, cell division and mitosis (Table 3). Thus, we proceed to study the cell cycle state and cell cycle exit in HD embryos from early striatal development. Here we show time and lineage-specific alterations in the cell cycle progression of the HD NPCs.

Our results also show an aberrant neurogenic program in Q175 embryos, affecting differently the different neurogenic stages, probably as a consequence of the cell cycle dysregulation. In the early NPCs expansion phase (at E12.5), Q175 embryos display an increased number of cells in S-phase and a decrease in the number of M-phase cells. In concordance, HD embryos display an increased precocious cell cycle exit of neural progenitors at this stage. In contrast, in the later expansion phase (at E14.5), HD embryos display a reduction in the S-phase cells, no changes in M-phase cells, together with a decrease in the cell cycle exit at this stage. We and others have detected alterations in the cell cycle progression in HD embryos<sup>319</sup>, despite the total number of cells in the GZ remain unchanged. This indicate that there is not an increase in the progenitor cell number but a distinct cell cycle regulation or distinct NPC population heterogeneity. The cell cycle phase length of subpallial progenitors could presumably play an important role in their expansion and the diversity of their neuronal output, as it does in the developing cortex<sup>315,316</sup>.

In line with and supporting our findings, it has been described that Sox2, an essential transcription factor for the cell stemness maintenance, is differently dysregulated during striatal development in HD models. It was found an initial reduction of Sox2 in HD striatal NPCs at E12.5, thus promoting

the cell cycle exit, and a later increase of Sox2 at E14.5 NPCs, thus promoting the proliferative state and inhibiting the cell cycle exit<sup>320</sup>.

In line with and supporting our findings, it has been described that Sox2, an essential transcription factor for the cell stemness maintenance, is differently dysregulated during striatal development in HD models. It was found an initial reduction of Sox2 in HD striatal NPCs at E12.5, thus promoting the cell cycle exit, and a later increase of Sox2 at E14.5 NPCs, thus promoting the proliferative state and inhibiting the cell cycle exit<sup>320</sup>. These HD NPC alterations can be explained by cell cycle regulation's intrinsic mechanisms, such as the energetic status, the transcriptional regulation of cell cycle-related genes or the mitotic spindle miss orientation, among others<sup>321</sup>. In this line, early alterations of brain cellular energy homeostasis have been described in HD models<sup>322</sup>. Previous evidence also demonstrate that Htt regulates cellular adhesion, polarity, and epithelial organization<sup>321,323</sup>. Moreover, it has been recently shown that mHtt disrupts the polarity of human and mouse neuroepithelium, and interferes with the cell cycle of apical progenitors by interfering with the orientation of the mitotic spindle, leading to fewer proliferating cells and more neural progenitors prematurely entering lineage specification over proliferation and self-renewal<sup>259</sup>.

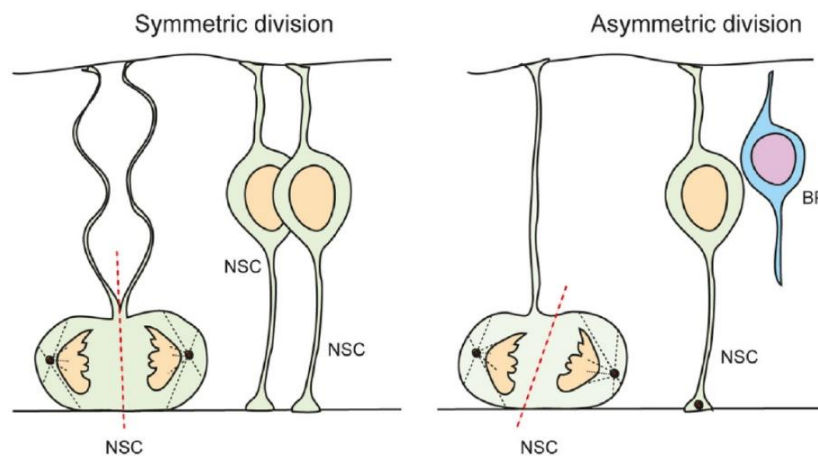


**Figure 74. Types of NSC divisions in the ventricular zone are determined by spindle orientation and the inheritance of cell fate determinants.** Symmetric divisions generate 2 NSCs, whereas asymmetric division generates 1 NSC and 1 differentiating daughter cell. During neural expansion, most divisions are symmetric, whereas during neurogenesis, most divisions are asymmetric. BP indicates basal progenitor; NSC, neural stem cell.

Other explanation is related with differences in the NPC population heterogeneity (Figure 75). As mentioned in the introduction, different NPCs can be found along time: aIPs are generated at earlier stages (E10.5-E12.5) and bIPs at later stages. It has been described differences in the cell cycle kinetics of these NPCs, being aIPs faster (17h) and with no more than one round of amplification, and bIPs slower (20h) with multiple rounds of amplification<sup>94,324</sup>. HD embryos could present distinct subpopulations proportions and identities compared to controls, thus affecting the NPCs behaviour, its kinetics, and the generation of their progeny. Differences in the symmetric/asymmetric divisions can also influence the NPCs heterogeneity pool<sup>325</sup> (Figure 74). For instance, an increase in the RG



asymmetric divisions give rise to a decrease in the RG population and an increase in the intermediate progenitor's (IPs) population. Complementary *in vitro* studies demonstrated clonal size reductions in association with impairments of striatal NPCs lineage restriction and specification of MSN subtypes, further illustrating the broad developmental consequence of HD deregulation of cell cycle parameters<sup>320</sup>.

Whether if these alterations and imbalances affect all NPCs or specific subpopulations, as well as how these alteration affects the NPCs pool maintenance remains still unknown. A deeper study defining the whole NPCs lineage scenario during wt and HD striatal development is crucial to further answer these questions.

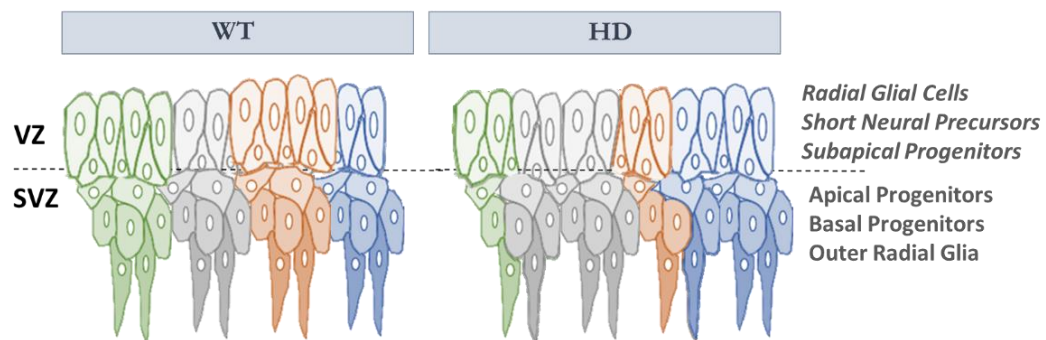


**Figure 75. Hypothesis for the NPCs alterations observed in HD embryos.** Regarding the same number of proliferating cells within the GZ, different cell cycle states may be reflecting differences in the proportion of the different NPCs populations, with different cell cycle potential and kinetics.

### 2.3. Direct and indirect pathway imbalance starts from early development in HD:

Basal ganglia circuitry balance and homeostasis is crucial for its correct function. Imbalances along this circuitry are related to several neurological and psychiatric diseases such as HD, PD, Tourette's syndrome, schizophrenia and depression, among many others<sup>326,327</sup>. Here we describe an early imbalance of the direct and indirect pathways, which could set the stage for the early pathophysiological abnormalities in HD.

DEGs obtained with by the bulkRNA-seq analyses show that there is a greater abundance of previously described<sup>271</sup> iMSN markers and a lower number of dMSN markers in the MZ of the samples HD with respect to wt (Figure 50 A), which can be interpreted as a larger proportion of iMSNs and a lower one proportion of dMSNs at this stage. It is well known that the iMSN population is specially altered in HD, although the reasons that lead to this differential affectation are unknown. These results show that both subpopulations of MSNs may be suffering from differing affectations during development and/or different developmental patterns. Differences in the formation of both

populations at the level of the embryo can lead to different degrees of vulnerability to stressors in the adult life of one of the subpopulations with respect to the other, as observed in the HD patients.

### 2.3.1. Precocious and enhanced neurogenesis of iMSNs:

Briefly, dMSNs are mostly generated during the early expansion phase while iMSNs are generated mainly during the later phase. Here we show an important increase in the production of lineage-specific iMSNs and, moreover, a precocious neurogenesis of that population in HD embryos, being erroneously born in the first neurogenic wave (E12.5). During the first neurogenic wave, NPCs are mainly early aIPs, which are committed to produce striosomal MSNs with likely no more than one single round of amplification. Around E13.5, an abrupt transition make that RGs shift to generate bIPs, which are fate-restricted to generate matrix MSNs. Provably, the increase in the early iMSNs generation at E12.5 can be due to an increase in the production of bIPs, due to an increase in the asymmetric divisions during early stages.

### 2.3.2. Specific iMSNs cell death during postnatal development:

Interestingly, these aberrantly born iMSNs undergo specific cell death postnatally. Removal of substantial numbers of neurons that are not yet completely integrated into the local circuits helps to ensure that maturation and homeostatic function of neuronal networks in the brain proceed correctly. Both the patch and matrix compartments undergo their entire cell death period by the end of the first postnatal week, when approximately 30% of striatal neurons are subject to cell death. It has been found that neurons with early projections to the substantia nigra survive this cell death period<sup>164,246</sup>. External signals from brain microenvironment together with intrinsic signalling pathways determine whether a particular neuron will die<sup>328–330</sup>. We hypothesize that aberrantly generated iMSNs are not capable to achieve its target connections, thus, they undergo a massive cell death during postnatal normal cell death period.

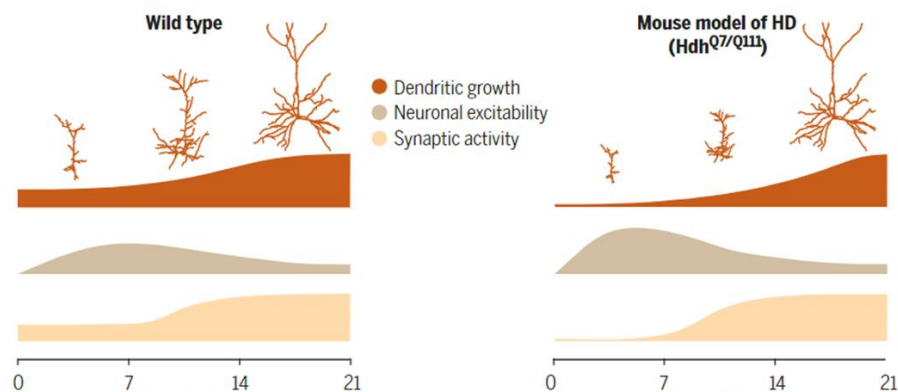


**Figure 76. Huntington's disease (HD) transiently alters cortical circuit function by decreasing synaptic activity, increasing excitability, and reducing the complexity of dendritic arborization.** Image extracted from Braş, B. Y., et al. (2022).



Some recent studies have investigated HD developmental alterations during the postnatal period. It has been described some postnatal HD alterations in the cortical circuit function by decreasing synaptic activity, increasing excitability, and reducing the complexity of dendritic arborization<sup>264</sup> (Figure 76). Moreover, a dopaminergic and glutamatergic imbalance has been reported in postnatal tgHD rat striatum, together with a down-regulation of the NR1, NR2B, and NR2C subunits of NMDARs of P10 HD rats<sup>331</sup>. Temporary reductions and enhancements in neural activity during the perinatal period can impact the functional connectivity and behaviour of an adult and may be responsible for early-onset neurological disorders such as schizophrenia, epilepsy, and autism spectrum disorders<sup>264</sup>. Developmental abnormalities can lay the groundwork for diseases that only appear in later life.

### 2.3.3. HD striatum ends up with an imbalance in dMSNs/iMSNs populations:

Our results show a reduction in the total number of iMSNs composing the mature striatum at the end of development (P21). The d/iMSNs lineage-specific dysfunction have been broadly explored in the adult HD, being iMSNs firstly affected in HD with an early reduction of this subpopulation during the disease progression. The early phases of disease progression in HD are dominated by hyperkinetic motor features, notably chorea. This has been attributed to this selective atrophy and early loss of iMSNs<sup>332,333</sup>.

Here we postulate that it is not that the iMSNs undergo neurodegeneration and cell death earlier than the dMSN's lineage, but they are in a decreased proportion in HD respect to controls from the very beginning because of their specific miss formation during development. Its specific disturbances during neuronal development may enhance iMSNs selective vulnerability to stressors, leading to the described iMSNs early dysfunction and loss.

## 2.4. Striatal Interneuron developmental alterations:

Interneurons represent a key regulator of cortical and striatal circuitry homeostasis. We found that HD developmental alterations also affects the interneuronal lineage.

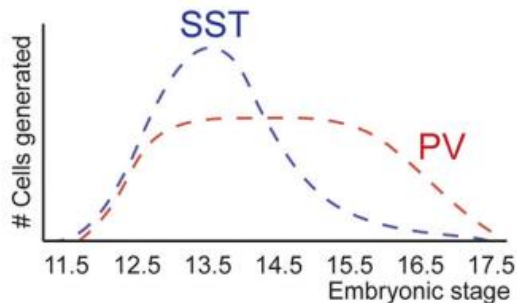


**Figure 77. Temporal biases in interneuron origin.** SST cells are mostly produced during early neurogenesis, while PV cell production remains nearly constant throughout the entire neurogenic window. *Image edited from Llorca, A., & Deogracias, R. (2022).*

We first detected a reduction in the SST<sup>+</sup>/NPY<sup>+</sup>/CR<sup>+</sup> expression at the E16.5 striatal MZ by bulkRNAseq. However, this reduction was not statistically significant when we histologically analysed the IN subpopulation within the striatal MZ at E18.5. This can be explained by three different factors. On the one hand, it could be possible that the reduction in the IN population detected in the E16.5 striatum is somehow compensated later at E18.5. On the second hand, when performing the histological analyses, we used the reporter mice Nkx2.1-CRE, that labels all the IN progeny, not only the SST<sup>+</sup>/NPY<sup>+</sup>/CR<sup>+</sup> IN subpopulation. Thus, reduction in specific subpopulations can be diluted when quantifying the total INs. Finally, the INs that we capture when dissecting the striatum at E16.5, can be either striatal residents or INs that are just crossing the striatum to their final destination in the cortex. Thus, may be is not that striatal INs are reduced in the striatum but a transient reduction in the INs migrating to the cortex. In this line, it has been found a selective reduction in SST<sup>+</sup> IN in the cortex of R6/1 HD mouse model<sup>334</sup>. Moreover, it has been shown that dysfunction of SST<sup>+</sup> striatal interneurons contributes to the increased GABA synaptic activity found in HD mouse models<sup>335</sup>.

When looking into the striatal INs neurogenic rates, we found that HD embryos have an increase in the IN generation at E14.5. We then would expect an increase in the striatal IN population later at E18.5. In this sense, we have just analyzed two timepoints from the whole IN neurogenesis timeline (E11.5-E17.5) (Figure 77) and, moreover, we have still not analyzed IN generation at E13.5, when there is the peak of neurogenesis of the SST<sup>+</sup>/NPY<sup>+</sup>/CR<sup>+</sup> IN subpopulation<sup>336</sup>. Thus, deeper analyses at different stages are needed to further understand what is happening during IN generation during HD development.

Although we still need a deeper analysis of the IN-lineage generation, migration and circuit integration to draw some conclusions, our preliminary results encourage to further investigate the IN developmental affection in HD.

## 2.5. Targeting HELT-expressing subpopulation as a candidate for HD:

We generated a robust developmental model by computationally integrating different human and mouse in vivo and in vitro scRNA-seq datasets (Figure 59). We were able to identify different important neuronal lineages such as the striatal dMSN lineage, the striatal iMSN lineage or the IN lineage (Figure 62). We did also identify different striatal NPCs and NBs populations (Figure 61). Moreover, our developmental model was conformed by both wt and HD cells, we could identify subpopulations specifically affected in HD. We then were able to extract specific markers of this populations. We focused on one of those genes, HELT, as it encoded for a BHLH TF.

BHLH TFs comprise an evolutionarily ancient group of proteins conserved across many species that mainly function as key regulators of cell-fate decisions and neuronal differentiation in the developing CNS of invertebrates and Vertebrates<sup>337,338</sup>. Here we identified a novel bHLH TF involved in striatal development, HELT/Mgn. HELT mRNA expression follows a specific and dynamic pattern in the embryonic CNS, which is developmentally regulated in a tissue-specific manner. Its expression shows a spatiotemporal correlation with GABAergic markers in several brain regions<sup>339</sup>. HELT is expressed early on E9.5, coinciding with the emergence of the first GABAergic neurons, and is then switched off in all GABAergic precursors once they become postmitotic.

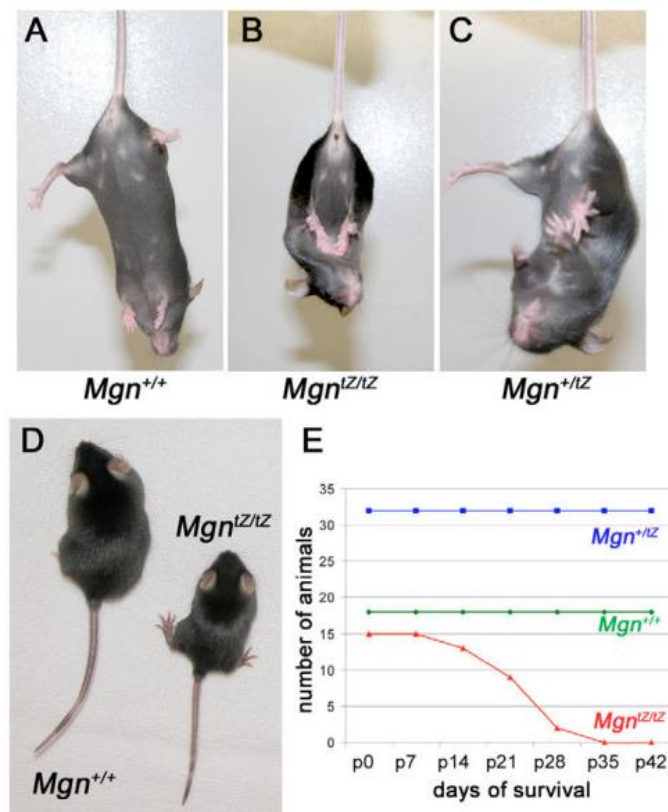


**Figure 78. HELT/Mgn KO mice. A-C)** Fore/hindlimb clasping phenotype in postnatal homozygous *Mgn*<sup>tZ/tZ</sup> mutant at postnatal day 20 (P20). **D)** Phenotypic comparison of *Mgn*<sup>+/+</sup> and *Mgn*<sup>tZ/tZ</sup> mice at P32. **E)** Survival curve of *Mgn*<sup>tZ/tZ</sup> mice.

HELT function has been widely described in the midbrain (MB)<sup>339</sup>. HELT mutant mice show normal brain histology and morphology. However, expression of GABAergic Gad65 and Gad67, is completely abolished in the superior colliculus (SC), and homozygous mutant animals display a clamping phenotype and symptoms resembling tonic-clonic seizures preceding postnatal death (Figure 78). These findings demonstrate the critical involvement of HELT in the correct development of GABAergic neurons in the SC and suggest that HELT plays a crucial role in postnatal survival during early development<sup>339,340</sup>.

Moreover, these studies also demonstrate HELT physically interacts with the proneural factor Ascl1. These studies demonstrate that these two cooperating bHLH factors are necessary for the acquisition of GABAergic identity in the MB (Figure 79)<sup>341,339</sup>. Moreover, HELT determines GABAergic over glutamatergic neuronal fate by repressing Ngn genes in the developing mesencephalon<sup>342</sup>.

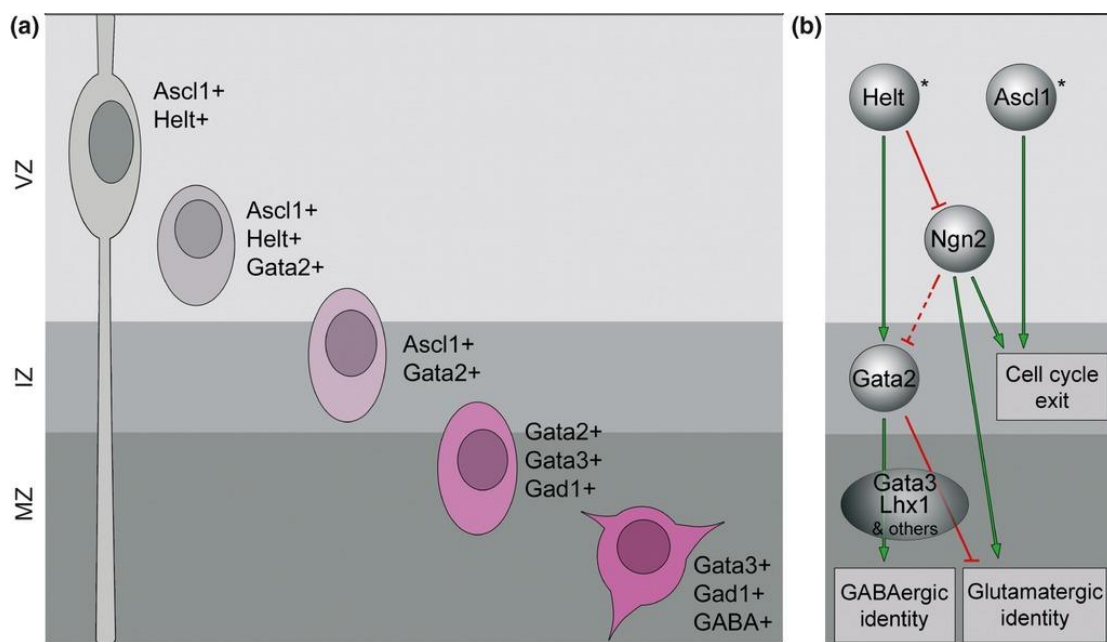


**Figure 79. Diagram illustrating the genetic network controlling the generation of midbrain-derived GABAergic neurons. A)** Schematic view of GABAergic neurogenesis in the midbrain. **B)** Genetic interactions between transcription factors controlling GABAergic vs. glutamatergic fate in the midbrain. Green arrows indicate activation and red blunted arrows inhibition. Edited from: Lahti, L., Achim, K., & Partanen, J. (2013)

Although HELT expression has never been related with striatal development, its important role in GABAergic midbrain neurogenesis and its cooperation with Ascl1 factor, let us to think that HELT TF could be a critical player also during striatal development. In this line, when looking into HELT expression along brain development, two main regions are highly enriched in this factor: midbrain and striatum (Figure 80).

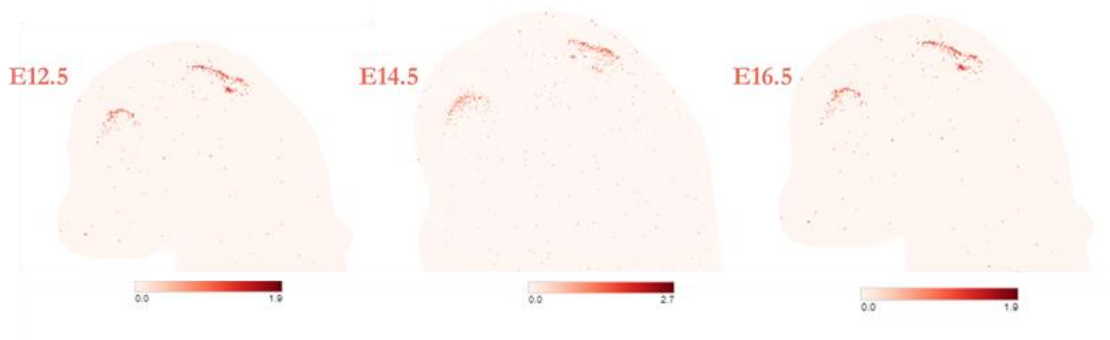


**Figure 80. HELT mRNA expression along brain development.**

Moreover, HELT KO mice show a fore/hindlimb cramping phenotype (Figure 78) which, interestingly, is a key feature observed in the HD mice<sup>343</sup>, suggesting a possible relationship between HELT expression and the HD adult phenotype. In this line, when we checked HELT expression during the *in vitro* differentiation of human control and HD iPSCs/ESCs to MSNs<sup>270</sup>, it was expressed during the striatal cell generation, showing its detection during GABAergic striatal neurogenesis. Moreover, HELT was specifically diminished in the HD cells during this process.

Here, we found an initial increase in HELT expression at E14.5, followed by a decrease in its expression later at E16.5 in HD embryos respect to controls. Moreover, gene expression pattern of the HELT<sup>+</sup> cells suggest that are involved in the iMSNs lineage, as they also express Six3 and SP8/9 indirect-lineage specific markers. This preliminary data encouraged us to further investigate this subpopulation and its affectation during HD striatal development.

### 3 INTEGRATIVE DISCUSSION

---

Our work provides evidences that developmental alterations can set the stage for the early pathophysiological abnormalities in HD by an early disruption of crucial developmental pathways. Here we show an early HD-like gene expression pattern in HD mouse embryos. Moreover, we show that iMSN lineage-specific developmental alterations lead to the formation of a neuronal imbalanced mature striatum. It has been demonstrated that the selective expression of mHtt just during development, until P21, is enough to generate an adult HD-phenotype<sup>344</sup>.

Asuming Huntington's Disease as an adult-onset neurodegenerative disorder with an early neurodevelopmental contribution represents an encouraging change in the HD paradigm. On the one hand, it shows the importance and the need to study the developmental contribution of HD which, in turn, will provide new information regarding the disease and its progression. On the other hand, it opens a range of therapeutic targets that aim to treat the disease in stages prior to the appearance of symptoms, before it becomes the massive neuronal loss.

We postulate that a Huntington's Disease is the result of the combination of different main factors:

- Neuronal generation is affected by both loss of function of wt Htt, the mHtt gain of function effects, and the attempt of the system to adapt and correct these defects.
- All these developmental events finally lead to a subtle imbalance in the basal ganglia circuitry which, in turn, tries to be compensated. This attempt is likely to be outbalanced, finally causing the first obvious symptoms of the disease to appear.
- The presence of mHtt and its toxic effects remain present in these unbalanced cells during the whole life, making them even more vulnerable to cell death.

Understanding the specific developmental disturbances and the interplay between compensatory and pathogenic mechanisms during the prodromal phases of HD, is crucial to better understand the disease progression and to identify candidate targets that potentially compensate for neurodevelopmental defects, restore neuronal homeostasis, and protect striatal MSNs from disease progression. Finding a cure that makes it possible to treat the disease long before the neurons die and, therefore, makes it possible to treat the disease before the symptoms appear, would represent a hopeful solution to cure and improve the lives of HD patients and their loved ones.



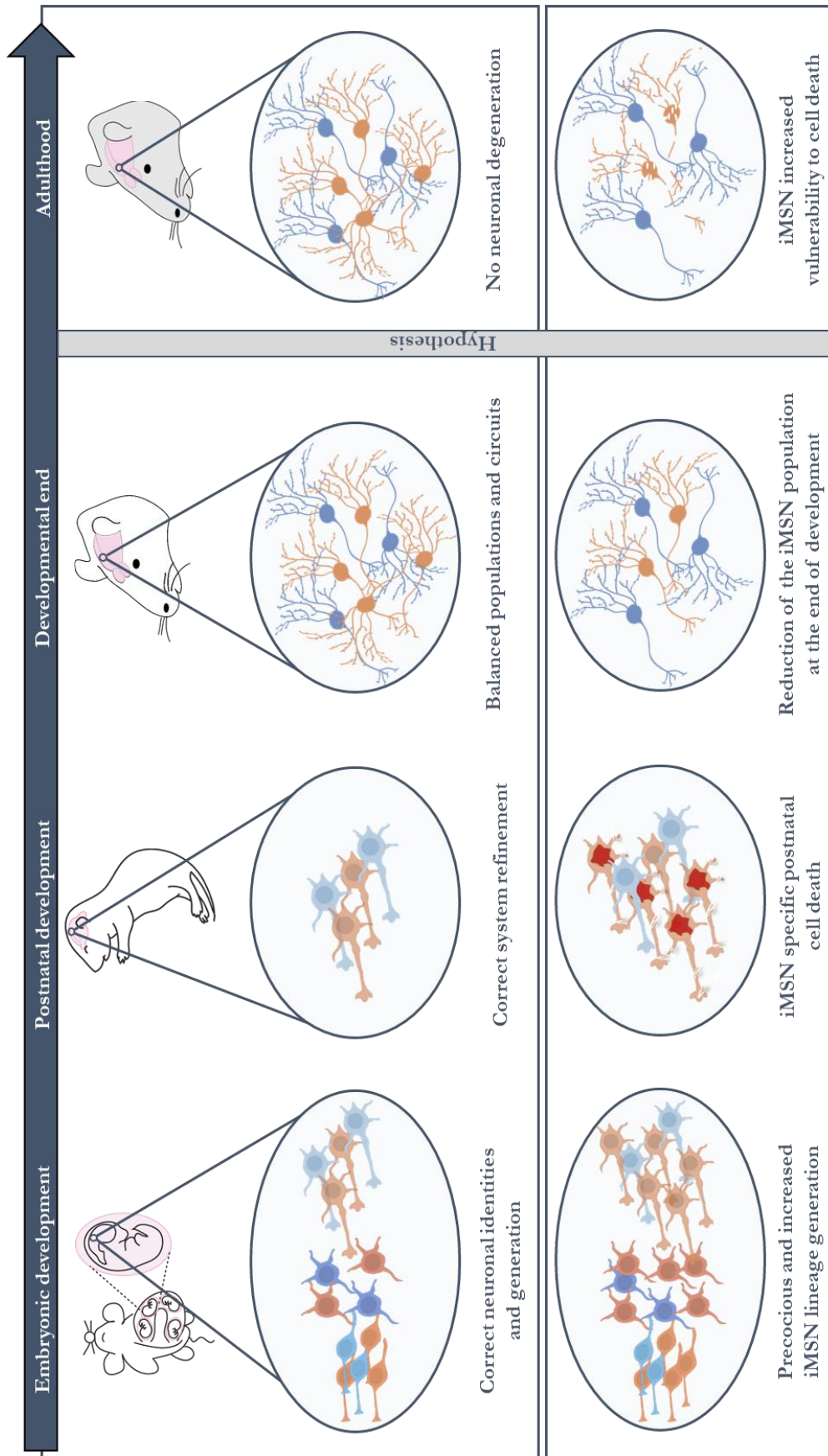


Figure 81. Schematic summary of the iMSN lineage developmental abnormalities.

# CONCLUSIONS

---





# CONCLUSIONS

1. Gene expression pattern is altered during mouse HD development and alterations are related with neurodegenerative disorders and locomotor conditions.
2. The gene expression pattern of HD embryos recapitulates the classic pathophysiological alterations described in the human adult HD.
3. Cell cycle regulation and identity of striatal neural progenitor cells are altered during HD development.
4. HD mouse embryos undergo a precocious neurogenesis during development.
5. Indirect lineage MSNs are generated prematurely and in excess during HD mouse development.
6. Striatal development ends up with an imbalance of its dMSNs/iMSNs population, with a reduction in the iMSNs population.
7. HELT emerges as a novel striatal transcription factor, which may have an important role during striatal GABAergic development.
8. HELT-expressing cell population is specifically affected during HD mouse development.
9. HELT-expressing NPCs may represent a potential target to further analyse the developmental aspects of HD and its contribution to the adult phenotype.



# BIBLIOGRAPHY

---



# BIBLIOGRAPHY

1. Parent, A. & Hazrati, L. N. Functional anatomy of the basal ganglia. I. The cortico-basal ganglia-thalamo-cortical loop. *Brain Research Reviews* (1995) doi:10.1016/0165-0173(94)00007-C.
2. THE Croonian Lectures ON SOME DISORDERS OF MOTILITY AND OF MUSCLE TONE., *Lancet* (1925) doi:10.1016/s0140-6736(01)20638-2.
3. DeLong, M. R. *et al.* Role of basal ganglia in limb movements. *Hum. Neurobiol.* (1984).
4. Schultz, W. Dopamine neurons and their role in reward mechanisms. *Curr. Opin. Neurobiol.* (1997) doi:10.1016/S0959-4388(97)80007-4.
5. Alexander, G. Models of information processing in the basal ganglia. *Electroencephalogr. Clin. Neurophysiol.* (1996) doi:10.1016/0921-884x(96)89703-7.
6. Balleine, B. W. & O'Doherty, J. P. Human and rodent homologies in action control: Corticostriatal determinants of goal-directed and habitual action. *Neuropsychopharmacology* (2010) doi:10.1038/npp.2009.131.
7. Redgrave, P., Prescott, T. J. & Gurney, K. The basal ganglia: A vertebrate solution to the selection problem? *Neuroscience* (1999) doi:10.1016/S0306-4522(98)00319-4.
8. Mink, J. W. The basal ganglia: Focused selection and inhibition of competing motor programs. *Prog. Neurobiol.* (1996) doi:10.1016/S0301-0082(96)00042-1.
9. McNab, F. & Klingberg, T. Prefrontal cortex and basal ganglia control access to working memory. *Nat. Neurosci.* (2008) doi:10.1038/nn2024.
10. O'Reilly, R. C. & Frank, M. J. Making working memory work: A computational model of learning in the prefrontal cortex and basal ganglia. *Neural Comput.* (2006) doi:10.1162/089976606775093909.
11. Alexander, G. E., DeLong, M. R. & Strick, P. L. Parallel organization of functionally segregated circuits linking basal ganglia and cortex. *Annu. Rev. Neurosci.* (1986) doi:10.1146/annurev.ne.09.030186.002041.
12. Middleton, F. A. & Strick, P. L. Basal-ganglia 'projections' to the prefrontal cortex of the primate. *Cereb. Cortex* (2002) doi:10.1093/cercor/12.9.926.
13. Schroeder, K. F., Hopf, A., Lange, H. & Thoerner, G. MORPHOMETRISCH-STATISTISCHE STRUKTURANALYSEN DES STRIATUM, PALLIDUM UND NUCLEUS SUBTHALAMICUS BEIM MENSCHEN. I. STRIATUM. *J. Hirnforsch.* (1975).

14. Gerfen, C. R. D1 and D2 dopamine receptor regulation of striatonigral and striatopallidal neurons. *Semin. Neurosci.* (1992) doi:10.1016/1044-5765(92)90009-Q.
15. Kubota, Y. & Kawaguchi, Y. Spatial distributions of chemically identified intrinsic neurons in relation to patch and matrix compartments of rat neostriatum. *J. Comp. Neurol.* **332**, 499–513 (1993).
16. Nopoulos, P. C. *et al.* Smaller intracranial volume in prodromal Huntington's disease: Evidence for abnormal neurodevelopment. *Brain* **134**, 137–142 (2011).
17. Mao, M., Nair, A. & Augustine, G. J. A novel type of neuron within the Dorsal striatum. *Front. Neural Circuits* (2019) doi:10.3389/fncir.2019.00032.
18. Darmopil, S., Muñetón-Gómez, V. C., De Ceballos, M. L., Bernson, M. & Moratalla, R. Tyrosine hydroxylase cells appearing in the mouse striatum after dopamine denervation are likely to be projection neurones regulated by L-DOPA. *Eur. J. Neurosci.* (2008) doi:10.1111/j.1460-9568.2008.06040.x.
19. Ibáñez-Sandoval, O., Xenias, H. S., Tepper, J. M. & Koós, T. Dopaminergic and cholinergic modulation of striatal tyrosine hydroxylase interneurons. *Neuropharmacology* (2015) doi:10.1016/j.neuropharm.2015.03.036.
20. Brimblecombe, K. R. & Cragg, S. J. The Striosome and Matrix Compartments of the Striatum: A Path through the Labyrinth from Neurochemistry toward Function. *ACS Chemical Neuroscience* (2017) doi:10.1021/acschemneuro.6b00333.
21. Gerfen, C. R., Herkenham, M. & Thibault, J. The neostriatal mosaic: II. Patch- and matrix-directed mesostriatal dopaminergic and non-dopaminergic systems. *J. Neurosci.* (1987) doi:10.1523/jneurosci.07-12-03915.1987.
22. Gerfen, C. R., Baimbridge, K. G. & Thibault, J. The neostriatal mosaic: III. Biochemical and developmental dissociation of patch-matrix mesostriatal systems. *J. Neurosci.* (1987) doi:10.1523/jneurosci.07-12-03935.1987.
23. Flaherty, A. W. & Graybiel, A. M. Output architecture of the primate putamen. *J. Neurosci.* (1993) doi:10.1523/jneurosci.13-08-03222.1993.
24. Tai, A. X., Cassidy, R. M. & Kromer, L. F. EphA7 expression identifies a unique neuronal compartment in the rat striatum. *J. Comp. Neurol.* (2013) doi:10.1002/cne.23308.
25. Janis, L. S., Cassidy, R. M. & Kromer, L. F. Ephrin-A binding and EphA receptor expression delineate the matrix compartment of the striatum. *J. Neurosci.* (1999) doi:10.1523/jneurosci.19-12-04962.1999.
26. Crittenden, J. R. & Graybiel, A. M. Basal Ganglia Disorders Associated with Imbalances in

- the Striatal Striosome and Matrix Compartments. *Front. Neuroanat.* **5**, (2011).
27. Gerfen, C. R. The neostriatal mosaic: multiple levels of compartmental organization. *Trends in Neurosciences* vol. 15 133–139 (1992).
  28. Crittenden, J. R. & Graybiel, A. M. Disease-Associated Changes in the Striosome and Matrix Compartments of the Dorsal Striatum. in *Handbook of Behavioral Neuroscience* vol. 24 783–802 (2017).
  29. Shipp, S. The functional logic of corticostriatal connections. *Brain Structure and Function* (2017) doi:10.1007/s00429-016-1250-9.
  30. Cavalcanti, J. R. L. P. *et al.* Nuclear organization of the substantia nigra, ventral tegmental area and retrorubral field of the common marmoset (*Callithrix jacchus*): A cytoarchitectonic and TH-immunohistochemistry study. *J. Chem. Neuroanat.* (2016) doi:10.1016/j.jchemneu.2016.05.010.
  31. Lanciego, J. L., Luquin, N. & Obeso, J. A. Functional neuroanatomy of the basal ganglia. *Cold Spring Harb. Perspect. Med.* (2012) doi:10.1101/cshperspect.a009621.
  32. Bolam, J. P., Izzo, P. N. & Graybiel, A. M. Cellular substrate of the histochemically defined striosome/matrix system of the caudate nucleus: A combined golgi and immunocytochemical study in cat and ferret. *Neuroscience* **24**, 853–875 (1988).
  33. Kojima, Y., Tam, O. H. & Tam, P. P. L. Timing of developmental events in the early mouse embryo. *Seminars in Cell and Developmental Biology* (2014) doi:10.1016/j.semcdb.2014.06.010.
  34. Iwakura, Y. Mechanism of Blastocyst Formation of the Mouse Embryo: (mouse embryo/blastocyst formation/ polarization/cell interaction/t12mutation/tunicamycin). *Development, Growth & Differentiation* (1989) doi:10.1111/j.1440-169X.1989.00523.x.
  35. Bardot, E. S. & Hadjantonakis, A. K. Mouse gastrulation: Coordination of tissue patterning, specification and diversification of cell fate. *Mech. Dev.* (2020) doi:10.1016/j.mod.2020.103617.
  36. Papenbrock, T., Wild, A. E. & Fleming, T. P. Cleavage and Gastrulation in Mouse Embryos. in *eLS* (2009). doi:10.1002/9780470015902.a0001068.pub2.
  37. Tam, P. P. L. & Behringer, R. R. Mouse gastrulation: The formation of a mammalian body plan. *Mech. Dev.* (1997) doi:10.1016/S0925-4773(97)00123-8.
  38. Sakai, Y. Neurulation in the mouse: Manner and timing of neural tube closure. *Anat. Rec.* (1989) doi:10.1002/ar.1092230212.
  39. Amadei, G. *et al.* Embryo model completes gastrulation to neurulation and organogenesis. *Nature* (2022) doi:10.1038/s41586-022-05246-3.



40. Altmann, C. R. & Brivanlou, A. H. Neural patterning in the vertebrate embryo. *International Review of Cytology* (2001) doi:10.1016/s0074-7696(01)03013-3.
41. Muhr, J., Jessell, T. M. & Edlund, T. Assignment of early caudal identity to neural plate cells by a signal from caudal paraxial mesoderm. *Neuron* (1997) doi:10.1016/S0896-6273(00)80366-9.
42. Wilson, S. W. & Rubenstein, J. L. R. Induction and dorsoventral patterning of the telencephalon. *Neuron* vol. 28 641–651 (2000).
43. Deacon, T. W., Pakzaban, P. & Isacson, O. The lateral ganglionic eminence is the origin of cells committed to striatal phenotypes: neural transplantation and developmental evidence. *Brain Res.* **668**, 211–219 (1994).
44. Stenman, J., Yu, R. T., Evans, R. M. & Campbell, K. Tlx and Pax6 co-operate genetically to establish the pallio-subpallial boundary in the embryonic mouse telencephalon. *Development* (2003) doi:10.1242/dev.00328.
45. Delgado, R. N. & Lim, D. A. Maintenance of positional identity of neural progenitors in the embryonic and postnatal telencephalon. *Front. Mol. Neurosci.* (2017) doi:10.3389/fnmol.2017.00373.
46. Carney, R. S. E., Cocas, L. A., Hirata, T., Mansfield, K. & Corbin, J. G. Differential regulation of telencephalic pallial-subpallial boundary Patterning by Pax6 and Gsh2. *Cereb. Cortex* (2009) doi:10.1093/cercor/bhn123.
47. Evans, A. E., Kelly, C. M., Precious, S. V. & Rosser, A. E. Molecular Regulation of Striatal Development: A Review. *Anat. Res. Int.* **2012**, 1–14 (2012).
48. Furuta, Y., Piston, D. W. & Hogan, B. L. M. Bone morphogenetic proteins (BMPs) as regulators of dorsal forebrain development. *Development* (1997) doi:10.1242/dev.124.11.2203.
49. Grove, E. A., Tole, S., Limon, J., Yip, L. W. & Ragsdale, C. W. The hem of the embryonic cerebral cortex is defined by the expression of multiple Wnt genes and is compromised in Gli3-deficient mice. *Development* (1998) doi:10.1242/dev.125.12.2315.
50. Monuki, E. S., Porter, F. D. & Walsh, C. A. Patterning of the dorsal telencephalon and cerebral cortex by a roof plate-lhx2 pathway. *Neuron* (2001) doi:10.1016/S0896-6273(01)00504-9.
51. Houart, C. *et al.* Establishment of the telencephalon during gastrulation by local antagonism of Wnt signaling. *Neuron* (2002) doi:10.1016/S0896-6273(02)00751-1.
52. Gunhaga, L. *et al.* Specification of dorsal telencephalic character by sequential Wnt and FGF signaling. *Nat. Neurosci.* (2003) doi:10.1038/nm1068.

53. Backman, M. *et al.* Effects of canonical Wnt signaling on dorso-ventral specification of the mouse telencephalon. *Dev. Biol.* (2005) doi:10.1016/j.ydbio.2004.12.010.
54. Campbell, K. Dorsal-ventral patterning in the mammalian telencephalon. *Current Opinion in Neurobiology* (2003) doi:10.1016/S0959-4388(03)00009-6.
55. Gunhaga, L., Jessell, T. M. & Edlund, T. Sonic hedgehog signaling at gastrula stages specifies ventral telencephalic cells in the chick embryo. *Development* (2000) doi:10.1242/dev.127.15.3283.
56. Marklund, M. *et al.* Retinoic acid signalling specifies intermediate character in the developing telencephalon. *Development* (2004) doi:10.1242/dev.01308.
57. Rallu, M., Corbin, J. G. & Fishell, G. Parsing the prosencephalon. *Nat. Rev. Neurosci.* (2002) doi:10.1038/nrn989.
58. Schuurmans, C. & Guillemot, F. Molecular mechanisms underlying cell fate specification in the developing telencephalon. *Current Opinion in Neurobiology* vol. 12 26–34 (2002).
59. Storm, E. E. *et al.* Dose-dependent functions for Fgf8 in regulating telencephalic patterning centers. *Development* (2006) doi:10.1242/dev.02324.
60. Casarosa, S., Fode, C. & Guillemot, F. Mash1 regulates neurogenesis in the ventral telencephalon. *Development* (1999) doi:10.1242/dev.126.3.525.
61. Fode, C. *et al.* A role for neural determination genes in specifying the dorsoventral identity of telencephalic neurons. *Genes Dev.* (2000) doi:10.1101/gad.14.1.67.
62. Corbin, J. G., Nery, S. & Fishell, G. Telencephalic cells take a tangent: Non-radial migration in the mammalian forebrain. *Nature Neuroscience* (2001) doi:10.1038/nn749.
63. Stoykova, A., Treichel, D., Hallonet, M. & Gruss, P. Pax6 modulates the dorsoventral patterning of the mammalian telencephalon. *J. Neurosci.* (2000) doi:10.1523/jneurosci.20-21-08042.2000.
64. Theil, T., Alvarez-Bolado, G., Walter, A. & Rüther, U. Gli3 is required for Emx gene expression during dorsal telencephalon development. *Development* (1999) doi:10.1242/dev.126.16.3561.
65. Tole, S., Goudreau, G., Assimacopoulos, S. & Grove, E. A. Emx2 is required for growth of the hippocampus but not for hippocampal field specification. *J. Neurosci.* (2000) doi:10.1523/jneurosci.20-07-02618.2000.
66. Yoshida, M. *et al.* Emx1 and Emx2 functions in development of dorsal telencephalon. *Development* (1997) doi:10.1242/dev.124.1.101.

67. Cecchi, C. *Emx2*: A gene responsible for cortical development, regionalization and area specification. *Gene* (2002) doi:10.1016/S0378-1119(02)00623-6.
68. Galceran, J., Miyashita-Lin, E. M., Devaney, E., Rubenstein, J. L. R. & Grosschedl, R. Hippocampus development and generation of dentate gyrus granule cells is regulated by LEF1. *Development* (2000) doi:10.1242/dev.127.3.469.
69. Pratt, T. *et al.* Disruption of early events in thalamocortical tract formation in mice lacking the transcription factors Pax6 or Foxg1. *J. Neurosci.* (2002) doi:10.1523/jneurosci.22-19-08523.2002.
70. Stenman, J. Tlx and Pax6 co-operate genetically to establish the pallio-subpallial boundary in the embryonic mouse telencephalon. *Development* **130**, 1113–1122 (2003).
71. Yun, K., Potter, S. & Rubenstein, J. L. R. Gsh2 and Pax6 play complementary roles in dorsoventral patterning of the mammalian telencephalon. *Development* (2001) doi:10.1242/dev.128.2.193.
72. Mason, H. A. *et al.* Notch signaling coordinates the patterning of striatal compartments. *Development* (2005) doi:10.1242/dev.02008.
73. Stenman, J., Toresson, H. & Campbell, K. Identification of two distinct progenitor populations in the lateral ganglionic eminence: Implications for striatal and olfactory bulb neurogenesis. *J. Neurosci.* (2003) doi:10.1523/jneurosci.23-01-00167.2003.
74. Lupo, G., Harris, W. A. & Lewis, K. E. Mechanisms of ventral patterning in the vertebrate nervous system. *Nature Reviews Neuroscience* (2006) doi:10.1038/nrn1843.
75. Martí, E., Takada, R., Bumcrot, D. A., Sasaki, H. & McMahon, A. P. Distribution of Sonic hedgehog peptides in the developing chick and mouse embryo. *Development* (1995) doi:10.1242/dev.121.8.2537.
76. Shimamura, K., Hartigan, D. J., Martinez, S., Puelles, L. & Rubenstein, J. L. R. Longitudinal organization of the anterior neural plate and neural tube. *Development* (1995) doi:10.1242/dev.121.12.3923.
77. Kohtz, J. D., Baker, D. P., Corte, G. & Fishell, G. Regionalization within the mammalian telencephalon is mediated by changes in responsiveness to Sonic Hedgehog. *Development* (1998) doi:10.1242/dev.125.24.5079.
78. Halilagic, A., Zile, M. H. & Studer, M. A novel role for retinoids in patterning the avian forebrain during presomite stages. *Development* (2003) doi:10.1242/dev.00423.
79. Halilagic, A. *et al.* Retinoids control anterior and dorsal properties in the developing forebrain. *Dev. Biol.* (2007) doi:10.1016/j.ydbio.2006.11.021.

80. Schneider, R. A., Hu, D., Rubenstein, J. L. R., Maden, M. & Helms, J. A. Local retinoid signaling coordinates forebrain and facial morphogenesis by maintaining FGF8 and SHH. *Development* (2001) doi:10.1242/dev.128.14.2755.
81. Toresson, H., De Urquiza, A. M., Fagerström, C., Perlmann, T. & Campbell, K. Retinoids are produced by glia in the lateral ganglionic eminence and regulate striatal neuron differentiation. *Development* (1999) doi:10.1242/dev.126.6.1317.
82. Shanmugalingam, S. *et al.* Ace/Fgf8 is required for forebrain commissure formation and patterning of the telencephalon. *Development* (2000) doi:10.1242/dev.127.12.2549.
83. Echevarria, D., Belo, J. A. & Martinez, S. Modulation of Fgf8 activity during vertebrate brain development. *Brain Research Reviews* (2005) doi:10.1016/j.brainresrev.2004.12.035.
84. Shimamura, K. & Rubenstein, J. L. R. Inductive interactions direct early regionalization of the mouse forebrain. *Development* (1997) doi:10.1242/dev.124.14.2709.
85. Xuan, S. *et al.* Winged helix transcription factor BF-1 is essential for the development of the cerebral hemispheres. *Neuron* (1995) doi:10.1016/0896-6273(95)90262-7.
86. Hardcastle, Z. & Papalopulu, N. Distinct effects of XBF-1 in regulating the cell cycle inhibitor p27(XIC1) and imparting a neural fate. *Development* (2000) doi:10.1242/dev.127.6.1303.
87. Dou, C. L., Li, S. & Lai, E. Dual role of brain factor-1 in regulating growth and patterning of the cerebral hemispheres. *Cereb. Cortex* (1999) doi:10.1093/cercor/9.6.543.
88. Miyoshi, G. *et al.* Genetic fate mapping reveals that the caudal ganglionic eminence produces a large and diverse population of superficial cortical interneurons. *J. Neurosci.* (2010) doi:10.1523/JNEUROSCI.4515-09.2010.
89. Sheth, A. N. & Bhide, P. G. Concurrent cellular output from two proliferative populations in the early embryonic mouse corpus striatum. *J. Comp. Neurol.* (1997) doi:10.1002/(SICI)1096-9861(19970630)383:2<220::AID-CNE8>3.0.CO;2-2.
90. Halliday, A. L. & Cepko, C. L. Generation and migration of cells in the developing striatum. *Neuron* (1992) doi:10.1016/0896-6273(92)90216-Z.
91. Castro, D. S. *et al.* A novel function of the proneural factor Ascl1 in progenitor proliferation identified by genome-wide characterization of its targets. *Genes Dev.* (2011) doi:10.1101/gad.627811.
92. Franco, S. J. & Müller, U. Shaping Our Minds: Stem and Progenitor Cell Diversity in the Mammalian Neocortex. *Neuron* (2013) doi:10.1016/j.neuron.2012.12.022.
93. Turrero García, M. & Harwell, C. C. Radial glia in the ventral telencephalon. *FEBS Letters* (2017) doi:10.1002/1873-3468.12829.

94. Pilz, G. A. *et al.* Amplification of progenitors in the mammalian telencephalon includes a new radial glial cell type. *Nat. Commun.* (2013) doi:10.1038/ncomms3125.
95. Noctor, S. C., Flint, A. C., Weissman, T. A., Dammerman, R. S. & Kriegstein, A. R. Neurons derived from radial glial cells establish radial units in neocortex. *Nature* (2001) doi:10.1038/35055553.
96. Gal, J. S. *et al.* Molecular and morphological heterogeneity of neural precursors in the mouse neocortical proliferative zones. *J. Neurosci.* (2006) doi:10.1523/JNEUROSCI.4499-05.2006.
97. Kowalczyk, T. *et al.* Intermediate neuronal progenitors (basal progenitors) produce pyramidal-projection neurons for all layers of cerebral cortex. *Cereb. Cortex* (2009) doi:10.1093/cercor/bhn260.
98. Shitamukai, A., Konno, D. & Matsuzaki, F. Oblique radial glial divisions in the developing mouse neocortex induce self-renewing progenitors outside the germinal zone that resemble primate outer subventricular zone progenitors. *J. Neurosci.* (2011) doi:10.1523/JNEUROSCI.4773-10.2011.
99. Petros, T. J., Bultje, R. S., Ross, M. E., Fishell, G. & Anderson, S. A. Apical versus Basal Neurogenesis Directs Cortical Interneuron Subclass Fate. *Cell Rep.* (2015) doi:10.1016/j.celrep.2015.09.079.
100. Harwell, C. C. *et al.* Wide Dispersion and Diversity of Clonally Related Inhibitory Interneurons. *Neuron* (2015) doi:10.1016/j.neuron.2015.07.030.
101. Brown, K. N. *et al.* Clonal production and organization of inhibitory interneurons in the neocortex. *Science* (80-. ). (2011) doi:10.1126/science.1208884.
102. Noctor, S. C., Martinez-Cerdeño, V., Ivic, L. & Kriegstein, A. R. Cortical neurons arise in symmetric and asymmetric division zones and migrate through specific phases. *Nat. Neurosci.* (2004) doi:10.1038/nn1172.
103. Knowles, R., Dehorter, N. & Ellender, T. From Progenitors to Progeny: Shaping Striatal Circuit Development and Function. *J. Neurosci.* (2021) doi:10.1523/jneurosci.0620-21.2021.
104. Cheffer, A., Tárnok, A. & Ulrich, H. Cell cycle regulation during neurogenesis in the embryonic and adult brain. *Stem Cell Rev. Reports* (2013) doi:10.1007/s12015-013-9460-5.
105. Calegari, F. & Huttner, W. B. An inhibition of cyclin-dependent kinases that lengthens, but does not arrest, neuroepithelial cell cycle induces premature neurogenesis. *J. Cell Sci.* (2003) doi:10.1242/jcs.00825.
106. Arai, Y. *et al.* Neural stem and progenitor cells shorten S-phase on commitment to neuron production. *Nat. Commun.* (2011) doi:10.1038/ncomms1155.

107. Bjornsson, C. S., Apostolopoulou, M., Tian, Y. & Temple, S. It takes a village: Constructing the neurogenic niche. *Developmental Cell* (2015) doi:10.1016/j.devcel.2015.01.010.
108. Alvarez-Buylla, A., García-Verdugo, J. M. & Tramontin, A. D. A unified hypothesis on the lineage of neural stem cells. *Nat. Rev. Neurosci.* (2001) doi:10.1038/35067582.
109. Götz, M. & Huttner, W. B. The cell biology of neurogenesis. *Nature Reviews Molecular Cell Biology* (2005) doi:10.1038/nrm1739.
110. Smart, I. H. A pilot study of cell production by the ganglionic eminences of the developing mouse brain. *J. Anat.* (1976).
111. Fentress, J. C., Stanfield, B. B. & Cowan, W. M. Observations on the development of the striatum in mice and rats. *Anat. Embryol. (Berl.)*. (1981) doi:10.1007/BF00315705.
112. Johnston, J. G., Gerfen, C. R., Haber, S. N. & van der Kooy, D. Mechanisms of striatal pattern formation: conservation of mammalian compartmentalization. *Dev. Brain Res.* (1990) doi:10.1016/0165-3806(90)90189-6.
113. Kelly, S. M. *et al.* Radial Glial Lineage Progression and Differential Intermediate Progenitor Amplification Underlie Striatal Compartments and Circuit Organization. *Neuron* (2018) doi:10.1016/j.neuron.2018.06.021.
114. Faull, R. L. M., Dragunow, M. & Villiger, J. W. The distribution of neurotensin receptors and acetylcholinesterase in the human caudate nucleus: evidence for the existence of a third neurochemical compartment. *Brain Res.* (1989) doi:10.1016/0006-8993(89)90735-X.
115. Minocha, S. *et al.* Nkx2.1 regulates the generation of telencephalic astrocytes during embryonic development. *Sci. Rep.* (2017) doi:10.1038/srep43093.
116. Anthony, T. E. & Heintz, N. Genetic lineage tracing defines distinct neurogenic and gliogenic stages of ventral telencephalic radial glial development. *Neural Dev.* (2008) doi:10.1186/1749-8104-3-30.
117. Cocas, L. A. *et al.* Emx1-lineage progenitors differentially contribute to neural diversity in the striatum and amygdala. *J. Neurosci.* (2009) doi:10.1523/JNEUROSCI.2525-09.2009.
118. Kohwi, M. *et al.* A subpopulation of olfactory bulb GABAergic interneurons is derived from Emx1- and Dlx5/6-expressing progenitors. *J. Neurosci.* (2007) doi:10.1523/JNEUROSCI.0254-07.2007.
119. Hirata, T. *et al.* Identification of distinct telencephalic progenitor pools for neuronal diversity in the amygdala. *Nat. Neurosci.* (2009) doi:10.1038/nn.2241.
120. Willaime-Morawek, S. *et al.* Embryonic cortical neural stem cells migrate ventrally and persist as postnatal striatal stem cells. *J. Cell Biol.* (2006) doi:10.1083/jcb.200604123.

121. Bartolini, G., Ciceri, G. & Marín, O. Integration of GABAergic Interneurons into Cortical Cell Assemblies: Lessons from Embryos and Adults. *Neuron* (2013) doi:10.1016/j.neuron.2013.08.014.
122. Flandin, P. *et al.* Lhx6 and Lhx8 Coordinately Induce Neuronal Expression of Shh that Controls the Generation of Interneuron Progenitors. *Neuron* **70**, 939–950 (2011).
123. Hamasaki, T., Goto, S., Nishikawa, S. & Ushio, Y. Neuronal cell migration for the developmental formation of the mammalian striatum. *Brain Research Reviews* vol. 41 1–12 (2003).
124. Ramon y Cajal, S. The structure and connexions of neurons. *Nobel Lect. Physiol. or Med. 1901-1921* (1906).
125. Rakic, P. Neuron-glia relationship during granule cell migration in developing cerebellar cortex. A Golgi and electronmicroscopic study in Macacus rhesus. *J. Comp. Neurol.* (1971) doi:10.1002/cne.901410303.
126. Rakic, P. Mode of cell migration to the superficial layers of fetal monkey neocortex. *J. Comp. Neurol.* (1972) doi:10.1002/cne.901450105.
127. Schmechel, D. E. & Rakic, P. A golgi study of radial glial cells in developing monkey telencephalon: Morphogenesis and transformation into astrocytes. *Anat. Embryol. (Berl)*. (1979) doi:10.1007/BF00300010.
128. Marín, O. & Rubenstein, J. L. R. A long, remarkable journey: Tangential migration in the telencephalon. *Nat. Rev. Neurosci.* (2001) doi:10.1038/35097509.
129. Gadisseux, J. F., Kadhim, H. J., van den Bosch de Aguilar, P., Caviness, V. S. & Evrard, P. Neuron migration within the radial glial fiber system of the developing murine cerebrum: an electron microscopic autoradiographic analysis. *Dev. Brain Res.* (1990) doi:10.1016/0165-3806(90)90220-S.
130. Gaiano, N., Nye, J. S. & Fishell, G. Radial glial identity is promoted by Notch1 signaling in the murine forebrain. *Neuron* (2000) doi:10.1016/S0896-6273(00)81172-1.
131. Heins, N. *et al.* Glial cells generate neurons: The role of the transcription factor Pax6. *Nat. Neurosci.* **5**, 308–315 (2002).
132. Levitt, P., Cooper, M. L. & Rakic, P. Coexistence of neuronal and glial precursor cells in the cerebral ventricular zone of the fetal monkey: An ultrastructural immunoperoxidase analysis. *J. Neurosci.* (1981) doi:10.1523/jneurosci.01-01-00027.1981.
133. Malatesta, P., Hartfuss, E. & Götz, M. Isolation of radial glial cells by fluorescent-activated cell sorting reveals a neural lineage. *Development* (2000) doi:10.1242/dev.127.24.5253.



134. Casper, K. B. & McCarthy, K. D. GFAP-positive progenitor cells produce neurons and oligodendrocytes throughout the CNS. *Mol. Cell. Neurosci.* (2006) doi:10.1016/j.mcn.2005.12.006.
135. Supèr, H., Soriano, E. & Uylings, H. B. M. The functions of the preplate in development and evolution of the neocortex and hippocampus. *Brain Res. Rev.* (1998) doi:10.1016/S0165-0173(98)00005-8.
136. De Carlos, J. A., López-Mascaraque, L. & Valverde, F. Dynamics of cell migration from the lateral ganglionic eminence in the rat. *J. Neurosci.* (1996) doi:10.1523/jneurosci.16-19-06146.1996.
137. Kakita, A. & Goldman, J. E. Patterns and dynamics of SVZ cell migration in the postnatal forebrain: Monitoring living progenitors in slice preparations. *Neuron* (1999) doi:10.1016/S0896-6273(00)80800-4.
138. Olsson, M., Björklund, A. & Campbell, K. Early specification of striatal projection neurons and interneuronal subtypes in the lateral and medial ganglionic eminence. *Neuroscience* (1998) doi:10.1016/S0306-4522(97)00532-0.
139. Anderson, S. A. *et al.* Mutations of the homeobox genes *Dlx-1* and *Dlx-2* disrupt the striatal subventricular zone and differentiation of late born striatal neurons. *Neuron* (1997) doi:10.1016/S0896-6273(00)80345-1.
140. Tessier-Lavigne, M. & Goodman, C. S. The molecular biology of axon guidance. *Science* (1996) doi:10.1126/science.274.5290.1123.
141. Tessier-Lavigne, M., Placzek, M., Lumsden, A. G. S., Dodd, J. & Jessell, T. M. Chemotropic guidance of developing axons in the mammalian central nervous system. *Nature* (1988) doi:10.1038/336775a0.
142. Hamasaki, T., Goto, S., Nishikawa, S. & Ushio, Y. A role of netrin-1 in the formation of the subcortical structure striatum: Repulsive action on the migration of late-born striatal neurons. *J. Neurosci.* (2001) doi:10.1523/jneurosci.21-12-04272.2001.
143. Heffron, D. S. & Golden, J. A. DM-GRASP is necessary for nonradial cell migration during chick diencephalic development. *J. Neurosci.* (2000) doi:10.1523/jneurosci.20-06-02287.2000.
144. Letinic, K. & Rakic, P. Telencephalic origin of human thalamic GABAergic neurons. *Nat. Neurosci.* (2001) doi:10.1038/nn0901-931.
145. Spassky, N. *et al.* Directional guidance of oligodendroglial migration by class 3 semaphorins and netrin-1. *J. Neurosci.* (2002) doi:10.1523/jneurosci.22-14-05992.2002.
146. Chen, L. *et al.* Rac1 controls the formation of midline commissures and the competency of



- tangential migration in ventral telencephalic neurons. *J. Neurosci.* (2007) doi:10.1523/JNEUROSCI.3509-06.2007.
147. Anderson, S. A., Marín, O., Horn, C., Jennings, K. & Rubenstein, J. L. R. Distinct cortical migrations from the medial and lateral ganglionic eminences. *Development* (2001) doi:10.1242/dev.128.3.353.
  148. Lavdas, A. A., Grigoriou, M., Pachnis, V. & Parnavelas, J. G. The medial ganglionic eminence gives rise to a population of early neurons in the developing cerebral cortex. *J. Neurosci.* (1999) doi:10.1523/jneurosci.19-18-07881.1999.
  149. Meyer, G., Soria, J. M., Martínez-Galán, J. R., Martín-Clemente, B. & Fairén, A. Different origins and developmental histories of transient neurons in the marginal zone of the fetal and neonatal rat cortex. *J. Comp. Neurol.* (1998) doi:10.1002/(SICI)1096-9861(19980810)397:4<493::AID-CNE4>3.0.CO;2-X.
  150. Kawaguchi, Y., Wilson, C. J., Augood, S. J. & Emson, P. C. Striatal interneurons: chemical, physiological and morphological characterization. *Trends in Neurosciences* (1995) doi:10.1016/0166-2236(95)98374-8.
  151. Marín, O., Anderson, S. A. & Rubenstein, J. L. R. Origin and molecular specification of striatal interneurons. *J. Neurosci.* (2000) doi:10.1523/jneurosci.20-16-06063.2000.
  152. Wichterle, H., Turnbull, D. H., Nery, S., Fishell, G. & Alvarez-Buylla, A. In utero fate mapping reveals distinct migratory pathways and fates of neurons born in the mammalian basal forebrain. *Development* (2001) doi:10.1242/dev.128.19.3759.
  153. Alifragis, P., Liapi, A. & Parnavelas, J. G. Lhx6 regulates the migration of cortical interneurons from the ventral telencephalon but does not specify their GABA phenotype. *J. Neurosci.* (2004) doi:10.1523/JNEUROSCI.1245-04.2004.
  154. Liodis, P. *et al.* Lhx6 activity is required for the normal migration and specification of cortical interneuron subtypes. *J. Neurosci.* (2007) doi:10.1523/JNEUROSCI.3055-06.2007.
  155. Parras, C. M. *et al.* Divergent functions of the proneural genes Mash1 and Ngn2 in the specification of neuronal subtype identity. *Genes Dev.* (2002) doi:10.1101/gad.940902.
  156. Pozas, E. & Ibáñez, C. F. GDNF and GFR $\alpha$ 1 promote differentiation and tangential migration of cortical GABAergic neurons. *Neuron* (2005) doi:10.1016/j.neuron.2005.01.043.
  157. Stumm, R. K. *et al.* CXCR4 regulates interneuron migration in the developing neocortex. *J. Neurosci.* (2003) doi:10.1523/jneurosci.23-12-05123.2003.
  158. Zhu, Y., Li, H. S., Zhou, L., Wu, J. Y. & Rao, Y. Cellular and molecular guidance of GABAergic neuronal migration from an extracortical origin to the neocortex. *Neuron* (1999)

doi:10.1016/S0896-6273(00)80801-6.

159. Herkenham, M. & Pert, C. B. Mosaic distribution of opiate receptors, parafascicular projections and acetylcholinesterase in rat striatum. *Nature* **291**, 415–418 (1981).
160. Ouimet, C. C., Lamantia, A. S., Goldman-Rakic, P., Rakic, P. & Greengard, P. Immunocytochemical localization of DARPP-32, a dopamine and cyclic- AMP-regulated phosphoprotein, in the primate brain. *J. Comp. Neurol.* (1992) doi:10.1002/cne.903230206.
161. Krushel, L. A., Fishell, G. & van der Kooy, D. Pattern Formation in the Mammalian Forebrain: Striatal Patch and Matrix Neurons Intermix Prior to Compartment Formation. *Eur. J. Neurosci.* (1995) doi:10.1111/j.1460-9568.1995.tb01111.x.
162. Krushel, L. A. & Van Der Kooy, D. Pattern formation in the developing mammalian forebrain: Selective adhesion of early but not late postmitotic cortical and striatal neurons within forebrain reaggregate cultures. *Dev. Biol.* (1993) doi:10.1006/dbio.1993.1175.
163. Song, D. D. & Harlan, R. E. Genesis and migration patterns of neurons forming the patch and matrix compartments of the rat striatum. *Dev. Brain Res.* (1994) doi:10.1016/0165-3806(94)00144-8.
164. Fishell, G. & Van Der Kooy, D. Pattern formation in the striatum: Neurons with early projections to the substantia nigra survive the cell death period. *J. Comp. Neurol.* (1991) doi:10.1002/cne.903120104.
165. Passante, L. *et al.* Temporal regulation of ephrin/Eph signalling is required for the spatial patterning of the mammalian striatum. *Development* (2008) doi:10.1242/dev.024778.
166. Garel, S., Marín, F., Grosschedl, R. & Charnay, P. Ebf1 controls early cell differentiation in the embryonic striatum. *Development* (1999).
167. Tinterri, A. *et al.* Active intermixing of indirect and direct neurons builds the striatal mosaic. *Nat. Commun.* (2018) doi:10.1038/s41467-018-07171-4.
168. Korematsu, K., Goto, S., Okamura, A. & Ushio, Y. Heterogeneity of cadherin-8 expression in the neonatal rat striatum: Comparison with striatal compartments. *Exp. Neurol.* **154**, 531–536 (1998).
169. Kirchgessner, A. L., Sclafani, A. & Nilaver, G. Histochemical identification of a PVN-hindbrain feeding pathway. *Physiol. Behav.* (1988) doi:10.1016/0031-9384(88)90154-0.
170. Sharpe, N. A. & Tepper, J. M. Postnatal development of excitatory synaptic input to the rat neostriatum: An electron microscopic study. *Neuroscience* (1998) doi:10.1016/S0306-4522(97)00583-6.
171. Liao, W. L. & Liu, F. C. RAR $\beta$  isoform-specific regulation of DARPP-32 gene expression:

- An ectopic expression study in the developing rat telencephalon. *Eur. J. Neurosci.* (2005) doi:10.1111/j.1460-9568.2005.04178.x.
172. Li, H. *et al.* A retinoic acid synthesizing enzyme in ventral retina and telencephalon of the embryonic mouse. *Mech. Dev.* (2000) doi:10.1016/S0925-4773(00)00352-X.
  173. Ruberte, E., Friederich, V., Chambon, P. & Morriss-Kay, G. Retinoic acid receptors and cellular retinoid binding proteins: III. Their differential transcript distribution during mouse nervous system development. *Development* (1993) doi:10.1242/dev.118.1.267.
  174. Zetterstrom, R. H., Simon, A., Giacobini, M. M. J., Eriksson, U. & Olson, L. Localization of cellular retinoid-binding proteins suggests specific roles for retinoids in the adult central nervous system. *Neuroscience* (1994) doi:10.1016/0306-4522(94)90482-0.
  175. Oulad-Abdelghani, M. *et al.* Meis2, a novel mouse Pbx-related homeobox gene induced by retinoic acid during differentiation of P19 embryonal carcinoma cells. *Dev. Dyn.* (1997) doi:10.1002/(SICI)1097-0177(199710)210:2<173::AID-AJA9>3.0.CO;2-D.
  176. Chang, C. W. *et al.* Identification of a developmentally regulated striatum-enriched zinc-finger gene, Nolz-1, in the mammalian brain. *Proc. Natl. Acad. Sci. U. S. A.* (2004) doi:10.1073/pnas.0308645100.
  177. Urbán, N. *et al.* Nolz1 promotes striatal neurogenesis through the regulation of retinoic acid signaling. *Neural Dev.* (2010) doi:10.1186/1749-8104-5-21.
  178. Toresson, H., Potter, S. S. & Campbell, K. Genetic control of dorsal-ventral identity in the telencephalon: Opposing roles for Pax6 and Gsh2. *Development* (2000) doi:10.1242/dev.127.20.4361.
  179. Szucsik, J. C. *et al.* Altered forebrain and hindbrain development in mice mutant for the Gsh-2 homeobox gene. *Dev. Biol.* (1997) doi:10.1006/dbio.1997.8733.
  180. Yun, K., Garel, S., Fischman, S. & Rubenstein, J. L. R. Patterning of the lateral ganglionic eminence by the Gsh1 and Gsh2 homeobox genes regulates striatal and olfactory bulb histogenesis and the growth of axons through the basal ganglia. *J. Comp. Neurol.* (2003) doi:10.1002/cne.10685.
  181. Toresson, H. & Campbell, K. A role Gsh1 in the developing striatum and olfactory bulb of Gsh2 mutant mice. *Development* (2001) doi:10.1242/dev.128.23.4769.
  182. Valerius, M. T. *et al.* Gsh-1: A novel murine homeobox gene expressed in the central nervous system. *Dev. Dyn.* (1995) doi:10.1002/aja.1002030306.
  183. Long, J. E., Cobos, I., Potter, G. B. & Rubenstein, J. L. R. Dlx1&2 and Mash1 transcription factors control MGE and CGE patterning and differentiation through parallel and

- overlapping pathways. *Cereb. Cortex* (2009) doi:10.1093/cercor/bhp045.
184. Pei, Z. *et al.* Homeobox genes *Gsx1* and *Gsx2* differentially regulate telencephalic progenitor maturation. *Proc. Natl. Acad. Sci. U. S. A.* (2011) doi:10.1073/pnas.1008824108.
  185. Corbin, J. G., Gaiano, N., Machold, R. P., Langston, A. & Fishell, G. The *Gsh2* homeodomain gene controls multiple aspects of telencephalic development. *Development* (2000) doi:10.1242/dev.127.23.5007.
  186. Porteus, M. H. *et al.* *DLX-2*, *MASH-1*, and *MAP-2* expression and bromodeoxyuridine incorporation define molecularly distinct cell populations in the embryonic mouse forebrain. *J. Neurosci.* (1994) doi:10.1523/jneurosci.14-11-06370.1994.
  187. Horton, S., Meredith, A., Richardson, J. A. & Johnson, J. E. Correct coordination of neuronal differentiation events in ventral forebrain requires the bHLH factor *MASH1*. *Mol. Cell. Neurosci.* (1999) doi:10.1006/mcne.1999.0791.
  188. Poitras, L., Ghanem, N., Hatch, G. & Ekker, M. The proneural determinant *MASH1* regulates forebrain *Dlx1/2* expression through the *l12b* intergenic enhancer. *Development* (2007) doi:10.1242/dev.02845.
  189. Waclaw, R. R., Wang, B., Pei, Z., Ehrman, L. A. & Campbell, K. Distinct Temporal Requirements for the Homeobox Gene *Gsx2* in Specifying Striatal and Olfactory Bulb Neuronal Fates. *Neuron* (2009) doi:10.1016/j.neuron.2009.07.015.
  190. Eisenstat, D. D. *et al.* *DLX-1*, *DLX-2*, and *DLX-5* expression define distinct stages of basal forebrain differentiation. *J. Comp. Neurol.* (1999) doi:10.1002/(SICI)1096-9861(19991115)414:2<217::AID-CNE6>3.0.CO;2-I.
  191. Bürglin, T. R. Analysis of TALE superclass homeobox genes (*MEIS*, *PBC*, *KNOX*, *Iroquois*, *TGIF*) reveals a novel domain conserved between plants and animals. *Nucleic Acids Res.* (1997) doi:10.1093/nar/25.21.4173.
  192. Chang, C. P. *et al.* *Meis* proteins are major in vivo DNA binding partners for wild-type but not chimeric *Pbx* proteins. *Mol. Cell. Biol.* (1997) doi:10.1128/mcb.17.10.5679.
  193. Moens, C. B. & Selleri, L. *Hox* cofactors in vertebrate development. *Developmental Biology* (2006) doi:10.1016/j.ydbio.2005.10.032.
  194. Choe, S. K., Vlachakis, N. & Sagerström, C. G. *Meis* family proteins are required for hindbrain development in the zebrafish. *Development* (2002) doi:10.1242/dev.129.3.585.
  195. Sagerström, C. G. *pbX* marks the spot. *Developmental Cell* (2004) doi:10.1016/j.devcel.2004.05.015.
  196. Su, Z. *et al.* *Dlx1/2*-dependent expression of *Meis2* promotes neuronal fate determination in

- the mammalian striatum. *Development* (2022) doi:10.1242/dev.200035.
197. Dorfman, R., Glazer, L., Weihe, U., Wernet, M. F. & Shilo, B. Z. Elbow and Noc define a family of zinc finger proteins controlling morphogenesis of specific tracheal branches. *Development* (2002) doi:10.1242/dev.129.15.3585.
  198. Hoyle, J., Tang, Y. P., Wietette, E. L., Wardle, F. C. & Sive, H. nlz Gene Family Is Required for Hindbrain Patterning in the Zebrafish. *Dev. Dyn.* (2004) doi:10.1002/dvdy.20001.
  199. Runko, A. P. & Sagerström, C. G. Nlz belongs to a family of zinc-finger-containing repressors and controls segmental gene expression in the zebrafish hindbrain. *Dev. Biol.* (2003) doi:10.1016/S0012-1606(03)00388-9.
  200. Von Ohlen, T., Syu, L. J. & Mellerick, D. M. Conserved properties of the Drosophila homeodomain protein, Ind. *Mech. Dev.* (2007) doi:10.1016/j.mod.2007.08.001.
  201. Chen, S. Y. *et al.* Parcellation of the striatal complex into dorsal and ventral districts. *Proc. Natl. Acad. Sci. U. S. A.* (2020) doi:10.1073/pnas.1921007117.
  202. Hagman, J., Gutch, M. J., Lin, H. & Grosschedl, R. EBF contains a novel zinc coordination motif and multiple dimerization and transcriptional activation domains. *EMBO J.* (1995) doi:10.1002/j.1460-2075.1995.tb07290.x.
  203. Wang, S. S., Betz, A. G. & Reed, R. R. Cloning of a novel Olf-1/EBF-like gene, O/E-4, by Degenerate Oligo-based Direct Selection. *Mol. Cell. Neurosci.* (2002) doi:10.1006/mcne.2002.1138.
  204. Wang, S. S., Tsai, R. Y. L. & Reed, R. R. The characterization of the Olf-1/EBF-like HLH transcription factor family: Implications in olfactory gene regulation and neuronal development. *J. Neurosci.* (1997) doi:10.1523/jneurosci.17-11-04149.1997.
  205. Garel, S. *et al.* Family of Ebf/Olf-1-related genes potentially involved in neuronal differentiation and regional specification in the central nervous system. *Dev. Dyn.* (1997) doi:10.1002/(SICI)1097-0177(199711)210:3<191::AID-AJA1>3.0.CO;2-B.
  206. Lobo, M. K., Yeh, C. & Yang, X. W. Pivotal role of early B-cell factor 1 in development of striatonigral medium spiny neurons in the matrix compartment. *J. Neurosci. Res.* **86**, 2134–46 (2008).
  207. Lobo, M. K., Karsten, S. L., Gray, M., Geschwind, D. H. & Yang, X. W. FACS-array profiling of striatal projection neuron subtypes in juvenile and adult mouse brains. *Nat. Neurosci.* **9**, 443–452 (2006).
  208. Bond, H. M. *et al.* Early hematopoietic zinc finger protein-zinc finger protein 521: A candidate regulator of diverse immature cells. *International Journal of Biochemistry and Cell Biology* (2008)

doi:10.1016/j.biocel.2007.04.006.

209. Hata, a *et al.* OAZ uses distinct DNA- and protein-binding zinc fingers in separate BMP-Smad and Olf signaling pathways. *Cell* **100**, 229–240 (2000).
210. Bond, H. M. *et al.* Early hematopoietic zinc finger protein (EHZF), the human homolog to mouse Evi3, is highly expressed in primitive human hematopoietic cells. *Blood* **103**, 2062–2070 (2004).
211. Wang, H. F. & Liu, F. C. Developmental restriction of the LIM homeodomain transcription factor Islet-1 expression to cholinergic neurons in the rat striatum. *Neuroscience* (2001) doi:10.1016/S0306-4522(00)00590-X.
212. Ehrman, L. A. *et al.* The LIM homeobox gene Isl1 is required for the correct development of the striatonigral pathway in the mouse. *Proc. Natl. Acad. Sci. U. S. A.* **110**, E4026-35 (2013).
213. Elshatory, Y. & Gan, L. The LIM-homeobox gene Islet-1 is required for the development of restricted forebrain cholinergic neurons. *J. Neurosci.* (2008) doi:10.1523/JNEUROSCI.5730-07.2008.
214. Long, J. E. *et al.* Dlx1&2 and Mash1 transcription factors control striatal patterning and differentiation through parallel and overlapping pathways. *J. Comp. Neurol.* (2009) doi:10.1002/cne.21854.
215. Garel, S., Marín, F., Grosschedl, R. & Charnay, P. Ebf1 controls early cell differentiation in the embryonic striatum. *Development* **126**, 5285–94 (1999).
216. Lobo, M. K., Karsten, S. L., Gray, M., Geschwind, D. H. & Yang, X. W. FACS-array profiling of striatal projection neuron subtypes in juvenile and adult mouse brains. *Nat. Neurosci.* (2006) doi:10.1038/nn1654.
217. Rebollo, A. & Schmitt, C. Ikaros, Aiolos and Helios: Transcription regulators and lymphoid malignancies. *Immunology and Cell Biology* vol. 81 171–175 (2003).
218. Agoston, D. V. *et al.* Ikaros is expressed in developing striatal neurons and involved in enkephalinergic differentiation. *J. Neurochem.* **102**, 1805–1816 (2007).
219. Martín-Ibáñez, R. *et al.* Ikaros-1 couples cell cycle arrest of late striatal precursors with neurogenesis of enkephalinergic neurons. *J. Comp. Neurol.* **518**, 329–351 (2010).
220. Onorati, M. *et al.* Molecular and functional definition of the developing human striatum. *Nat. Neurosci.* **17**, 1–15 (2014).
221. Martín-Ibáñez, R. *et al.* Helios transcription factor expression depends on Gsx2 and Dlx1&2 function in developing striatal matrix neurons. *Stem Cells Dev.* **21**, 2239–51 (2012).

222. Zhang, Q. *et al.* The Zinc Finger Transcription Factor Sp9 Is Required for the Development of Striatopallidal Projection Neurons. *Cell Rep.* (2016) doi:10.1016/j.celrep.2016.06.090.
223. Waclaw, R. R. *et al.* The zinc finger transcription factor Sp8 regulates the generation and diversity of olfactory bulb interneurons. *Neuron* (2006) doi:10.1016/j.neuron.2006.01.018.
224. Ma, T. *et al.* A subpopulation of dorsal lateral/caudal ganglionic eminence-derived neocortical interneurons expresses the transcription factor Sp8. *Cereb. Cortex* (2012) doi:10.1093/cercor/bhr296.
225. Xu, Z. *et al.* SP8 and SP9 coordinately promote D2-type medium spiny neuron production by activating Six3 expression. *Dev.* (2018) doi:10.1242/dev.165456.
226. Arlotta, P. *et al.* Neuronal subtype-specific genes that control corticospinal motor neuron development in vivo. *Neuron* **45**, 207–221 (2005).
227. Leid, M. *et al.* CTIP1 and CTIP2 are differentially expressed during mouse embryogenesis. *Gene Expr Patterns* **4**, 733–739 (2004).
228. Arlotta, P., Molyneaux, B. J., Jabaudon, D., Yoshida, Y. & Macklis, J. D. Ctip2 controls the differentiation of medium spiny neurons and the establishment of the cellular architecture of the striatum. *J. Neurosci.* (2008) doi:10.1523/JNEUROSCI.2986-07.2008.
229. Ferland, R. J., Cherry, T. J., Preware, P. O., Morrissey, E. E. & Walsh, C. A. Characterization of Foxp2 and Foxp1 mRNA and protein in the developing and mature brain. *J. Comp. Neurol.* (2003) doi:10.1002/cne.10654.
230. Tamura, S., Morikawa, Y., Iwanishi, H., Hisaoka, T. & Senba, E. Expression pattern of the winged-helix/forkhead transcription factor Foxp1 in the developing central nervous system. *Gene Expr. Patterns* (2003) doi:10.1016/S1567-133X(03)00003-6.
231. Sussel, L., Marin, O., Kimura, S. & Rubenstein, J. L. R. Loss of Nkx2.1 homeobox gene function results in a ventral to dorsal molecular respecification within the basal telencephalon: Evidence for a transformation of the pallidum into the striatum. *Development* (1999) doi:10.1242/dev.126.15.3359.
232. Métin, C., Baudoin, J. P., Rakić, S. & Parnavelas, J. G. Cell and molecular mechanisms involved in the migration of cortical interneurons. *European Journal of Neuroscience* (2006) doi:10.1111/j.1460-9568.2006.04630.x.
233. Wonders, C. P. & Anderson, S. A. The origin and specification of cortical interneurons. *Nature Reviews Neuroscience* (2006) doi:10.1038/nrn1954.
234. Guo, J. *et al.* In silico analysis indicates a similar gene expression pattern between human brain and testis. *Cytogenet. Genome Res.* **103**, 58–62 (2003).



235. Fragkouli, A. *et al.* Loss of forebrain cholinergic neurons and impairment in spatial learning and memory in LHX7-deficient mice. *Eur. J. Neurosci.* (2005) doi:10.1111/j.1460-9568.2005.04141.x.
236. Flandin, P., Kimura, S. & Rubenstein, J. L. R. The progenitor zone of the ventral medial ganglionic eminence requires Nkx2-1 to generate most of the globus pallidus but few neocortical interneurons. *J. Neurosci.* (2010) doi:10.1523/JNEUROSCI.4228-09.2010.
237. Nóbrega-Pereira, S. *et al.* Postmitotic Nkx2-1 Controls the Migration of Telencephalic Interneurons by Direct Repression of Guidance Receptors. *Neuron* (2008) doi:10.1016/j.neuron.2008.07.024.
238. Parsons, M. P. & Raymond, L. A. Huntington disease. in *Neurobiology of Brain Disorders: Biological Basis of Neurological and Psychiatric Disorders, Second Edition* (2022). doi:10.1016/B978-0-323-85654-6.00042-3.
239. Nguyen, H. H. P. & Weydt, P. Huntington disease. *Medizinische Genetik* (2018) doi:10.1007/s11825-018-0190-6.
240. Huntington, G. On chorea. George Huntington, M.D. *The Journal of neuropsychiatry and clinical neurosciences* (2003) doi:10.1176/jnp.15.1.109.
241. Pringsheim, T. *et al.* The incidence and prevalence of Huntington's disease: A systematic review and meta-analysis. *Movement Disorders* (2012) doi:10.1002/mds.25075.
242. Warby, S. C. *et al.* HTT haplotypes contribute to differences in Huntington disease prevalence between Europe and East Asia. *Eur. J. Hum. Genet.* (2011) doi:10.1038/ejhg.2010.229.
243. Hodgson, J. G. *et al.* A YAC Mouse Model for Huntington's Disease with Full-Length Mutant Huntingtin, Cytoplasmic Toxicity, and Selective Striatal Neurodegeneration to 35 of a CAG trinucleotide repeat in the HD gene. *Neuron* (1999).
244. Bates, G. P. *et al.* Huntington disease. *Nature Reviews Disease Primers* (2015) doi:10.1038/nrdp.2015.5.
245. Rosas, H. D. *et al.* Evidence for more widespread cerebral pathology in early HD: An MRI-based morphometric analysis. *Neurology* (2003) doi:10.1212/01.WNL.0000065888.88988.6E.
246. Rosas, H. D. *et al.* Cerebral cortex and the clinical expression of Huntington's disease: Complexity and heterogeneity. *Brain* (2008) doi:10.1093/brain/awn025.
247. Galvan, A. & Wichmann, T. GABAergic circuits in the basal ganglia and movement disorders. *Progress in Brain Research* (2007) doi:10.1016/S0079-6123(06)60017-4.
248. Alexander, G. E. & Crutcher, M. D. Functional architecture of basal ganglia circuits: neural substrates of parallel processing. *Trends in Neurosciences* (1990) doi:10.1016/0166-



249. Van Vugt, M. Community identification moderating the impact of financial incentives in a natural social dilemma: Water conservation. *Personal. Soc. Psychol. Bull.* (2001) doi:10.1177/01461672012711005.
250. Rothwell, J. C. *et al.* Magnetic stimulation: motor evoked potentials. The International Federation of Clinical Neurophysiology. *Electroencephalogr. Clin. Neurophysiol. Suppl.* (1999).
251. Mestre, T. A. & Ferreira, J. J. An evidence-based approach in the treatment of Huntington's disease. *Parkinsonism and Related Disorders* (2012) doi:10.1016/j.parkreldis.2011.10.021.
252. Duyao, M. P. *et al.* Inactivation of the mouse huntington's disease gene homolog Hdh. *Science* (80-. ). (1995) doi:10.1126/science.7618107.
253. Zeitlin, S., Liu, J. P., Chapman, D. L., Papaioannou, V. E. & Efstratiadis, A. Increased apoptosis and early embryonic lethality in mice nullizygous for the Huntington's disease gene homologue. *Nat. Genet.* (1995) doi:10.1038/ng1095-155.
254. Arteaga-Bracho, E. E. *et al.* Postnatal and adult consequences of loss of huntingtin during development: Implications for Huntington's disease. *Neurobiol. Dis.* **96**, 144–155 (2016).
255. Mehler, M. F. *et al.* Loss-of-huntingtin in medial and lateral ganglionic lineages differentially disrupts regional interneuron and projection neuron subtypes and promotes huntington's disease-associated behavioral, cellular, and pathological hallmarks. *J. Neurosci.* (2019) doi:10.1523/JNEUROSCI.2443-18.2018.
256. Burrus, C. J. *et al.* Striatal Projection Neurons Require Huntingtin for Synaptic Connectivity and Survival. *Cell Rep.* (2020) doi:10.1016/j.celrep.2019.12.069.
257. Godin, J. D., Poizat, G., Hickey, M. A., Maschat, F. & Humbert, S. Mutant huntingtin-impaired degradation of  $\beta$ -catenin causes neurotoxicity in Huntington's disease. *EMBO J.* (2010) doi:10.1038/emboj.2010.117.
258. Godin, J. D. & Humbert, S. Mitotic spindle: Focus on the function of huntingtin. *International Journal of Biochemistry and Cell Biology* (2011) doi:10.1016/j.biocel.2011.03.009.
259. Molina-Calavita, M. *et al.* Mutant huntingtin affects cortical progenitor cell division and development of the mouse neocortex. *J. Neurosci.* (2014) doi:10.1523/JNEUROSCI.0715-14.2014.
260. Lim, R. G. *et al.* Developmental alterations in Huntington's disease neural cells and pharmacological rescue in cells and mice. *Nat. Neurosci.* **20**, (2017).
261. Molero, A. E. *et al.* Impairment of developmental stem cell-mediated striatal neurogenesis and pluripotency genes in a knock-in model of Huntington's disease. *Proc. Natl. Acad. Sci. U. S. A.*

- (2009) doi:10.1073/pnas.0912171106.
262. McKinstry, S. U. *et al.* Huntingtin is required for normal excitatory synapse development in cortical and striatal circuits. *J. Neurosci.* (2014) doi:10.1523/JNEUROSCI.4699-13.2014.
  263. Deng, Y. P., Wong, T., Bricker-Anthony, C., Deng, B. & Reiner, A. Loss of corticostriatal and thalamostriatal synaptic terminals precedes striatal projection neuron pathology in heterozygous Q140 Huntington's disease mice. *Neurobiol. Dis.* (2013) doi:10.1016/j.nbd.2013.08.009.
  264. Braz, B. Y. *et al.* Treating early postnatal circuit defect delays Huntingtin<sup>TM</sup>s disease onset and pathology in mice. *Science* (80-. ). (2022) doi:10.1126/science.abq5011.
  265. Lee, C. Y. D., Cattle, J. P. & Yang, X. W. Genetic manipulations of mutant huntingtin in mice: New insights into Huntington's disease pathogenesis. *FEBS Journal* (2013) doi:10.1111/febs.12418.
  266. Heikkinen, T. *et al.* Characterization of Neurophysiological and Behavioral Changes, MRI Brain Volumetry and 1H MRS in zQ175 Knock-In Mouse Model of Huntington's Disease. *PLoS One* (2012) doi:10.1371/journal.pone.0050717.
  267. Menalled, L. B. *et al.* Comprehensive Behavioral and Molecular Characterization of a New Knock-In Mouse Model of Huntington's Disease: ZQ175. *PLoS One* (2012) doi:10.1371/journal.pone.0049838.
  268. Zhang, J. *et al.* c-Fos facilitates the acquisition and extinction of cocaine-induced persistent changes. *J. Neurosci.* (2006) doi:10.1523/JNEUROSCI.3795-06.2006.
  269. Durieux, P. F. *et al.* D<sup>2</sup>R striatopallidal neurons inhibit both locomotor and drug reward processes. *Nat. Neurosci.* (2009) doi:10.1038/nn.2286.
  270. Comella-Bolla, A. *et al.* Human Pluripotent Stem Cell-Derived Neurons Are Functionally Mature In Vitro and Integrate into the Mouse Striatum Following Transplantation. *Mol. Neurobiol.* (2020) doi:10.1007/s12035-020-01907-4.
  271. Gokce, O. *et al.* Cellular Taxonomy of the Mouse Striatum as Revealed by Single-Cell RNA-Seq. *Cell Rep.* **16**, 1126–1137 (2016).
  272. Bocchi, V. D. *et al.* The coding and long noncoding single-cell atlas of the developing human fetal striatum. *Science* (80-. ). (2021) doi:10.1126/science.abf5759.
  273. Grzybowska, E. A. Human intronless genes: Functional groups, associated diseases, evolution, and mRNA processing in absence of splicing. *Biochemical and Biophysical Research Communications* (2012) doi:10.1016/j.bbrc.2012.06.092.
  274. Dey, B. K., Mueller, A. C. & Dutta, A. Long non-coding rnas as emerging regulators of

- differentiation, development, and disease. *Transcription* vol. 5 (2014).
275. Nagano, T. & Fraser, P. No-nonsense functions for long noncoding RNAs. *Cell* vol. 145 178–181 (2011).
  276. Geisler, S. & Coller, J. RNA in unexpected places: Long non-coding RNA functions in diverse cellular contexts. *Nature Reviews Molecular Cell Biology* vol. 14 699–712 (2013).
  277. Ponting, C. P., Oliver, P. L. & Reik, W. Evolution and Functions of Long Noncoding RNAs. *Cell* vol. 136 629–641 (2009).
  278. Hutchinson, J. N. *et al.* A screen for nuclear transcripts identifies two linked noncoding RNAs associated with SC35 splicing domains. *BMC Genomics* **8**, (2007).
  279. Johnson, R. Long non-coding RNAs in Huntington’s disease neurodegeneration. *Neurobiology of Disease* vol. 46 245–254 (2012).
  280. Sunwoo, J. S. *et al.* Altered Expression of the Long Noncoding RNA NEAT1 in Huntington’s Disease. *Mol Neurobiol* (2016) doi:10.1007/s12035-016-9928-9.
  281. Lipovich, L. *et al.* Activity-dependent human brain coding/noncoding gene regulatory networks. *Genetics* **192**, 1133–1148 (2012).
  282. Yan, W., Chen, Z. Y., Chen, J. Q. & Chen, H. M. LncRNA NEAT1 promotes autophagy in MPTP-induced Parkinson’s disease through stabilizing PINK1 protein. *Biochem. Biophys. Res. Commun.* **496**, 1019–1024 (2018).
  283. Bernard, D. *et al.* A long nuclear-retained non-coding RNA regulates synaptogenesis by modulating gene expression. *EMBO J.* **29**, 3082–3093 (2010).
  284. McCluggage, F. & Fox, A. H. Paraspeckle nuclear condensates: Global sensors of cell stress? *BioEssays* (2021) doi:10.1002/bies.202000245.
  285. Hirose, T. *et al.* NEAT1 long noncoding RNA regulates transcription via protein sequestration within subnuclear bodies. *Mol. Biol. Cell* **25**, 169–183 (2014).
  286. Choudhry, H. *et al.* Tumor hypoxia induces nuclear paraspeckle formation through HIF-2 $\alpha$  dependent transcriptional activation of NEAT1 leading to cancer cell survival. *Oncogene* **34**, 4482–4490 (2015).
  287. Mao, Y. S., Zhang, B. & Spector, D. L. Biogenesis and function of nuclear bodies. *Trends in Genetics* (2011) doi:10.1016/j.tig.2011.05.006.
  288. Morimoto, M. & Boerkoel, C. F. The role of nuclear bodies in gene expression and disease. *Biology* (2013) doi:10.3390/biology2030976.
  289. Nakagawa, S., Naganuma, T., Shioi, G. & Hirose, T. Paraspeckles are subpopulation-specific

- nuclear bodies that are not essential in mice. *J. Cell Biol.* **193**, 31–39 (2011).
290. Fox, A. H. & Lamond, A. I. Paraspeckles. *Cold Spring Harbor perspectives in biology* vol. 2 (2010).
  291. Fox, A. H., Nakagawa, S., Hirose, T. & Bond, C. S. Paraspeckles: Where Long Noncoding RNA Meets Phase Separation. *Trends in Biochemical Sciences* (2017) doi:10.1016/j.tibs.2017.12.001.
  292. Keryer, G. *et al.* Ciliogenesis is regulated by a huntingtin-HAP1-PCM1 pathway and is altered in Huntington disease. *J. Clin. Invest.* **121**, 4372–4382 (2011).
  293. McGuire, J. R., Rong, J., Li, S. H. & Li, X. J. Interaction of Huntingtin-associated protein-1 with kinesin light chain: Implications in intracellular trafficking in neurons. *J. Biol. Chem.* **281**, 3552–3559 (2006).
  294. Martin, E. J. *et al.* Analysis of huntingtin-associated protein 1 in mouse brain and immortalized striatal neurons. *J. Comp. Neurol.* **403**, 421–430 (1999).
  295. Metzger, S. *et al.* Huntingtin-associated protein-1 is a modifier of the age-at-onset of Huntington's disease. *Hum. Mol. Genet.* **17**, 1137–1146 (2008).
  296. Rao, D. S. *et al.* Huntingtin Interacting Protein 1 Is a Clathrin Coat Binding Protein Required for Differentiation of late Spermatogenic Progenitors. *Mol. Cell. Biol.* **21**, 7796–7806 (2001).
  297. Metzler, M. *et al.* HIP1 Functions in Clathrin-mediated Endocytosis through Binding to Clathrin and Adaptor Protein 2. *J. Biol. Chem.* **276**, 39271–39276 (2001).
  298. Block, R. C., Dorsey, E. R., Beck, C. A., Brenna, J. T. & Shoulson, I. Altered cholesterol and fatty acid metabolism in Huntington disease. *Journal of Clinical Lipidology* vol. 4 17–23 (2010).
  299. Duan, W., Jiang, M. & Jin, J. Metabolism in HD: Still a relevant mechanism? *Movement Disorders* vol. 29 1366–1374 (2014).
  300. Naseri, N. N. *et al.* Abnormalities in the tricarboxylic Acid cycle in Huntington disease and in a Huntington disease mouse model. *J Neuropathol Exp Neurol* **74**, 527–537 (2015).
  301. Waldvogel, H. J., Kim, E. H., Tippet, L. J., Vonsattel, J. P. G. & Faull, R. L. M. The neuropathology of Huntington's disease. *Curr. Top. Behav. Neurosci.* **22**, 33–80 (2014).
  302. Harding, R. J. & Tong, Y. F. Proteostasis in Huntington's disease: Disease mechanisms and therapeutic opportunities. *Acta Pharmacologica Sinica* (2018) doi:10.1038/aps.2018.11.
  303. Mitra, S. & Finkbeiner, S. The ubiquitin-proteasome pathway in Huntington's disease. *TheScientificWorldJournal* (2008) doi:10.1100/tsw.2008.60.
  304. Ortega, Z. & Lucas, J. J. Ubiquitin-proteasome system involvement in huntington's disease. *Front. Mol. Neurosci.* (2014) doi:10.3389/fnmol.2014.00077.

305. Li, X. J. & Li, S. Proteasomal dysfunction in aging and Huntington disease. *Neurobiology of Disease* (2011) doi:10.1016/j.nbd.2010.11.018.
306. Stoykova, a, Götz, M., Gruss, P. & Price, J. Pax6-dependent regulation of adhesive patterning, R-cadherin expression and boundary formation in developing forebrain. *Development* **124**, 3765–3777 (1997).
307. Neyt, C., Welch, M., Langston, a, Kohtz, J. & Fishell, G. A short-range signal restricts cell movement between telencephalic proliferative zones. *J. Neurosci.* **17**, 9194–203 (1997).
308. Stoykova, a, Fritsch, R., Walther, C. & Gruss, P. Forebrain patterning defects in Small eye mutant mice. *Development* **122**, 3453–3465 (1996).
309. Toresson, H., Potter, S. S. & Campbell, K. Genetic control of dorsal-ventral identity in the telencephalon: opposing roles for Pax6 and Gsh2. *Development* **127**, 4361–4371 (2000).
310. Chapouton, P., Gärtner, A. & Götz, M. The role of Pax6 in restricting cell migration between developing cortex and basal ganglia. *Development* **126**, 5569–79 (1999).
311. Götz, M., Stoykova, A. & Gruss, P. Pax6 controls radial glia differentiation in the cerebral cortex. *Neuron* **21**, 1031–1044 (1998).
312. Andrews, G. L. & Mastick, G. S. R-cadherin is a Pax6-regulated, growth-promoting cue for pioneer axons. *J. Neurosci.* **23**, 9873–80 (2003).
313. Redies, C. *et al.* Patch/matrix patterns of gray matter differentiation in the telencephalon of chicken and mouse. in *Brain Research Bulletin* vol. 57 489–493 (2002).
314. Zhou, C. *et al.* Lhx6 and Lhx8: Cell fate regulators and beyond. *FASEB Journal* vol. 29 4083–4091 (2015).
315. Hindley, C. & Philpott, A. Co-ordination of cell cycle and differentiation in the developing nervous system. *Biochemical Journal* (2012) doi:10.1042/BJ20112040.
316. Dehay, C. & Kennedy, H. Cell-cycle control and cortical development. *Nature Reviews Neuroscience* (2007) doi:10.1038/nrn2097.
317. Da Veiga Moreira, J. *et al.* Cell cycle progression is regulated by intertwined redox oscillators. *Theoretical Biology and Medical Modelling* (2015) doi:10.1186/s12976-015-0005-2.
318. Park, Y. Y., Ahn, J. H., Cho, M. G. & Lee, J. H. ATP depletion during mitotic arrest induces mitotic slippage and APC/CCdh1-dependent cyclin B1 degradation. *Exp. Mol. Med.* (2018) doi:10.1038/s12276-018-0069-2.
319. Lim, R. G. *et al.* Developmental alterations in Huntington's disease neural cells and pharmacological rescue in cells and mice. *Nat. Neurosci.* **20**, 648–660 (2017).

320. Molero, A. E. *et al.* Impairment of developmental stem cell-mediated striatal neurogenesis and pluripotency genes in a knock-in model of Huntington's disease. *Proc. Natl. Acad. Sci.* (2009) doi:10.1073/pnas.0912171106.
321. Godin, J. D. *et al.* Huntingtin Is Required for Mitotic Spindle Orientation and Mammalian Neurogenesis. *Neuron* (2010) doi:10.1016/j.neuron.2010.06.027.
322. Mochel, F. *et al.* Early alterations of brain cellular energy homeostasis in huntington disease models. *J. Biol. Chem.* (2012) doi:10.1074/jbc.M111.309849.
323. Matsuzaki, F. & Shitamukai, A. Cell division modes and cleavage planes of neural progenitors during mammalian cortical development. *Cold Spring Harb. Perspect. Biol.* (2015) doi:10.1101/cshperspect.a015719.
324. Knowles, R., Dehorter, N. & Ellender, T. From Progenitors to Progeny: Shaping Striatal Circuit Development and Function. *J. Neurosci.* **41**, 9483–9502 (2021).
325. Mukhtar, T. & Taylor, V. Untangling Cortical Complexity During Development. *Journal of Experimental Neuroscience* (2018) doi:10.1177/1179069518759332.
326. Fazl, A. & Fleisher, J. Anatomy, Physiology, and Clinical Syndromes of the Basal Ganglia: A Brief Review. *Semin. Pediatr. Neurol.* (2018) doi:10.1016/j.spen.2017.12.005.
327. Ring, H. A. & Serra-Mestres, J. Neuropsychiatry of the basal ganglia. *Journal of Neurology Neurosurgery and Psychiatry* (2002) doi:10.1136/jnnp.72.1.12.
328. Dekkers, M. P. J. & Barde, Y. A. Programmed cell death in neuronal development. *Science* (2013) doi:10.1126/science.1236152.
329. Pfisterer, U. & Khodosevich, K. Neuronal survival in the brain: Neuron type-specific mechanisms. *Cell Death and Disease* (2017) doi:10.1038/cddis.2017.64.
330. Yamaguchi, Y. & Miura, M. Programmed cell death in neurodevelopment. *Developmental Cell* (2015) doi:10.1016/j.devcel.2015.01.019.
331. Siebzehnürbl, F. A. *et al.* Early postnatal behavioral, cellular, and molecular changes in models of Huntington disease are reversible by HDAC inhibition. *Proc. Natl. Acad. Sci. U. S. A.* (2018) doi:10.1073/pnas.1807962115.
332. Sapp, E. *et al.* Evidence for a preferential loss of enkephalin immunoreactivity in the external globus pallidus in low grade Huntington's disease using high resolution image analysis. *Neuroscience* (1995) doi:10.1016/0306-4522(94)00427-7.
333. Deng, X., Kang, J. koo & Low, B. S. Corporate social responsibility and stakeholder value maximization: Evidence from mergers. *J. financ. econ.* (2013) doi:10.1016/j.jfineco.2013.04.014.

334. Voelkl, K., Schulz-Trieglaff, E. K., Klein, R. & Dudanova, I. Distinct histological alterations of cortical interneuron types in mouse models of Huntington's disease. *Front. Neurosci.* (2022) doi:10.3389/fnins.2022.1022251.
335. Holley, S. M. *et al.* Major contribution of somatostatin-expressing interneurons and cannabinoid receptors to increased GABA synaptic activity in the striatum of Huntington's disease mice. *Front. Synaptic Neurosci.* (2019) doi:10.3389/fnsyn.2019.00014.
336. Llorca, A. & Deogracias, R. Origin, Development, and Synaptogenesis of Cortical Interneurons. *Frontiers in Neuroscience* (2022) doi:10.3389/fnins.2022.929469.
337. Jan, Y. N. & Jan, L. Y. Genetic control of cell fate specification in *Drosophila* peripheral nervous system. *Annual Review of Genetics* (1994) doi:10.1146/annurev.ge.28.120194.002105.
338. Kageyama, R. & Nakanishi, S. Helix-loop-helix factors in growth and differentiation of the vertebrate nervous system. *Curr. Opin. Genet. Dev.* (1997) doi:10.1016/S0959-437X(97)80014-7.
339. Guimera, J., Weisenhorn, D. V. & Wurst, W. Megane/Heslike is required for normal GABAergic differentiation in the mouse superior colliculus. *Development* (2006) doi:10.1242/dev.02557.
340. Wende, C. Z. *et al.* Hairy/Enhancer-of-split MEGANE and proneural MASH1 factors cooperate synergistically in midbrain GABAergic neurogenesis. *PLoS One* (2015) doi:10.1371/journal.pone.0127681.
341. Li, S., Joshee, S. & Vasudevan, A. Mesencephalic GABA neuronal development: No more on the other side of oblivion. *Biomolecular Concepts* (2014) doi:10.1515/bmc-2014-0023.
342. Nakatani, T., Minaki, Y., Kumai, M. & Ono, Y. Helt determines GABAergic over glutamatergic neuronal fate by repressing Ngn genes in the developing mesencephalon. *Development* (2007) doi:10.1242/dev.02870.
343. Yamamoto, A., Lucas, J. J. & Hen, R. Reversal of neuropathology and motor dysfunction in a conditional model of Huntington's disease. *Cell* (2000) doi:10.1016/S0092-8674(00)80623-6.
344. Molero, A. E. *et al.* Selective expression of mutant huntingtin during development recapitulates characteristic features of Huntington's disease. *Proc. Natl. Acad. Sci.* **113**, 5736–5741 (2016).